The Role of Intracellular Ca^{2+} in Cigarette Smoke-Induced CFTR Internalisation

Waseema Salim Patel

Thesis submitted for the degree of Doctor of Philosophy

Date of submission: June 2017

Institute for Cell & Molecular Biosciences,

Faculty of Medical Sciences, Newcastle University

Marsico Lung Institute/ Cystic Fibrosis Center

The University of North Carolina at Chapel Hill

Abstract

Chronic obstructive pulmonary disease (COPD), the third leading cause of death worldwide, is characterised by airflow obstruction and is primarily caused by smoking. In contrast, another obstructive pulmonary disease, cystic fibrosis (CF), has orphan disease status. However, patients with either COPD or CF present with similar clinical lung problems. Importantly, cystic fibrosis transmembrane conductance regulator (CFTR) activity is reduced in both diseases. Recent work from our lab showed that cigarette smoke-induced increases in cytosolic Ca^{2+} were consequential in reducing plasma membrane expression of CFTR by an unknown mechanism. Therefore, the major aim of my project was to identify the molecular mechanism underlying the loss of CFTR activity brought about by an increase in cytosolic Ca^{2+}.

Whole cell patch clamp recordings in HEK 293T cells transiently transfected with CFTR showed that an increase in cytosolic Ca^{2+} significantly reduced CFTR-mediated conductance. Characterisation of the dynamic changes in cytosolic Ca^{2+}, induced by a range of agonists, showed that a sustained increase in Ca^{2+} was not essential for the loss of CFTR-mediated conductance, but it did involve a dynamin-dependent internalisation of the channel. Confocal imaging further confirmed that an increase in cytosolic Ca^{2+} caused a reduction in plasma membrane CFTR expression, and a reciprocal increase in intracellular CFTR.

Activation of the MEK/ERK pathway has previously been linked to smoke-induced internalisation of CFTR. Similarly, inhibition of the pathway prevented a Ca^{2+}-induced internalisation of CFTR, indicating this pathway also plays a role in Ca^{2+}-induced CFTR internalisation. Importantly, inhibition of the Ca^{2+} dependent phosphatase calcineurin with cyclosporin A prevented both Ca^{2+} as well as smoke-induced loss of CFTR, suggesting that the mechanism of internalisation is linked to dephosphorylation, possibly of CFTR itself. Furthermore, either an increase in Ca^{2+}, or exposure to cigarette smoke, increased calcineurin activity, further implicating this phosphatase as a key effector. Functionally, inhibition of calcineurin prevented against a smoke-induced reduction in ASL height whilst having no effect on physiological changes in height induced by G protein-coupled receptor agonists; signifying calcineurin only gets activated under conditions of stress. These findings highlight a role for cytosolic Ca^{2+} in modulating CFTR activity. Additionally, these data may lead to novel therapeutic strategies aimed at correcting ASL hydration in smokers as well as in people with CF.

Dedicated to the memory of my brother.

This is for you, Q

Acknowledgments

I would like to express my gratitude and thanks to my supervisors, Dr Mike Gray and Dr Rob Tarran, for their time, guidance, and constructive critique throughout my PhD, all of which have allowed me to develop my ability as a research scientist. I would also like to extend my thanks for the unique opportunity of working towards my PhD in both of their labs, on either side of the Atlantic. As such, both of my supervisors have at some point advised me from afar but have always been available when needed and provided valuable insights into my project.

I was lucky enough to work in two labs during my PhD; my experience in each lab would not have been the same without the encouragement from my colleagues and the enjoyable work environment they created. In particular, I would like to thank Dr Mark Turner and Dr Salam Ibrahim for their help and support in the early days of my PhD and throughout my time at Newcastle University. I would like to thank Dr Bernard Verdon and the Pearson lab for always keeping their office open for advice and for welcoming any questions I had. I would also like to thank members of the Epithelial Research Group at Newcastle University for their advice, the insightful conversations, and their friendship.

I would like to thank the members of the Tarran lab, past and present, for welcoming me to Chapel Hill and for all their support, advice, and assistance during the last half of my PhD. I would particularly like to thank Dr Saira Ahmad, Dr Megan Webster, Dr Abigail Marklew, and Dr Patrick Moore for making my time especially enjoyable both in and out of the lab. Additionally, I would like to thank members of the Wolfgang, Ehre, and Kesimer labs for all the stimulating discussions... sometimes related to science. I would also like to thank my friends in Chapel Hill and Durham for making my time in the states so much easier knowing I had a great group of friends.

I would like to thank my family for their unwavering support, encouragement, and dedication, all of which were invaluable and were a constant regardless of whether I was on the opposite side of England or in another country altogether. Finally, I would like to thank my friends at home in Blackburn for their enthusiasm, their support, and for always making my trips back home all the more fun.

Table of Contents

List of Figures

List of Tables

List of Abbreviations

$[Ca^{2+}]_i$	The concentration of intracellular Ca^{2+}
ABC	ATP binding cassette
Ado	Adenosine
AKAP	A kinase anchoring protein
AM	Acetoxymethylester
AMPK	5’ adenosine monophosphate-activated protein kinase
Ano1	Anoctamin 1
Anx 2	Annexin 2
AQP	Aquaporin
ASL	Airway surface liquid
ATP	Adenosine triphosphate
AUC	Area under curve
BAPTA	1,2-Bis(2-aminophenoxy)ethane-N,N,N′,N′-tetraacetic acid tetrakis
BCA	Bicinchoninic acid
BHK	Baby hamster kidney
BSA	Bovine serum albumin
CaCC	Ca^{2+}-activated Cl^- channel
cAMP	Cyclic adenosine monophosphate
CAP	Channel activated protease
CB	Chronic bronchitis
CBF	Ciliary beat frequency
CF	Cystic fibrosis
CFTR	Cystic fibrosis transmembrane conductance regulator
Cn	Calcineurin
COP	Coat protein complex
COPD	Chronic obstructive pulmonary disease
CS	Cigarette smoke
CsA	Cyclosporin A
CSC	Cigarette smoke condensate
CSE	Cigarette smoke extract
DAPI	4’,6-Diamidino-2-Phenylindole dihydrochloride
DMEM	Dulbecco’s Modified Eagle’s Medium
DMSO	Dimethyl sulfoxide

EDTA	Ethylenediaminetetraacectic acid
EGTA	Ethylene glycol-bis(β-aminoethyl ether)-N,N,N’,N’-tetraacetic acid
ENaC	Epithelial Na^+ channel
Epac	Exchange protein activated by cAMP
ER	Endoplasmic reticulum
ERK	Extracellular signal related kinase
FBS	Foetal bovine serum
Fura 2	2-[6-[Bis[2-[(acetyloxy)methoxy]-2-oxoethyl]amino]-5-[2-[2-[bis[2-[(acetyloxy)methoxy]-2-oxoethyl]amino]-5-methylphenoxy]ethoxy]-2-benzofuranyl]-5-oxazolecarboxylic acid
Fsk	Forskolin
GFP	Green fluorescent protein
GPN	Glycyl-L-phenylalanine-β-napthylamide
HBEC	Human bronchial epithelial cell
HEK	Human embryonic kidney
HyD	Hybrid detector
IP_3	Inositol-1,4,5-trisphosphate
ISO	International organisation for standardisation
IV	Current-voltage
KSR2	Kinase suppressor of Ras 2
LAMP1	Lysosomal associated membrane protein 1
LAS AF	Leica Application Suite: Advanced Fluorescence
MAPK	Mitogen activated protein kinase
MCC	Mucociliary clearance
MEK	Mitogen activated protein kinase kinase
MSD	Membrane spanning domain
NAADP	Nicotinic acid adenine dinucleotide phosphate
NBD	Nucleotide binding domain
NFAT	Nuclear factor of activated T cells
NKCC	$Na^+/K^+/2\ Cl^-$ cotransporter
NNK	Nicotine-derived nitrosamine ketone
nS	Nanosiemen
OA	Okadaic acid
PBS	Phosphate buffered saline
PCL	Periciliary liquid

PDZ	Post synaptic density protein (PSD-95), drosophila disc large tumour suppressor (Dlg 1) and zona occludens 1 protein (ZO-1)
pF	picofarad
PFC	Perfluorocarbon
PIP_2	Phosphatidylinositol 4,5-bisphosphate
PIP_3	Phosphatidylinositol 3,4,5-trisphosphate
PKA	Protein kinase A
PKC	Protein kinase C
PMT	Photomultiplier
P_o	Open probability
PP2	Protein phosphatase 2
Pyk2	Proline rich tyrosine kinase 2
Rab	Ras associated binding
RACK1	Receptor for activated C kinase
SEM	Standard error of mean
SERCA	Sarcoendoplasmic reticulum Ca^{2+} ATPase
SPLUNC	Short palate, lung and nasal epithelial clone
STIM1	Stromal interaction molecule 1
TG	Thapsigargin
TGN	*Trans* Golgi network
TIRF	Total internal reflection fluorescence
TPC	Two-pore channel
TRP	Transient receptor potential
UTP	Uridine 5'-triphosphate
UV	Ultraviolet
V_m	Membrane potential
WCS	Whole cigarette smoke

Chapter 1.0 Introduction

1.1 Anatomy of the airways

The airways form a continuous tract that allows the passage of air to the lungs, with the predominant role being to protect against inhaled pathogens and provide a suitable mechanism for gas exchange, allowing oxygen to reach the rest of the body. The airways can be split into two broad regions, the upper and lower airways, which function to allow the passage of air to the lungs. The nasal cavities, pharynx, larynx, trachea, bronchi and bronchioles form the upper airway. The respiratory bronchiole, alveolar ducts, and sacs form the lower airway (Ganesan et al., 2013). The purpose of the upper airways is to condition and moisten inhaled air, thus allowing sterile air to flow to the lower airways (Pohunek, 2004). The lower airways on the other hand, are primarily responsible for gas exchange. Anatomically, the airways possess 20-25 generations or branch points with a progressive increase in the surface area (Knowles and Boucher, 2002). The first 10 airway generations are characterised as having cartilaginous rings, seen from the trachea to the bronchi. Between generations 10-15th, there is a loss of cartilage in the conducting bronchioles. Between generations 15-20, are respiratory bronchioles and after generation 20 are the alveolar ducts, continuously lined with alveoli.

As mentioned earlier, the airways serve to protect the host from inhaled agents. This is accomplished by cells in the upper airway acting synchronously to prevent any inhaled pathogens reaching the respiratory airways (Saint-Criq and Gray, 2017). The airways are lined by a pseudostratified epithelium that progressively becomes a cuboidal layer followed by a thin epithelial layer (Hermans and Bernard, 1999). It has been estimated that 50-90% of cells in the conducting airway are ciliated; these cells beat in a co-ordinated manner to expel any inhaled toxins or pathogens. Submucosal glands, goblet and club cells are responsible for most mucus secretion into the airways, which helps remove inhaled agents. The secreted fluid and mucins form a layer of solution, the airway surface liquid (ASL), which traps inhaled particles and transports them, via ciliary beating towards the mouth (Fig. 1.01). The process by which the ASL clears trapped pollutants from the distal airway to the pharynx is known as mucociliary clearance (MCC) and the efficiency of this process depends on the composition of the airway surface liquid (Boucher, 2004).

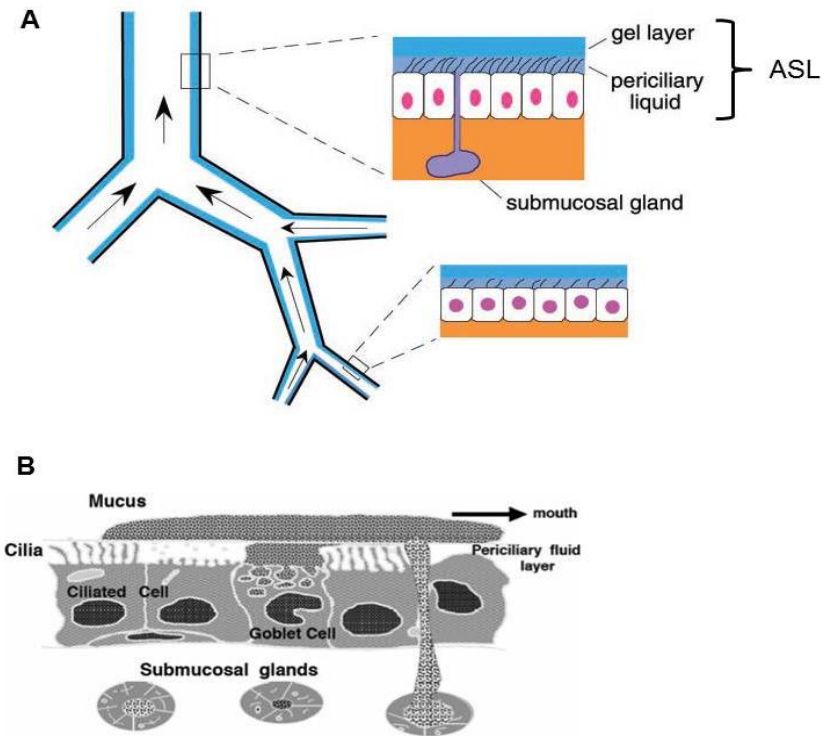

Figure 1.01. Airway surface liquid and mucociliary clearance in the airways. (A) Diagram showing airway surface liquid (ASL) in large and small airways. The ASL is composed of a periciliary fluid layer, which is the same thickness as cilia and a mucus gel layer. The direction of fluid movement throughout the airways is indicated. Taken from (Verkman et al., 2003). **(B)** Detailed diagram showing the components that constitute mucociliary clearance. Mucus is carried towards the mouth to clear bacteria and toxins away from the airways. Taken from (Bennett et al., 2010).

1.2 The airway surface liquid

The airway surface liquid, approximately 7-10 µm in height, serves to lubricate epithelial cells and is composed of the periciliary liquid layer (PCL) and a mucus layer (Matsui et al., 1998b). The PCL is a low viscosity solution that is roughly the same height as cilia and functions to sustain an environment which maintains efficient ciliary beating. The PCL also contains a mesh layer that prevents movement of substances from the mucus layer into the PCL (Fig. 1.02). This mesh layer is composed of membrane spanning mucins including MUC1, MUC4 and MUC16 and also contains mucopolysaccharides (Button et al., 2012). The height of the PCL is maintained by a balance between the absorption of Na^+ through the epithelial Na^+ channel (ENaC) and the secretion of Cl^- through the cystic fibrosis transmembrane conductance regulator (CFTR) and Ca^{2+}-activated Cl^- channels (CaCC; discussed in more detail in section 1.3). The importance of the PCL height in the airways was

highlighted by Tarran et al., (2001) who showed that despite multiple manoeuvres to change ASL hydration, the PCL height remained constant (Tarran et al., 2001a). The researchers observed that the mucus layer absorbed the changes in height to maintain a PCL height of ~7 μm, adding to existing evidence suggesting that the mucus layer acts as a reservoir for the PCL (Kilburn, 1968).

In addition to maintaining PCL height, the mucus layer also serves to bind and trap inhaled pathogens (Thornton et al., 2008). The mucus layer is effective at binding a variety of pathogens due to the expression of multiple carbohydrate epitopes. The mucins predominantly found in the airways are MUC5AC and MUC5B which are produced by goblet cells and submucosal glands, respectively (Hovenberg et al., 1996, Wickström et al., 1998). Mucus and any trapped pathogens are subsequently removed by the tips of cilia contacting the underside of the mucus layer and propelling it towards the mouth (Knowles and Boucher, 2002).

The control of ASL height occurs locally with mediators in the ASL acting as feedback molecules to regulate and maintain ASL height. The control of basal ASL height is regulated by adenosine which causes an increase in Cl^- secretion through pathways linked to the activation of G protein-coupled receptors (Lazarowski et al., 2004, Tarran et al., 2005, Tarran et al., 2006b). The reporter molecules contained within the ASL include purine nucleotides and channel activated proteases (CAPs). Vallet et al (1997) identified CAPs and CAP inhibitors as regulators of ENaC activity, with CAPs cleaving ENaC and causing an increase in activity (Vallet et al., 1997). Donaldson and colleagues further suggested that the main CAP in airway epithelia is prostatin (Donaldson et al., 2002). In addition to CAPS, the protease inhibitor, short palate, lung and nasal epithelial clone 1 (SPLUNC1) also functions as a reporter molecule by binding to ENaC directly to inhibit channel activity (Garcia-Caballero et al., 2009, Gaillard et al., 2010).

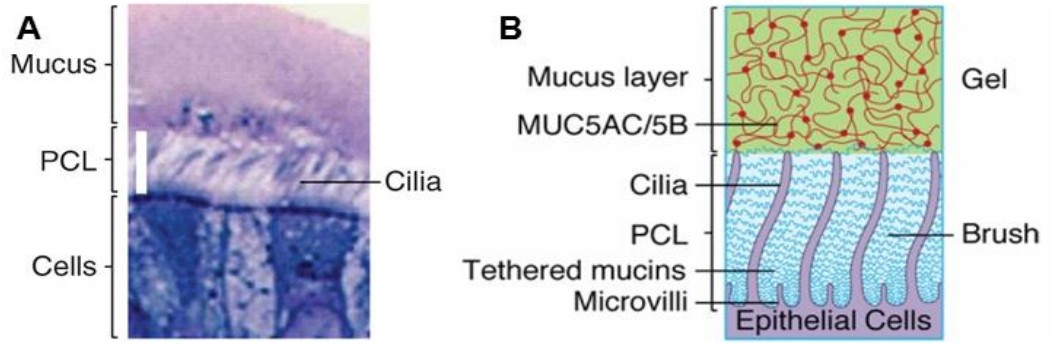

Figure 1.02. Model of the airway surface liquid. (A) Airway surface liquid (ASL) in fixed human bronchial epithelial cells. Scale bar represents 7 µm. Taken from (Matsui et al., 1998a). **(B)** Model detailing composition of the layers of the ASL. The mucus gel layer contains the mucins MUC5AC and MUC5B. The periciliary liquid (PCL) layer is the same height as cilia and contains mucins such as MUC4 to form a mesh and prevent constituents of the mucus layer entering the PCL. Taken from (Button et al., 2012).

1.3 Ion transport in the airway

As indicated in section 1.2, the activity of ion channels, transporters and pumps must be co-ordinated for efficient MCC. Therefore, an understanding of transepithelial ion transport in the airway and what governs these fluxes is of importance. In particular, the movement of Na^+ and Cl^- is of interest as Na^+ absorption is associated with a reduction in ASL height and Cl^- secretion with increases in ASL height.

The concentrations of Na^+ and K^+ in the cell are regulated by the Na^+/K^+ ATPase at the basolateral membrane which loads K^+ into the cell and exports Na^+. The $Na^+/K^+/2$ Cl^- cotransporter (NKCC) at the basolateral membrane consequently uses the Na^+ gradient created by the Na^+/K^+ ATPase to accumulate Cl^- into the cell along with Na^+ and K^+. Cl^- subsequently leaves the cell passively through channels expressed on the apical membrane whilst K^+ is recycled from the cell via the action of K^+ channels at the apical and basolateral membrane (McCann and Welsh, 1990).

ENaC, a heterotrimer made up of α, β and γ subunits, is responsible for the transepithelial absorption of Na^+ from the luminal space to blood (Canessa et al., 1994). ENaC is inhibited by CFTR activity, as an elevation of cyclic adenosine monophosphate (cAMP) activates protein kinase A (PKA), resulting in phosphorylation of ENaC and a decrease in channel gating (Fig. 1.03) (Stutts et al., 1995, Konstas et al., 2003). Alternatively, ENaC is activated by anionic lipid such as

phosphatidylinositol 3,4,5-trisphosphate (PIP_3) phosphatidylinositol 4,5-bisphosphate (PIP_2) and phosphatidylserine. Thus, PIP_2 has been shown to prevent the rundown of ENaC activity by binding to all three subunits of ENaC (Ma et al., 2002).

Cl^- secretion through the apical plasma membrane is predominantly mediated by CFTR which responds to increases in cAMP (discussed in more detail in next section). Additionally, CaCC channels, which respond to increases in cytosolic Ca^{2+}, also mediate Cl^- secretion. CaCC are thought to be encoded by the Anoctamin 1/TMEM16 A gene (Caputo et al., 2008, Schroeder et al., 2008, Yang et al., 2008). However, in intestinal and airway epithelia, TMEM16A may only contribute for a small amount of CaCC (Namkung et al., 2011). CaCC activity is stimulated by nucleotides such as ATP. Once released in the airways, nucleotides bind to $P2Y_2$ receptors and cause an increase in cytosolic Ca^{2+} through phospholipase C (PLC). This pathway also leads to inhibition of ENaC through a reduction in PIP_2 (Chambers et al., 2007). Increased secretion Cl^- into the ASL by ATP has been reported to increase ASL height and mucus hydration, although the effects have been shown to be short-lived due to the rapid metabolism of ATP by 5'-ectonucleotideases (Tarran, 2004). The metabolism of ATP however, yields adenosine which can stimulate CFTR activity through increasing intracellular PKA (Lazarowski et al., 2004, Picher et al., 2004).

The movement of K^+ is also of importance within airway epithelia as the movement of this ion creates the electrical driving force for the movement of Cl^- out of the cell (Silva et al., 1977). Within airway epithelia, the basolateral membrane expresses voltage gated K^+ channels, K_vLQT1 (also known as K_v7.1, *KCNQ1*) channels which respond to an increase in cAMP with the secretion of K^+ (Fig. 1.03). Thus, these channels act in parallel with the activation in CFTR to maximise Cl^- secretion (Mall et al., 2000). Another K^+ channel, SK4, also known as K_{ca}3.1 (*KCNN4*), is also expressed at the basolateral membrane of airway epithelia and respond to an increase in cytosolic Ca^{2+} (Mall et al., 2003). As with K_vLQT1, SK4 channels act in concert with the activation of CaCC channels to maximise Cl^- efflux from the cell. K_vLQT1 and SK4 have also been found to be expressed at the apical membrane, where these channels may interact with CFTR (Bernard et al., 2003, Moser et al., 2008, Klein et al., 2016). Furthermore, Davis and Cowley identified two-pore domain K^+ channels at the apical plasma membrane, which also facilitate anion efflux (Davis and Cowley, 2006).

The movement of Na^+ and Cl^- creates local osmotic gradients allowing the movement of water, either passively through the paracellular pathway or transcellularly through aquaporins (AQP). Within airway epithelia, AQP 5 is expressed at the apical membrane, whilst AQP 3 and 4 are expressed at the basolateral membrane (Schreiber et al., 1999). Furthermore, Schrieber and colleagues showed that activation of CFTR was also linked to an increase in water permeability through AQP3, suggesting changes in cAMP can influence water transport through the cell (Schreiber et al., 1999).

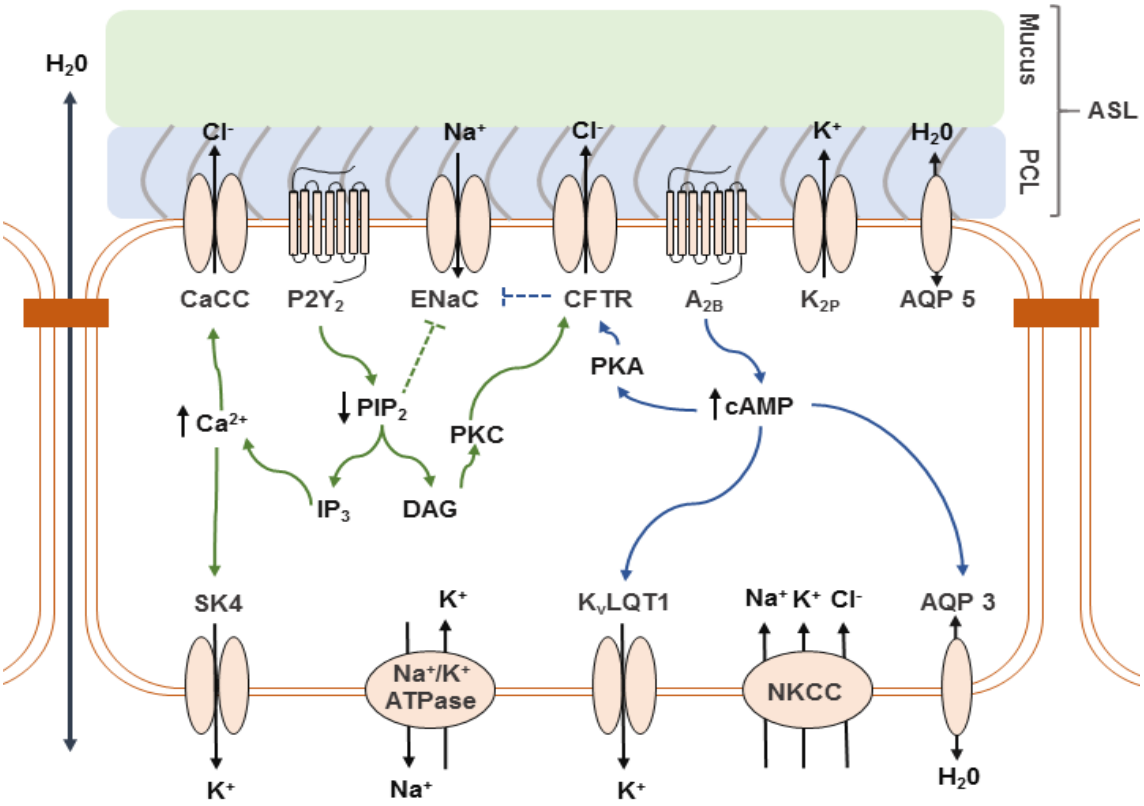

Figure 1.03. Ion transport in airway epithelia. Ion transport at the apical plasma membrane is controlled by the actions of the epithelial Na^+ channel (ENaC), the cystic fibrosis transmembrane conductance regulator (CFTR), Ca^{2+} activated Cl^+ channels (CaCC) and K^+ channels. Ion transport at the basolateral membrane is controlled by the $Na^+/K^+/2$ Cl^- cotransporter (NKCC), Na^+/K^+ ATPase and K^+ channels. Water moves by paracellularly or through aquaporins (AQP). The activity of channels expressed in airway epithelia is regulated by increases in protein kinase A (PKA) linked to cAMP, which in turn is stimulated by activation of the A_{2B} receptor. Alternatively, channels can be regulated by increases in Ca^{2+} through activation of the Gq pathway induced by UTP/ATP binding to $P2Y_2$ receptors. Solid arrows represent positive regulation through these pathways whereas dashed lines indicate inhibition. The secretion of Cl^- and absorption of Na^+ at the apical membrane consequently influence the height of the airway surface liquid (ASL), composed of a periciliary layer (PCL) and mucus layer.

1.4 CFTR

1.4.1 CFTR structure and function

CFTR is an anion channel found on the apical membrane of polarised epithelial cells and is a member of ATP-binding cassette (ABC) transporter family (Riordan et al., 1989). As with other members of this superfamily, CFTR consists of two membrane spanning domains (MSD), composed of six transmembrane α-helices and two nucleotide binding domains (NBD; Fig. 1.04). Amongst the ABC transporter family, the regulatory (R) domain and long N and C terminal tails are specific to CFTR (Rab et al., 2013, Riordan, 2005, Moran and Zegarra-Moran, 2008, Lubamba et al., 2012).

The R domain of the channel contains multiple consensus sites for serine/threonine phosphorylation by either PKA or PKC. In a non-active state, the R domain is bound to NBD1, inhibiting dimerisation of CFTR (Aleksandrov et al., 2007). Phosphorylation of the channel releases the R domain from binding to NBD1 and causes the binding of the R domain to C terminus of CFTR, allowing channel activation (Baker et al., 2007, Seavilleklein et al., 2008). The channel pore is formed by the two membrane spanning domains in response to the binding of ATP by the Walker A and B motifs. The Walker motifs bind ATP in a head to tail orientation and interruption of this conformation requires ATP hydrolysis. The opening of the channel is brought about by the dimerisation of the two NBD domains and the movement of the transmembrane domains to an outward facing conformation (Vergani et al., 2005). In addition, rotation of the transmembrane domains during channel gating is thought to facilitate channel opening. The pore has been characterised as a having a narrow central region (~5.3 Å) flanked by larger inner and outer vestibules (Linsdell and Hanrahan, 1998). In particular, the transmembrane segments 1, 6, 11 and 12 are involved in pore formation and line the inner vestibule; roles for transmembrane regions 3 and 9 in the cytoplasmic region of the pore have also been suggested (Wang et al., 2014). Transmembrane region 2 and extracellular loop 1 have been associated with forming the outer vestibule and attracting Cl^- to the pore (Zhou et al., 2008).

CFTR has a single channel conductance of 8-11 pS and an ohmic Cl^- conductance (Gray et al., 1989, Berger et al., 1991, Sheppard and Welsh, 1999). Notably, CFTR is not only selective for Cl^-, but other ions can also permeate through the channel. The permeability sequence through the channel is as $SCN^->NO_3^->Br^->Cl^->I^->$formate$>F^-$

(Anderson and Gregory, 1991). It has been found that the permeability sequence of ions through CFTR follows a lyotropic sequence, determined by a selectivity filter in the channel pore. Therefore, ions that are easily dehydrated have a higher permeability through CFTR (Linsdell et al., 1997). Indeed, it has been shown that ions are dehydrated as they pass through the pore (Smith et al., 1999). The permeation of Cl^- ions through CFTR is of particular interest because Cl^- has the highest conductance through the channel with the conductance sequence being as follows, $Cl^->NO_3^->Br^->formate>F^-,SCN^-,I^-$. The conductance of ions through CFTR is in turn determined by the affinity of ions for the inner vestibule (Linsdell, 2016, Linsdell, 2017).

Using the cell attached configurations of the patch clamp technique, Gray et al., (1989) showed that channel activity has a characteristic profile. Initial channel activation of CFTR is typified by a burst phase in which the channel shows flickering (Gray et al., 1989). The burst phase is followed by the channel being in a closed state (Zhou et al., 2001). This profile of CFTR channel activity involves the channel being in three states, open, closed or open-ready. It has been suggested that the channel is open when ATP is bound with the binding of ATP causing the opening of a gate within the channel pore and allowing access to the cytoplasmic region of the channel. Likewise, ATP hydrolysis results in the channel being closed (Wang and Linsdell, 2012). Further, the length of channel opening has been correlated to the time for ATP hydrolysis (Li et al., 1996).

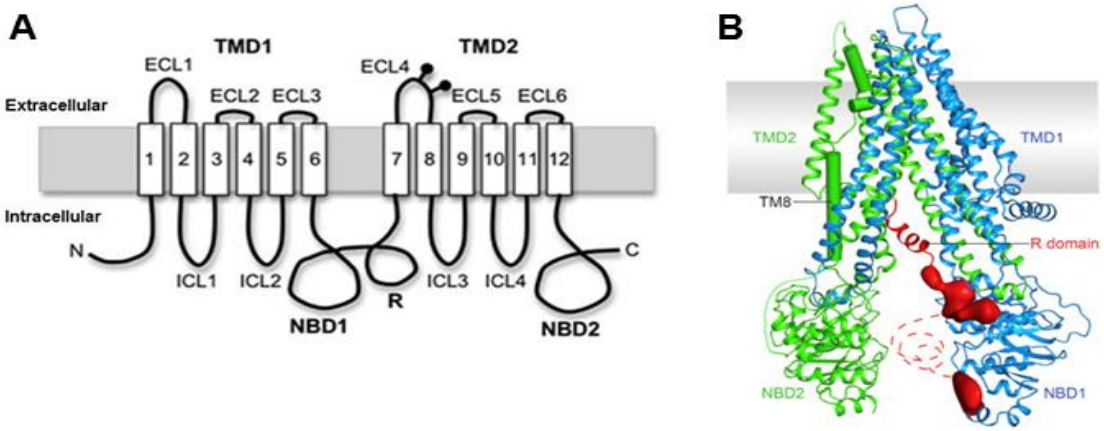

Figure 1.04. Model of CFTR. (A) CFTR is composed of two transmembrane domains (TMD) that are each composed of six transmembrane helices. The protein also contains two nucleotide binding domains (NBD) which are the site for nucleotide hydrolysis and a regulatory (R) domain which is unique to CFTR. Extracellular loops (ECL) and intracellular loops (ICL) are also indicated. (Kim and Skach, 2012). **(B)** Model of human CFTR. Taken from (Liu et al., 2017).

1.4.2 Biogenesis and trafficking of CFTR

CFTR synthesis occurs on cytosolic ribosomes, which are subsequently targeted and inserted into the endoplasmic reticulum (ER) (Skach, 2000, Farinha et al., 2013). The protein is assembled in the ER, with each domain of CFTR folding separately after which interdomain assembly occurs. CFTR undergoes quality control in the ER, with chaperones such as calnexin and Aha acting in concert with the cytosolic proteins Hsp 40/70/90, the co-chaperones Hdj2, HsBp1, Hop and p23, and CHIP to assess CFTR folding (Yang et al., 1993, Pind et al., 1994, Loo et al., 1998, Farinha et al., 2002). If CFTR fails to be deemed suitable, the protein is targeted for ER associated degradation. Furthermore, along with Hsp70, CHIP can also mediate degradation of misfolded CFTR by targeting the protein for ubiquitination and subsequent proteasomal degradation (Meacham et al., 1999, Meacham et al., 2001).

Following assembly, CFTR is transferred to an ER-Golgi intermediate compartment via COPII vesicles. At the Golgi apparatus, CFTR undergoes further quality control and may be targeted back to the ER for further modification (Bannykh et al., 2000, Ellgaard and Helenius, 2003). Alternatively, CFTR can be modified by N-linked glycosylation, however it has been suggested that this modification is not necessary for CFTR to proceed to the plasma membrane (Yu et al., 2007). The next step in the processing of CFTR involves the protein being targeted to the apical plasma membrane, via endosomes. In total, it has been suggested that only 30% of synthesised protein reaches the plasma membrane (Ameen et al., 2007, Cant et al., 2014).

Exocytosis of CFTR in to the apical plasma membrane is regulated by the interaction of CFTR with post synaptic density protein (PSD-95), drosophila disc large tumour suppressor (Dlg 1) and zona occludens 1 protein (ZO-1; PDZ) proteins. CFTR's PDZ binding motif (DTRL) is located at the C-terminus of the channel. The importance of this interaction has been evidenced by truncation of the C-terminus of CFTR resulting in the production of protein that was not targeted to the apical membrane (Moyer et al., 1999). PDZ proteins thought to be involved in CFTR localisation include ezrin-radixin-moesin (ERM)-binding phosphoprotein (EBP50/NHERF1), which has been shown to bind to the actin cytoskeleton, CAP70 which is found in the apical region of airway cells and also binds the cytoskeleton and CAL, which is localised below the

apical membrane and may be associated with the *trans* Golgi network (TGN) (Short et al., 1998, Wang et al., 2000, Cheng et al., 2002).

In addition to tethering CFTR to the apical plasma membrane, the interaction of CFTR with PDZ proteins also helps regulate CFTR activity; CAP70 and EBP50 have been shown to increase the open probability of CFTR. Wang and colleagues suggested CAP70 increased the open probability of CFTR by promoting the interaction of CFTR monomers with other CFTR monomers (Wang et al., 2000). Raghuram and colleagues also suggested EBP50 may act to increase P_o through promoting dimerisation of CFTR (Raghuram et al., 2001). Furthermore, ezrin has been suggested to act as an A kinase anchor protein (AKAP) and bind to EBP50 to facilitate the recruitment of PKA to the plasma membrane (Sun et al., 2000). Through interaction with EBP50 or CAP70, it has been suggested PLC can also be recruited to the plasma membrane. Additionally, PKC can also be tethered to EBP50 through interaction with a receptor for activated C kinase (RACK1; Fig. 1.05 (Jia et al., 1997). Thus, it has been suggested that recruitment of other proteins to the plasma membrane by PDZ proteins can potentiate CFTR activity.

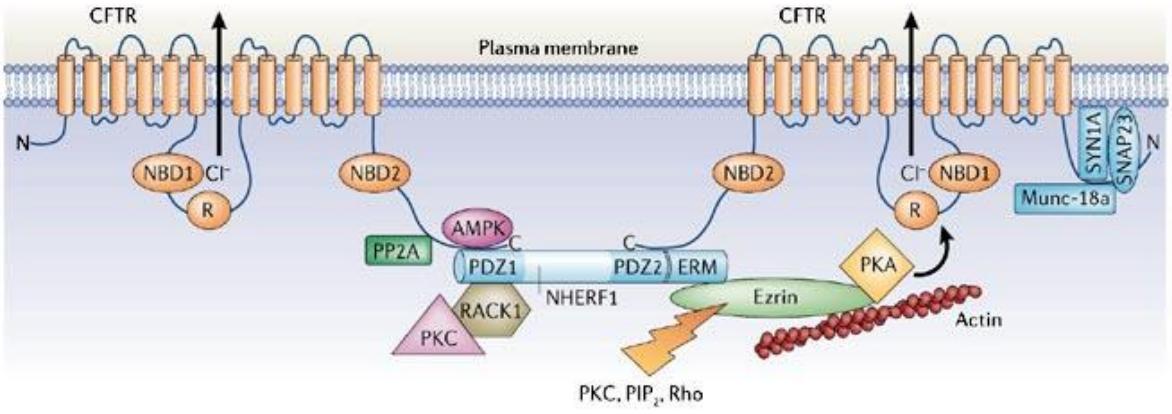

Figure 1.05. Protein interactions of CFTR at the plasma membrane. CFTR is contained in a complex with proteins that regulate CFTR activity. Furthermore, the complex tethers CFTR to the apical plasma membrane through interaction with actin. Taken from (Guggino and Stanton, 2006).

Mature CFTR has a half-life of between 24 - 48 hours at the plasma membrane with the activity of CFTR at the plasma membrane being dependent on both the number of channels present at the plasma membrane and the conductivity of the channels (Heda et al., 2001, Swiatecka-Urban et al., 2002). This can be summarised by the equation; $I=iNP_o$ where I represents the macroscopic current, i the unitary

conductance of the channel, *N* the number of channels at the plasma membrane and P_o represents the open probability of the channel. Thus, factors that affect trafficking usually affect *N* and so have consequent effects on conductance (Ameen et al., 2007).

Regulation of CFTR density at the cell membrane is dependent upon endocytic pathways. Removal of CFTR from the membrane is thought to be dependent upon clathrin mediated pathways and has been shown to be a rapid process, with a capability of removing up to 10% of total CFTR per minute (Prince et al., 1994). This rapid internalisation of CFTR occurs due to the presence of tyrosine-based and dileucine-based internalisation motifs within the C terminus of CFTR. The tyrosine-based motif consists of either a NPXY signal where X is a variable amino acid or the more common YXXΦ signal where Φ represents a large hydrophobic amino acid (Goldstein et al., 1979, Ameen et al., 2007). The dileucine-based motif consists of D/EXXXLL/I or DXXLL and is important in regulating protein trafficking to endosomes/lysosomes (von Essen et al., 2002, Ameen et al., 2007).

Clathrin-mediated endocytosis of CFTR is facilitated by the C terminus of CFTR binding to the μ2 subunit of an endocytic adaptor complex known as AP-2 (Weixel and Bradbury, 2001). Once endocytosed, approximately 50% of CFTR may be recycled back to the cell membrane (Picciano et al., 2003). Therefore, CFTR also undergoes trafficking between intracellular organelles and the plasma membrane. The Ras associated binding (Rab) GTPase, Rab5 has been shown to modulate trafficking of CFTR from the plasma membrane to early endosomes whilst Rab7 facilitates movement from endosomes to lysosomes. Rab11 has been shown to modulate trafficking of CFTR from endosomes to the TGN and plays a role, via recycling endosomes, in trafficking CFTR back to plasma membrane (Gentzsch et al., 2004, Ameen et al., 2007, Farinha et al., 2013). Further, the recycling of CFTR back to the plasma membrane is facilitated by Rme-1 which regulates the movement of CFTR from the endosome recycling compartment to the plasma membrane (Picciano et al., 2003). Thus, the recycling of CFTR back to the plasma membrane allows cells to maintain a relatively high proportion of CFTR ready for transport to the membrane, if required (Fig. 1.06).

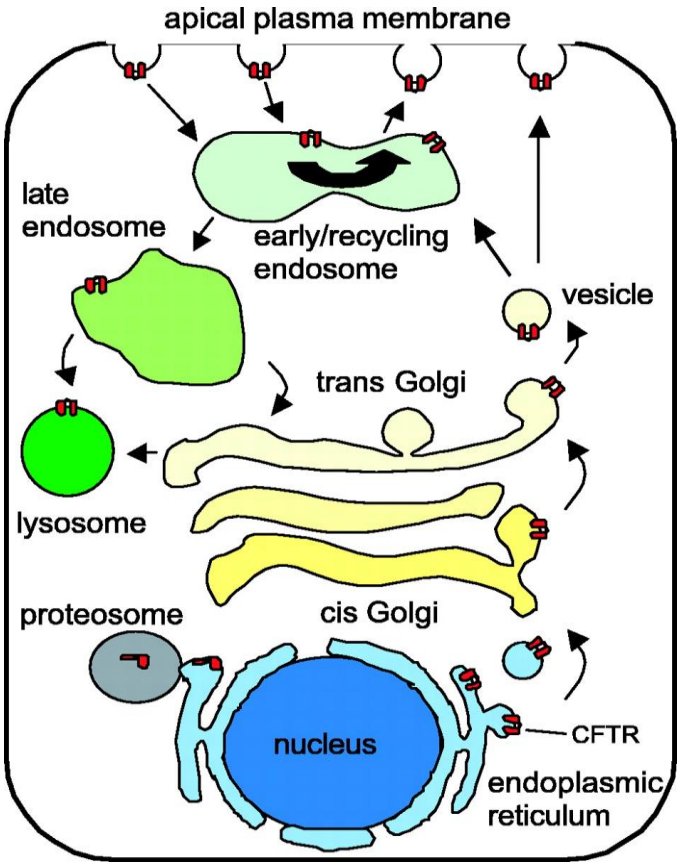

Figure 1.06. Trafficking of CFTR. CFTR is synthesised in ribosomes and then transferred to the ER. Following transport to the ER, CFTR is transported to the *trans* Golgi network and then onto the plasma membrane. Following this, CFTR is transported to endosomes through internalisation signals present on CFTR. CFTR can be cycled back to the cell membrane from endosomes or to lysosomes for degradation. Misfolded CFTR can also be targeted to the proteasome for degradation. Taken from (Bertrand and Frizzell, 2003).

1.4.3 Regulation of CFTR channel activity by phosphorylation

The activity of CFTR is controlled by phosphorylation at multiple sites on the R domain of the channel. Particularly, the balance between the phosphorylation by kinases and phosphatases that remove phosphoryl groups determine the amount of Cl^- secretion through CFTR. Phosphorylation at various sites on the R domain can be either stimulatory or inhibitory; however, phosphorylation at multiple sites is required for full activation of CFTR. Furthermore, phosphorylation at one site can influence the phosphorylation of other sites on the R domain (Chappe et al., 2004, Hegedűs et al., 2009).

The key kinase linked to the activation of CFTR is PKA, identified through the large number of PKA consensus sites on the R domain of CFTR (Anderson et al., 1991).

Accordingly, there are up to 19 sites on the R domain which have been predicted to be phosphorylation sites for PKA (Picciotto et al., 1992, Gadsby and Nairn, 1999). Phosphorylation of CFTR by PKA results in the R domain binding to other domains of CFTR to allow channel activation (Chappe et al., 2005). Consequently, there is an increase in the open probability of the channel. In addition to phosphorylation at the R domain, it has also been suggested that PKA may phosphorylate sites near NBD1, as identified in NBD1-R domain peptides. Indeed, mutation of these sites when phosphorylation sites on the R domain are also mutated has been found to cause further loss of channel activity (Townsend et al., 1996, Neville et al., 1997, Neville et al., 1998). Conversely, mutation of phosphorylation sites in the R domain only does not abolish all CFTR channel activity, adding further evidence for the functional significance of sites outside the R domain (Seibert et al., 1995).

Consensus sites for PKC have also been identified, with 6 sites on the R domain being suggested as targets for PKC phosphorylation (Chappe et al., 2004). However, this kinase causes a smaller activation of CFTR in comparison to PKA. Instead, phosphorylation of CFTR by PKC has been found to facilitate the activation of the channel by PKA by shifting the PKA concentration dependence of the channel (Jia et al., 1997, Chappe et al., 2003). Furthermore, phosphorylation of CFTR by PKC has been shown to be crucial for PKA induced configurational changes involving binding of the R domain to CFTR. It has been suggested that the configurational change in CFTR when stimulated with PKA and PKC in combination, causes CFTR to be more conductive (Seavilleklein et al., 2008). Interestingly, Picciotto and colleagues showed that exposure of a portion of the R domain to supraphysiological levels of Ca^{2+} caused an inhibition of PKC dependent phosphorylation of CFTR (Picciotto et al., 1992).

Further to phosphorylation by protein kinases, Fischer and colleagues showed that CFTR activation can occur through tyrosine phosphorylation, independent of the action of PKA. Through measuring changes in channel activity using inside out patches, the researchers identified the tyrosine kinases p60c-Src and proline-rich tyrosine kinase 2 (Pyk2) as kinases capable of activating CFTR. Moreover, the activation of CFTR induced by tyrosine kinases was comparable to that caused by PKA (Fischer and Machen, 1996, Billet et al., 2013). The kinase, CK2, has also been shown to play role in the activation of CFTR. CK2 binds to CFTR at the apical

membrane and phosphorylates the channel, thus increasing Cl^- secretion (Treharne et al., 2009). Furthermore, CK2 has also been linked to the processing and trafficking of CFTR, with CK2 inhibition resulting in the production of CFTR that is not stable at the plasma membrane (Luz et al., 2011). Finally, 5' adenosine monophosphate-activated protein kinase (AMPK) has been linked to the phosphorylation of CFTR. However, unlike the other protein kinases previously discussed, phosphorylation by AMPK has been linked to inactivation of CFTR. AMPK directly binds to CFTR and inactivates the channel, possibly through preventing the phosphorylation of CFTR by PKA and PKC (Hallows et al., 2000, Kongsuphol et al., 2009).

As the activity of CFTR is controlled by the phosphorylation of the channel, it follows that there are a variety of phosphatases linked to the regulation of CFTR activity. Phosphatases that have been linked to CFTR function predominantly include protein phosphatase 2 (PP2). Specifically, the isoforms PP2A, PP2B and PP2C have been linked to an inhibition of CFTR activity. *In vitro,* PP2A and PP2C are known to have relevant roles in the regulation of CFTR activity (Berger et al., 1993, Luo et al., 1998). CFTR has been shown to act as a substrate for PP2A, with the C terminus of CFTR being physically linked to the catalytic and regulatory subunits of PP2A. Furthermore, PP2A activity has been shown to have functionally important consequences for basal CFTR activity, as inhibition of PP2A can prevent the rundown of CFTR channel activity when measured in outside-out membrane patches. This response was physiologically related to an increase in ASL height (Thelin et al., 2005). Alongside controlling basal CFTR activity, PP2A is capable of causing an inhibition of activated CFTR (Luo et al., 1998). PP2C requires the presence of Mg^{2+} to be active. Studies have indicated that addition of PP2C is able to cause an inhibition of CFTR activity faster than PP2A. Furthermore, under basal conditions, PP2C and CFTR are tethered together, possibly to enable deactivation of the channel following cAMP stimulation (Dahan et al., 2001). PP2A and PP2C show different patterns of effects on CFTR gating after inhibition suggesting they act on different sites on CFTR (Luo et al., 1998). Importantly, neither PP2A nor PP2C causes a complete inhibition of CFTR activity alone, suggesting that multiple phosphatases are required to fully deactivate CFTR (Luo et al., 1998).

PP2B or calcineurin, which requires the presence of Ca^{2+} and calmodulin for activity, has also been implicated in the regulation of CFTR activity. Using the specific

inhibitors, cyclosporin A and deltamethrin, Fischer and colleagues showed that calcineurin caused an inhibition of either PKA or PKC stimulated CFTR activity. However, there has been some uncertainty regarding the role of PP2B, with the regulation of CFTR by PP2B appearing to be cell type dependent (Fischer et al., 1998). Lastly, alkaline phosphatase has also been implicated in the regulation of CFTR activity. Using the inhibitor, bromotetramisole, in intact cells and membrane patches, Becq and colleagues (1994) found that inhibition of alkaline phosphatase stimulated CFTR activity. Furthermore, inhibition of alkaline phosphatase also increased channel activity of CFTR channels with a cystic fibrosis causing (G551D) mutation (detailed in next section (Becq et al., 1994).

The major kinases and phosphatases involved in the regulation of CFTR exist in a macromolecular complex. The kinases and phosphatases contained within this complex include PKA, PKC, AMPK, PP2A and PP2C. Although calcineurin has not been shown to be contained within this complex, AKAP79, which binds to calcineurin, has been found to be tethered to CFTR. As discussed in section 1.4.2, CFTR is also tethered to a complex including EBP50, CAP70 and CAL (Bozoky et al., 2013). The arrangement of proteins in this complex highlights the tight regulation of CFTR activity.

1.5 Diseases in the airway due to defective CFTR

1.5.1 Cystic Fibrosis

Cystic fibrosis (CF) is an autosomal recessive disease, deemed an ‘orphan disease’ which affects approximately 80,000 people worldwide (Lubamba et al., 2012, Rab et al., 2013). Broadly, CF is a consequence of a loss of Cl^- permeability through CFTR. Clinically, the loss of CFTR causes a multi organ disease which adversely affects the lungs, gastrointestinal and reproductive tracts. Critically, deterioration of lung function is the major determinant of morbidity (Davis, 2006).

To date, >2000 mutations in CFTR have been associated with development of cystic fibrosis, however, only approximately 10% of these mutations have been directly associated as causative in CF (www.genet.sickkids.on.ca/cftr, https://www.cftr2.org/). The mutations in CFTR have effects ranging from the production of protein with defects in gating, conductance, or reduced expression at the plasma membrane. However, around 90% of patients harbour the same mutation, the deletion of

phenylalanine 508 (F508) located in NBD1 (Davis, 2006). This mutation results in a loss of CFTR at the plasma membrane due a temperature sensitive processing defect where the protein is retained in the ER (Dalemans and Barbry, 1991, Amarai et al., 1992, Okiyoneda et al., 2004). Consequently, only ~1% of translated protein reaches the apical membrane. However, Swiatecka-Urban et al., (2005) showed that this protein also had a reduced half-life of ~4 hours at the plasma membrane and a defect in channel gating with the channels spending an increased proportion of time in the closed state when compared to wild type CFTR (Lukacs et al., 1993, Heda et al., 2001, Swiatecka-Urban et al., 2005).

Within the airways, the loss of CFTR from the plasma membrane causes a loss of Cl^- secretion and an increase in Na^+ absorption due to the activity of ENaC no longer being negatively regulated by CFTR. CaCC is functional in CF patients and provides a route for Cl^- efflux; however, this can be compromised by infection (Chambers et al., 2007). This altered ion channel activity leads to reduced Cl^- secretion and increased Na^+ absorption which causes dehydration of the airways and a reduction in the volume of the PCL (Davis, 2006). The net effect of reduced ASL volume is that patients suffer from mucus accumulation (Tarran et al., 2006a).

As the F508 deletion represents the most predominant CF causing mutation, treatment strategies have focused on alleviating this protein defect. Currently available CFTR modulators are potentiators, such as ivacaftor, which increase CFTR channel activity at the plasma membrane and correctors, such as lumacaftor, which targets the defect in CFTR processing by enabling movement of the protein to the plasma membrane (Clancy et al., 2012, Rowe and Verkman, 2013).

1.5.2 Chronic Obstructive Pulmonary Disease

Chronic obstructive pulmonary disease (COPD), the third leading cause of death worldwide, is characterised by airflow obstruction and is primarily caused by smoking (World Health Organisation, 2014). The disease can also be brought about by environmental exposure to heavy metals and toxic fumes. A small proportion of patients develop COPD due to mutation of α1 antitrypsin (Gerald and Bailey, 2002). Clinically, COPD is a manifestation of either emphysema, chronic bronchitis (CB), or a combination of both. Chronic bronchitis is clinically defined as a chronic cough that

persists for two months or more and the progression of CB causes a loss of lung function similar to that in CF (Boucher, 2004).

COPD usually leads to lung inflammation that continues even after smoking cessation. Disease progression leads to obstruction of the small airways due to mucus production and accumulation. Furthermore, the chronic inflammatory environment results in structural changes in airway epithelia with an increase in smooth muscle and fibrosis resulting in thickening of the basement membrane and lamina reticularis just beneath the basement membrane of airway walls (Yoshida and Tuder, 2007, Tuder and Petrache, 2012). Along with smoking cessation and mucolytics, treatment strategies for COPD involve the use of corticosteroids to reduce inflammation and β adrenergic receptor agonists to increase ciliary beat frequency and mucus hydration (Kim and Criner, 2013).

The similar clinical symptoms between patients with COPD and CF, suggest there may be a common mechanism for the initiation of both diseases (Boucher, 2004). Accordingly, sufferers of both COPD and CF show impaired mucus clearance from the airways due to the production of thick, viscous mucus, brought about by defective ion homeostasis in the airways. The common spectrum of clinical manifestations of the two diseases led to the initial speculation that both diseases could be due to dysfunction of CFTR. Indeed, research has found that CFTR function is reduced in COPD (Dransfield et al., 2013). Furthermore, although chronic bronchitis has been highlighted as being clinically similar to CF, Bodas et al., (2011) linked the loss of CFTR to the progression of emphysema (Bodas et al., 2011). The similarities between COPD and CF also extend to the bacterial infections seen with *Staphylococcus aureus* and *Pseudomonas aeruginosa* common in both CF and COPD patients (Kahl et al., 1998, Soler et al., 1998, Murphy et al., 2008). Furthermore, the treatment regimens used for CF patients have applications for COPD patients. For example, ivacaftor is effective in treating the CFTR defect caused by smoke exposure (Raju et al., 2017).

1.6 The effect of cigarette smoke on CFTR

In recent years, several groups have proposed that cigarette smoke (CS) affects CFTR with the observation that smoke exposure negatively regulates CFTR in multiple ways. CS exposure has been shown to reduce CFTR at the mRNA level,

along with the amount of protein expressed at the membrane in Calu-3 cells (Cantin et al., 2006). Furthermore, Kreindler and colleagues showed the ionic fluxes were altered in cells exposed to cigarette smoke extract. Using human bronchial epithelial cells as a model, the researchers showed that transepithelial Cl^- transport was decreased via a reduction in both Cl^- secretion and Cl^- uptake via NKCC1. The effect of this was an increased net Na^+ absorption, as with CF cells (Kreindler et al., 2005).

The link between cigarette smoke exposure and CFTR dysfunction has not only been found in airway epithelia, but also in sweat ducts, pancreatic and intestinal epithelia. A study by Raju et al., 2013 looked at the effect of CS on extrapulmonary organs isolated from smokers and non-smokers, the researchers found that CFTR in multiple organs including the intestine was dysfunctional. Moreover, the researchers showed acrolein, which is a toxic component of CS, was likely the cause of extrapulmonary CFTR dysfunction (Jia et al., 2007, Raju et al., 2013). Indeed, many papers have speculated that smoking causes a systemic defect in CFTR function, creating a pseudo-CF phenotype (Cantin et al., 2006, Raju et al., 2013).

Recently, work from our lab has shown that exposure to the volatile phase of cigarette smoke causes an increase in cytosolic Ca^{2+} (Rasmussen et al., 2014). Further to the increase in Ca^{2+}, cigarette smoke exposure caused activation of the MEK/ERK pathway (Xu et al., 2015). Both cellular effects of smoke were linked to a decrease in plasma membrane expression of CFTR and the internalisation of CFTR into insoluble aggregates. Interestingly, the effect of smoke was specific to CFTR. Na^+ transport was unaffected by CS, as evidenced by the expression of the α subunit of ENaC being unchanged after CS exposure. Cl^- secretion through CaCC was also unaffected by CS as agonists such as ATP were still able to induce Cl^- efflux after CS exposure (Clunes et al., 2012).

It has been previously suggested that although cigarette smoke is composed of thousands of constituents, the toxic effects of smoke are a consequence of a few chemicals. Cadmium and acrolein have been used to mimic the effect of smoke exposure and linked to a reduction in CFTR activity (Raju et al., 2013, Rennolds et al., 2010). Indeed, specific components of smoke underlying the increase in cytosolic Ca^{2+} were identified by Sassano et al., (2017) who showed that nicotine and

formaldehyde were amongst the constituents linked to substantial increases in cytosolic Ca^{2+} (Sassano et al., 2017).

Although CS has been shown to have numerous effects on cells, an important caveat to consider is that many of the studies cited above use differing methods of exposing cells to CS. Furthermore, cigarette smoke exposure protocols vary between laboratories, with each lab having their own method of exposure. CS is composed of a volatile phase, which comprises approximately 95% of CS and a particulate phase composed of lipid and water-soluble particulates, which constitutes 5% of CS. Typically used formulations include cigarette smoke condensate (CSC), which is prepared by passing whole cigarette smoke (WCS) through a filter pad and then sonicating the filter pad in DMSO to collect the lipid soluble phase. Alternatively, groups have also used cigarette smoke extract (CSE) which is prepared by passing WCS through a buffer solution to collect the aqueous phase of CS. Other labs have exposed cells to specific components of CS such as nicotine, acrolein, cadmium or reactive oxygen species. Finally, studies have also puffed the volatile or gaseous phase of cigarette smoke over cells directly, with the particulate phase typically excluded from exposure due to the highly fluorescent nature of this phase. Importantly, Clunes et al., (2008) showed that this method of smoke exposure most closely resembles *in vivo* smoke exposure. By comparing nicotine concentrations in the airway surface liquid from smoke exposed cells to concentrations found in sputum from smokers, Clunes et al., (2008) found WCS was more effective than CSE at replicating *in vivo* smoke exposure (Clunes et al., 2008).

1.7 Calcium signalling

Ca^{2+} is a ubiquitous second messenger, able to control many cellular processes within a cell. The sensitivity of cells to Ca^{2+} is achieved by the high concentration gradient between cytosolic Ca^{2+} and either intracellular organelles or the extracellular space. The relatively low cytosolic Ca^{2+} is achieved by the action of Ca^{2+} influx and efflux pumps and transporters. At the plasma membrane, the plasma membrane Ca^{2+} ATPase and the Na^{+}/Ca^{2+} exchanger act to extrude Ca^{2+} from the cell and maintain a low resting Ca^{2+} in the range of ~100 nM. Alongside pumps expressed at the plasma membrane, the sarcoendoplasmic reticulum Ca^{2+} ATPase (SERCA) restores cytoplasmic Ca^{2+} by transporting Ca^{2+} to the ER stores (Brini and Carafoli, 2009).

Mitochondria can also take up cytosolic Ca^{2+} via the mitochondrial uniporter which couple Ca^{2+} uptake to the mitochondrial membrane potential (Berridge et al., 2000, Berridge et al., 2003). Finally, lysosomal Ca^{2+} channels also play a role in cytosolic Ca^{2+} uptake by coupling the uptake of Ca^{2+} to H^+ transport (Galione and Churchill, 2002).

Cellular cytoplasmic Ca^{2+} signals are encoded by not only the duration of Ca^{2+} signal but also the frequency and amplitude of the signal. Thus, a large variety of responses can be elicited after a change in cytosolic Ca^{2+} due to effectors that respond to distinct spatiotemporal signals. Furthermore, Ca^{2+} binding proteins and buffers can help to fine tune changes in cytosolic Ca^{2+}. The buffers have different properties, with the fast buffers, calretinin and calbindin, having a low affinity for Ca^{2+} and the slow buffer, parvalbumin, having a higher affinity for Ca^{2+} (Bootman et al., 2001, Berridge et al., 2003).

The ER represents a large cellular store of Ca^{2+} and for the most part, Ca^{2+} release from intracellular stores is derived from the ER. As the ER spans the entire cell, release of Ca^{2+} from this store can create global increases in cytosolic Ca^{2+}. Release of Ca^{2+} from the ER is usually triggered by Ca^{2+} itself or by second messengers including inositol-1,4,5-trisphosphate (IP_3), cyclic ADP ribose, nicotinic acid adenine dinucleotide triphosphate and sphingosine-1-phosphate. The process of Ca^{2+} induced Ca^{2+} release can help create a large increase in cytosolic Ca^{2+} over a short timeframe and the generation of repetitive Ca^{2+} waves (Berridge et al., 2003). Furthermore, depletion of the ER stores can activate store operated Ca^{2+} entry, the molecular components of which are composed of the ER Ca^{2+} sensor, STIM1 and the plasma membrane channel, Orai1 (Clapham, 2007).

Mitochondria can also act as sources for Ca^{2+}. Mitochondria take up Ca^{2+} via a uniporter which is controlled by the mitochondrial membrane potential and can modulate Ca^{2+} uptake and release in response to local changes in Ca^{2+}. Furthermore, mitochondria can release Ca^{2+} through a Na^+ dependent exchanger (Bootman et al., 2001, Rizzuto et al., 2012). Mitochondria have also been shown to act as Ca^{2+} buffers for Ca^{2+} released from the ER (Bakowski et al., 2012). Importantly, within airway epithelial cells, mitochondria have been shown to act as Ca^{2+} buffers, limiting the release of Ca^{2+} to either the apical or basolateral poles of

the cell (Ribeiro et al., 2003). Indeed, Rasmussen et al., (2014) also speculated that the mitochondria buffered some of the Ca^{2+} released after smoke exposure (Rasmussen et al., 2014). However, it has been suggested mitochondria do not buffer modest cytosolic elevations in Ca^{2+}, and so may not respond to physiological changes in Ca^{2+} (Ribeiro et al., 2003).

Research from our lab associated Ca^{2+} release from lysosomal stores as being responsible for the smoke-induced rise in cytosolic Ca^{2+}. Ca^{2+} uptake into lysosomes is proton dependent and has been suggested to facilitate the endocytic pathway (Galione and Churchill, 2002). Ca^{2+} entry into lysosomes is thought to occur through secondary active transport due to proton transport into lysosomes, however the transporter responsible is unknown (Jha et al., 2014). It has also been suggested that Ca^{2+} uptake can occur from the extracellular space, but the contribution of Ca^{2+} uptake through this method is unclear (Christensen et al., 2002, Xiong and Zhu, 2016). Lysosomal Ca^{2+} release has been shown to be sensitive to NAADP and occur through two-pore channels (TPC) although there is conflicting evidence as to whether TPC channels transport Ca^{2+} (Wang et al., 2012). Furthermore, it has been suggested that Ca^{2+} release from lysosomes can be increased by release from ER stores and Ca^{2+} induced Ca^{2+} release (Calcraft et al., 2009, Morgan et al., 2011). It has also been suggested that members of the transient receptor potential (TRP) family of channels, in particular TRPML1, may mediate Ca^{2+} release from lysosomes as these channels have been shown to be NAADP sensitive, although with a much lower affinity than TPC channels (Zhu et al., 2010). Finally, $P2X_4$ channels have been shown to cause pH dependent Ca^{2+} release such that the channels are active at neutral pH (Huang et al., 2014, Cao et al., 2015).

1.7.1 Ca^{2+} signalling in airway epithelia

Ca^{2+} plays an important role in influencing mucociliary clearance in airway epithelia. Airway epithelial Ca^{2+} release is elicited by activation of apical or basolateral G protein-coupled receptors. The receptors are linked to phospholipase C (PLC), which release Ca^{2+} from the ER store through the generation of IP_3. Alternatively, nucleotides released into the airways are coupled to purinoceptors ($P2Y_2$) which also cause Ca^{2+} release from ER stores via PLC (Antigny et al., 2011). Additionally, acetylcholine released from parasympathetic nerve endings at the basolateral membrane can also stimulate Ca^{2+} release by binding to M3 muscarinic acetylcholine

receptors that are coupled to PLC activation (Eichstaedt et al., 2008, Billet et al., 2013, Widdicombe and Wine, 2015).

Within airway epithelia, changes in Ca^{2+} help regulate a multitude of processes. As discussed earlier, changes in cytosolic Ca^{2+} can affect Cl^- secretion through CaCC and therefore have secondary effects on ASL height (Tarran et al., 2001b, Tarran, 2004, Schroeder et al., 2008, Yang et al., 2008). In addition to influencing ion channel activity, ciliary beat frequency (CBF) is also regulated by changes in cytosolic Ca^{2+}. The basal level of CBF is regulated by changes in Ca^{2+}. Furthermore, ciliary beat frequency also increases in response to specific oscillatory Ca^{2+} changes in cytosolic Ca^{2+} (Di Benedetto et al., 1991, Evans and Sanderson, 1999). In accordance with Ca^{2+} regulating ciliary beat frequency, smoke has been shown to cause a reduction in CBF (Dalhamn, 1959). This is particularly important as efficient ciliary beating is needed to maintain MCC (Stanley et al., 1986). Interestingly, the reduction in CBF due to smoke exposure has been linked to changes induced by smoke independent of Ca^{2+}. Ciliary beating can also be stimulated by increases in cAMP linked to PKA; conversely activation of PKC causes an inhibition of ciliary beating. CS has been shown to activate PKC and consequently decrease ciliary beat frequency and the number of ciliated cells (Simet et al., 2010).

The secretion of mucins is a Ca^{2+} dependent process with the exocytosis of mucin granules requiring an increase in cytosolic Ca^{2+} (Davis and Dickey, 2008). Importantly, Ca^{2+} regulates mucin secretion at multiple stages with the movement of secretory granules towards the plasma membrane, the priming of secretory granules so they are fusion competent, and the fusion of granules with the plasma membrane all being dependent on Ca^{2+} (Klenchin and Martin, 2000, Rossi et al., 2007). Likewise, the secretion of mucin is increased when airway goblet cells are exposed to Ca^{2+} ionophores or conversely, inhibited when Ca^{2+} is chelated (Abdullah et al., 1997, Conway et al., 2003). The importance of Ca^{2+} in mucin secretion has also been underscored with the finding that regulation of secretion by PKC, previously thought to be a Ca^{2+} independent process, is also reliant on Ca^{2+} (Rossi et al., 2004).

1.8 Aims

Recent work from our lab and others, has found that cigarette smoke negatively affects CFTR (Kreindler et al., 2005, Cantin et al., 2006, Clunes et al., 2008). However, our lab was the first to show cigarette smoke induced CFTR internalisation and that a smoke-induced increase in cytosolic Ca^{2+} was essential for CFTR internalisation (Clunes et al., 2012, Rasmussen et al., 2014). These data, along with research from other groups, leads me to hypothesise that increases in cytosolic Ca^{2+} can modulate the presence of CFTR at the plasma membrane, specifically, by causing a reduction in the channels present at the plasma membrane (Bargon et al., 1992, Bozoky et al., 2017). However, the direct effect of an increase in cytosolic Ca^{2+} on CFTR function and expression has not yet been investigated. Thus, a better understanding of this process would be of value in determining how changes in Ca^{2+} affect CFTR activity and expression. As an increase in cytosolic Ca^{2+} is crucial for the effect of smoke on CFTR, these data would directly help understand the deleterious effects of CS on epithelial function. Moreover, the data could have consequences for the development of new therapeutics for COPD.

Therefore, the specific aims of my project were to;

- Determine if an increase in cytosolic Ca^{2+} affects whole cell CFTR-mediated conductance
- Characterise if a change in cytosolic Ca^{2+} was temporally related to a change in CFTR-mediated conductance
- Compare the effects of an increase in cytosolic Ca^{2+}, induced by pharmacological agents, on CFTR to that caused by cigarette smoke
- Identify the molecular mechanism by which an increase in cytosolic Ca^{2+} affects CFTR function and validate these findings in primary human bronchial epithelial cells

Chapter 2.0 Methods

2.1 Reagents

All reagents were purchased from Sigma-Aldrich, except for ionomycin and $CFTR_{inh}$-172 (Calbiochem), Fura-2 acetoxymethyl ester (AM; Invitrogen), forskolin, cyclosporin A and H89 (Tocris). Drugs used are listed in table 1; stock solutions of each drug were made up in dimethyl sulfoxide (DMSO). Culture media was purchased from either Sigma-Aldrich or Gibco. All culture flasks and plates were purchased from Corning. The pIRES2-EGFP-CFTR vector was a gift from Dr Linsdell of Dalhousie University; STIM1 mCherry was a gift from Dr Dolmetsch of Stanford University. Antibodies were purchased from Cell Signalling Technology apart from the calreticulin antibody (Abcam). The cell lines, HEK 293T, A6, SL-29 and VSW were purchased from ATCC; Sf9 cells were kindly donated by Dr Hammond at the University of North Carolina, Chapel Hill.

Reagent	Stock concentration	Working concentration
Forskolin	100 mM	5 µM
$CFTR_{inh}$-172	50 mM	10 µM
Thapsigargin	2 mM	200 nM
Ionomycin	5 mM	1 µM
GPN	500 mM	100 µM
Dynasore	100 mM	80 µM
H89	5 mM	500 nM
Staurosporine	1 mM	100 nM
Cyclosporin A	100 mM	1 µM
Okadaic Acid	1 mM	10 nM
U0126	10 mM	10 µM
PD98059	10 mM	10 µM
BAPTA-AM	20 mM	50 µM
Fura-2 AM	1mM	5 µM

Table 1.01. List of reagents and the concentrations they were used at.

2.2 Cell culture

Tissue culture was carried out in class II laminar flow hoods. All media and supplements were filtered through a 0.2 µm filter unit before use. Media was pre-warmed to 37ºC in a water bath and media and tissue culture equipment were sterilised before use. All cultures were maintained in 75 cm^2 flasks with 25 mls of growth media and were grown to ~90% confluence. To subculture cells, culture media was removed and cells were rinsed with phosphate buffered saline (PBS) twice. Cells were then incubated in 5 mls of a 0.05% trypsin and 0.02% ethylenediaminetetraacectic acid (EDTA) solution for 2-5 minutes at 37ºC to detach cells from the culture flasks. Following detachment, trypsin was neutralised by the addition of 10 mls media and cells were centrifuged at 500 rpm for 5 minutes. The supernatant was discarded and the pellet was resuspended in 10 mls of fresh media. The cell density was then calculated using a haemocytometer (Fisher Scientific) and cells were reseeded to maintain cultures.

Human embryonic kidney (HEK) 293T cells for patch clamp experiments were cultured in Dulbecco's Modified Eagle's Medium (DMEM) supplemented with 2 mM L-glutamine, 1% non-essential amino acids, 10% foetal bovine serum (FBS), 100 Uml^{-1} penicillin and 100 μgml^{-1} streptomycin. Cells were subcultured every 7 days and used between passages 10-50. HEK 293T cells used for imaging experiments were cultured in DMEM supplemented with 10% FBS, 100 Uml^{-1} penicillin and 100 μgml^{-1} streptomycin. Cells were subcultured every 2-5 days and used between passages 5-40. All cells were grown at 37ºC in a humidified 5% CO_2 atmosphere.

Xenopus laevis kidney cells, A6, were grown in NCTC 109 medium supplemented with 15% distilled water, 10% FBS, 100 Uml^{-1} penicillin and 100 μgml^{-1} streptomycin. Cells were grown at 26ºC in a 5% CO_2 atmosphere and subcultured approximately every 10 days. Cells were used up to passage 10.

Chicken embryonic fibroblast cells, SL-29, were grown in DMEM supplemented with 5% tryptose phosphate broth, 5% FBS, 100 Uml^{-1} penicillin and 100 μgml^{-1} streptomycin. Cells were grown to confluence at 37ºC in a 5% CO_2 atmosphere and subcultured approximately every 10 days. Cells were used up to passage 7.

Splenic Russell's viper cells, VSW, were grown in Eagle's minimum essential medium supplemented with 10% FBS, 100 Uml^{-1} penicillin and 100 μgml^{-1} streptomycin. Cells were grown at 30^{o}C in a 5% CO_2 atmosphere and subcultured approximately every 7 days. Cells were used up to passage 5.

Ovarian fall armyworm cells, Sf9, were cultured in Grace's Insect medium supplemented with 10% FBS, 100 Uml^{-1} penicillin and 100 μgml^{-1} streptomycin. Cells were grown at 27^{o}C in atmospheric air and subcultured every 7 days. Cells were subcultured by removing spent growth medium from the cultures and adding 10 mls of fresh media. Cells were subsequently agitated until they detached. Cells were then centrifuged and reseeded.

Primary human bronchial epithelial cells (HBECs) were obtained by the University of North Carolina's Cystic Fibrosis Center Tissue Core in a procedure approved by the University of North Carolina Institutional Committee for the Protection of the Rights of Human Subjects. Epithelial cells were isolated from the cartilaginous bronchi of excess donor lungs. Cells were plated at a density of 2.5 x 10^4 onto 12 mm polyester clear transwell supports with a 0.4 µM pore size (Costar, USA). Transwells were coated with human type IV placental collagen and ultraviolet (UV) sterilised before use. Cells were grown using a base media of DMEM-H: LHC (50:50) with additives as detailed previously (Fulcher et al., 2005, Hill and Button, 2012, Fulcher and Randell, 2013). Cells were grown at a liquid-liquid interface until the cells formed a monolayer (usually 7 days' post seeding); after which cells were grown under air-liquid interface conditions. Only primary cells were used for experiments. Basolateral media was replenished three times a week and cells were washed with PBS once a week. Cultures were maintained at 37^{o}C in a 5% CO_2 humidified atmosphere and studied after fully differentiated (approximately 3-5 weeks).

2.3 Transfection

HEK 293T cells were transiently transfected with the bicistronic pIRES2-EGFP-CFTR vector (https://www.addgene.org/vector-database/3178/) to co-express wild type CFTR and enhanced green fluorescent protein (GFP) for patch clamp experiments (Gong et al., 2002). Cells were transfected one day post seeding. Briefly, DNA was pre-complexed with Lipofectamine 2000 (Invitrogen) and Opti-MEM with GlutaMAX (Invitrogen) for 15 minutes at room temperature. DNA was then diluted in culture

media to 1 μgml^{-1} and added to cells. Following 6 hours incubation at 37^{o}C, cells were left to incubate overnight in Opti-MEM with 10% FBS after which cells were transferred back to culture media. Cells were studied 48-72 hrs post transfection at ~50% confluency.

For imaging experiments, cells were transfected with wild type CFTR with a GFP tag on the N terminus of channel and STIM1 with a mCherry tag on the C terminus of STIM1 (Park et al., 2009). Cells plated on coverslips were transfected with 1 μg of CFTR and 0.5 μg of STIM1 one day post seeding. DNA and Lipofectamine 2000 (Invitrogen) were diluted in Opti-MEM and the mixtures were incubated for 5 minutes at room temperature. Following the incubation, the diluted DNA was mixed with the diluted Lipofectamine 2000 and incubated for 15 minutes at room temperature. The cells were transferred to growth media without antibiotics and the transfection mix was added dropwise. Cells were incubated for 4 hours at 37^{o}C after which the transfection mix was aspirated and the cells were transferred back to culture media. Cells were used 48 hrs post transfection.

2.4 Cigarette smoke exposure

Reference cigarettes (3R4F) from the University of Kentucky (Lexington, Kentucky) were used to produce cigarette smoke. These cigarettes are produced for research purposes only and are manufactured with known amounts of constituents that resemble commercial cigarettes, allowing for reproducibility between experiments (Chepiga et al., 2000). The blend specifications for the 3R4F cigarette are; flue-cured 35.41%, burley 21.62%, oriental 12.07%, maryland 1.35%, reconstituted (Schweitzer process) 29.55%, glycerine (dry weight basis at 11.6% oven volatiles) 2.67% and isosweet (sugar) 6.41%.

Whole cigarette smoke was generated using the LC1 Borgwaldt smoke engine (Borgwaldt, Hamburg, Germany). Cells were smoked according to the standards set by the International Organisation for Standardisation (ISO) to mimic *in vivo* smoke exposure (Clunes et al., 2008). Cells were exposed to 13 x 35 ml puffs of 2s duration every 30s, which was the equivalent of one research cigarette. The particulate fraction of smoke, which is highly fluorescent, was collected by placing a Cambridge filter pad in the output line. The filter pad collects 99.9% of the particulate fraction with a size greater than 0.1 μm (Clunes et al., 2008). Before exposure, cells were

rinsed twice in pyruvate Ringer's solution and left to incubate in Ringer's for 5 minutes at 37^{o}C. Following incubation, the excess Ringer's solution was tipped off, to represent the 'thin film' conditions in the airways (Tarran et al., 2006a). Cells were then exposed to smoke or room air in dedicated chambers for each. Following exposure, cells remained in the chambers for a further 5 minutes after which the Ringer's solution was removed and cells were put back into media and incubated for the times necessary.

Cigarette smoke condensate, which captures the particulate fraction of cigarette smoke, was prepared by puffing three full reference cigarettes, through a Cambridge filter pad. The filter pad was then cut in half and each half was sonicated in 1 ml DMSO for 15 minutes to collect the particulate fraction (Clunes et al., 2008). The concentration of particulate matter was calculated by weighing the filter pad before and after smoke exposure. On average, this method gave a yield of 16 mgml^{-1} of particulate matter; the condensate was stored at -20^{o}C until use.

2.5 Electrophysiology

HEK 293T cells were seeded at a density of 5 x 10^{5} per coverslip and used 2-3 days post transfection. Whole cell recordings, which allow for changes in current through the membrane of the whole cell to be measured, were carried out on single cells and all experiments were conducted at room temperature (Sakmann and Neher, 1984, Sheppard et al., 2004). Pipettes were pulled from borosilicate glass capillaries (GC120F; Harvard Apparatus, Kent) using the P-87 Sutter Flaming/Brown micropipette puller. All pipettes had resistances between 3-5 MΩ after fire-polishing. The pipette solution was filtered through a 0.2 µm filter before use.

Cells were viewed under phase-contrast microscopy and gigaohm seals were obtained by applying gentle suction once the pipette had touched the cell (Fig. 2.01). Further suction was then applied to disrupt the membrane and provide electrical access to the cell (Hamill et al., 1981). Experiments were carried out using an Axopatch 200B (Molecular Devices Inc) patch clamp amplifier and data was captured using pClamp10 software. The reference electrode was a silver/silver chloride wire connected to a 150 mM NaCl agar bridge. Cells were held at 0 mV and voltage steps were applied between ±100 mV in 20 mV increments. Each voltage step lasted 250 ms and there was a 1 s interval between subsequent steps. Data was filtered at 1

kHz and sampled at 2 kHz with a four pole Bessel filter. The average current obtained between a 100 ms period starting 80 ms into the voltage step was used to construct current-voltage (I-V) plots.

Liquid junction potentials, which arise from the charge generated due to the different mobility's of ions present in the pipette and bath solutions, were corrected for and applied to membrane potentials (V_m) (Neher, 1992, Wright et al., 2004). The Axopatch 200B amplifier was used to compensate for series resistance; 70% compensation was used for all whole cell recordings. The input capacitance of cells was measured before each experiment and compensated for; the mean capacitance of HEK 293T cells was 19.3 ± 0.9 pF (n=79). Slope conductance was calculated by fitting a linear regression to each I-V plot. Single cell slope conductance was divided by cell capacitance to normalise data to cell size and therefore this allowed a comparison between different experiments.

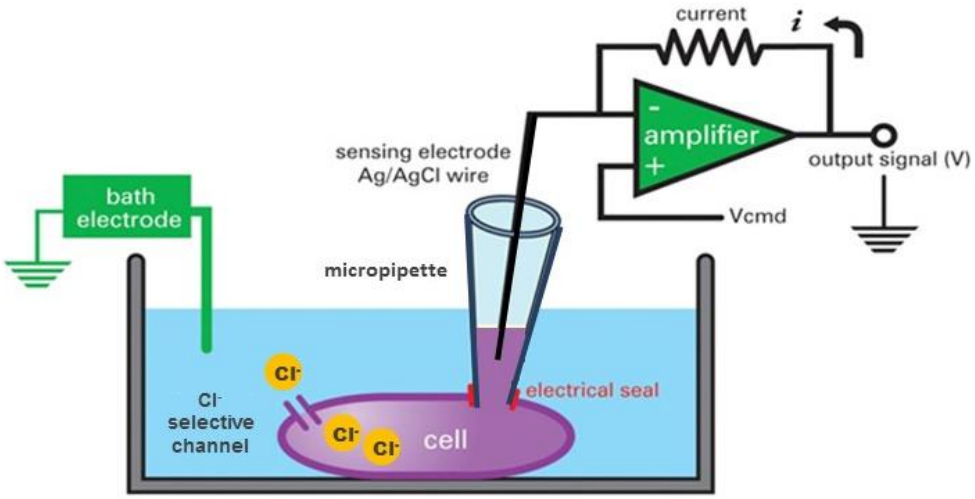

Figure 2.01. Set up for whole-cell patch clamp recording technique. A micropipette is attached to the cell and suction applied to form a high resistance seal between the cell and the micropipette. The seal allows for current through ion channels on the surface of the membrane to be detected with minimal background noise. Electrical contact to the solution was provided by silver electrode. The electrode measures current and the current measured is transferred to a high resistance amplifier. The voltage measured by the sensing electrode is compared to the reference 'bath electrode' which sets the zero current value. Image adapted from (Clare, 2010).

2.6 Measurement of intracellular Ca^{2+}

The Ca^{2+} sensitive dye, Fura-2 acetoxymethylester (AM; 5 µM) was used to measure changes in the concentration of intracellular Ca^{2+} ($[Ca^{2+}]_i$) (Grynkiewicz et al., 1985).

Experiments were conducted 2-4 days post seeding and all experiments were carried out at room temperature. To load cells with dye, culture media was removed and cells were rinsed with NaHEPES solution. Cells were then loaded with Fura-2 AM for 1 hour at 37^{o}C. Following incubation, cells were again rinsed in NaHEPES solution and left to de-esterify for 15 minutes at room temperature.

Experiments were carried out on an inverted epifluorescence microscope (Nikon, UK) and cells were viewed under an oil immersion lens (Nikon, Fluor 40, numerical aperture 1.3). The microscope was equipped with a 300W xenon lamp and computer controlled filter changer and shutter that contained 340 nm and 380 nm bandpass filters; emission at 510 nm was measured using a photomultiplier (PMT). Data was acquired every 250 ms and was captured using InCyt PM-2 software (Intracellular Imaging Inc).

For experiments in which cells were exposed to cigarette smoke or air within the experiment, cells were placed in chambers with entry and exit ports for smoke or air. Cells were manually exposed to either one reference cigarette or the equivalent of room air per ISO standard conditions. Single cells were selected as regions of interest and images were acquired every 30s with HCImageLive software (Hamamatsu). Experiments were carried out using an inverted microscope (Nikon, USA) and were viewed under an oil immersion lens (Nikon, Fluor 40, numerical aperture 1.3). The microscope was equipped with a 200 W metal halide lamp and shutter that contained 340 nm and 380 nm bandpass filters; emission at 510 nm was measured using an Orca CCD camera (Hamamatsu).

The excitation ratio of the 340 nm and 380 nm wavelengths was taken to be a read out of $[Ca^{2+}]_i$ (Grynkiewicz et al., 1985, Boese et al., 2000, Stewart et al., 2001). Counts were corrected for background fluorescence and cell autofluorescence. Data was analysed using ImageJ software (National Institutes of Health, Bethesda, Maryland, http://rsb.info.nih.gov/ij/); changes in $[Ca^{2+}]_i$ are expressed as maximum changes in the 340/380 ratio induced by each agent from the resting ratio. These values indicate the peak response seen minus the baseline value before the addition of the reagent. Area under the curve (AUC) was also chosen to indicate changes in Ca^{2+} as this gives an estimation of the magnitude of any changes as well as any

subsequent recovery. AUC was calculated for the duration the reagent was added to the cells.

2.7 Confocal microscopy

HEK 293T cells were seeded at a density of 7.5 x 10^4 per coverslip and transfected with the construct of interest as detailed earlier. Cells were treated 48 hrs post transfection and fixed with methanol after treatment. Briefly, cells were washed twice with PBS and incubated in ice-cold 100% methanol at -20^{o}C for 10 minutes. Cells were then rinsed again in PBS twice and stored in the dark at 4^{o}C until use. Nuclei were counter stained with 1 µgml^{-1} 4',6-Diamidino-2-Phenylindole dihydrochloride (DAPI) for 10 minutes on ice. Cells were then rinsed twice with PBS and imaged. All cells were imaged within 24 hrs of fixation.

Cells were imaged using the Leica TCS SP8 confocal laser scanning microscope. Images were captured using a 63x oil immersion lens (numerical aperture 1.4); with a bidirectional scan frequency of 700 Hz and a pinhole of 1 airy unit. DAPI, GFP and mCherry were excited with the 405 nm, 488 nm line of an argon laser and 561 nm laser, respectively. The hybrid detector (HyD) was used for excitation at 488 nm whilst the PMT lasers were used for all other wavelengths. Images were captured using a sequential scan to avoid possible overlap between the excitation and emission spectra of the various wavelengths. Images were captured using the Leica Application Suite: Advanced Fluorescence (LAS AF) software; 6-12 images were taken to obtain approximately 50 cells per coverslip. Images were taken on a 12-bit scale with a line average of between 3-5 and a frame accumulation of 2. Images were taken from two coverslips on at least three separate occasions.

Images were analysed offline using ImageJ by manually selecting 6 regions of interest from the membrane and 6 regions of interest from the intracellular space (Fig. 2.02). The average intensity of these regions was then determined for each cell. The average values of all the cells from either vehicle treated and air exposed cells were collected and were taken as one; all other treatments were normalised to the controls. All confocal images were arranged and enhanced (brightness enhanced ~40%) in Adobe Photoshop.

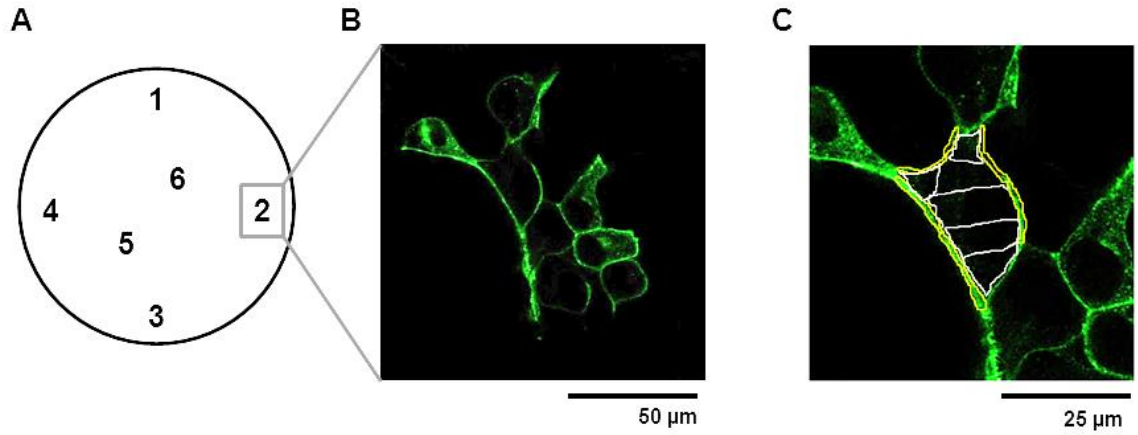

Figure 2.02. Image selection and analysis for confocal micrographs. (A) Diagrammatic representation of a coverslip and the points at which images were taken. **(B)** Example of an image taken at a point indicated in A. **(C)** Regions to measure the intensity of fluorescence at the membrane (indicated in yellow) and the intracellular space (indicated in white) were drawn using the 'freehand line selection' on ImageJ.

2.8 Airway surface liquid height measurements

HBECs were washed with PBS for 1 hr to remove excess mucus before all experiments. Cells were then loaded with 1 mgml^{-1} tetramethylrhodamine conjugated to 10 kDa dextran which has been shown to diffuse into the airway surface liquid (ASL) without crossing the epithelial barrier (Worthington and Tarran, 2011). Before imaging, the cultures were transferred to Ringer's solution and 100 µl perfluorocarbon (PFC, FC-770; Acros Organics) was added mucosally to prevent evaporation of the ASL (Tarran et al., 2001b). PFC has been shown to have no effect on ASL height, mucus transport or ion transport (Tarran et al., 2001a, Tarran and Boucher, 2002). Following measurement of the ASL, cells were transferred back to media and kept at 37^{o}C in a 5% CO_2 incubator between time points.

For experiments in which the effect of smoke on secretion of Cl^- into the ASL was being tested, cultures were loaded with dextran for 30 minutes. Excess dextran was then aspirated to set a starting ASL height of ~8 µm cells. As cultures were pre-treated bilaterally with compounds, the dextran and basolateral media contained the appropriate compounds. For experiments measuring the long-term effect of compounds on ASL height, the dextran and basolateral media again contained the compounds. However, dextran was added to the cultures and left to absorb overnight. Compounds added apically in these experiments were suspended as a dry powder in PFC and sonicated for 10 minutes (Tarran et al., 2001b).

ASL was imaged using a XZ scan on a confocal laser scanning microscope (Leica SP5) with a 63x glycerol immersion lens and the 561 nm laser. Images were captured on an 8-bit scale using a bidirectional scan frequency of 700 Hz, with a line average of 2 and a pinhole of 1 airy unit. At least three transwells were taken per condition in experiment. Images were taken at 15 predefined points on the transwell; the first 10 images were taken forward for analysis. Any images which captured the edge of the transwell and therefore imaged the meniscus were excluded. Images were analysed offline using ImageJ software by measuring the height of the ASL and correcting for the zoom on the microscope to calculate the ASL height in microns (Fig. 2.03).

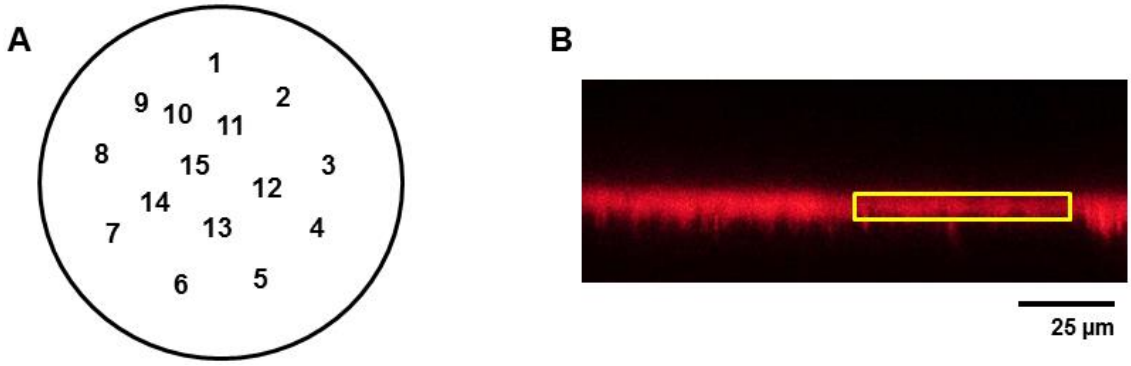

Figure 2.03. Imaging and measurement of airway surface liquid height. (A) Representation of 15 pre-defined points on a transwell used to image airway surface liquid (ASL). **(B)** Typical image obtained at a point on the transwell, the yellow box indicates the 'bounding rectangle' function used on ImageJ to measure ASL height.

2.9 Immunocytochemistry

HEK 293T cells were seeded at a density of 7.5 x 10^4 per coverslip and transfected with GFP-CFTR one day post seeding. Cells were treated and fixed 48 hrs post transfection. Following treatment, cells were fixed with methanol as described earlier. Next, cells were blocked for 1 hr at room temperature in a solution consisting of PBS, 5% (v/v) normal goat serum and 1% (w/v) bovine serum albumin. Cells were then probed with antibodies against the lysosomal marker, LAMP1 (rabbit anti-LAMP1, 1:200), the endoplasmic reticulum marker, calreticulin (mouse anti-calreticulin, 1:200) or a marker of the Golgi apparatus, GM130 (rabbit anti-GM130, 1:200). Cells were probed for the relevant markers for 3 hours at room temperature or overnight at 4^{o}C. Following incubation, cells were washed three times with PBS, for 5 minutes each.

Cells were then probed with secondary antibodies (1:500) for 1 hour at room temperature. Secondary antibodies used were either goat anti-rabbit conjugated to Dylight 649 or goat anti-mouse conjugated to Alexa Fluor 568. Cells were then given three 5 min washes with PBS and loaded with 1 $\mu g ml^{-1}$ DAPI, following which cells were imaged using the SP8 confocal microscope.

Images were captured using the LAS AF software with the 405 nm, 488 nm line of an argon laser and either 561 nm or 633 nm lasers. Images were taken using a sequential scan; 6-10 images were taken per coverslip to obtain approximately 50 cells per coverslip. Images were taken from two coverslips on at least three separate occasions. Co-localisation between two proteins of interest was also calculated using LAS AF software (Fig. 2.04). Single cell regions of interest were selected manually and the percentage co-localisation was calculated by the software using the equation; *percent co-localisation = co-localisation area/ area foreground, where area foreground = image area/image background*.

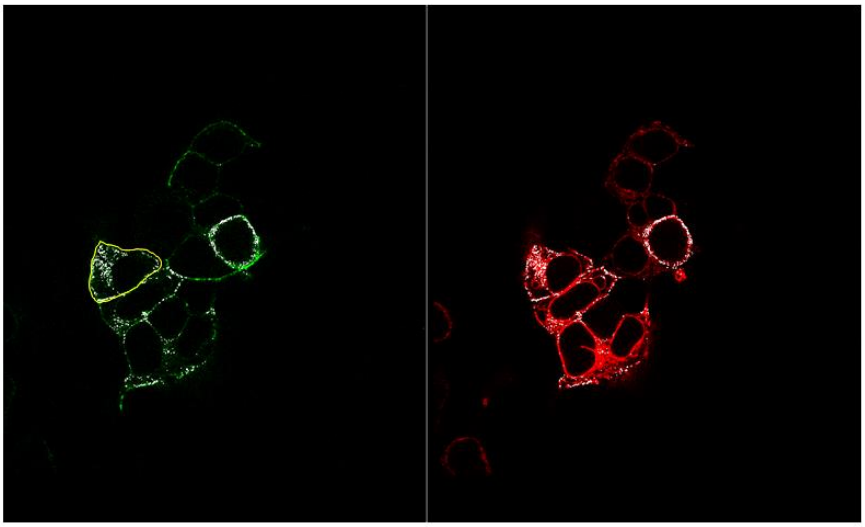

Figure 2.04. Example co-localisation analysis between CFTR and STIM1. Representative images taken as indicated in Fig. 2.02. Example image showing co-localisation between CFTR (green) and STIM1 (red) calculated using LAS AF software. CFTR fluorescence was superimposed onto STIM1 fluorescence (indicated in white) and single cells were selected as regions of interest (indicated in yellow) to calculate co-localisation.

2.10 Total internal reflection fluorescence microscopy

HEK 293T cells were plated onto glass coverslips at a density of 7.5 x 10^4 and transfected with CFTR with a GFP tag on the N terminus as detailed above. Cells were treated and fixed with ice-cold methanol 48 hrs post transfection. Total internal

reflection fluorescence microscopy (TIRF) was performed on a Leica SR GSD microscope. GFP was excited using the 488 nm line of an argon laser and images were taken using a 100x oil immersion lens. The penetration depth of the evanescent wave set to 90 nm. Images were captured on a 16-bit scale using the LAS AF software; 6-10 images were taken per coverslip to obtain approximately 40 cells per condition. Images were taken from two coverslips on at least three separate occasions

Images were analysed offline using ImageJ software. The threshold function was used to select regions of interest and the integrated density, which accounts for the mean grey value and the area of the selected region, was measured and used to compare between treatments (Fig. 2.05).

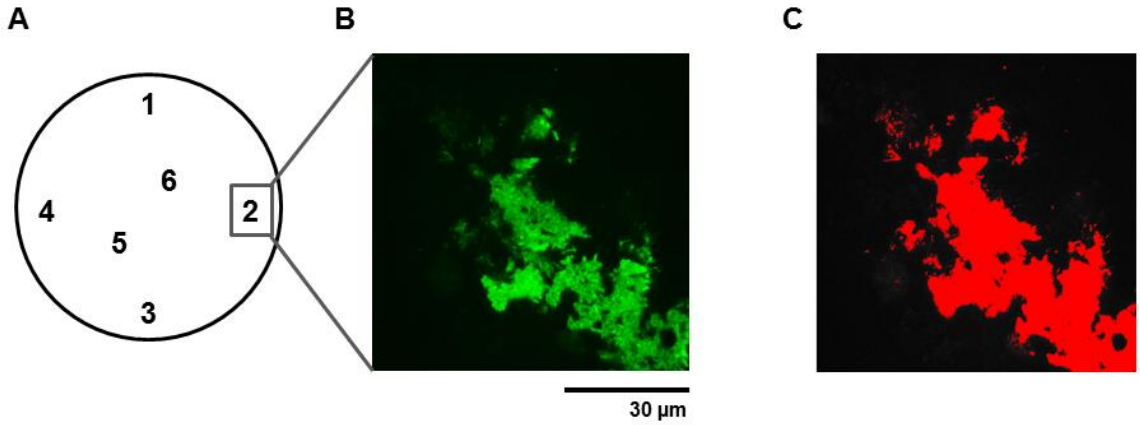

Figure 2.05. Example of total internal reflection fluorescence microscopy image acquisition and analysis. (A) Representation of the points on a coverslip at which images were taken and **(B)** example image taken from a point on the coverslip. **(C)** The 'threshold' function on ImageJ was used to select regions of interest (indicated in red) and the integrated density of these areas used for analysis.

2.11 Measurement of calcineurin phosphatase activity

Calcineurin phosphatase activity in cell lysates was measured using a colorimetric assay per manufacturer's instructions (Enzo life sciences). HEK 293T cells were seeded onto 60 mm culture dishes at a density of 1 x 10^6 per dish and treated 24 hrs later. Cells were then washed with ice-cold Tris buffered saline solution, lysed and stored at -80^{o}C. Excess phosphates and nucleotides were removed from the lysates by passing the samples through a chromatography column. The desalted samples were subsequently stored at -80^{o}C. To ensure an equal amount of protein was run in the assay for each sample, a bicinchoninic acid (BCA) assay was run according

manufacturer's instructions. Total protein in the samples was calculated using a standard curve generated from known bovine serum albumin (BSA) standards (Fig. 2.06).

Following the BCA assay, 3 µg of protein per sample was used for the calcineurin phosphatase assay. Total phosphatase activity in the samples was detected by addition of the phosphopeptide substrate, RII, in assay buffer. The assay plate was then equilibrated to the reaction temperature for 10 minutes at 37ºC. Following the equilibration, sample lysates were added to the assay plate and the plate was incubated at 37ºC for 30 minutes. The free phosphate was then measured by the addition of BIOMOL GREEN reagent and colour was allowed to develop for 30 minutes at 37ºC. Absorbance at 620 nm was then measured. Results were corrected for background, which was obtained by measuring absorbance without the addition of the RII phosphopeptide substrate.

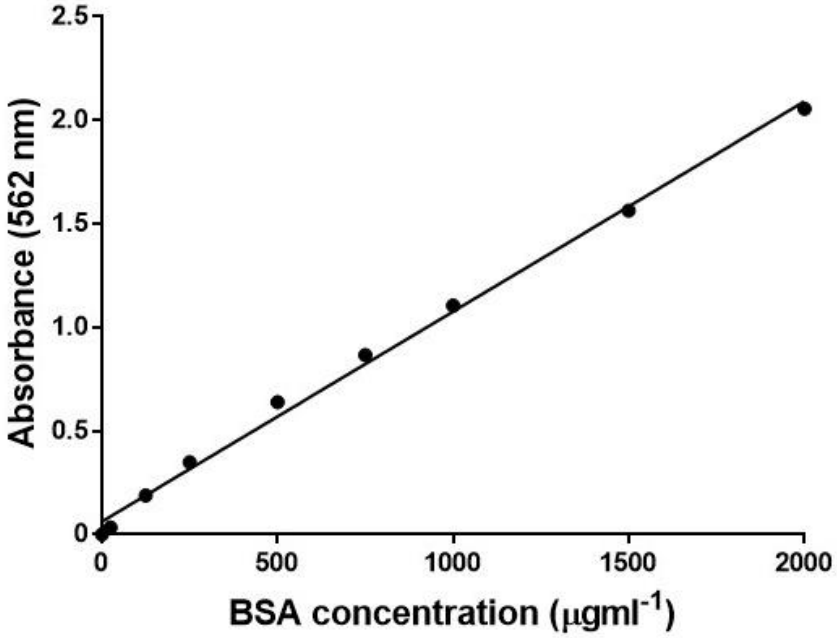

Figure 2.06. Example BCA assay used to quantify protein in lysates generated for the calcineurin phosphatase activity assay. Known concentrations of bovine serum albumin (BSA) were used to generate a standard curve. Data was generated from the average of standards run in triplicate r^2= 0.9957

2.12 Solutions

For patch clamp experiments, the high EGTA pipette solution contained in mM; 120 CsCl, 2 $MgCl_2$, 5 EGTA, 10 HEPES and 1 Na_2ATP, set to pH 7.2 with CsOH. The low EGTA solution contained in mM; 120 CsCl, 2 $MgCl_2$, 0.2 EGTA, 10 HEPES, 1

Na_2ATP and 13 mannitol, set to pH 7.2 with CsOH. Pipette solution osmolarity was typically 260 mOsm. The bath solution contained in mM; 130 NaCl, 5 KCl, 1 $CaCl_2$, 1 $MgCl_2$, 10 HEPES, 10 glucose and 20 mannitol, set to pH 7.4 with HCl. Bath solution osmolarity was typically 310 mOsm.

The solutions used for Ca^{2+} imaging experiments consisted of the same NaHEPES solution as that used in patch clamp experiments, but without the addition of mannitol. Experiments conducted with a 0 mM Ca^{2+} solution contained in mM; 130 NaCl, 5 KCl, 1 EGTA, 1 $MgCl_2$, 10 HEPES, 10 glucose and 20 mannitol, set to pH 7.4 with HCl. For experiments conducted with a nominally Ca^{2+} free bath solution, the solution consisted of in mM; 130 NaCl, 5 KCl, 2 $MgCl_2$, 10 HEPES, 10 glucose and 20 mannitol, set to pH 7.4 with HCl.

The pyruvate Ringer's solution used for cigarette smoke exposure consisted of, in mM; 120 NaCl, 12 $NaHCO_3$, 24 HEPES, 1.2 $MgCl_2$, 5.2 KCl, 1 NaPyruvate, 1% non-essential amino acids, 10 glucose, 1.2 $CaCl_2$, set to pH 7.4 with NaOH.

PBS consisted of, in mM; 137 NaCl, 2.7 KCl, 1.5 KH_2PO_4, 8.1 Na_2HPO_4, pH 7.0 - 7.3.

Tris buffered saline consisted of, in mM; 20 Tris, 150 NaCl, pH 7.2.

Lysis buffer consisted of, in mM; 50 Tris, 0.1 EDTA, 0.1 EGTA, 1 DTT, 0.2% NP-40, pH 7.5.

2.13 Statistical analysis

Data was collected using Microsoft Excel 2007; Graphpad Prism v6.0 was used to carry out all analyses. All data are presented as mean ± standard error of the mean. For patch clamp experiments, data was analysed using a repeated measures ANOVA with a Tukey's multiple comparison post-test. For imaging experiments, data was analysed using Students' t-tests or one-way ANOVA were used where appropriate; $p<0.05$ was considered statistically significant.

Chapter 3.0 An Increase in Cytosolic Ca^{2+} Causes a Loss of CFTR-Mediated Conductance and Internalisation of CFTR

3.1 Introduction

Recently, several labs have proposed that cigarette smoke causes a reduction in CFTR expression and activity (Kreindler et al., 2005, Cantin et al., 2006, Clunes et al., 2012, Dransfield et al., 2013). Our lab and others have shown that cigarette smoke and its constituents are linked to an increase in cytosolic Ca^{2+} in a variety of different cell lines (Misonou et al., 2006, Rasmussen et al., 2014, Lin et al., 2015). Using confocal microscopy and fluorescent Ca^{2+} measurements, our lab was the first to show that a smoke-induced increase in intracellular Ca^{2+} ($[Ca^{2+}]_i$), irrespective of the source, caused internalisation of CFTR. Furthermore, this research showed that Ca^{2+} release from internal stores, such as the endoplasmic reticulum, was sufficient to cause CFTR internalisation (Rasmussen et al., 2014). Therefore, I sought to further understand the effect of an increase in cytosolic Ca^{2+} on CFTR at a functional level. This chapter details the effect of an increase in $[Ca^{2+}]_i$, released from different intracellular stores, on CFTR-mediated conductance, measured using the whole cell patch clamp technique. Additionally, the effect of the various Ca^{2+} agonists on cytosolic Ca^{2+} within HEK 293T cells were characterised using fluorescent Ca^{2+} measurements.

3.2 Stable CFTR-mediated currents can be activated in transfected HEK 293 cells

To investigate the effect of an increase in $[Ca^{2+}]_i$ on CFTR, experiments were carried out on HEK 293T cells transiently transfected with CFTR. This system results in robust expression of CFTR, allowing changes in CFTR-mediated current to be easily measured using the whole cell configuration of the patch clamp technique. Furthermore, preliminary experiments carried out in Calu-3 cells, a cell line derived from serous cells of the submucosal glands, showed that activated CFTR current was variable between different cultures of cells, making it difficult to compare between cultures or treatments (data not shown; (Shen et al., 1994).

To characterise the activity of CFTR, transfected cells were perfused with forskolin to stimulate CFTR and the inhibitor $CFTR_{inh}$-172 used to test the specificity of the activated current. Overall, activation of CFTR with forskolin (5 µM) caused a 58.3 ± 38.9 fold increase in conductance to 2.0 ± 0.5 nS/pF (8 mins post addition) from a baseline of 0.07 ± 0.02 nS/pF (n=4, $p<0.005$, Fig. 3.01). The forskolin activated current was found to reach a peak between 6 - 8 minutes after the addition of forskolin and was relatively stable for ~20 minutes, with the conductance at 18 minutes post addition being 1.6 ± 0.5 nS/pF (n=4, $p<0.005$, Fig. 3.01) and the conductance at 28 minutes post addition being 1.4 ± 0.5 nS/pF (n=4, Fig. 3.01D). The remaining forskolin stimulated increase in conductance was sensitive to inhibition with $CFTR_{inh}$-172 (10 µM), with the conductance being reduced to 0.3 ± 0.1 nS/pF after 8 minutes of exposure ($p<0.05$, Fig. 3.01D). As the data indicated approximately 69.4 ± 10.0% of activated current remained following a prolonged exposure to forskolin, this model provided a system whereby temporal changes in conductance could be studied in response to test compounds.

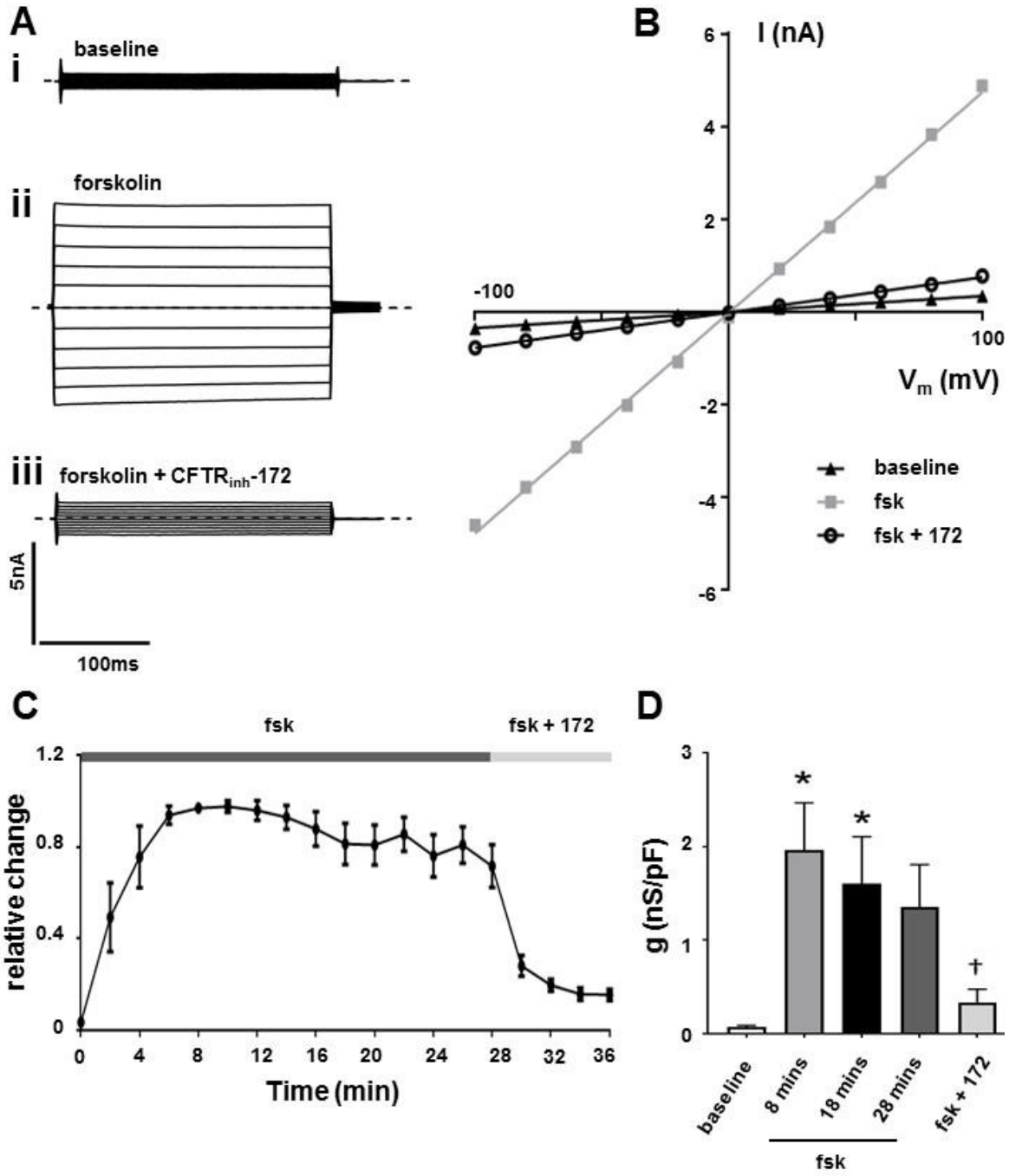

Figure 3.01. Time course for CFTR activation. (A) Representative fast whole cell current traces obtained by holding the membrane potential at 0 mV and applying voltage steps between ±100 mV in 20 mV increments under **(i)** basal conditions and after 8 mins perfusion with **(ii)** forskolin (fsk; 5 µM) and **(iii)** fsk and $CFTR_{inh}$-172 (10 µM). Dashed line indicates the zero current level. **(B)** Current-voltage (I-V_m) plot for the traces shown in A. **(C)** Mean changes in conductance plotted relative to the maximum current reached at +100 mV when cells were perfused with fsk. **(D)** Changes in conductance under conditions indicated. Conductance was normalised to cell size. Data are mean ± SEM (n=4) *p<0.005 when compared to baseline conductance. † p<0.05 when compared to fsk (8 mins) stimulated conductance.

3.3 An increase in Ca^{2+} has no effect on conductance in cells that do not express CFTR

3.3.1 Non-transfected HEK 293T cells show no change in conductance when exposed to an increase in cytosolic Ca^{2+}

To determine whether an increase in cytosolic Ca^{2+} would affect CFTR-mediated conductance, it was first necessary to test whether untransfected cells showed any changes in conductance when exposed to an increase in $[Ca^{2+}]_i$. The endoplasmic reticulum (ER) represents one of the major stores of Ca^{2+} within the cell, therefore cells were exposed to the sarcoendoplasmic reticulum Ca^{2+} ATPase (SERCA) pump inhibitor, thapsigargin (Lytton et al., 1991). Thapsigargin irreversibly binds the SERCA pump when it is in a conformational state acquired in the absence of Ca^{2+} (Inesi and Sagara, 1992, Sagara et al., 1992). The SERCA pumps usually acts to refill endoplasmic reticulum stores with Ca^{2+} from the cytosol, thus inhibition of the pump leads to an elevation of cytosolic Ca^{2+}. To study the effect of an increase in $[Ca^{2+}]_i$ on CFTR, cells were initially stimulated with forskolin (5 µM) for 8 minutes to activate CFTR, and then exposed to thapsigargin (200 nM) for 10 minutes to increase $[Ca^{2+}]_i$. Current was monitored for a further 10 minute wash out period in the presence of forskolin alone. Finally, cells were exposed to $CFTR_{inh}$-172 (10 µM) for 8 minutes to test whether there was any residual CFTR-dependent current.

Overall, untransfected cells showed no substantial changes in conductance after the addition of thapsigargin. On average, the baseline conductance of these cells was 0.3 ± 0.1 nS/pF, and after addition of forskolin; conductance remained at 0.3 ± 0.1 nS/pF. Subsequent addition of thapsigargin also had no effect, with the conductance remaining at 0.3 ± 0.1 nS/pF 10 minutes post addition. Whole cell conductance showed no change 10 minutes after wash out of thapsigargin (0.3 ± 0.1 nS/pF). Furthermore, addition of the inhibitor, $CFTR_{inh}$-172, also had no effect (0.3 ± 0.1 nS/pF n=8, Fig. 3.02D). The absence of an increase in conductance upon exposure to forskolin or thapsigargin suggested there is no endogenous CFTR, Ca^{2+}-activated chloride channel (CaCC) or Ca^{2+} activated non-selective cation channels present in HEK 293T cells.

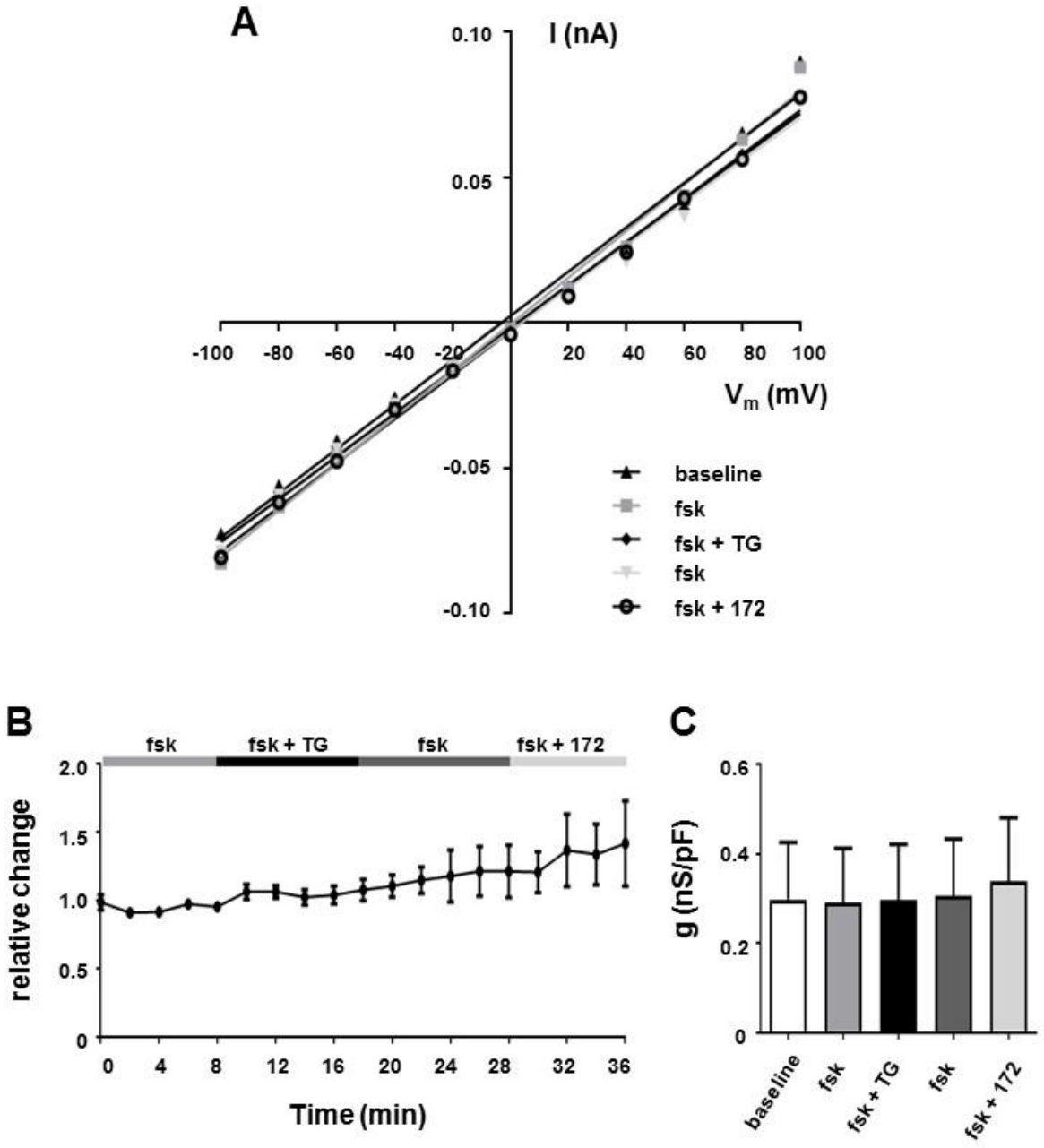

Figure 3.02. An increase in cytosolic Ca^{2+} has no effect on conductance in untransfected cells. HEK 293T cells were exposed to forskolin (fsk; 5 µM) followed by thapsigargin (TG; 200 nM) and the inhibitor $CFTR_{inh}$-172 (172; 10 µM). **(A)** Representative current-voltage (I-V_m) plot under conditions indicated. **(B)** Mean changes in conductance plotted relative to the maximum current reached at +100 mV when cells were perfused with forskolin. **(C)** Changes in conductance under conditions indicated; conductance was normalised to cell size. Data are mean ± SEM (n=8).

3.3.2 HEK 293T cells transfected with vehicle only show no change in conductance when exposed to an increase in cytosolic Ca^{2+}

In addition to the experiments detailed above, cells which had been transfected with water only, which was the vehicle for the CFTR construct, were also exposed to thapsigargin. On average, these cells had a resting conductance of 0.1 ± 0.04 nS/pF, which showed no change with the addition of forskolin (0.10 ± 0.05 nS/pF after 8 minutes' exposure). Addition of thapsigargin caused little change in the conductance (0.14 ± 0.07 nS/pF after 10 minutes) and the conductance remained at 0.14 ± 0.06 nS/pF after 10 minutes wash out of thapsigargin. $CFTR_{inh}$-172 also had no effect on the conductance after 8 minutes of exposure (0.18 ± 0.09 nS/pF, n=3, Fig. 3.03D). As these cells also showed no significant change in conductance after addition of forskolin or thapsigargin, the data indicated that the transfection protocol or vehicle provided no artefacts in forskolin or Ca^{2+} stimulated conductance's and that any changes observed would be due to the expression of CFTR.

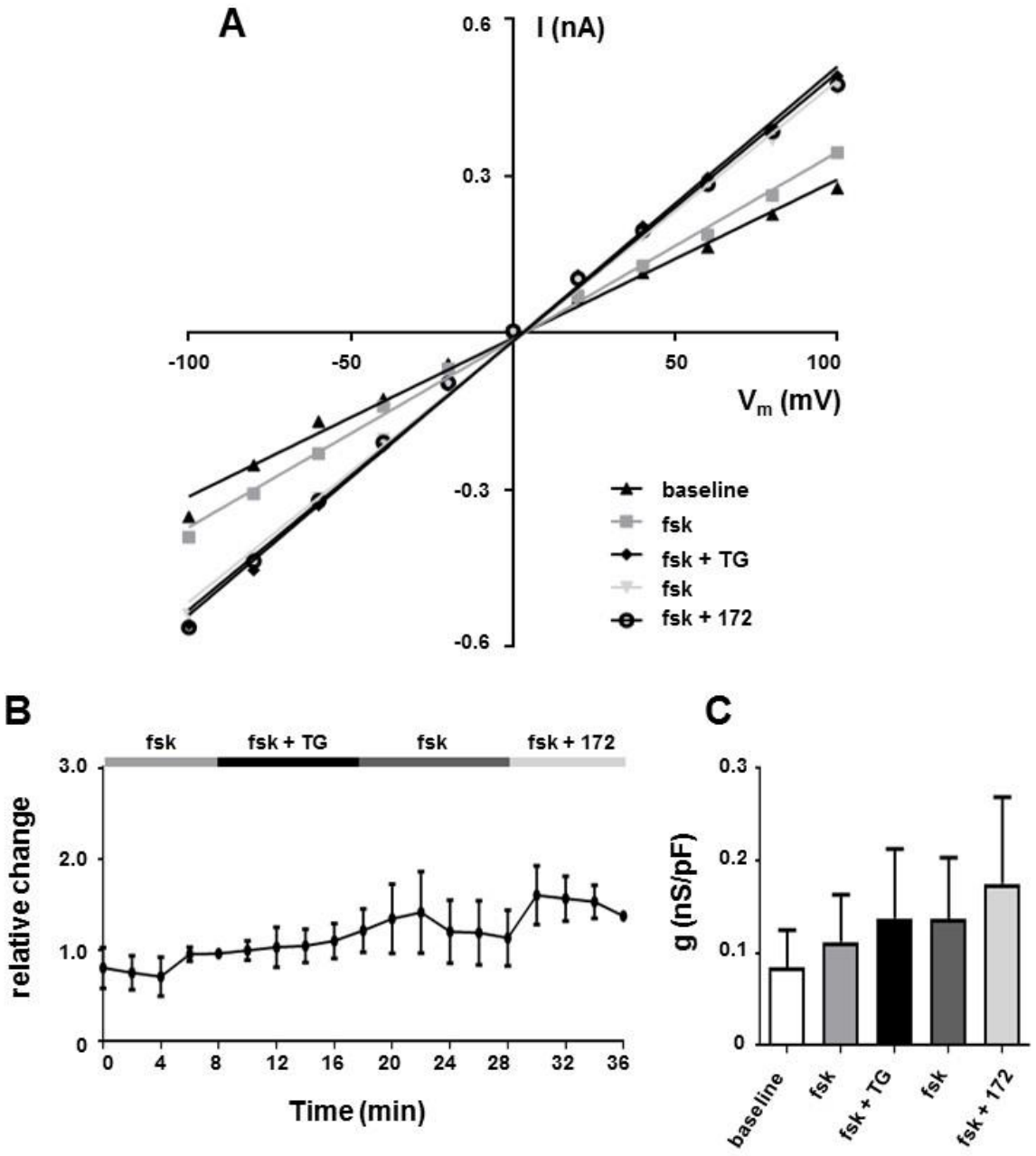

Figure 3.03. An increase in cytosolic Ca^{2+} has no effect on conductance in cells transfected with vehicle only. HEK 293T cells were exposed to forskolin (fsk; 5 µM) followed by thapsigargin (TG; 200 nM) and the inhibitor $CFTR_{inh}$-172 (172; 10 µM) **(A)** Representative current-voltage (I-V_m) plot under conditions indicated. **(B)** Mean changes in conductance plotted relative to the maximum current reached at +100 mV when cells were perfused with forskolin. **(C)** Changes in conductance under conditions indicated. Conductance was normalised to cell size. Data are mean ± SEM (n=3).

3.4 Exposure to the SERCA pump inhibitor, thapsigargin causes a decrease in CFTR-mediated conductance and internalisation of the channel

3.4.1 The effect of endoplasmic reticulum Ca^{2+} release on CFTR conductance

To study the effect of an increase in cytosolic Ca^{2+} on CFTR, transfected HEK 293T cells were exposed to forskolin to activate CFTR and then exposed to thapsigargin to induce an increase in cytosolic Ca^{2+}. Thus, any effect of thapsigargin on CFTR could be directly assessed.

On average, stimulation with forskolin caused an increase in conductance to 2.7 ± 0.5 nS/pF from a baseline of 0.1 ± 0.06 nS/pF (n=8, $p<0.05$, Fig. 3.04). Cells were subsequently exposed to thapsigargin for 10 minutes. This caused a decline in conductance to 1.9 ± 0.4 nS/pF after 10 minutes exposure. After a further 10 minutes in which cells were exposed to forskolin alone, there was a further decrease in conductance to 1.0 ± 0.3 nS/pF (n=8, $p<0.05$, Fig. 3.04). On average, after 20 minutes of exposure to thapsigargin, 40.0 ± 6.5% of the forskolin stimulated conductance remained. This remaining conductance was still sensitive to inhibition by $CFTR_{inh}$-172 with the conductance being reduced to 0.4 ± 0.06 nS/pF (n=8, $p<0.05$, Fig. 3.04D).

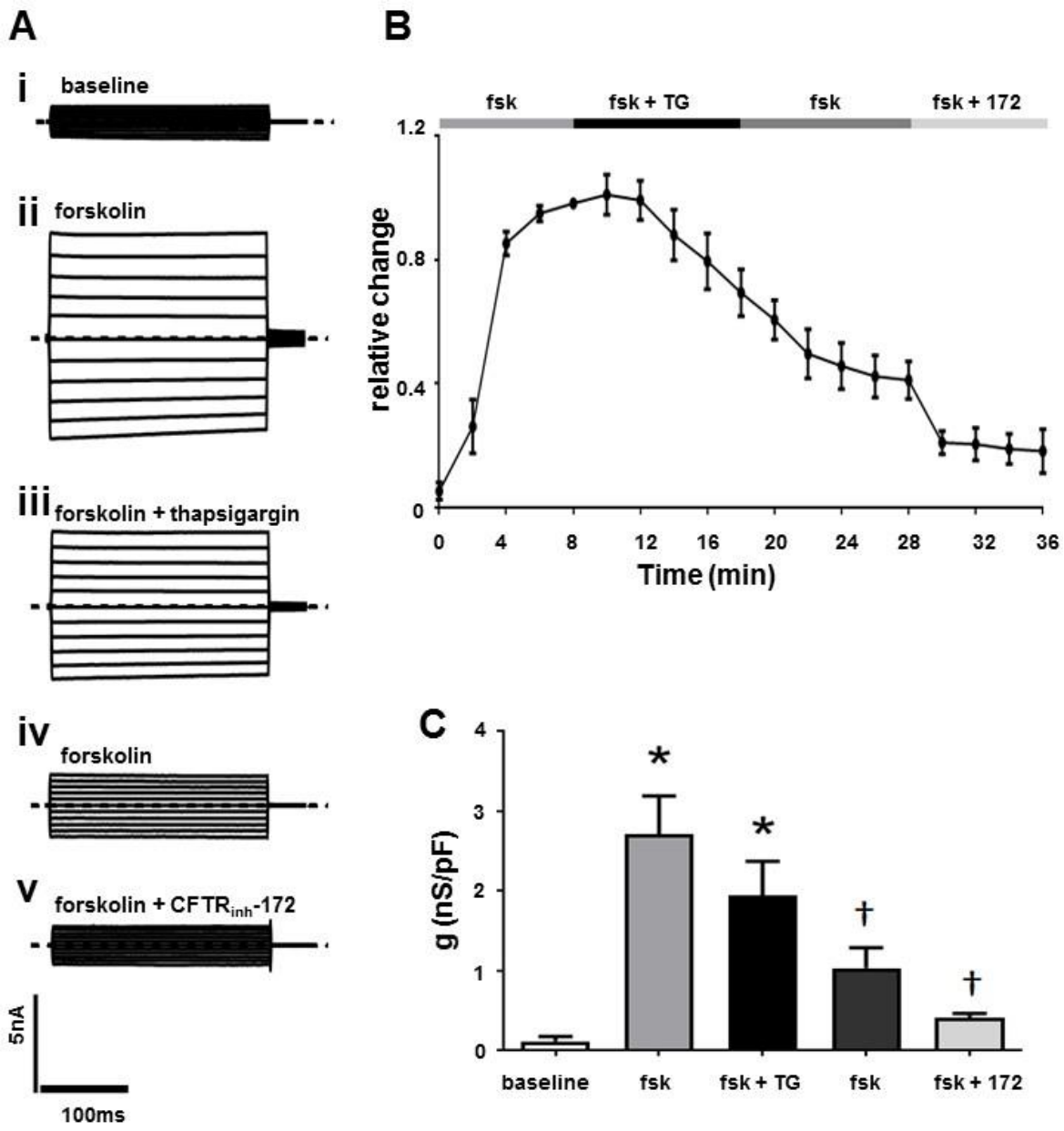

Figure 3.04. Thapsigargin causes a decrease in CFTR-mediated conductance. (A) Representative fast whole cell current traces obtained by holding the membrane potential at 0 mV and applying voltage steps between ±100 mV in 20 mV increments under **(i)** basal conditions **(ii)** after 8 mins perfusion with forskolin (fsk; 5 µM) **(iii)** 10 mins perfusion with fsk and thapsigargin (TG; 200 nM) **(iv)** 10 mins perfusion with fsk alone and **(v)** 8 mins perfusion with fsk and $CFTR_{inh}$-172 (10 µM). Dashed line indicates the zero current level. **(B)** Mean changes in conductance plotted relative to the maximum current reached at +100 mV when cells were perfused with fsk. **(C)** Changes in conductance under the conditions indicated. Conductance was normalised to cell size. Data are mean ± SEM (n=8). *p<0.05 when compared to baseline. † p<0.05 when compared to maximal forskolin stimulated conductance.

Alongside characterising the effect of thapsigargin on CFTR-mediated conductance, I also followed changes in cytosolic Ca^{2+} following exposure to thapsigargin. As mentioned in section 3.3.1, thapsigargin inhibits the action of the SERCA pump, which would lead to an elevation of cytosolic Ca^{2+} (Sagara et al., 1992). The increase in Ca^{2+} was found to gradually reach a peak followed by a slow decline to a maintained plateau greater than baseline (n=3; Fig. 3.05). Although the environment within the cells being patch clamped and imaged using Fura-2 AM would differ, the time frames of the patch clamp experiments and the Ca^{2+} imaging experiments were similar. Furthermore, the experiments were performed in the presence of forskolin as with patch clamp experiments. Therefore, these experiments gave an approximation of how Ca^{2+} may change when cells were exposed to thapsigargin in patch clamp experiments. Together, these data indicate that the increase in cytosolic Ca^{2+} correlated to a loss of CFTR-dependent conductance.

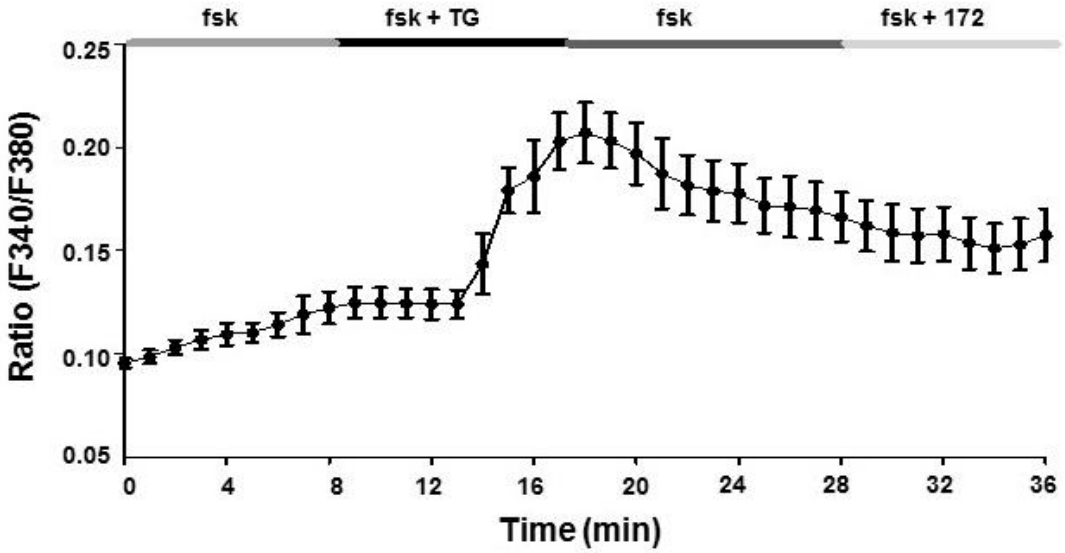

Figure 3.05. Thapsigargin causes a sustained increase in cytosolic Ca^{2+}. Mean change in $[Ca^{2+}]_i$, as indicated by the 340/380 ratio, when cells were exposed to TG in a bath solution containing 1mM Ca^{2+} (n=3).

3.4.2 Preventing an increase in cytosolic Ca^{2+} prevents a loss of CFTR-mediated conductance

To verify that the changes in $[Ca^{2+}]_i$ induced by thapsigargin were indeed responsible for the reduction in CFTR dependent current seen in earlier experiments, the EGTA concentration in the pipette solution was increased from 0.2 to 5 mM in an attempt to buffer out the increase in $[Ca^{2+}]_i$ induced by thapsigargin (Gray et al., 1994).

As before, CFTR was stimulated using forskolin, which caused an increase in conductance to 3.0 ± 2.1 nS/pF after 8 minutes exposure compared to a baseline of 0.4 ± 0.2 nS/pF. Addition of thapsigargin for 10 minutes failed to cause a decrease in conductance (3.4 ± 2.4 nS/pF). Following a 10 minute wash out period, the conductance remained at 3.4 ± 2.5 nS/pF. This remaining conductance was mostly reduced with $CFTR_{inh}$-172 (1.1 ± 0.8 nS/pF, n=3, Fig. 3.06D).

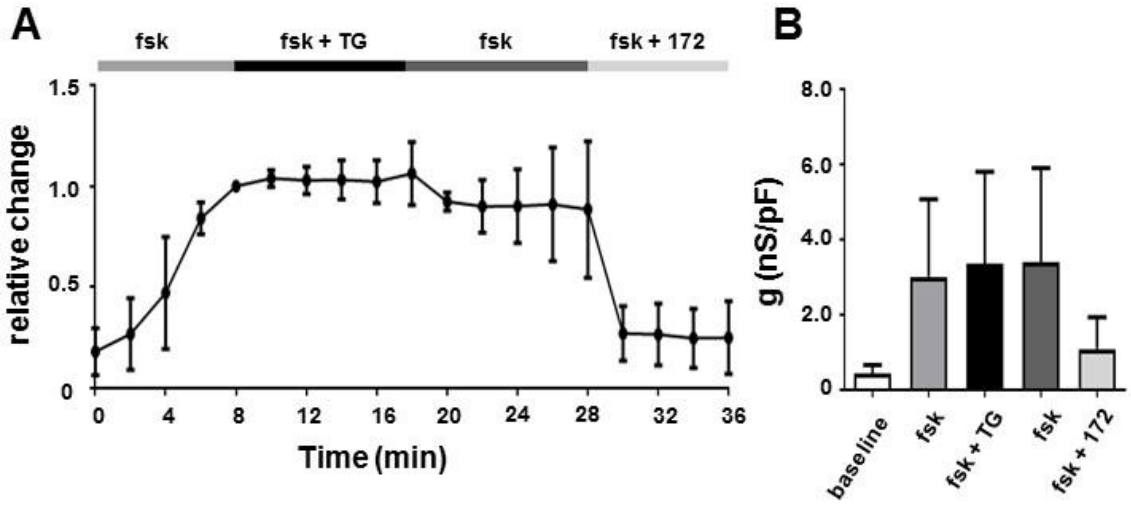

Figure 3.06. An increase in the concentration of EGTA in the patch pipette solution prevents the thapsigargin-induced decrease in CFTR conductance. HEK 293T cells were exposed to forskolin (fsk; 5 µM) followed by thapsigargin (TG; 200 nM) and the inhibitor $CFTR_{inh}$-172 (172; 10 µM) **(A)** Changes in current were measured using the fast whole cell configuration of the patch clamp technique. Data are plotted as mean changes in conductance plotted relative to the maximum current reached at +100 mV when cells were perfused with forskolin. **(B)** Changes in conductance under conditions indicated. Conductance was normalised to cell size. Data are mean ± SEM (n=3).

For calcium imaging experiments, cells were pre-incubated with the Ca^{2+} chelator, BAPTA-AM (50 µM) for 1 hour before an experiment. Cells were exposed to thapsigargin in the presence of forskolin as earlier, however, the profile of the change in $[Ca^{2+}]_i$ differed in that the cells showed no substantial change in $[Ca^{2+}]_i$ (n=3; Fig. 3.07).

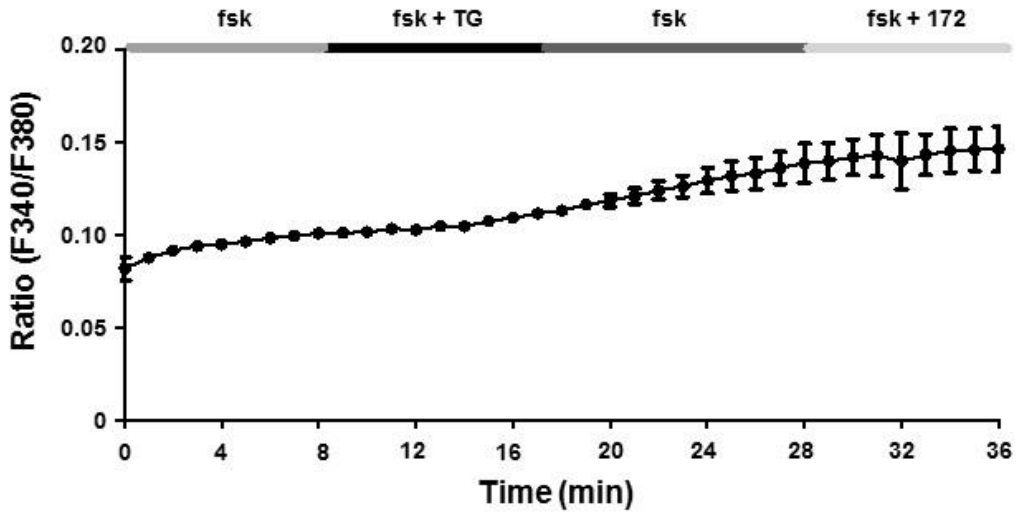

Figure 3.07. Pre-incubation of HEK 293T cells with BAPTA-AM prevents a thapsigargin induced increase in cytosolic Ca^{2+}. Mean change in $[Ca^{2+}]_i$ when cells were exposed to TG in a bath solution containing 1mM Ca^{2+}, as indicated by the 340/380 ratio, after pre-incubation with BAPTA-AM (50 µM; n=3).

3.4.3 An increase in cytosolic Ca^{2+} causes internalisation of CFTR via a dynamin-dependent mechanism

Rasmussen and colleagues (2014) recently showed exposure to either tobacco smoke or a Ca^{2+} agonist causes internalisation of CFTR, seen as the movement of GFP-tagged CFTR from the cell membrane into intracellular aggregates (Rasmussen et al., 2014). To test whether CFTR was also being internalised under these conditions, HEK 293T cells were pre-incubated with an inhibitor of the dynamin GTPase, dynasore (Macia et al., 2006).

Cells were pre-incubated with 80 µM dynasore in media at 37^{o}C for 30 - 60 min and were studied within 20 minutes post incubation. On average, cells showed an increase in conductance to 3.0 ± 0.9 nS/pF when stimulated with forskolin compared to 0.04 ± 0.02 nS/pF at baseline (n=7, $p<0.05$, Fig. 3.08B). The conductance remained at 2.9 ± 0.9 nS/pF 10 minutes after addition of thapsigargin and showed a small decrease to 2.5 ± 0.9 nS/pF after 10 minutes wash out of thapsigargin. Addition of $CFTR_{inh}$-172 inhibited the conductance to 0.5 ± 0.3 nS/pF ($p<0.05$, n=7, Fig. 3.08B). Thus, dynasore largely prevented the thapsigargin induced decrease in CFTR activity, with 86.2 ± 14.8% of the forskolin stimulated conductance remaining 20 minutes post exposure to thapsigargin. These data suggest that an increase in

cytosolic Ca^{2+} causes a reduction in CFTR-mediated conductance through internalisation of the channel in a dynamin dependent manner.

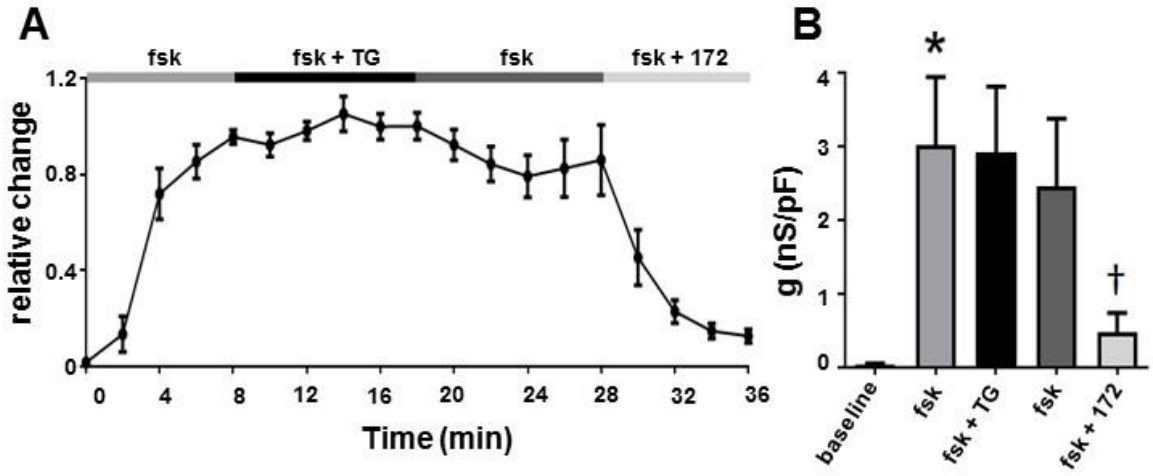

Figure 3.08. Dynasore prevents the thapsigargin-induced decrease in CFTR conductance. Cultures were pre-treated with dynasore (80 µM) for 30 - 60 min in media at 37°C and then exposed to thapsigargin (TG; 200 nM) and the inhibitor, $CFTR_{inh}$-172 (172; 10 µM). **(A)** Changes in current were measured using the fast whole cell configuration of the patch clamp technique. Data are plotted as mean changes in conductance plotted relative to the maximum current reached at +100 mV when cells were perfused with forskolin (fsk; 5 µM). **(B)** Changes in conductance under conditions indicated. Conductance was normalised to cell size. Data are mean ± SEM (n=7). *p<0.001 when compared to baseline. † p<0.05 when compared to initial forskolin exposure.

To validate the effect of dynasore was through preventing the internalisation of CFTR and not through an indirect effect on cytosolic Ca^{2+}, I characterised the effect of dynasore on Ca^{2+}. Cells were pre-treated with dynasore as for patch clamp experiments and exposed to TG in the presence of forskolin. Overall, the change in $[Ca^{2+}]_i$ showed the same trend in cells pre-treated with dynasore. On average, cells pre-treated with dynasore showed an increase in ratio to 1.4 ± 0.03 ratio units from a baseline of 1.0 ± 0.01 ratio units. In comparison, cells pre-treated with vehicle showed an increase in ratio to 1.7 ± 0.2 ratio units from a baseline of 1.1 ± 0.05 ratio units. Likewise, the area under the curve in cells pre-treated with dynasore was 14.5 ± 0.9 ratio.min compared to 27.0 ± 2.8 ratio.min in vehicle treated cells (n=3; Fig. 3.09). These data suggest that the ability of dynasore to prevent a thapsigargin-induced CFTR internalisation in patch clamp experiments, could in part, be due an effect on the thapsigargin-induced increase in cytosolic Ca^{2+}.

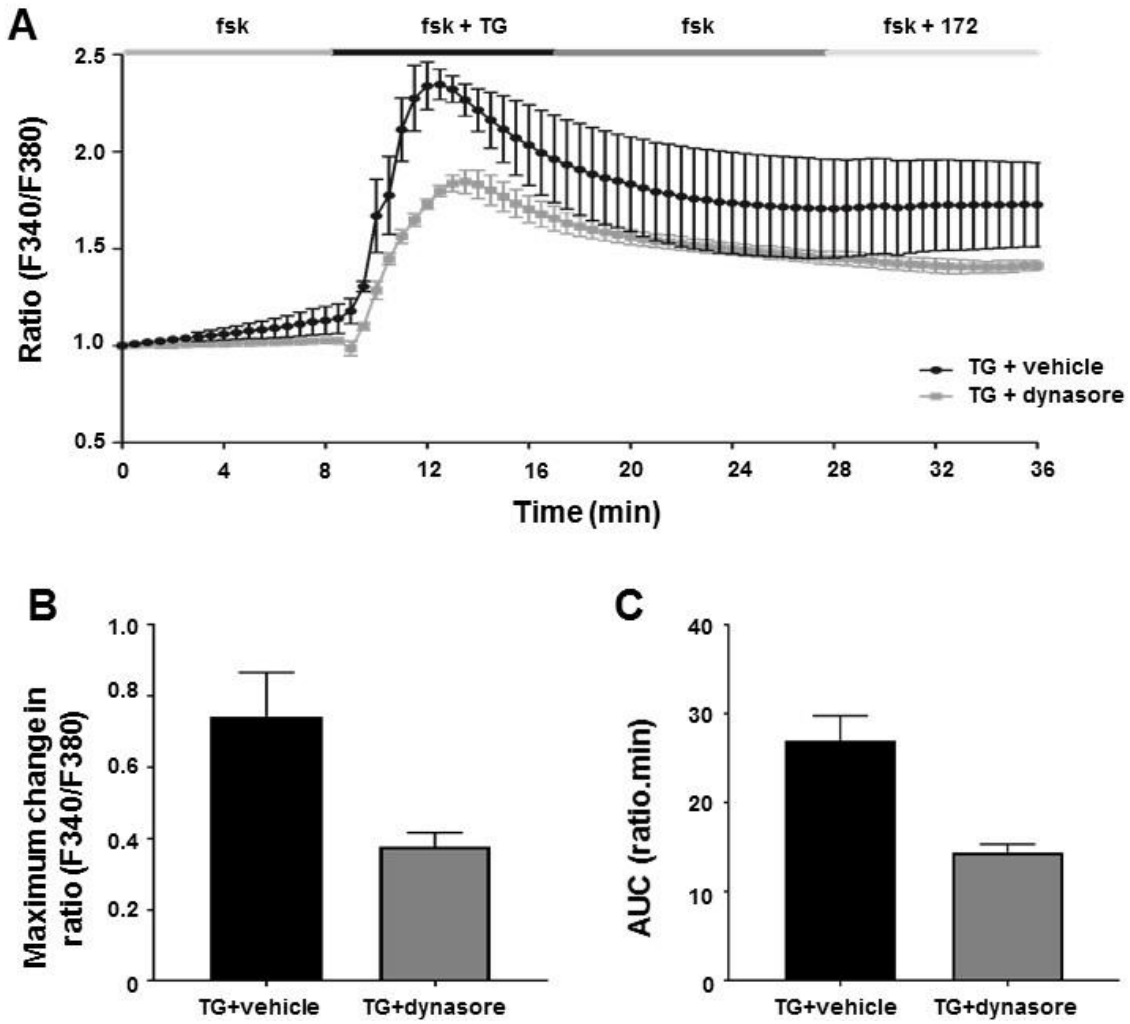

Figure 3.09. Effect of dynasore on intracellular Ca^{2+}. (A) Mean change in $[Ca^{2+}]_i$, as indicated by the 340/380 ratio, when cells were pre-treated with vehicle (black trace) or dynasore (grey trace; 80 µM) for 30 minutes at 37°C and exposed to thapsigargin (TG; 200 nM) in a bath solution containing 1mM Ca^{2+}. Mean changes in **(B)** Fura-2 ratio and **(C)** area under the curve (AUC). Data are mean ± SEM (n=3).

3.5 Extracellular Ca^{2+} is not required for a Ca^{2+} dependent loss of CFTR-mediated conductance

3.5.1 CFTR can be activated without the presence of extracellular Ca^{2+}

It has been previously reported that extracellular Ca^{2+} is not required for tobacco smoke to increase cytosolic Ca^{2+}, determined by exposing cells to cigarette smoke in Ca^{2+} free conditions (Rasmussen et al., 2014). Before testing whether extracellular Ca^{2+} was required for a Ca^{2+}-induced loss of CFTR-mediated conductance, experiments were first conducted to determine whether CFTR could be activated without extracellular Ca^{2+}. Cells were perfused with a nominally Ca^{2+} free solution, as

the addition of EGTA to the bath solution has been shown to result in the activation of hemichannels (Contreras et al., 2003). The free Ca^{2+} in this solution could be estimated to be approximately less than 100 µM based on measurements of free Ca^{2+} carried out in similar solutions (Stewart et al., 2001).

On average, the conductance 8 minutes after removal of extracellular Ca^{2+} was 0.39 ± 0.18 nS/pF which was not significantly different to a resting conductance of 0.2 ± 0.1 nS/pF. Following the removal of Ca^{2+}, CFTR was activated with forskolin, which caused a large increase in conductance to 1.3 ± 0.5 nS/pF and this increase was sensitive to inhibition with $CFTR_{inh}$-172 (0.5 ± 0.2 nS/pF; n=7; Fig. 3.10).

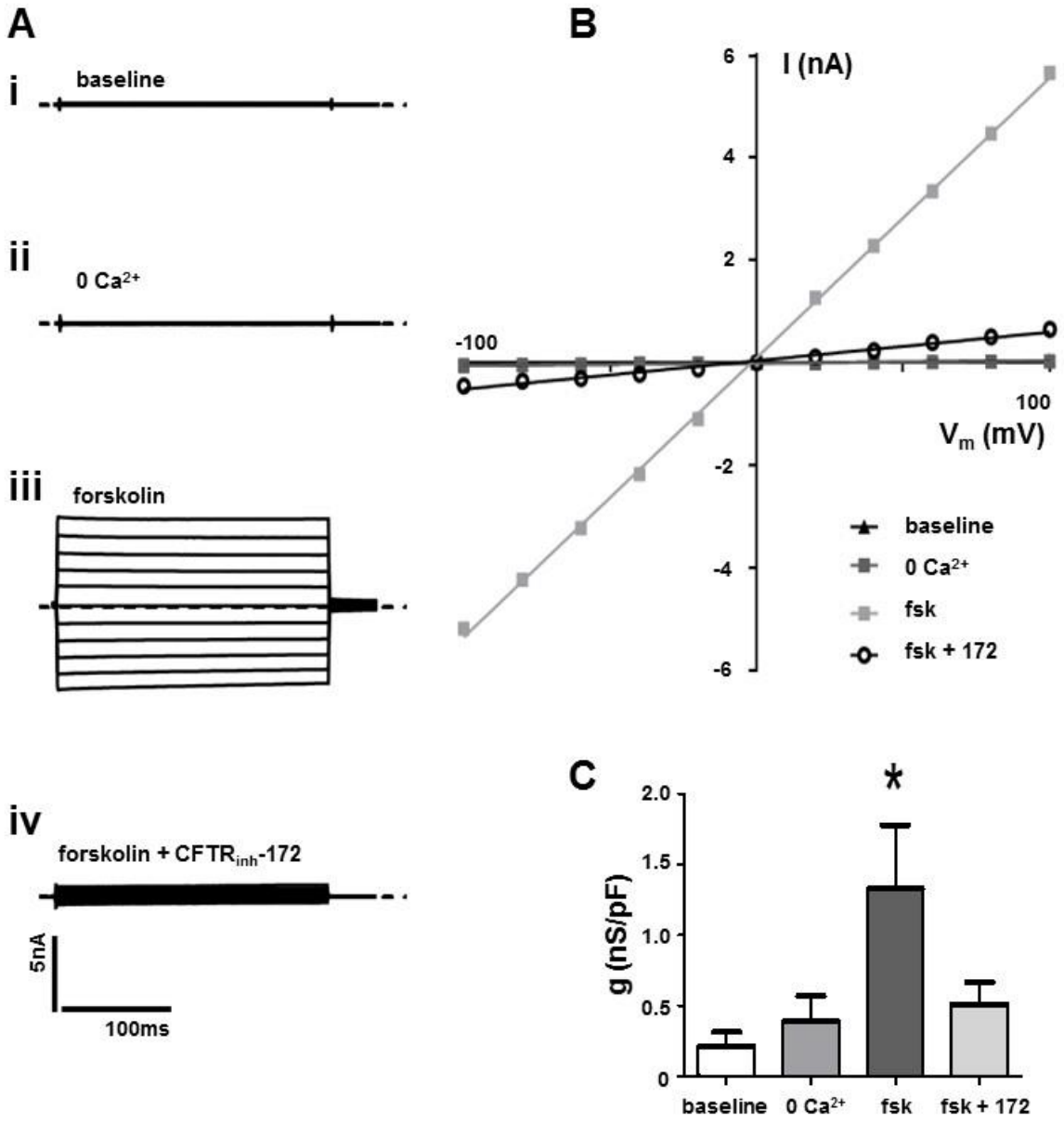

Figure 3.10. CFTR activation in the absence of extracellular Ca^{2+}. (A) Representative fast whole cell current traces obtained by holding the membrane potential at 0 mV and applying voltage steps between ±100 mV in 20 mV increments under **(i)** basal conditions **(ii)** after 8 mins perfusion with a nominally Ca^{2+} free solution and **(iii)** forskolin (fsk; 5 µM, 8 mins post addition) **(iv)** fsk and $CFTR_{inh}$-172 (10 µM, 8 mins exposure). Dashed line indicates the zero current level. **(B)** Current-voltage ($I\text{-}V_m$) plot for the traces shown in A. **(C)** Changes in conductance under conditions indicated. Conductance was normalised to cell size. Data are mean ± SEM (n=7).

As earlier, I also followed the change in the forskolin stimulated conductance overtime. Cells were exposed to forskolin for 28 minutes and then to $CFTR_{inh}$-172. On average, forskolin caused an increase in conductance to 1.0 ± 0.3 nS/pF compared to a baseline of 0.1 ± 0.04 nS/pF. The conductance remained at 1.1 ± 0.4

nS/pF (n=3) at 18 minutes post addition and 1.1 ± 0.2 nS/pF at 28 minutes. The forskolin stimulated increase in conductance was sensitive to inhibition with $CFTR_{inh}$-172, with the conductance being reduced to 0.3 ± 0.1 nS/pF (n=2, Fig. 3.11B). Similar to time course experiments in the presence of Ca^{2+}, these experiments indicated the forskolin activated conductance was stable for the duration of the experiment.

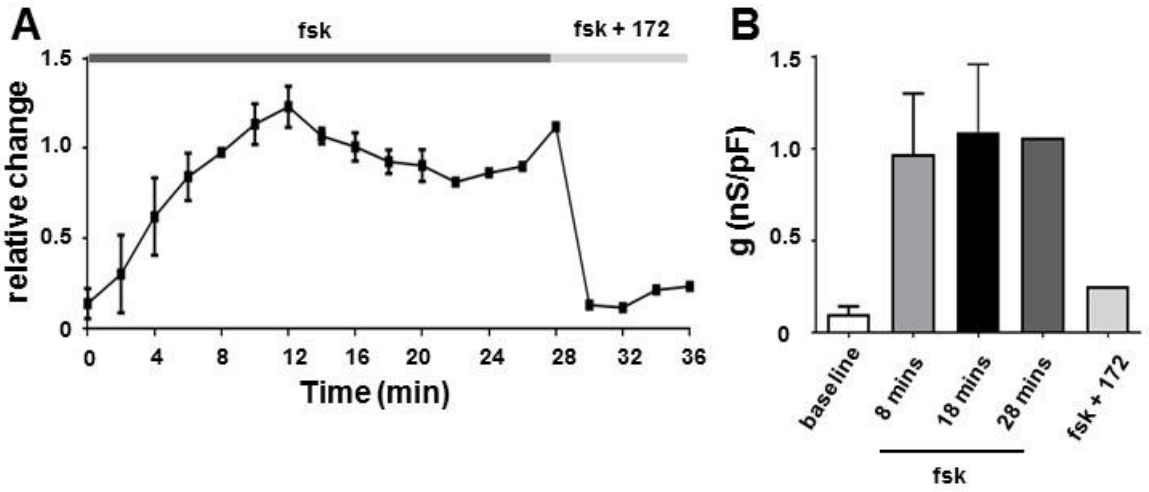

Figure 3.11. Time course for CFTR activation in the absence of extracellular Ca^{2+}. (A) Changes in current were measured using the fast whole cell configuration of the patch clamp technique. Data are plotted as mean changes in conductance plotted relative to the maximum current reached at +100 mV when cells were perfused with forskolin. **(B)** Changes in conductance under conditions indicated. Conductance was normalised to cell size. Note that one cell was lost at 20 mins. Data are mean ± SEM (n=2-3).

3.5.2 Extracellular Ca^{2+} is not needed for the Ca^{2+} dependent loss of current

I next tested whether addition of thapsigargin to a nominally Ca^{2+} free bath solution would cause a decrease in CFTR conductance. On average, when stimulated with forskolin, cells showed an increase in conductance to 1.6 ± 0.3 nS/pF from a baseline of 0.03 ± 0.01 nS/pF (n=7, $p<0.05$, Fig. 3.12). Addition of thapsigargin for 10 minutes reduced this conductance to 1.3 ± 0.4 nS/pF. After a further 10 minutes, in which cells were perfused with forskolin alone, the conductance further declined to 0.8 ± 0.2 nS/pF. Addition of $CFTR_{inh}$-172 inhibited the remaining conductance to 0.2 ± 0.1 nS/pF (n=7, $p<0.05$, Fig. 3.12B). Thus, the data showed exposure to thapsigargin in a nominally Ca^{2+} free bath solution caused a 52.8 ± 9.7% reduction in the forskolin stimulated conductance. In comparison, when cells were exposed to thapsigargin in a bath solution containing 1 mM Ca^{2+}, there was a similar reduction (60.0 ± 6.5%) in forskolin stimulated conductance.

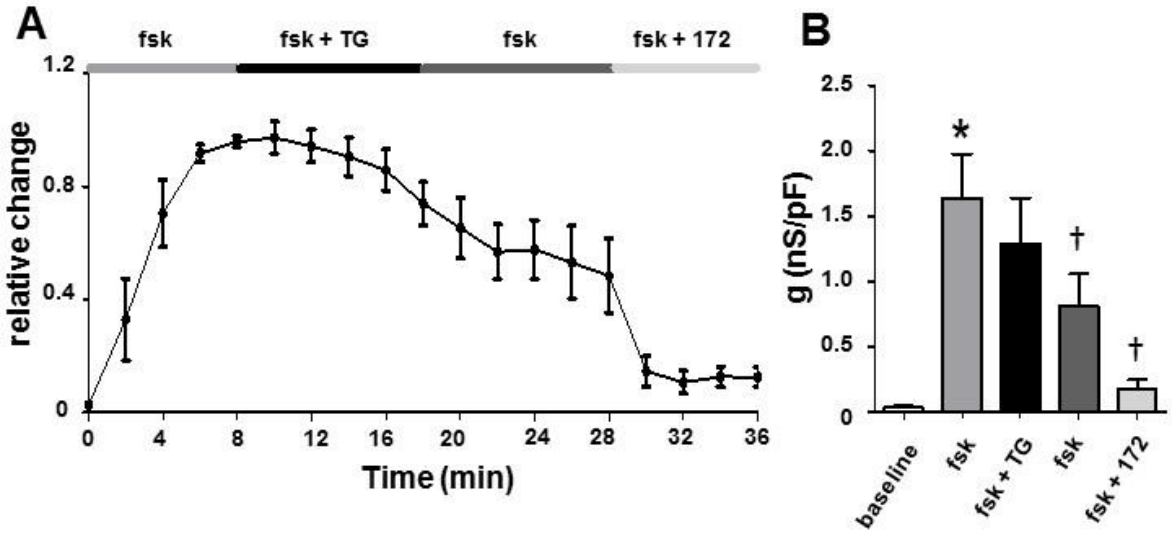

Figure 3.12. Thapsigargin decreases CFTR-mediated conductance in the absence of extracellular Ca^{2+}. HEK 293T cells were exposed to forskolin (fsk; 5 µM) followed by thapsigargin (TG; 200 nM) and the inhibitor $CFTR_{inh}$-172 (172; 10 µM). **(A)** Changes in current were measured using the fast whole cell configuration of the patch clamp technique. Data are plotted as mean changes in conductance plotted relative to the maximum current reached at +100 mV when cells were perfused with forskolin. **(B)** Changes in conductance under conditions indicated. Conductance was normalised to cell size. Data are mean ± SEM (n=7). *p<0.05 when compared to baseline, † p<0.05 when compared to initial forskolin exposure.

The effect of thapsigargin on cytosolic Ca^{2+} was also characterised. In a nominally Ca^{2+} free solution, exposure to thapsigargin in the presence of forskolin caused a transient increase in $[Ca^{2+}]_i$ which was seen as a slow rise to a peak followed by a decline (n=3, Fig. 3.12). Thus, these data along with patch clamp data indicate that a sustained increase in $[Ca^{2+}]_i$ is not needed for thapsigargin to cause a significant decrease in CFTR-mediated conductance. Furthermore, the data suggests that extracellular Ca^{2+} does not need to be present for thapsigargin-induced CFTR internalisation (further detailed in Fig. 3.26).

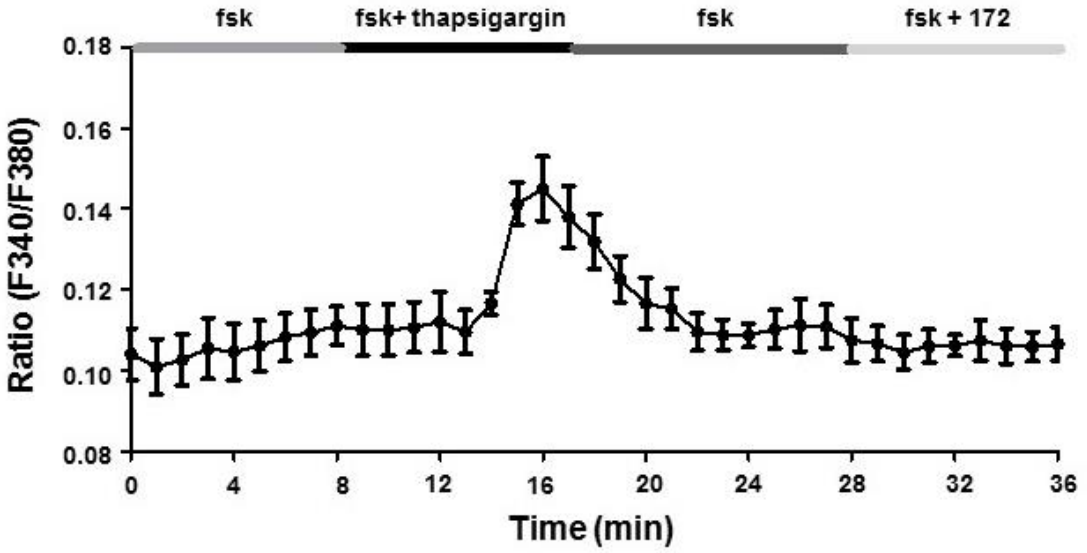

Figure 3.13. Thapsigargin in a nominally Ca^{2+} free bath solution causes a transient increase in cytosolic Ca^{2+}. Mean change in $[Ca^{2+}]_i$, as indicated by the 340/380 ratio, when cells were exposed to TG (200 nM) in a nominally Ca^{2+} free bath solution (n=3).

3.6 The effect of other Ca^{2+} agonists on CFTR-mediated conductance

3.6.1 The effect of ionophore mediated Ca^{2+} release on CFTR conductance

Along with thapsigargin, I also characterised the effect of several other Ca^{2+} agonists on CFTR-mediated conductance to further understand how a change in cytosolic Ca^{2+} was related to a loss of CFTR-mediated conductance. Cells were exposed to the ionophore, ionomycin which creates Ca^{2+} permeable pores in intracellular membranes (Liu and Hermann, 1978, Morgan and Jacob, 1994).

Like earlier experiments with thapsigargin, cells were exposed to ionomycin (1 µM) in a bath solution containing 1 mM Ca^{2+} for 10 minutes. Current was then monitored for a further 10 minutes after the wash out of ionomycin but in the presence of forskolin. Finally, $CFTR_{inh}$-172 was added to test whether there was any residual CFTR activity. On average, cells showed an increase in conductance to 2.2 ± 0.4 nS/pF from a baseline of 0.2 ± 0.07 nS/pF. The conductance was reduced to 0.7 ± 0.2 nS/pF 10 minutes after addition of ionomycin (n=6, $p<0.001$, Fig. 3.14B). After a further 10 minutes, 22.9 ± 7.2% of the forskolin stimulated conductance remained with the conductance being reduced to 0.4 ± 0.1 nS/pF. Addition of $CFTR_{inh}$-172 did not affect the remaining conductance with the average being 0.39 ± 0.1 nS/pF (n=6, $p<0.005$, Fig. 3.14B). On average, ionomycin caused a faster loss of forskolin stimulated conductance (5.1 ± 0.7% per minute) when compared to thapsigargin (3.2 ± 0.4% per

minute, p<0.05). Indeed, when single cell profiles were studied, 63.7 ± 12.9% of forskolin stimulated conductance was lost within the first ten minutes of exposure (Fig.3.14A, blue trace).

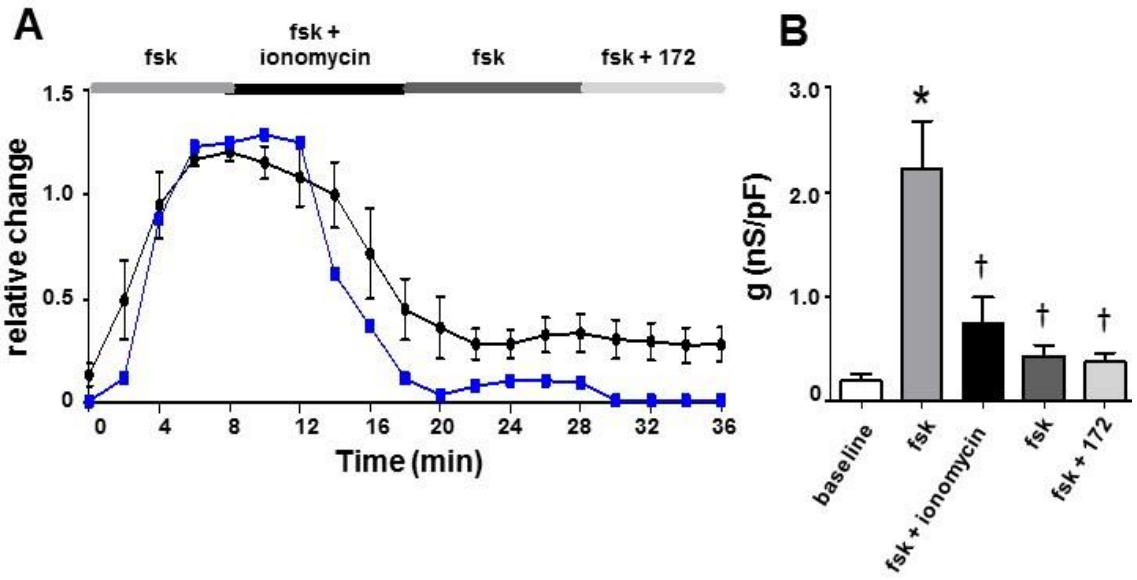

Figure 3.14. Ionomycin causes a loss of CFTR-mediated conductance. HEK 293T cells were exposed to forskolin (fsk; 5 µM) followed by ionomycin (1 µM) and the inhibitor $CFTR_{inh}$-172 (172; 10 µM). **(A)** Changes in current were measured using the fast whole cell configuration of the patch clamp technique. Data are plotted as mean changes in conductance plotted relative to the maximum current reached at +100 mV when cells were perfused with forskolin (fsk; black trace, n=6). The blue trace depicts a representative example of the change in conductance induced by ionomycin in a single cell. **(B)** Changes in conductance under the conditions indicated. Conductance was normalised to cell size. Data are mean ± SEM. *p<0.001 when compared to baseline. † p<0.005 when compared to initial forskolin exposure.

In Ca^{2+} imaging experiments, exposure of cells to ionomycin in the presence of forskolin caused a sharper rise in cytosolic Ca^{2+} followed by a more sustained increase in cytosolic Ca^{2+}, when compared to thapsigargin. This different profile in Ca^{2+} change could account for the faster and more complete loss of CFTR dependent conductance, as indicated by the lack of any $CFTR_{inh}$-172 sensitive conductance. This data further confirms an increase in Ca^{2+}, regardless of the source, can reduce CFTR activity.

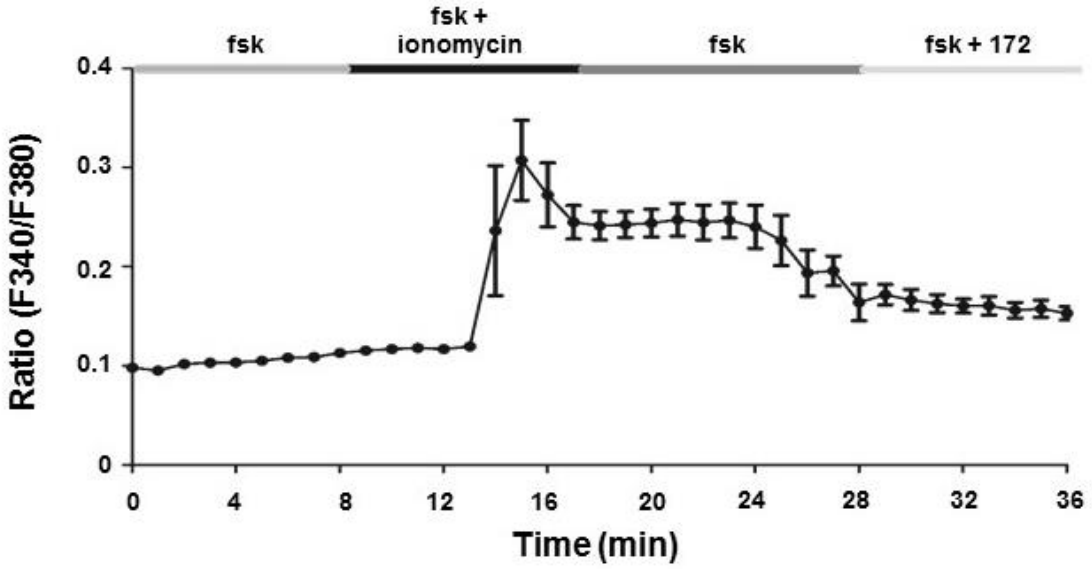

Figure 3.15. Ionomycin increases intracellular Ca^{2+}. Mean change in $[Ca^{2+}]_I$, as indicated by the 340/380 ratio, when cells were exposed to ionomycin (1 µM) in a bath solution containing 1mM Ca^{2+} (n=3).

3.6.2 The effect of lysosomal Ca^{2+} release on CFTR mediated conductance

Tobacco smoke induced Ca^{2+} release has been shown to arise from lysosomal stores (Rasmussen et al., 2014). In order to determine the effect of lysosomal Ca^{2+} release on CFTR, I tested the effect of the compound glycyl-L-phenylalanine-β-napthylamide (GPN), which releases Ca^{2+} from lysosomal stores (Haller et al., 1996).

Cells were treated with concentrations of GPN ranging from 100-500 µM. In patch clamp experiments, however, I could not test the effect of 500 µM GPN as this concentration was found to be toxic to cells in that I either lost the high resistance seal between the cell and the patch pipette or the cells died within minutes of exposure to GPN (n=5, data not shown).

Therefore, cells were exposed to 100 µM GPN. On average, cells showed an increase in conductance to 1.5 ± 0.4 nS/pF when stimulated with forskolin compared to a baseline of 0.04 ± 0.02 nS/pF (n=6, $p<0.05$, Fig. 3.16B). The conductance was reduced to 0.8 ± 0.2 nS/pF following a 10 minute exposure to 100 µm GPN in a bath solution containing 1 mM Ca^{2+}. After a further 10 minute wash out, the conductance was 0.7 ± 0.2 nS/pF. Addition of $CFTR_{inh}$-172 caused a reduction in the forskolin stimulated conductance to 0.4 ± 0.1 nS/pF (n=6, Fig. 3.16). However, the cells showed mixed responses to GPN; out of the 6 cells tested, 3 cells showed a further

activation of current that was sensitive to $CFTR_{inh}$-172 and 3 cells showed a reduction in CFTR dependent conductance. The mixture of responses seen made it difficult to draw any firm conclusions regarding the effect of lysosomal Ca^{2+} on CFTR.

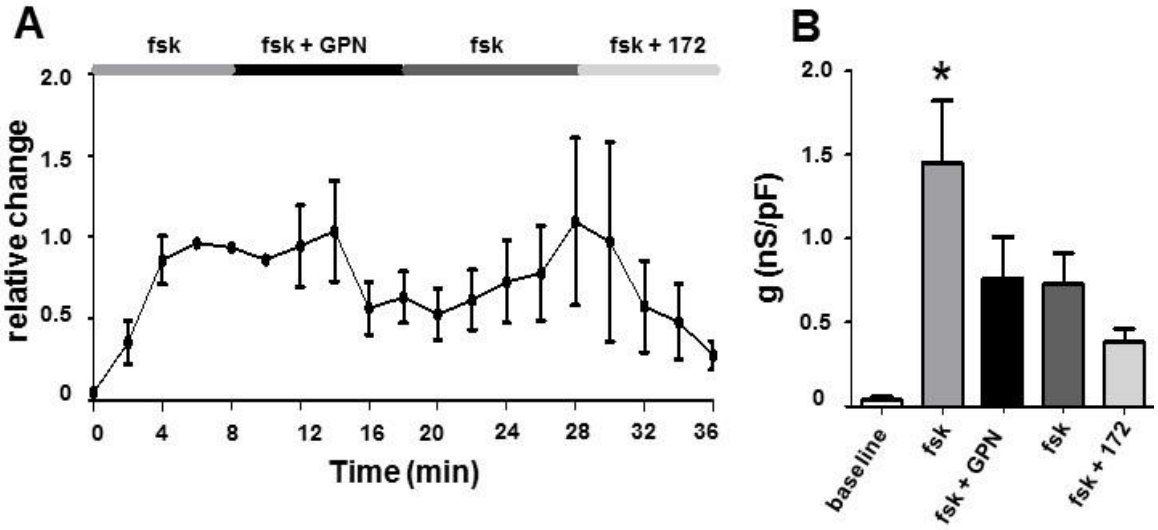

Figure 3.16. Effect of GPN on CFTR-mediated conductance. HEK 293T cells were exposed to forskolin (fsk; 5 µM) followed by the lysosomal Ca^{2+} release agent, glycyl-L-phenylalanine-β-napthylamide (GPN; 100 µM) and the inhibitor, $CFTR_{inh}$-172 (172; 10 µM). **(A)** Changes in current were measured using the fast whole cell configuration of the patch clamp technique. Data are plotted as mean changes in conductance plotted relative to the maximum current reached at +100 mV when cells were perfused with forskolin. **(B)** Changes in conductance under the conditions indicated. Conductance was normalised to cell size. Data are mean ± SEM (n=6). *p<0.05 when compared to baseline conductance.

Despite the mixed responses seen to GPN in patch clamp experiments, the release of lysosomal Ca^{2+} was found to cause a sustained increase in cytosolic Ca^{2+} when exposed to cells in a bath solution containing 1 mM Ca^{2+} (n=3, Fig. 3.17).

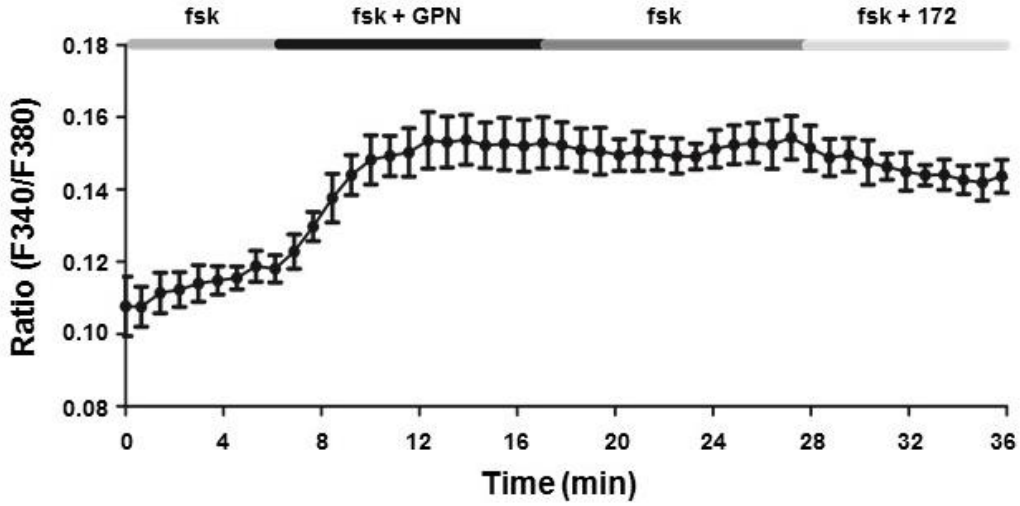

Figure 3.17. Effect of GPN on intracellular Ca^{2+}. Mean change in $[Ca^{2+}]_i$, as indicated by the 340/380 ratio, when cells were exposed to GPN (100 µM) in a bath solution containing 1mM Ca^{2+} (n=3).

3.6.3 The particulate fraction of cigarette smoke does not affect CFTR-mediated current

Tobacco smoke can be separated into two fractions, the volatile fraction, which comprises 95% of whole cigarette smoke and is composed of gaseous vapours and the particulate fraction, which forms the other 5% and is composed of lipid and water soluble particulates (Clunes et al., 2008). Rasmussen and colleagues (2014) have previously shown that exposure of cells to either the volatile phase alone or complete smoke results in a similar degree of internalisation of CFTR (Rasmussen et al., 2014).

To further investigate whether the particulate fraction affects CFTR, cells were exposed to a cigarette smoke condensate (CSC), which collects the lipid soluble phase. On average, cells showed an increase in conductance to 1.7 ± 0.7 nS/pF from a baseline of 0.03 ± 0.01 nS/pF (n=4, $p<0.05$, Fig.3.18B). Exposure of cells to 32 $\mu g ml^{-1}$ cigarette smoke condensate for 4 minutes caused little change in conductance (1.6 ± 0.6 nS/pF). The conductance dropped to 1.0 ± 0.6 nS/pF following wash out of the condensate and this remaining conductance was sensitive to inhibition to $CFTR_{inh}$-172, with the conductance being reduced to 0.4 ± 0.2 nS/pF (n=4; Fig. 3.18).

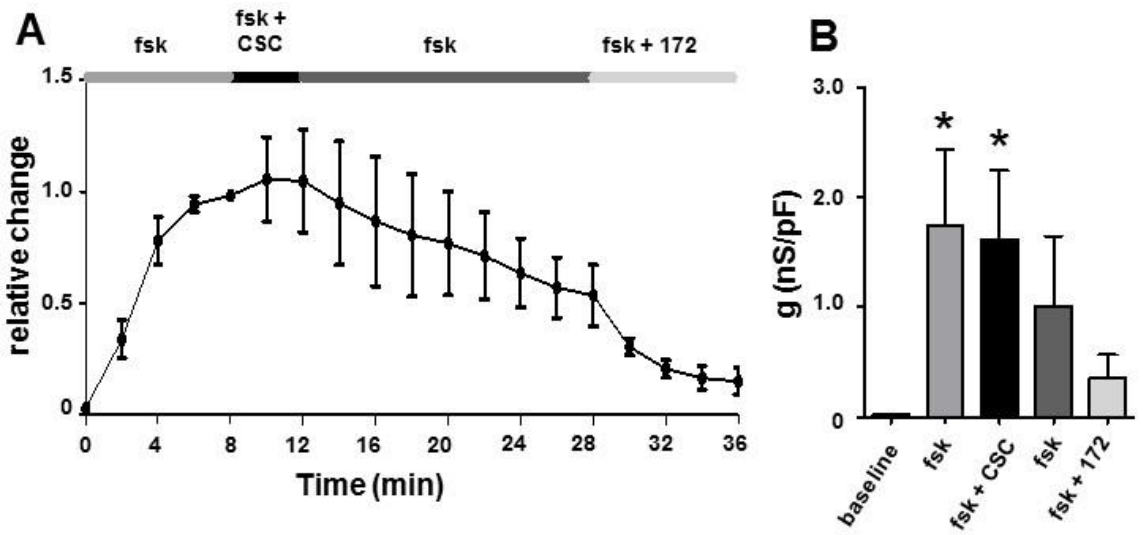

Figure 3.18. Effect of cigarette smoke condensate on CFTR-mediated conductance. HEK 293T cells were exposed to forskolin (fsk; 5 µM) followed by cigarette smoke condensate (CSC; 32 µgml^{-1}) and the inhibitor, CFTR$_{inh}$-172 (172; 10 µM). **(A)** Changes in current were measured using the fast whole cell configuration of the patch clamp technique. Data are plotted as mean changes in conductance plotted relative to the maximum current reached at +100 mV when cells were perfused with forskolin. **(B)** Changes in conductance under the conditions indicated. Conductance was normalised to cell size. Data are mean ± SEM (n=4). *p<0.05 when compared to baseline.

When the same concentration of cigarette smoke condensate was tested in Ca^{2+} imaging experiments, the condensate caused no substantial changes in cytosolic Ca^{2+} (n=3, Fig. 3.19). Furthermore, the profile of Ca^{2+} changes did not follow that of cells exposed to GPN, suggesting that the condensate did not cause Ca^{2+} release from lysosomes. These data suggested that for the condensate, the effect on CFTR-mediated conductance was not due to an increase in cytosolic Ca^{2+}.

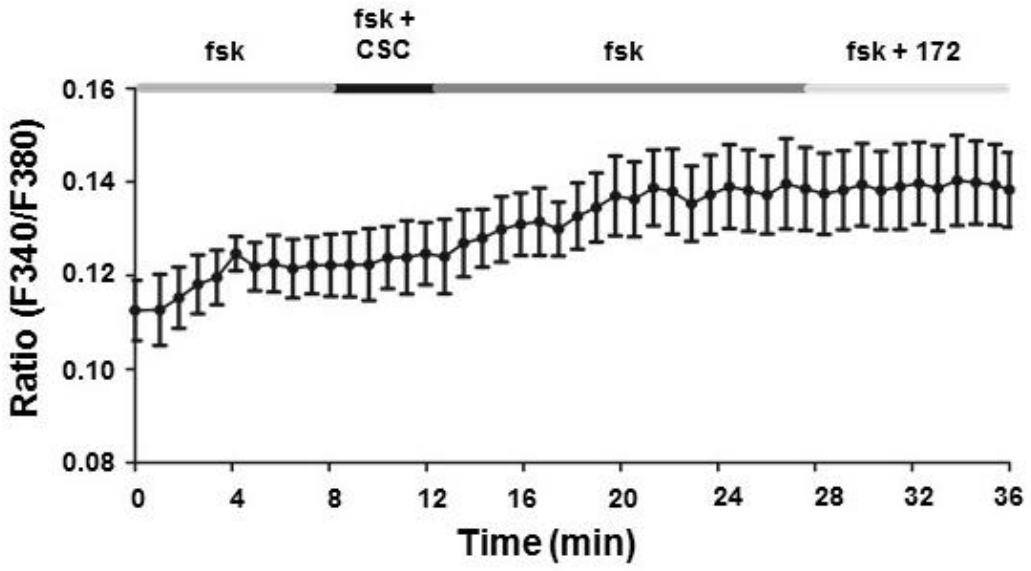

Figure 3.19. Effect of cigarette smoke condensate on intracellular Ca^{2+}. Mean change in $[Ca^{2+}]i$, as indicated by the 340/380 ratio, when cells were exposed to cigarette smoke condensate (CSC; 32 $\mu g ml^{-1}$) in a bath solution containing 1mM Ca^{2+} (n=3)

To further understand how cigarette smoke condensate affected CFTR-mediated conductance, experiments were carried out on vehicle treated cells. Cells were exposed to an equivalent concentration of DMSO (0.2% v/v) as that used for CSC. In patch clamp experiments, cells showed an increase in conductance to 1.4 ± 0.1 nS/pF when treated with forskolin compared to a baseline conductance of 0.1 ± 0.1 nS/pF (n=4, $p<0.05$, Fig. 3.20B). When exposed to DMSO for 4 minutes, the conductance showed a small decrease to 1.2 ± 0.2 nS/pF. Following wash out of DMSO, the conductance was reduced to 0.4 ± 0.2 nS/pF. This remaining conductance was reduced to 0.2 ± 0.1 nS/pF with $CFTR_{inh}$-172 (n=4, Fig. 3.20).

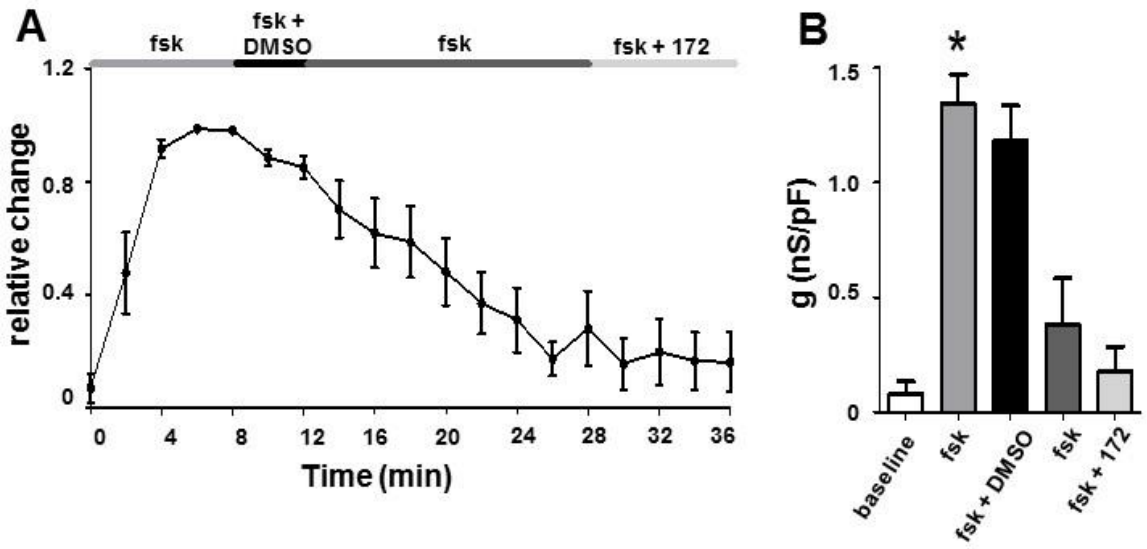

Figure 3.20. Effect of dimethyl sulfoxide on CFTR-mediated conductance. HEK 293T cells were exposed to forskolin (fsk; 5 µM) followed by dimethyl sulfoxide (DMSO; 0.2% v/v) and the inhibitor, $CFTR_{inh}$-172 (172; 10 µM) **(A)** Changes in current were measured using the fast whole cell configuration of the patch clamp technique. Data are plotted as mean changes in conductance plotted relative to the maximum current reached at +100 mV when cells were perfused with forskolin. **(B)** Changes in conductance under the conditions indicated. Conductance was normalised to cell size. Data are mean ± SEM (n=4). *p<0.01 when compared to baseline

Similar to Ca^{2+} imaging experiments with cigarette smoke condensate; DMSO had no substantial effect on cytosolic Ca^{2+} (n=3, Fig. 3.21). These experiments showed that exposure of cells to DMSO caused a similar loss of CFTR-mediated conductance and had no effect on cytosolic Ca^{2+}, suggesting that CSC alone has no effect on CFTR and the active compound against CFTR must be found in the volatile phase of tobacco smoke.

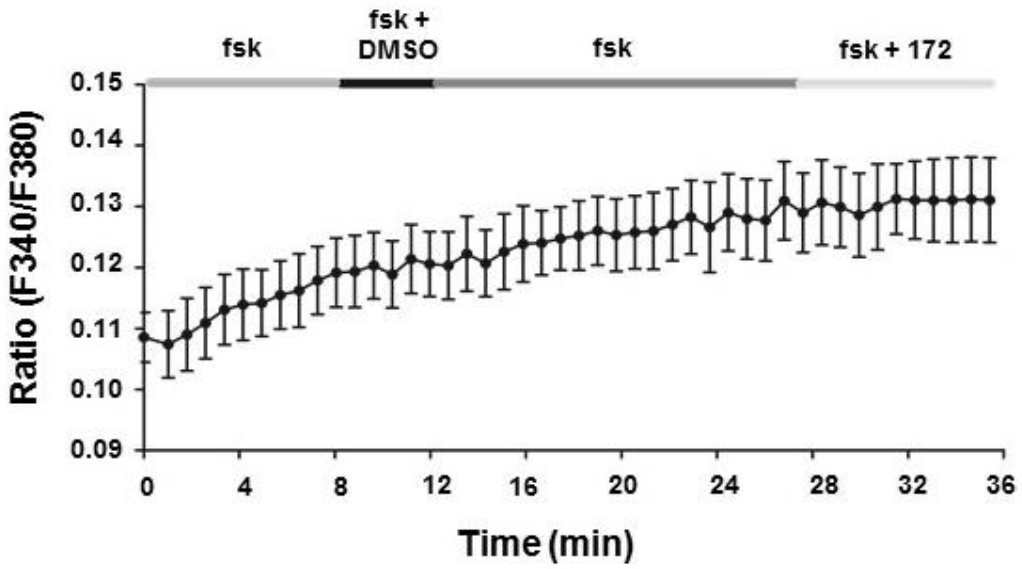

Figure 3.21. Effect of DMSO on intracellular Ca^{2+} and CFTR. Mean change in $[Ca^{2+}]_i$, as indicated by the 340/380 ratio, when cells were exposed to DMSO (0.2% v/v) in a bath solution containing 1mM Ca^{2+} (n=3).

3.6.4 The effect of physiological increases in cytosolic Ca^{2+} on CFTR-mediated conductance

To test whether physiological Ca^{2+} increases could also cause internalisation of CFTR, cells were exposed to ATP. On average, cells showed an increase in conductance with forskolin to 1.2 ± 0.3 nS/pF from a baseline of 0.1 ± 0.03 nS/pF (n=6, $p<0.05$, Fig. 3.22B). The conductance was reduced to 0.7 ± 0.2 nS/pF following addition of ATP. After a further 10 min wash out, the conductance was reduced to 0.4 ± 0.1 nS/pF (n=6, $p<0.05$, Fig. 3.22B). Addition of $CFTR_{inh}$-172 inhibited the forskolin stimulated conductance to 0.2 ± 0.1 nS/pF (n=6, $p<0.05$, Fig. 3.22B).

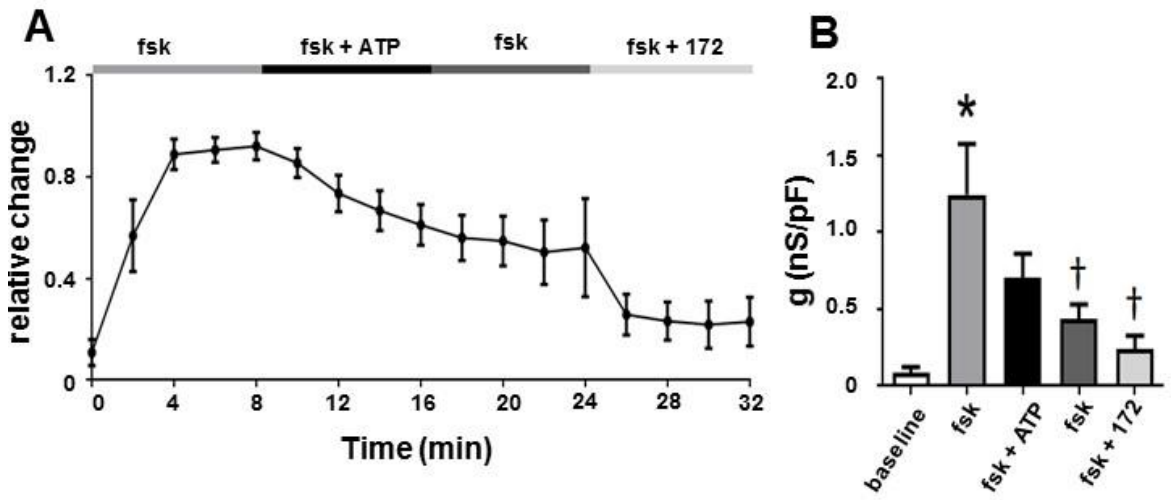

Figure 3.22. Effect of ATP on CFTR-mediated conductance. (A) Changes in current were measured using the fast whole cell configuration of the patch clamp technique. Data are plotted as mean changes in conductance plotted relative to the maximum current reached at +100 mV when cells were perfused with forskolin. **(B)** Changes in conductance under the conditions indicated. Conductance was normalised to cell size. Data are mean ± SEM (n=6). *p<0.05 when compared to baseline. † p<0.005 when compared to initial forskolin exposure.

However, the individual responses to ATP seen could be split into 3 groups. Out of the 6 cells tested, 1 cell responded by showing little change in conductance after exposure to ATP. 3 cells responded to ATP by showing a gradual decrease in CFTR conductance and 2 cells showed a transient decrease, with the conductance starting to recover after wash out of ATP (Fig. 3.23).

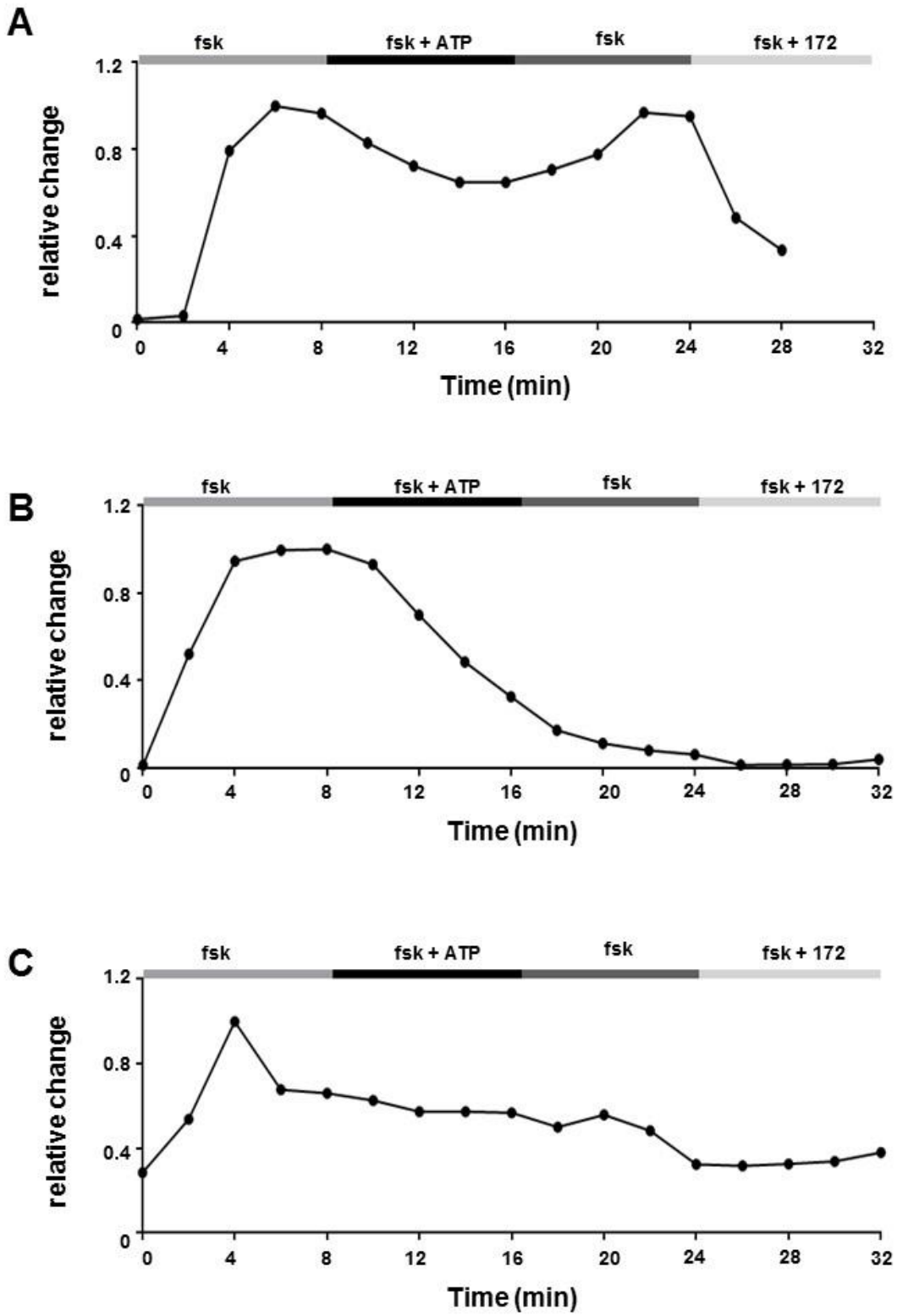

Figure 3.23. Changes in CFTR conductance seen following exposure to ATP. Representative traces showing the different responses seen in CFTR activity after addition of ATP. **(A)** 2 cells showed a transient decrease in CFTR conductance **(B)** 3 cells showed a reduction in conductance following exposure to ATP and **(C)** 1 cell responded by showing little change in conductance after exposure to ATP.

When cells were exposed to ATP with forskolin in Ca^{2+} imaging experiments, there was a transient increase in cytosolic Ca^{2+}, with the Ca^{2+} being released from ER stores (Fig. 3.24). The transient response was likely due to the breakdown of ATP, or the desensitisation of the $P2Y_2$ receptor (Lazarowski and Boucher, 2001).

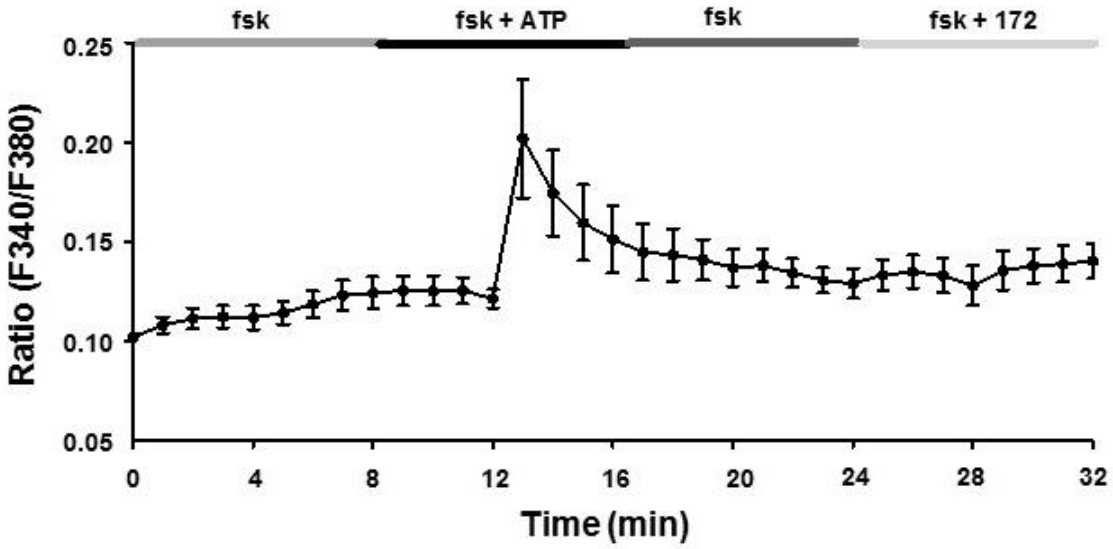

Figure 3.24. Effect of ATP on intracellular Ca^{2+}. Mean change in $[Ca^{2+}]_I$, as indicated by the 340/380 ratio, when cells were exposed to ATP (100 µM) in a bath solution containing 1mM Ca^{2+} (n=3).

3.7 An increase in cytosolic Ca^{2+} does not change CFTR open channel probability in lipid bilayers

The data presented thus far has indicated that an increase in cytosolic Ca^{2+} causes a decrease in CFTR dependent conductance. Further, the data suggested that this loss of conductance was due to the removal of functional channels from the membrane via dynamin dependent endocytosis. However, it could be argued that the loss of CFTR activity could be due to a decrease in the open state probability of the channel (P_o). To test whether Ca^{2+} was indeed causing a change in the P_o of CFTR, open probability was measured in purified CFTR incorporated into lipid bilayers (Aleksandrov and Riordan, 1998, Aleksandrov et al., 2002). Experiments were conducted by Dr Aleksandrov in the Riordan lab at the University of North Carolina at Chapel Hill.

Single channel kinetics were measured after exposing bilayers to solutions with or without Ca^{2+} on the cytoplasmic side of CFTR. On average, these experiments

showed that there was no significant variation in the conductance of the channel (14.1 pS in Ca^{2+} free vs 14.2 pS with Ca^{2+}), the open probability (0.81 in Ca^{2+} free vs 0.79 with Ca^{2+}), the time the channel was open (190 ms in Ca^{2+} free vs 200 ms with Ca^{2+}) or the closed time (45 ms in Ca^{2+} free vs 55 ms with Ca^{2+}; Fig. 3.25). Thus, the data show that addition of Ca^{2+} to the cytoplasmic side of CFTR causes no differences in single channel kinetics; suggesting Ca^{2+} increases do not affect CFTR function.

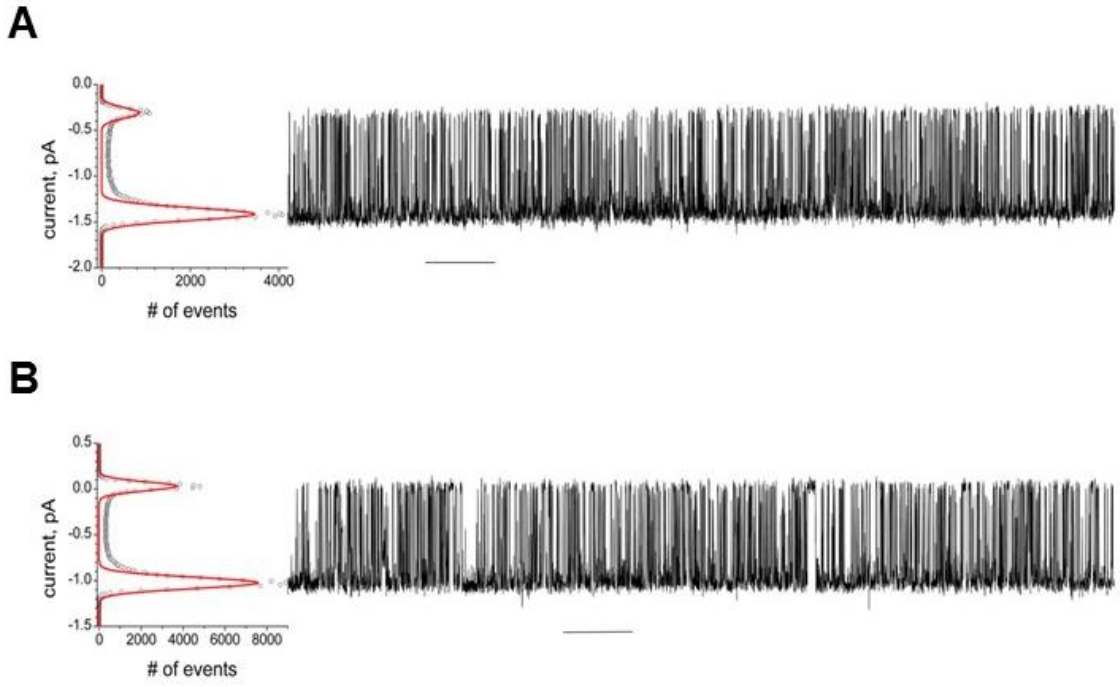

Figure 3.25. An increase in cytosolic Ca^{2+} does not affect CFTR single channel function. Single channel function (on the right) and all points histogram (on the left) used to calculate single channel conductance and open state probability for CFTR at 37°C in **(A)** Ca^{2+} free conditions and **(B)** after addition of 1.5 mM Ca^{2+} to the cytoplasmic side of the channel. Scale bar represents 10s interval. Experiments were performed by Dr Aleksandrov at the University of North Carolina, Chapel Hill.

3.8 Correlating changes in cytosolic Ca^{2+} to changes in CFTR-mediated conductance

To further understand how changes in cytosolic Ca^{2+} affect CFTR, a comparison of the agonists used to increase cytosolic Ca^{2+} was carried out, in terms of their effect on CFTR-mediated conductance. When the data was collated, ionomycin caused the biggest increase in Ca^{2+}, determined by the maximum change induced in the 340/380 ratio, as well as the biggest magnitude of response, determined by the change in the

area under the curve. When cells were exposed to thapsigargin in a nominally Ca^{2+} free solution or ATP, a bigger change in the 340/380 ratio was induced by ATP. However, the magnitude of the response induced by thapsigargin and ATP were similar (Fig. 3.26). A caveat to the data, however, is that the changes in the Fura-2 ratio were not calibrated, thus any changes in Fura-2 ratio measured do not reflect absolute changes in cytosolic Ca^{2+}.

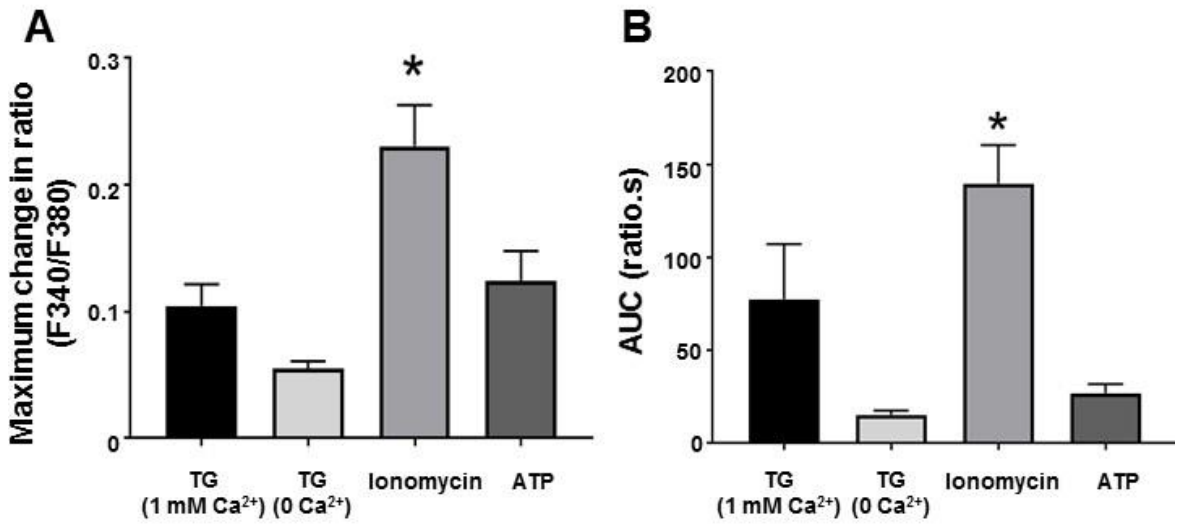

Figure 3.26. Summary diagram comparing the effect of various Ca^{2+} agonists on cytosolic Ca^{2+}. The agonists detailed were compared by analysing changes they induced in the **(A)** maximum change in 340/380 ratio calculated using the difference in the Fura-2 AM ratio before addition of the agonist and at the end of the exposure period. **(B)** Area under the curve (AUC) was also used as a comparison and was calculated for the duration of exposure to each agonist. Data are mean ± SEM (n=3). *p<0.05 compared to TG (1 mM Ca^{2+}).

The effects of the various agonists were also compared in terms of their effect on CFTR-mediated conductance. This was determined by calculating the percentage decrease induced in the maximal forskolin stimulated conductance. Similar to the trends seen in the Ca^{2+} imaging experiments, ionomycin caused the biggest inhibition in CFTR-mediated conductance, causing the conductance to fall by 5.1 ± 0.7% per minute (Fig. 3.27). Earlier analyses carried out showed that thapsigargin in either a Ca^{2+} containing or Ca^{2+} free solution could cause a significant reduction in CFTR-mediated conductance. These agonists both induced a similar loss of CFTR-mediated conductance, with 3.2 ± 0.4% in Ca^{2+} containing solution and 2.5 ± 0.4% in the absence of Ca^{2+}. Patch clamp experiments showed the loss in CFTR-mediated conductance induced by ATP was significant. However, ATP caused a similar percentage inhibition per minute (3.3 ± 0.5%) to cells that were exposed to

thapsigargin in a Ca^{2+} containing solution. Taken together with the data from the Ca^{2+} imaging experiments, these data suggest that the rate at which a Ca^{2+} agonist causes inhibition of CFTR-mediated conductance may be of importance in determining whether an increase in $[Ca^{2+}]_i$ is able to induce a significant loss of CFTR-mediated conductance.

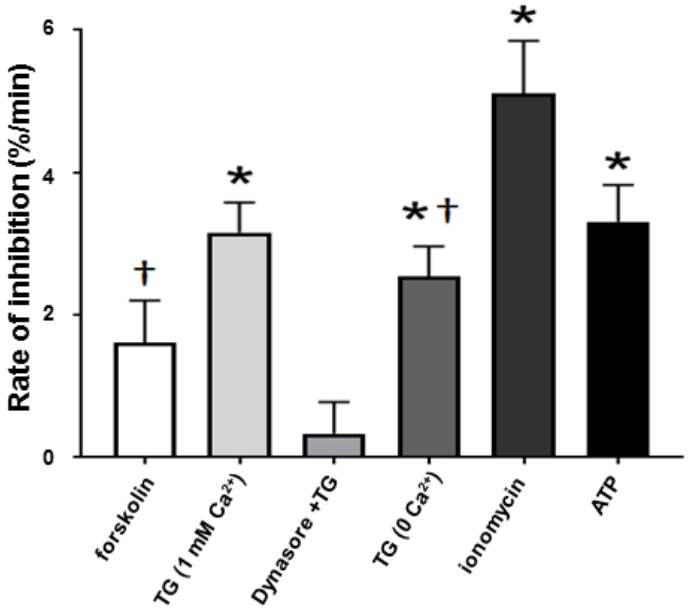

Figure 3.27. The effect of various Ca^{2+} agonists on CFTR-mediated conductance. The effect of various agonists on CFTR-mediated conductance, determined by the percentage inhibition per minute of forskolin stimulated conductance induced by each agonist. Data are mean ± SEM. *p<0.05 compared to dynasore + TG † p<0.005 when compared to ionomycin.

To further understand the relationship between the change in cytosolic Ca^{2+} and CFTR-mediated conductance, the correlation between the two variables was tested. Regression analysis between the rate the inhibition and both the maximum change in Fura-2 AM ratio and area under the curve showed that changes in cytosolic Ca^{2+} were indeed related to loss of CFTR-mediated conductance (Fig. 3.28). Thus, the data from this chapter indicated an increase in cytosolic Ca^{2+} caused a loss of CFTR-mediated conductance, with the magnitude of the increase in Ca^{2+} being related to the magnitude of the loss of CFTR-mediated conductance.

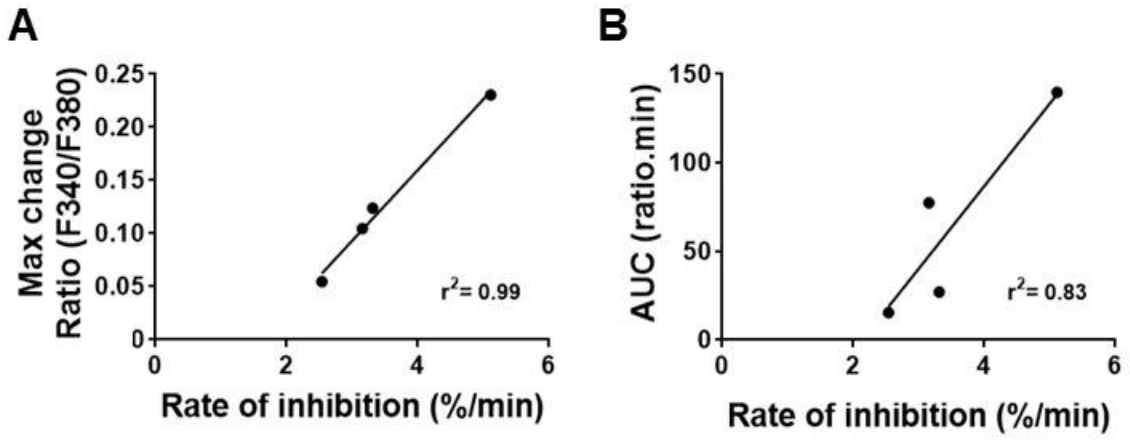

Figure 3.28. Correlation between changes in cytosolic Ca^{2+} and inhibition of CFTR-mediated conductance. The relationship between increases in cytosolic Ca^{2+} and loss of CFTR-mediated conductance was assessed by testing the correlation between the average rate of inhibition and **(A)** maximum change in Fura-2 AM ratio and **(B)** area under the curve (AUC) induced by each agonist.

3.9 Discussion

Tobacco smoke has been shown to cause internalisation of CFTR through a smoke-induced increase in cytosolic Ca^{2+} (Rasmussen et al., 2014). The data presented in this chapter showed that increases in cytosolic Ca^{2+}, regardless of the source, caused a decrease in CFTR-mediated conductance, perhaps via internalisation of the channel. Therefore, the data is consistent with the work from Rasmussen et al., (2014).

Increases in $[Ca^{2+}]_i$ induced by the SERCA pump inhibitor, thapsigargin, showed that this lead to a decrease in CFTR-mediated conductance. The decrease in conductance caused by thapsigargin was further supported by the loss of CFTR-mediated conductance by ionomycin. The change in Ca^{2+} induced by ionomycin was larger than that of thapsigargin and likewise, ionomycin induced a greater loss of conductance. Interestingly, Bargon and colleagues (1992) found that exposure of colon carcinoma (HT-29) cells to agents that increased the intracellular concentration of divalent cations including Ca^{2+}, caused a reduction in CFTR mRNA and protein in a time and dose dependent manner (Bargon et al., 1992). Furthermore, Bozoky and colleagues (2017) found that an increase in cytosolic Ca^{2+} caused a reduction CFTR activity. The researchers also found that the effect of an increase in cytosolic Ca^{2+} on CFTR depended on the phosphorylation status of CFTR. Similar to the findings detailed in this chapter, Bozoky et al., (2017) found that phosphorylated CFTR showed a decrease in activity when exposed to an increase in cytosolic Ca^{2+}. However, in the absence of PKA phosphorylation, an increase in $[Ca^{2+}]_i$ caused an increase in CFTR activity (Bozoky et al., 2017).

In the present study, when cells were exposed to thapsigargin after exposure to forskolin, the whole cell conductance declined. However, Billet and Hanrahan (2013) have suggested that there may be a role for CFTR to act as a Ca^{2+} activated Cl^- channel (Billet and Hanrahan, 2013). Indeed, Billet and colleagues (2013) found that there was a Ca^{2+} dependent component to the activation of CFTR. The researchers found that activation of the M3 muscarinic receptor via carbachol in baby hamster kidney (BHK) cells caused stimulation of CFTR (Billet et al., 2013). Further support comes from the observation that the efficacy of agents thought to increase Cl^- secretion through CaCC is lowered in CF. Indeed, CF pig nasal turbinates show a reduction in fluid secretion in response to stimulation with carbachol (Cho et al.,

2011). Thus, Billet and Hanrahan (2013) suggested that the effect of Ca^{2+} may be cell type dependent (Billet and Hanrahan, 2013). However, investigating the effect of a muscarinic receptor agonist may be of value in further understanding how changes in cytosolic Ca^{2+} modulate CFTR-mediated conductance.

The data in this thesis suggested that extracellular Ca^{2+} was not necessary for the loss of CFTR-mediated conductance, and therefore store operated Ca^{2+} entry does not need to occur. Similarly, Rasmussen and colleagues have previously shown that if cells were exposed to cigarette smoke in the absence of extracellular Ca^{2+}, the increase in $[Ca^{2+}]_i$ was similar to that seen when Ca^{2+} was present (Rasmussen et al., 2014). These data suggested a transient increase in Ca^{2+} was sufficient to cause CFTR internalisation. Thus, the data in this chapter also supports the finding that Ca^{2+} release from internal stores alone is sufficient to cause a reduction in CFTR at the membrane.

To test the effect of a physiological agonist on CFTR-mediated conductance, cells were exposed to ATP. ATP is usually released in the airways in response to the mechanical stresses seen during breathing; the subsequent effect is the release of Ca^{2+} from endoplasmic reticulum stores (Paradiso et al., 2001). Exposure to ATP in patch clamp experiments induced a variety of responses in terms of CFTR conductance. A proportion of the cells showed a transient loss of conductance; it is known that stimulation of the $P2Y_2$ receptor causes activation of the G_q pathway and the activation of PKC via this pathway has been shown to result in the phosphorylation of CFTR, through potentiating the effect of PKA (Paradiso et al., 2001). Furthermore, ATP is broken down to adenosine by ectonucleotidases which would stimulate CFTR activity in a autocrine/paracrine manner through the action of adenosine on the A_{2B} receptor (Lazarowski et al., 2004). Likewise, the activation of the A_{2B} receptor has been shown to be coupled to cAMP accumulation via G_s (Cooper et al., 1997, Gao et al., 1999). Therefore, it could be that the increase in $[Ca^{2+}]_i$ induced by ATP caused a loss in conductance, but the recovery was due to one of the effects listed above. The majority of cells tested showed some decrease in conductance, either as an initial decrease followed by a plateau or a gradual decline in conductance. This suggests that the increase in cytosolic Ca^{2+} caused by ATP may have overwhelmed the ability of the various mechanisms listed above to prevent a big loss in conductance. Interestingly, activation of A_{2B} receptors in HEK 293 cells

has been shown to result in the activation of the extracellular signal regulated kinases (ERK) 1/2 pathway (Gao et al., 1999). This is of significance as Xu and colleagues (2015) showed that activation of the MEK/ERK pathway can cause CFTR internalisation (Xu et al., 2015).

As it has been previously suggested that smoke induced Ca^{2+} release is from the lysosomal store, the lysosomal Ca^{2+} release agent, GPN, was tested. GPN is hydrolysed by the lysosomal cathepsin C which causes osmotic swelling of the lysosomal membrane and allows for leak of small molecular weight substances including Ca^{2+} (Patel and Docampo, 2010, Kilpatrick et al., 2013). Exposure to GPN in HEK 293 cells was found to cause a slow sustained change in cytosolic Ca^{2+}, which induced variable effects on forskolin stimulated increases in CFTR conductance in patch clamp experiments. It is possible that release of substances from the lysosome was toxic to the cell and so caused a loss of the high resistance seal or the variability in the responses seen.

Overall, when all the Ca^{2+} agonists were compared in terms of their effect on CFTR-mediated conductance, the data showed that the rate at which agonists induced a loss of CFTR-mediated conductance was an important determinant of whether there was a significant loss of conductance. Furthermore, increases in $[Ca^{2+}]_I$, determined by changes in Fura-2 ratio,, were correlated to the loss of CFTR-mediated conductance. This suggests, albeit indirectly, that cytosolic Ca^{2+} levels can directly affect the activity of CFTR. Conversely, it has been suggested that CFTR itself can regulate Ca^{2+} influx. CFTR has been shown to prevent the insertion of Orai1 channels into the membrane, which causes a net effect of decreasing Ca^{2+} entry into the cell during store operated Ca^{2+} entry. This effect is lost in CF which allows for the creation of more STIM1/Orai1 complexes during store-operated Ca^{2+} entry and causes a larger influx of Ca^{2+} into the cells (Balghi et al., 2011). If cigarette smoke exposure causes the same effect i.e. the loss of Orai1 channel regulation, CFTR loss induced by the smoke induced increase in Ca^{2+} would create a positive feedback loop whereby the loss of CFTR would allow for further entry of Ca^{2+} into the cells due to the failure of Orai1 channel regulation by CFTR.

The data suggested a Ca^{2+} dependent decrease in conductance was due to a decrease in functional CFTR channels present at the membrane, via dynamin

dependent endocytosis, and no change in channel gating. This was evidenced by the ability of dynasore, a dynamin GTPase inhibitor (Macia et al., 2006), to prevent a Ca^{2+}-induced decrease in conductance. Dynamin is the primary protein involved in scission of clathrin coated pits from the cell membrane and dynasore prevents the GTPase activity of dynamin by preventing the hydrolysis of GTP (Hinshaw, 2000). Previous studies have shown that dynasore is able to prevent the endocytosis of CFTR under resting conditions, suggesting that the initial mechanism by which CFTR is internalised resembles that of the normal trafficking process (Young et al., 2009). Interestingly, Ca^{2+} increases have been linked to regulating the balance between endocytosis and exocytosis. In synaptosomes, Marks et al., (1998) showed that an increase in Ca^{2+} was able to cause endocytosis at concentrations lower than that needed for exocytosis (Marks and McMahon, 1998). Furthermore, in nerve terminals, an increase in cytosolic Ca^{2+}, and binding of Ca^{2+} to calmodulin, has been shown to be linked to the initiation of endocytosis. The researchers also found that increasing the rate of Ca^{2+} influx was linked to a corresponding increase in the rate of endocytosis (Wu et al., 2009). However, a caveat to my data was that Ca^{2+} imaging experiments suggested that the effect of dynasore could be in part, due to a reduction in the increase in cytosolic Ca^{2+} induced by thapsigargin. Thus, further experiments would be needed to definitively conclude that thapsigargin was inducing the internalisation of CFTR.

Experiments carried out to measure the single channel gating kinetics showed that there was no significant change in the conductance, open probability, open time or closed time when bilayers expressing the purified channel were exposed to an increase in cytosolic Ca^{2+}. Similar findings were reported by Clunes et al., (2012) who carried out the same experiments in bilayers that had been exposed to cigarette smoke (Clunes et al., 2012). The data supports the evidence that either exposure to smoke or an increase in cytosolic Ca^{2+} causes a reduction in CFTR via an effect on the number of channels present on the membrane and not the gating kinetics. However, Raju and colleagues showed that exposure of inside out patches from HEK 293 cells to the cigarette smoke component, acrolein, was able to cause a reduction in the open probability of CFTR (Raju et al., 2013). It is possible that testing the effect of one component of smoke alone, however, is not sufficient to gage the effect whole cigarette smoke would have on CFTR gating. The same group has also shown that exposure to cigarette smoke extract to HEK 293 cells causes a reduction in the open

probability of CFTR (Raju et al., 2017). However, the researchers used cigarette smoke extract, not whole phase cigarette smoke for these studies. Furthermore, they found that acute exposure of cells to extract had no effect on CFTR. Cigarette smoke condensate, used in this study, is prepared by capturing the particulate fraction in DMSO. However, cigarette smoke extract, is prepared by bubbling cigarette smoke into either media or buffer solution (Tamashiro et al., 2009). It is possible that because cigarette smoke extract only captures a fraction of smoke, it takes longer for it to be effective. Indeed, the data detailed in section 3.6.3 (discussed below) showed that acute exposure to cigarette smoke condensate had no effect on CFTR conductance.

Cigarette smoke condensate captures the particulate fraction of smoke, which comprises 5% of whole smoke. When the condensate was tested, cells showed no substantial decrease in CFTR-mediated conductance compared to vehicle treated cells. Rasmussen and colleagues previously showed that CFTR internalisation was the same whether they used whole cigarette smoke or the volatile phase only, suggesting that the particulate fraction has no effect on CFTR internalisation (Rasmussen et al., 2014). However, as mentioned above, there is conflicting evidence as to the effect of cigarette smoke extract on CFTR. Welsh and colleagues (1983) showed that exposure of CS to canine tracheal cells caused a reduction in Cl^- mediated short circuit current. In contrast to the data detailed in this chapter, Moran and colleagues (2014) found that exposure to CSC caused an inhibition of CFTR-mediated conductance (Moran et al., 2014). Other researchers have previously showed that cigarette smoke extract is able to induce a decrease in CFTR protein. For example, cigarette smoke extract has been shown to cause a reduction in CFTR short circuit current and protein (Kreindler et al., 2005, Cantin et al., 2006). Furthermore, the deleterious effects of CS extract are not limited to CFTR; the free radicals within the CS extract have been shown to cause an opening of hemichannels which propagate Ca^{2+} increases between cells (Ramachandran et al., 2007). As there is no standardised protocol for the development of cigarette smoke condensate and the preparation varies between labs, it is possible different extracts capture different constituents of smoke, accounting for the differing effects seen.

When cells were exposed to a relatively high concentration of DMSO, there was a large decrease in CFTR-mediated conductance. However, Ca^{2+} imaging experiments

indicated there was little change in cytosolic Ca^{2+}. Tamagnini and colleagues showed that pre-treatment with a low concentration (0.05%) of DMSO had permanent effects on excitable cells such as reducing action potential output, under patch clamp conditions. Furthermore, the researchers found the effects remained after wash out of the DMSO (Tamagnini et al., 2014). It has also been suggested that DMSO is able to cause changes in the structure of membranes, including changing the orientation of components such as cholesterol (de Ménorval et al., 2012). Indeed, it has been suggested that changing cholesterol in the plasma membrane can cause the redistribution of CFTR in primary human bronchial epithelial cells (Abu-Arish et al., 2015). It could therefore be possible that although there was little change in $[Ca^{2+}]_i$ upon the addition of DMSO, there was a large effect on conductance due to non-specific effects of DMSO.

In summary, the findings of this chapter are;

- An increase in $[Ca^{2+}]_i$ caused a significant reduction in CFTR-mediated conductance.
- An increase in $[Ca^{2+}]_i$ caused an inhibition of CFTR-mediated conductance in the absence of extracellular Ca^{2+}. These data suggested that a transient increase in $[Ca^{2+}]_i$, from internal stores is sufficient to induce loss of CFTR-mediated conductance.
- The different agonists used to increase cytosolic Ca^{2+} indicated that the magnitude of the increase in $[Ca^{2+}]_i$ correlated to the degree of CFTR-mediated conductance lost.
- An increase in $[Ca^{2+}]_i$ causes internalisation of CFTR via dynamin-dependent endocytosis and has no effect on the gating of channels present at the membrane.

Chapter 4.0 An Increase in Cytosolic Ca^{2+} Causes CFTR Internalisation via the MEK/ERK Pathway and the Activation of Calcineurin

4.1 Introduction

The findings from the previous chapter showed that an increase in cytosolic Ca^{2+} induced a decrease in CFTR-mediated conductance via internalisation of the channel. CFTR expression at the plasma membrane is tightly regulated, once removed from the membrane; much of the protein is recycled back to the plasma membrane via recycling endosomes (Farinha et al., 2013). As discussed in section 1.4.2, CFTR is routed to late endosomes or lysosomes for degradation, if not recycled back to the plasma membrane (Gentzsch et al., 2004). Previous research from our lab has shown that tobacco smoke exposure does not cause CFTR to be routed to the lysosome for degradation, due to smoke induced disruption of lysosomal function (Rasmussen et al., 2014). Therefore, I sought to further understand the trafficking process undertaken by CFTR once exposed to an increase in cytosolic Ca^{2+}. Further to the internalisation route taken by CFTR following cigarette smoke exposure, our lab has shown that activation of the mitogen activated protein kinase (MEK)/ extracellular signal related kinase (ERK) pathway plays a role in the smoke-induced internalisation of the channel (Xu et al., 2015). Cigarette smoke has been shown to cause the activation of the MEK/ERK pathway, however, previous studies had not identified the MEK/ERK pathway as having a role in regulating plasma membrane expression of CFTR (Mercer and D Armiento, 2006). Thus, I tested whether this pathway could regulate CFTR expression after an increase in cytosolic Ca^{2+}. As the experiments carried out in chapter 3 studied the effect of an increase in cytosolic Ca^{2+} on phosphorylated CFTR, the effect of the phosphorylation status on CFTR internalisation was also investigated. In this chapter, I used confocal microscopy to further understand the movement of CFTR following an increase in cytosolic Ca^{2+} induced by either Ca^{2+} agonists or cigarette smoke. Furthermore, I sought to identify the mechanism by which an increase in cytosolic Ca^{2+} affects CFTR expressed at the plasma membrane. Many of the studies cited above have used HEK 293 cells as a simpler model system that replicated the signalling pathways found in human airway epithelial cell lines, such as the MEK/ERK pathway. Thus, I used HEK 293T cells to further investigate the mechanism behind how

increases in cytosolic Ca^{2+} affect CFTR. Primary airway cells were then used to validate if the same signalling pathways were affected as those in HEK 293 cells.

4.2 Cigarette smoke exposure causes internalisation of CFTR

Experiments detailed in the previous chapter showed that an increase in cytosolic Ca^{2+} caused a reduction in CFTR-mediated conductance via internalisation of the channel. As a control for the Ca^{2+} agonists, cigarette smoke, which has been previously shown to cause an increase in cytosolic Ca^{2+} and CFTR internalisation via confocal microscopy, was used as an agonist for internalisation (Rasmussen et al., 2014).

HEK 293T cells were exposed to one full research grade cigarette under thin film conditions and incubated for 30 minutes in media before fixation (detailed in section 2.7). For these experiments, cells were co-transfected with CFTR and STIM1. On average, exposure to cigarette smoke caused an increase in intracellular fluorescence of CFTR to 4.2 ± 0.2 A.U (n=228 cells, $p<0.001$), compared to 1.0 ± 0.04 A.U (n=227 cells) in cells exposed to air. Likewise, the plasma membrane fluorescence of CFTR in cells exposed to smoke showed a decrease to 0.7 ± 0.2 A.U compared to 1.0 ± 0.03 A.U in cells treated with air ($p<0.001$, Fig. 4.01).

Experiments in the lab have previously indicated that smoke exposure caused the movement of CFTR to the endoplasmic reticulum (Marklew, 2016). To further confirm this observation, cells were co-transfected with stromal interaction molecule 1 (STIM1) which acts as a Ca^{2+} sensor in the endoplasmic reticulum. Specifically, STIM1 couples to and activates Orai1 channels on the plasma membrane upon depletion of the endoplasmic reticulum store to form Ca^{2+} release activated channels (Baba et al., 2006). Exposure to smoke caused an increase in co-localisation of CFTR and STIM1 to 51.7 ± 2.3% ($p<0.001$) compared 37.7 ± 1.9% in air exposed cells.

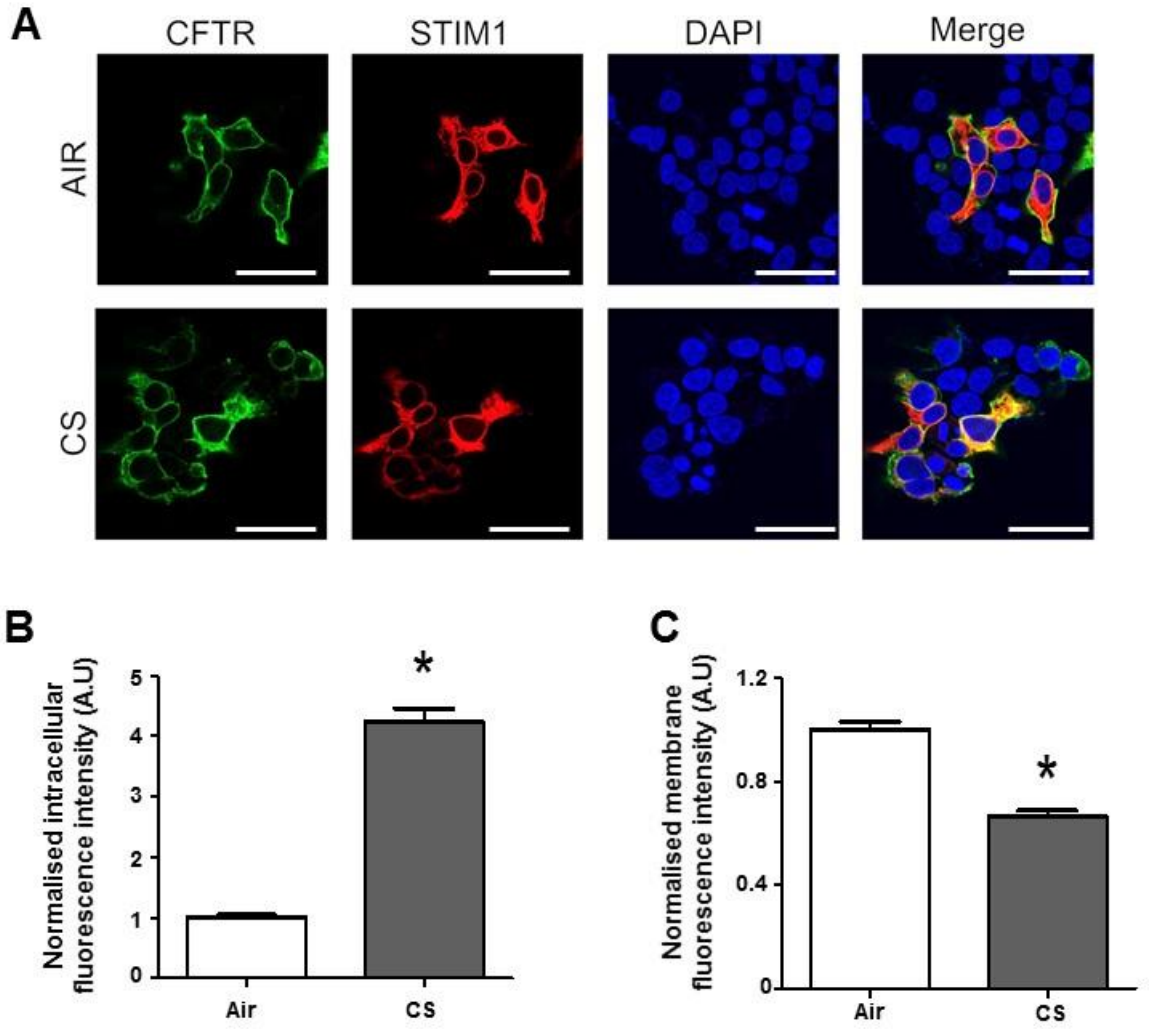

Figure 4.01. Exposure to the cigarette smoke causes internalisation of CFTR. (A) Representative images showing the effect of either 13 puffs of air (n=228 cells) or cigarette smoke (CS; n=227 cells) as indicated. HEK 293 cells were transfected with GFP CFTR (green) and STIM1 mCherry (red). Nuclei were counter stained with DAPI (blue). Changes in **(B)** intracellular and **(C)** membrane fluorescence. Data are mean ± SEM (coverslips were imaged in duplicate from 3 independent experiments). Scale bar represents 50 µm. *p<0.001 compared to air exposed cells.

4.3 Increases in cytosolic Ca^{2+} cause internalisation of CFTR

4.3.1 Exposure to the SERCA pump inhibitor thapsigargin, causes internalisation of CFTR but not Ano1

Data in the previous chapter showed thapsigargin caused a reduction of CFTR-mediated conductance via a dynamin-dependent mechanism. Therefore, the effect of thapsigargin and dynasore on CFTR internalisation was tested.

Using same protocol as earlier, cells were co-transfected with CFTR and STIM1. On average, HEK 293 cells treated with vehicle had an internal fluorescence of 1.0 ± 0.1 A.U (n=201 cells) for CFTR. Exposure to 200 nM thapsigargin for 30 minutes caused an increase in internal fluorescence to 4.5 ± 0.2 A.U (n=199 cells, $p<0.005$) whereas cells pre-treated with 80 µM dynasore showed little increase in fluorescence (1.2 ± 0.1 A.U; n=238 cells, $p<0.001$) after exposure to thapsigargin. Likewise, plasma membrane fluorescence of CFTR in vehicle treated cells had an average fluorescence of 1.0 ± 0.03 A.U. Cells exposed to thapsigargin showed a reduction in plasma membrane fluorescence to 0.6 ± 0.02 A.U whereas cells treated with dynasore showed no loss in membrane fluorescence (1.0 ± 0.03 A.U, $p<0.001$, Fig. 4.02). Therefore, pre-treatment with dynasore completely prevented the thapsigargin-induced internalisation of CFTR.

As with earlier experiments, co-localisation between CFTR and STIM1 was quantified. On average, cells treated with vehicle had a percentage co-localisation of 20.5 ± 1.7% whereas cells exposed to thapsigargin showed an increase in co-localisation to 44.5 ± 2.6% ($p<0.001$). Pre-treatment of cells with dynasore caused a reduction in co-localisation to 32.3 ± 2.1% ($p<0.001$).

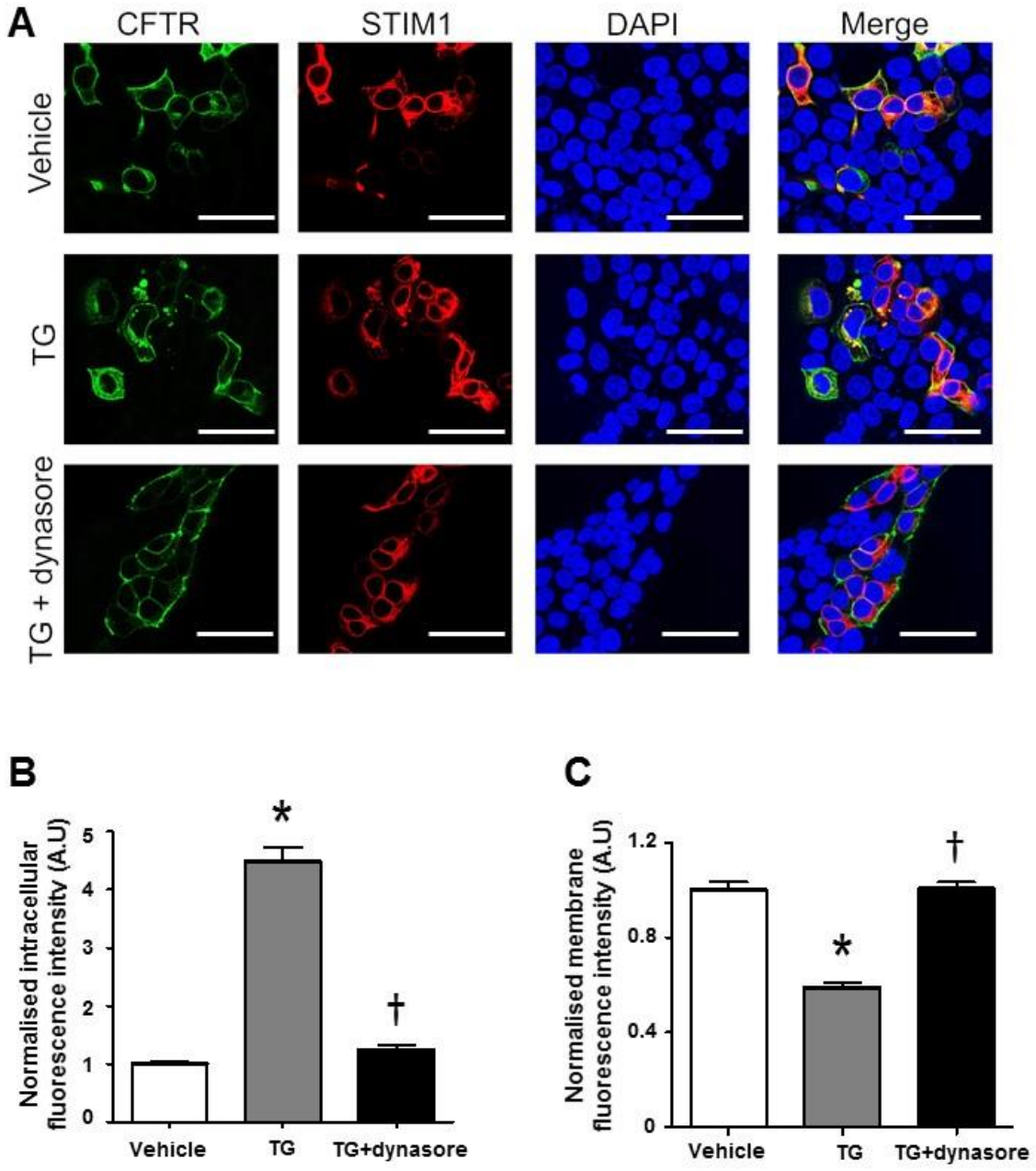

Figure 4.02. Exposure to thapsigargin causes internalisation of CFTR via a dynamin dependent mechanism. (A) Representative images showing the effect of vehicle (n=201 cells), 200 nM thapsigargin (TG; n=199 cells) and 80 µM dynasore + thapsigargin (n=238 cells) on CFTR. HEK 293 cells were transfected with GFP CFTR (green) and STIM1 mCherry (red). Nuclei were counter stained with DAPI (blue). Changes in **(B)** intracellular and **(C)** membrane fluorescence. Data are mean ± SEM (coverslips were imaged in duplicate from 3 independent experiments). Scale bar represents 50 µm. *p<0.001 compared to vehicle treated cells † p<0.001 compared to TG.

Total internal reflection fluorescence microscopy, which directly measures changes in protein expressed at the plasma membrane, was used to further investigate the effect

of an increase in cytosolic Ca^{2+} on CFTR expressed at the plasma membrane (Axelrod, 2001). Furthermore, to test whether the effect of an increase in cytosolic Ca^{2+} was specific to CFTR, cells were co-transfected with Anoctamin 1 (Ano1). Ano1 encodes the Ca^{2+} activated chloride channel (CaCC) which is responsible for Cl^- secretion into the airways in response to an increase in cytosolic Ca^{2+} (Caputo et al., 2008, Schroeder et al., 2008, Yang et al., 2008).

Upon exposure to thapsigargin, CFTR expressed at the plasma membrane showed a decrease in fluorescence to 0.7 ± 0.1 A.U ($p<0.05$), in contrast to cells treated with vehicle (1.0 ± 0.1 A.U). On the other hand, Ano1 expressed at the plasma membrane showed a little change in fluorescence (0.9 ± 0.2 A.U), when compared to Ano1 expressed at the plasma membrane in vehicle treated cells (1.0 ± 0.1 A.U; Fig. 4.03). These data indicated that the effect of an increase in cytosolic Ca^{2+} was specific to CFTR and did not affect Ano1 and potentially other plasma membrane Cl^- transporters expressed in HEK 293 cells.

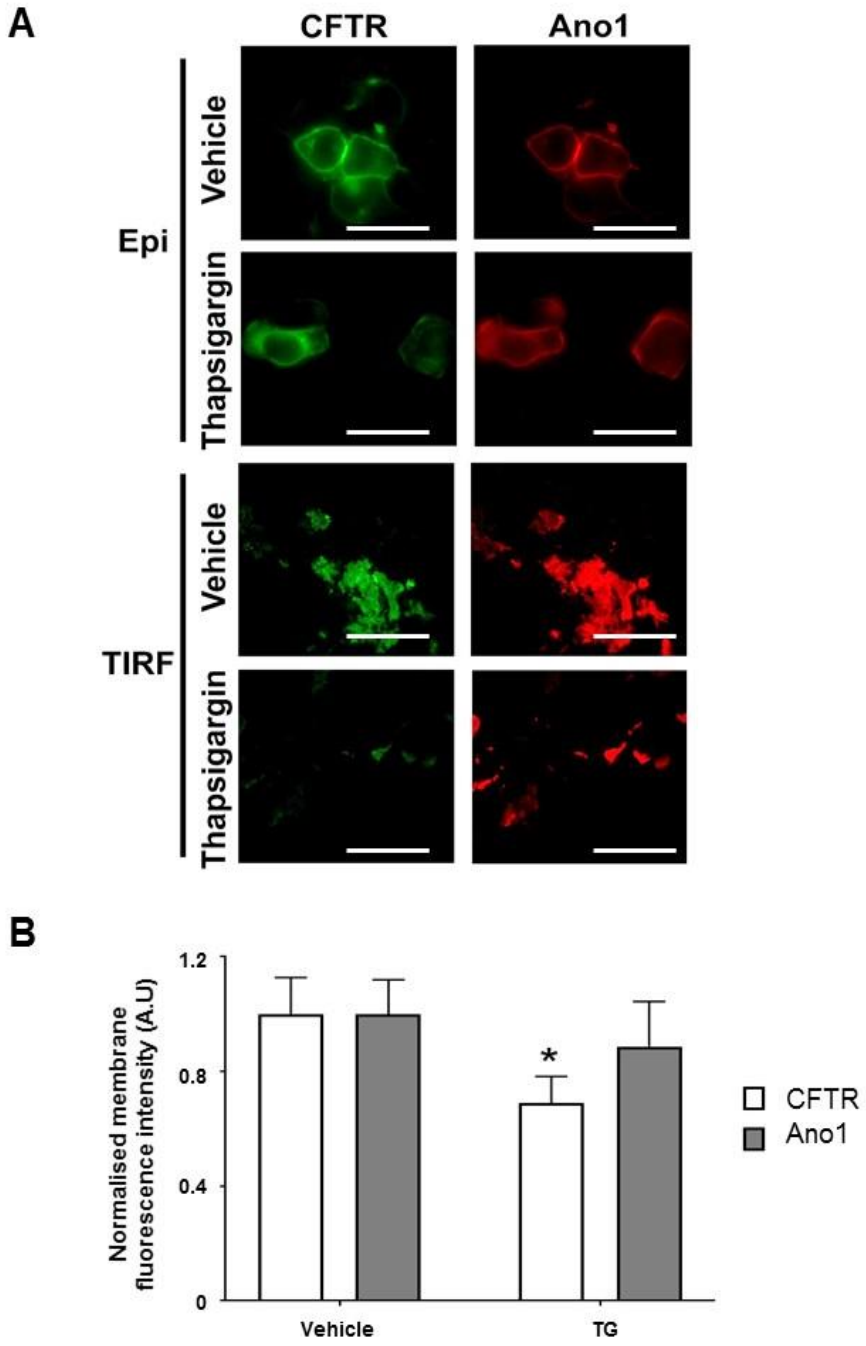

Figure 4.03. Exposure to thapsigargin causes loss of CFTR expressed at the membrane. (A) Representative images showing CFTR (green) and Ano1 (red) imaged using total internal reflection fluorescence microscopy and epifluorescent microscopy after treatment with either vehicle or 200 nM thapsigargin (TG). **(B)** Changes in relative membrane fluorescence, calculated using TIRF images. Data are mean ± SEM (coverslips were imaged in duplicate from 3 independent experiments). Scale bar represents 30 µm. *p<0.05 compared to vehicle treated cells.

4.3.2 Exposure to the ionophore, ionomycin, causes internalisation of CFTR

As with experiments detailed in chapter 3, further Ca^{2+} agonists were tested to complement the data from cells treated with thapsigargin. Exposure to the ionophore,

ionomycin, for 30 minutes caused an increase in intracellular fluorescence of CFTR to 4.1 ± 0.2 A.U (n=228 cells, p<0.001) compared to cells treated with vehicle (1.0 ± 0.03 A.U, n=227 cells). Likewise, plasma membrane fluorescence of CFTR decreased to 0.5 ± 0.01 A.U in ionomycin exposed cells, compared to 1.0 ± 0.02 A.U in vehicle exposed cells (Fig. 4.04). Accordingly, co-localisation between CFTR and STIM1 showed an increase to 54.6 ± 2.0% in ionomycin exposed cells, compared to cells treated with vehicle alone (37.7 ± 1.1%, p<0.001).

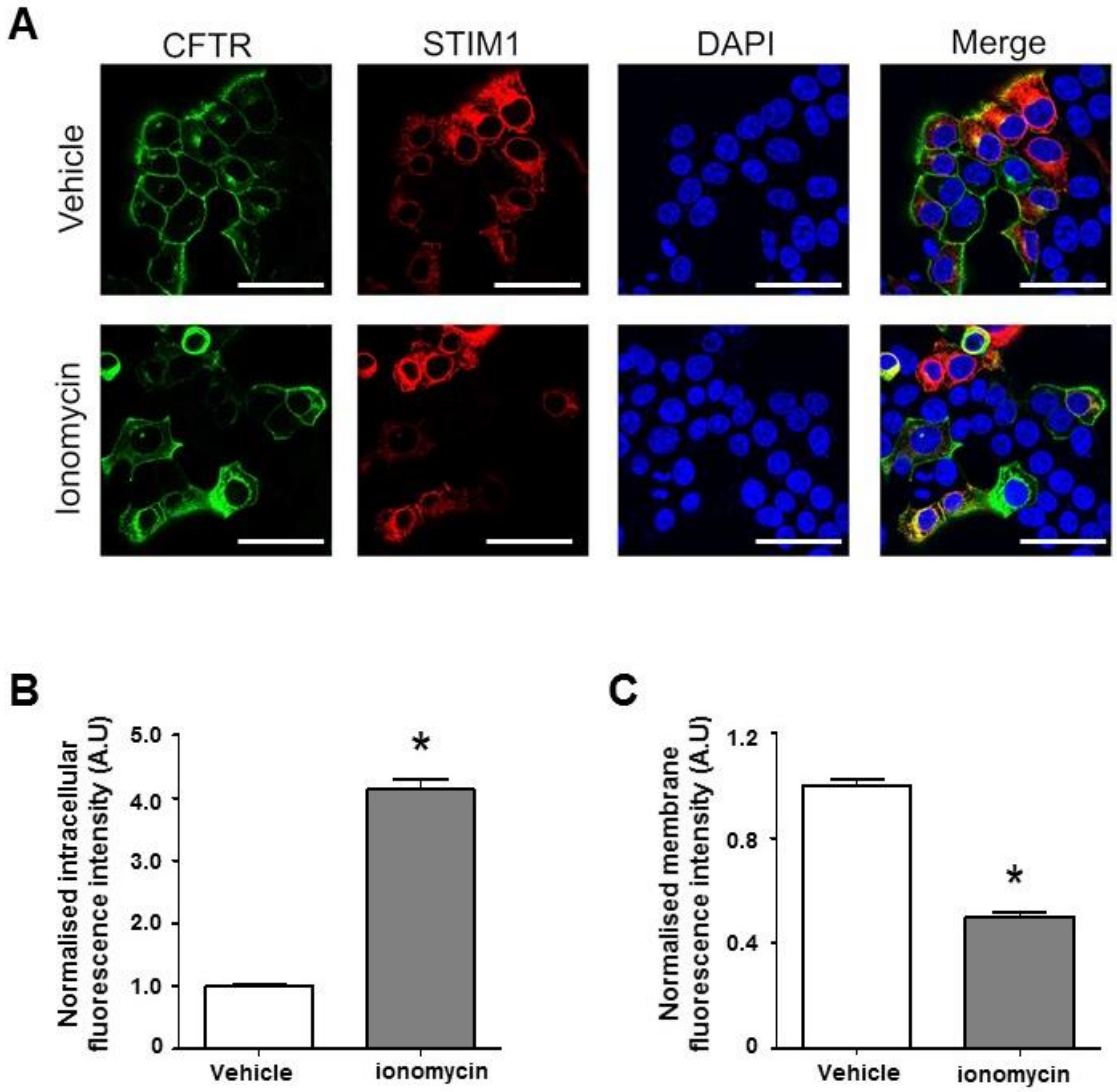

Figure 4.04. Ionomycin causes internalisation of CFTR. (A) Representative images showing the effect of vehicle (n=227 cells) and 1 µM ionomycin (n=228 cells). HEK 293 cells were transfected with GFP CFTR (green) and STIM1 mCherry (red). Nuclei were counter stained with DAPI (blue). Changes in **(B)** intracellular and **(C)** membrane fluorescence. Data are mean ± SEM (coverslips were imaged in duplicate from 3 independent experiments). Scale bar represents 50 µm. *p<0.001 compared to vehicle treated cells.

4.3.3 Exposure to a physiological agonist, ATP, causes internalisation of CFTR

The effect of the physiological agonist, ATP was also tested; cells were exposed to 100 µM ATP or vehicle for 30 minutes. Exposure to ATP caused an increase in intracellular CFTR to 1.9 ± 0.2 A.U (n=213 cells, p<0.001) compared to 1.0 ± 0.1 A.U (n=210 cells) for vehicle treated cells. Likewise, ATP treated cells showed a reduction in plasma membrane expressed CFTR (0.8 ± 0.02 A.U) compared to vehicle treated cells (1.0 ± 0.3 A.U, p<0.001, Fig. 4.05). As with earlier experiments, co-localisation between CFTR and STIM1 was analysed. Exposure to ATP caused an increase in co-localisation to 38.9 ± 1.7% in comparison to cells exposed to vehicle (30.2 ± 1.4%, p<0.001).

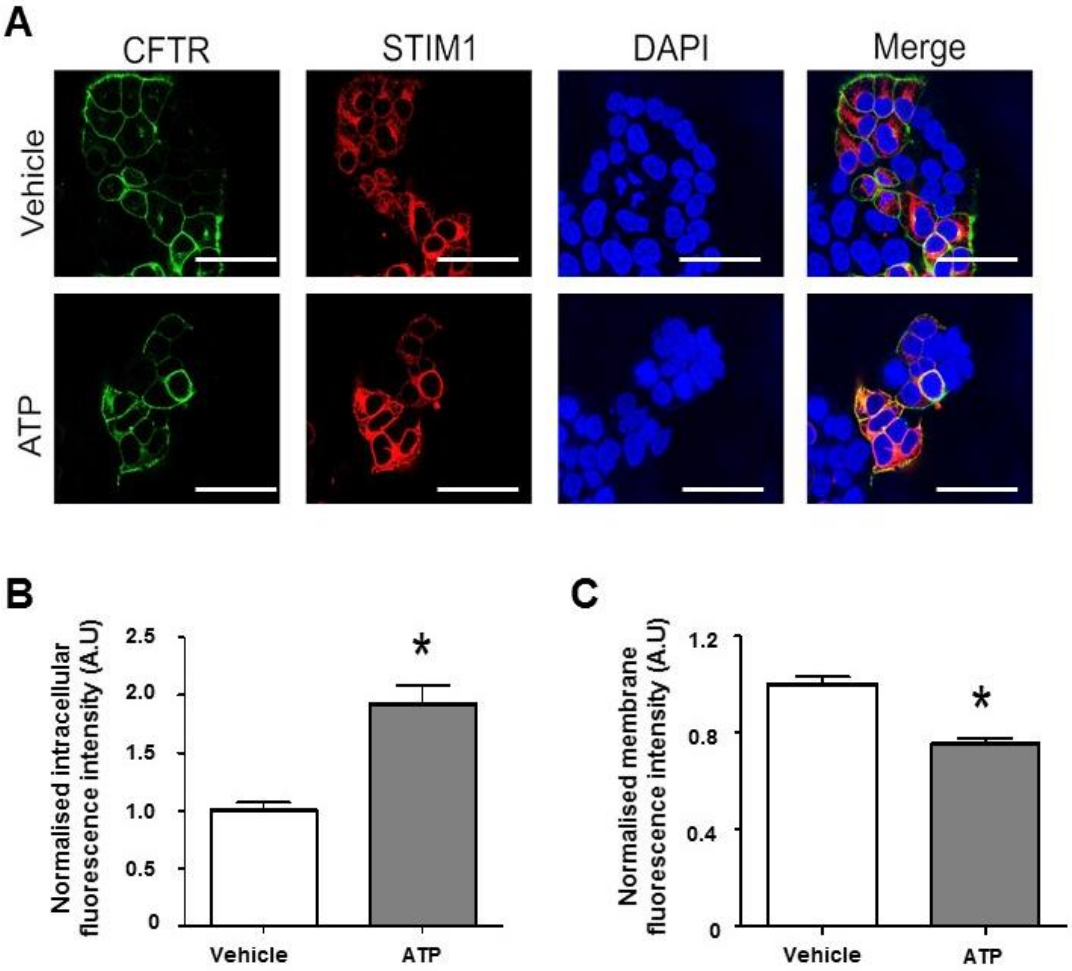

Figure 4.05. Exposure to the physiological agonist, ATP, causes internalisation of CFTR. (A) Representative images showing the effect of vehicle (n=213 cells) and 100 µM ATP (n=210 cells) on CFTR. Cells were transfected with GFP CFTR (green) and STIM1 mCherry (red).). Nuclei were counter stained with DAPI (blue). Changes in **(B)** intracellular and **(C)** membrane fluorescence under conditions indicated. Data are mean ± SEM (coverslips were imaged in duplicate from 3 independent experiments). Scale bar represents 50 µm. *p<0.001 compared to vehicle.

4.4 Comparison of the effect of cigarette smoke and Ca^{2+} agonists on CFTR expression

The data detailed in chapter 3 showed that thapsigargin, ionomycin and ATP all elicited different temporal changes in cytosolic Ca^{2+}. In order to try and correlate the changes in Ca^{2+} to changes in expression of CFTR, a comparison of the effects of the agonists detailed above to CS was carried out. When compiled, the data indicated that thapsigargin and ionomycin induced a bigger change in both intracellular and plasma membrane CFTR expression compared to smoke ($p<0.05$, Fig. 4.06). Furthermore, the change in both intracellular and plasma membrane expression of CFTR was similar between thapsigargin and ionomycin exposed cells, despite the differences in Ca^{2+} induced by both agonists. In contrast, ATP caused a smaller increase in intracellular fluorescence when compared to smoke ($p<0.05$, Fig. 4.06) and caused a loss of plasma membrane fluorescence that was comparable to cigarette smoke.

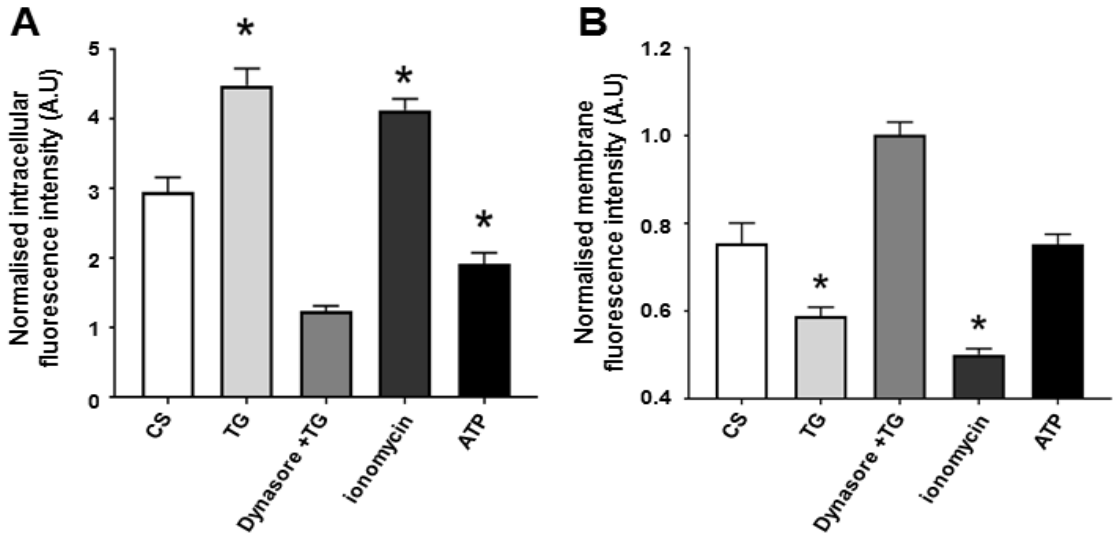

Figure 4.06. Comparison of the effect of cigarette smoke and Ca^{2+} agonists on CFTR expression. Effect of indicated Ca^{2+} agonists on relative amounts of **(A)** intracellular and **(B)** plasma membrane CFTR; cigarette smoke (CS), thapsigargin (TG). Data are mean ± SEM (coverslips were imaged in duplicate from 3 independent experiments). *$p<0.05$ compared to CS.

4.5 A thapsigargin-induced increase in cytosolic Ca^{2+} causes CFTR to be routed to the endoplasmic reticulum

4.5.1 Internalised CFTR co-localises with calreticulin

Smoke internalised CFTR is thought to be routed to aggresome like compartments, possibly due to lysosomal function being compromised by smoke exposure

(Rasmussen et al., 2014). The experiments detailed above using STIM1 as a marker for the endoplasmic reticulum have shown CFTR was routed to the ER. To further confirm this observation and use a conventional marker for the endoplasmic reticulum, staining was carried out with the ER marker, calreticulin (Milner et al., 1991). Cells exposed to thapsigargin showed an increase in co-localisation between CFTR and calreticulin to 53.2 ± 1.3% (n=265 cells, p<0.001) when compared to vehicle treated cells (39.0 ± 1.0%, n=355 cells, Fig. 4.07), further indicating that CFTR is routed to the endoplasmic reticulum following an increase in cytosolic Ca^{2+}.

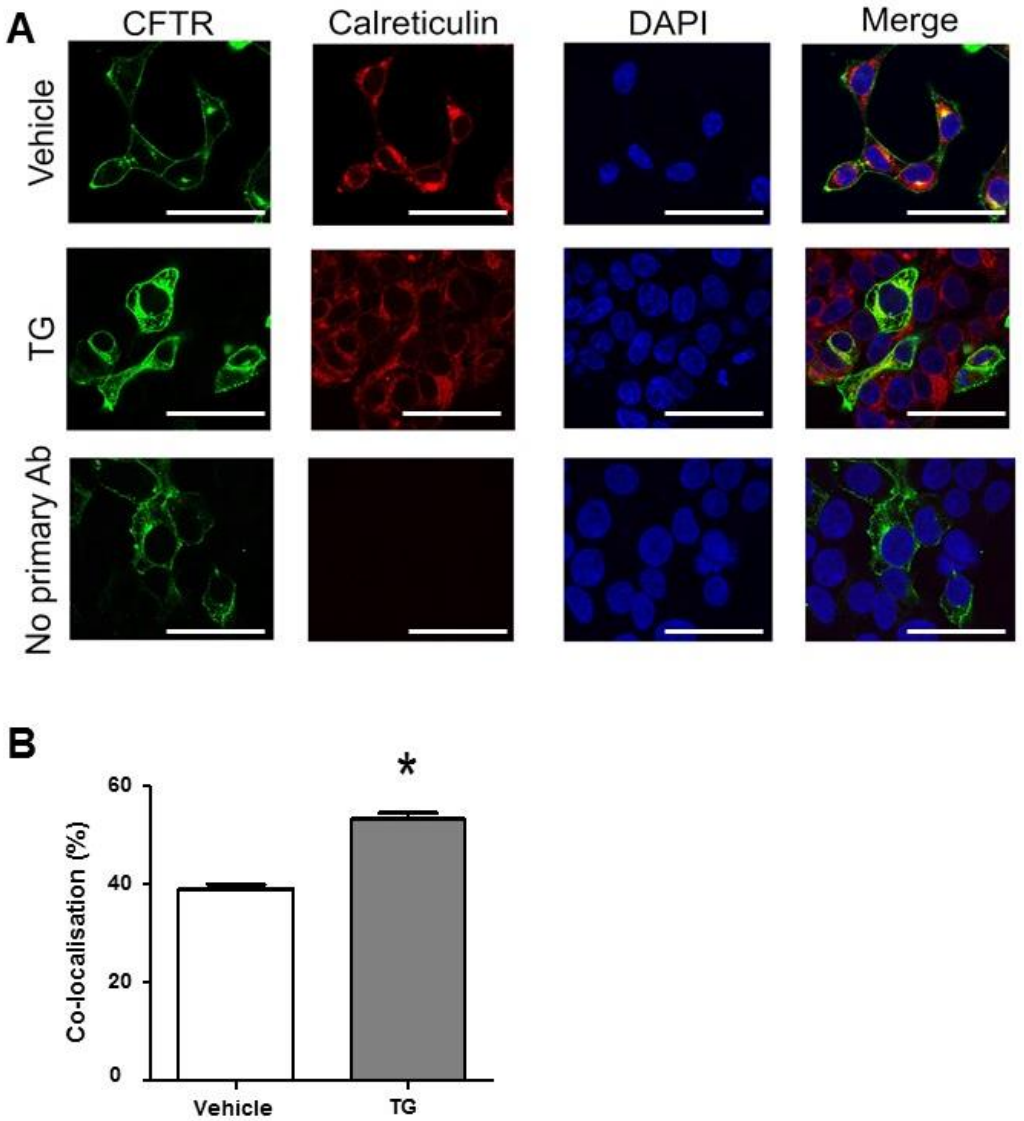

Figure 4.07. Exposure to thapsigargin causes an increase in CFTR in the endoplasmic reticulum. (A) Representative images showing the effect of vehicle (n=355 cells) or 200 nM thapsigargin (TG; n=265 cells) on CFTR. HEK 293 cells were transfected with GFP CFTR (green) and stained for calreticulin (red). Nuclei were counter stained with DAPI (blue). (**B)** Co-localisation between CFTR and calreticulin under conditions indicated. Data are mean ± SEM (coverslips were imaged in duplicate from 3 independent experiments). Scale bar represents 50 µm *p<0.001 compared to vehicle treated cells.

4.5.2 Internalised CFTR is not routed to the lysosome

Research from the lab has shown that CFTR is not routed to lysosomes following exposure to cigarette smoke (Rasmussen et al., 2014). To test whether an increase in cytosolic Ca^{2+} causes the same pattern of trafficking, cells were stained for lysosomal associated membrane protein 1 (LAMP1) (Meikle et al., 1997). On average, thapsigargin exposed cells had a co-localisation of 39.0 ± 0.9% (n=300 cells), similar to vehicle treated cells (37.0 ± 0.8%, n= 362 cells, Fig. 5.08), suggesting CFTR is not routed to the lysosome following an increase in cytosolic Ca^{2+}.

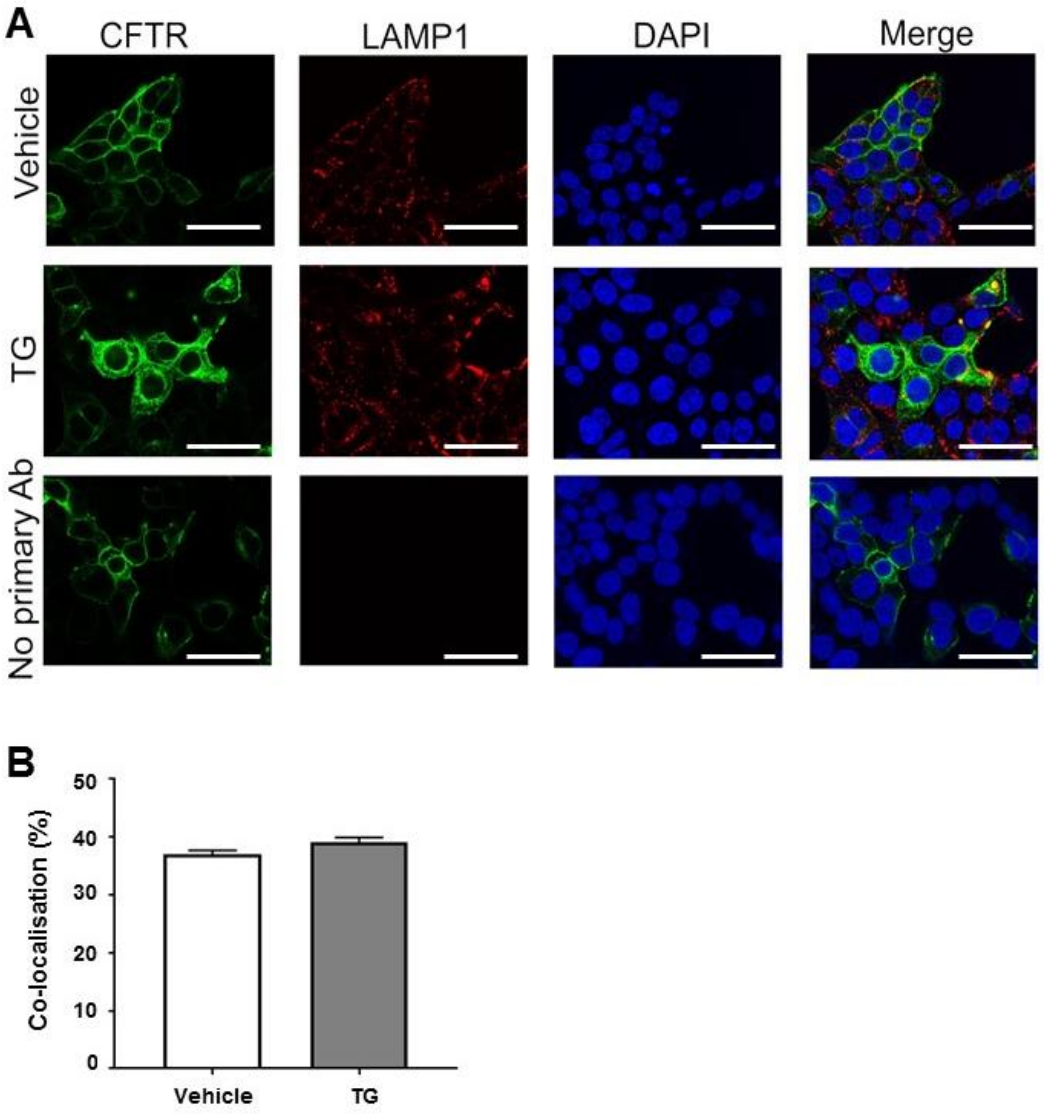

Figure 4.08. Exposure to thapsigargin does not change CFTR expression in lysosomes. (A) Representative images showing the effect of vehicle (n=362 cells) or 200 nM thapsigargin (TG; n=300 cells). HEK 293 cells were transfected with GFP CFTR (green) and stained for LAMP1 (red). Nuclei were counter stained with DAPI (blue). (**B)** Co-localisation between CFTR and LAMP1 under conditions indicated. Data are mean ± SEM (coverslips were imaged in duplicate from 3 independent experiments). Scale bar represents 50 µm.

4.5.3 CFTR is not routed to the Golgi apparatus following an increase in cytosolic Ca^{2+}

To determine whether CFTR was being routed to the Golgi apparatus, cells were stained for the *cis* Golgi apparatus marker, GM130 (Nakamura et al., 1995). On average, cells treated with vehicle had a co-localisation of 21.0 ± 0.8% (n=247 cells) and exposure to thapsigargin caused no change in co-localisation (20.2 ± 1.1%, n=187 cells, Fig. 4.09). These data suggest that for the timeframe recorded for these experiments, CFTR is not routed to the Golgi apparatus.

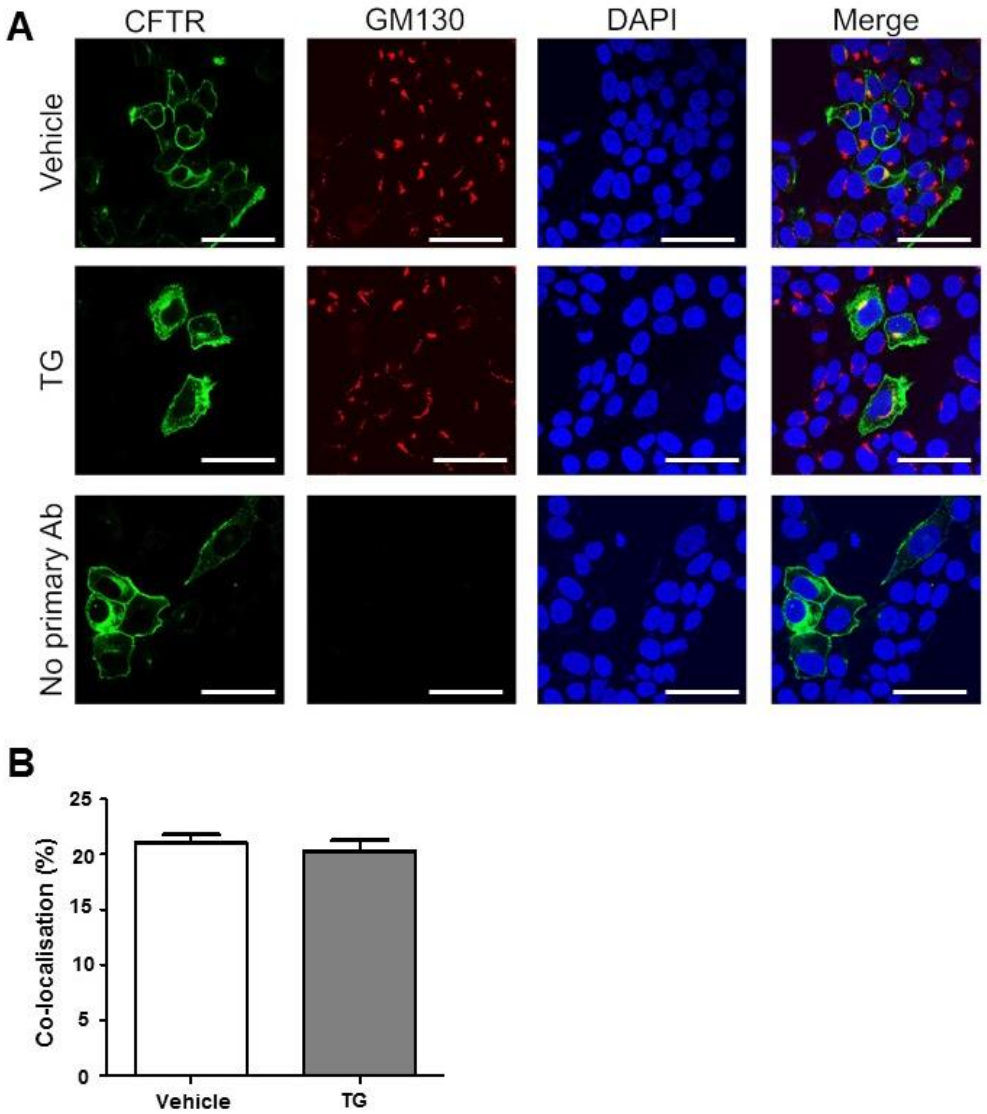

Figure 4.09. Exposure to thapsigargin causes no change in CFTR present in the Golgi apparatus. (A) Representative images showing the effect of vehicle (n=247 cells) or 200 nM thapsigargin (TG; n=187 cells). HEK 293 cells were transfected with GFP CFTR (green) and stained for GM130 (red). Nuclei were counter stained with DAPI (blue). (**B)** Co-localisation between CFTR and GM130 under conditions indicated. Data are mean ± SEM (coverslips were imaged in duplicate from 3 independent experiments). Scale bar represents 50 µm.

4.6 Inhibitors of the MEK/ERK pathway prevent a thapsigargin-induced internalisation of CFTR

Research from the has previously shown that inhibition of the MEK/ERK pathway can prevent tobacco smoke-induced internalisation of CFTR (Xu et al., 2015). To test whether the MEK/ERK pathway is involved in Ca^{2+}-induced internalisation of CFTR, cells were pre-treated for 30 minutes with U0126 (10 µM) which binds to MEK1 and MEK2 at specific residues, without competing with ERK or ATP, and thus provides selective inhibition of MEK (Duncia et al., 1998, Favata et al., 1998). Cells were also pre-treated with PD98059 (10 µM) which binds to the inactive form of MAPKK, preventing its activation (Alessi et al., 1995, Dudley et al., 1995).

On average, exposure to 200 nM thapsigargin caused an increase in intracellular fluorescence of CFTR to 5.7 ± 0.3 A.U (n=322 cells, $p<0.05$) from a baseline of 1.0 ± 0.1 A.U (n=307 cells). This increase was significantly blunted when cells were pre-treated with U0126 (1.5 ± 0.1 A.U, n=341 cells) or PD98059 (1.6 ± 0.1 A.U, n=386 cells, Fig. 4.10B). Likewise, plasma membrane fluorescence of CFTR decreased to 0.6 ± 0.01 A.U when cells were treated with thapsigargin, however, this decrease was prevented after pre-treatment with U0126 (1.0 ± 0.03 A.U) or PD98059 (1.0 ± 0.02 A.U, Fig. 4.10C).

As earlier, percentage co-localisation between CFTR an STIM1 was also quantified. On average, vehicle treated cells had a co-localisation of 35.2 ± 1.4% which was increased to 54.8 ± 2.1% ($p<0.05$) when cells were exposed to thapsigargin. This increase was blunted when cells were pre-treated with either U0126 (42.6 ± 1.7%, $p<0.05$) or PD98059 (46.8 ± 2.1%, $p<0.05$). Thus, these data indicate that the activation of the MEK/ERK pathway plays a role in Ca^{2+}-induced CFTR internalisation.

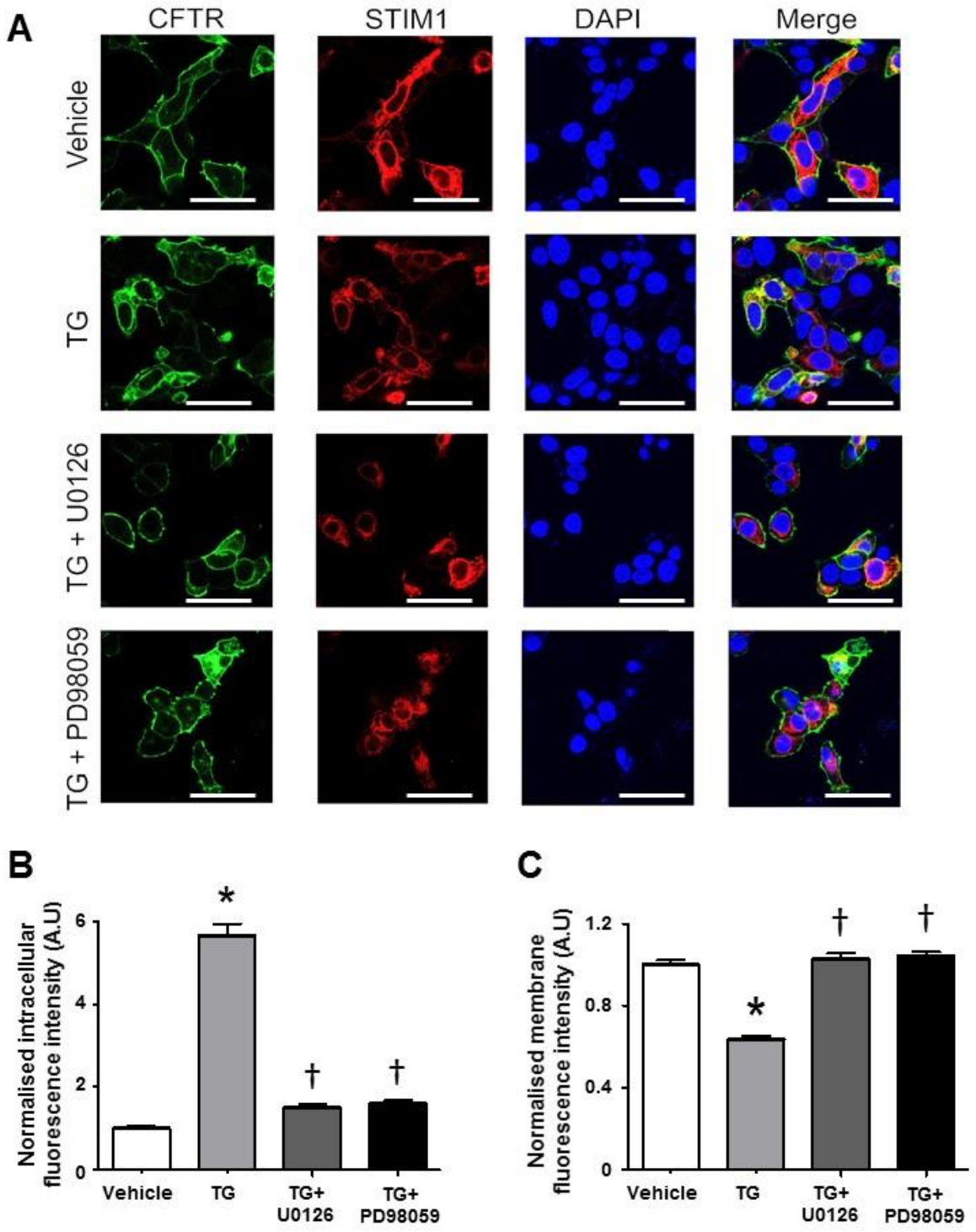

Figure 4.10. Effect of MEK/ERK inhibitors on thapsigargin-induced CFTR internalisation. (A) Representative images showing the effect of vehicle (n=307 cells), 200 nM thapsigargin (TG; n=322 cells), TG + 10 µM U0126 (n=341 cells) and TG + 10 µM PD98059 (n=386 cells). Cells were transfected with GFP CFTR (green) and STIM1 mCherry (red). Nuclei were counter stained with DAPI (blue). Changes in **(B)** intracellular and **(C)** membrane fluorescence under conditions indicated. Data are mean ± SEM (coverslips were imaged in duplicate from 3 independent experiments). Scale bar represents 50 µm *p<0.001 compared to vehicle treated cells † p<0.001 compared to TG.

4.7 Effects of altered cAMP/PKA activity on CFTR internalisation

4.7.1 Increasing cAMP does not affect thapsigargin-induced CFTR internalisation

Patch clamp experiments detailed in the previous chapter studied the effect of an increase in cytosolic Ca^{2+} on CFTR after the channel had first been activated with forskolin. To test whether the phosphorylation of CFTR could affect internalisation, cells were pre-treated with forskolin for 10 minutes before addition of thapsigargin, similar to the exposure period used in patch clamp experiments.

On average, in cells exposed to vehicle, CFTR had an intracellular fluorescence of 1.0 ± 0.05 A.U (n=323 cells) and exposure to 200 nM thapsigargin caused an increase in intracellular fluorescence to 5.1 ± 0.3 A.U (n=279 cells, $p<0.001$). Exposure to thapsigargin in cells that had been pre-treated with 5 µM forskolin caused a similar increase in intracellular fluorescence (4.7 ± 0.2 A.U; n=289 cells, $p<0.001$, Fig. 4.11B). Likewise, plasma membrane fluorescence of CFTR in vehicle exposed cells was 1.0 ± 0.03 A.U whereas cells exposed to thapsigargin showed a reduction in plasma membrane fluorescence to 0.6 ± 0.02 A.U as did cells treated with forskolin and thapsigargin (0.6 ± 0.02 A.U, Fig. 4.11C). These data suggested that in forskolin stimulated cells, which should activate and phosphorylate CFTR, an increase in cytosolic Ca^{2+} had the same effect as cells in which CFTR has not been activated. Thus, Ca^{2+}-induced CFTR internalisation was independent of phosphorylation status of CFTR.

Similar trends were seen in the co-localisation between CFTR and STIM1. On average, vehicle treated cells had a co-localisation of 20.1 ± 1.6% which was increased to 40.0 ± 2.4% ($p<0.05$) in thapsigargin exposed cells and similarly increased to 44.0 ± 1.9% ($p<0.05$) in forskolin and thapsigargin exposed cells.

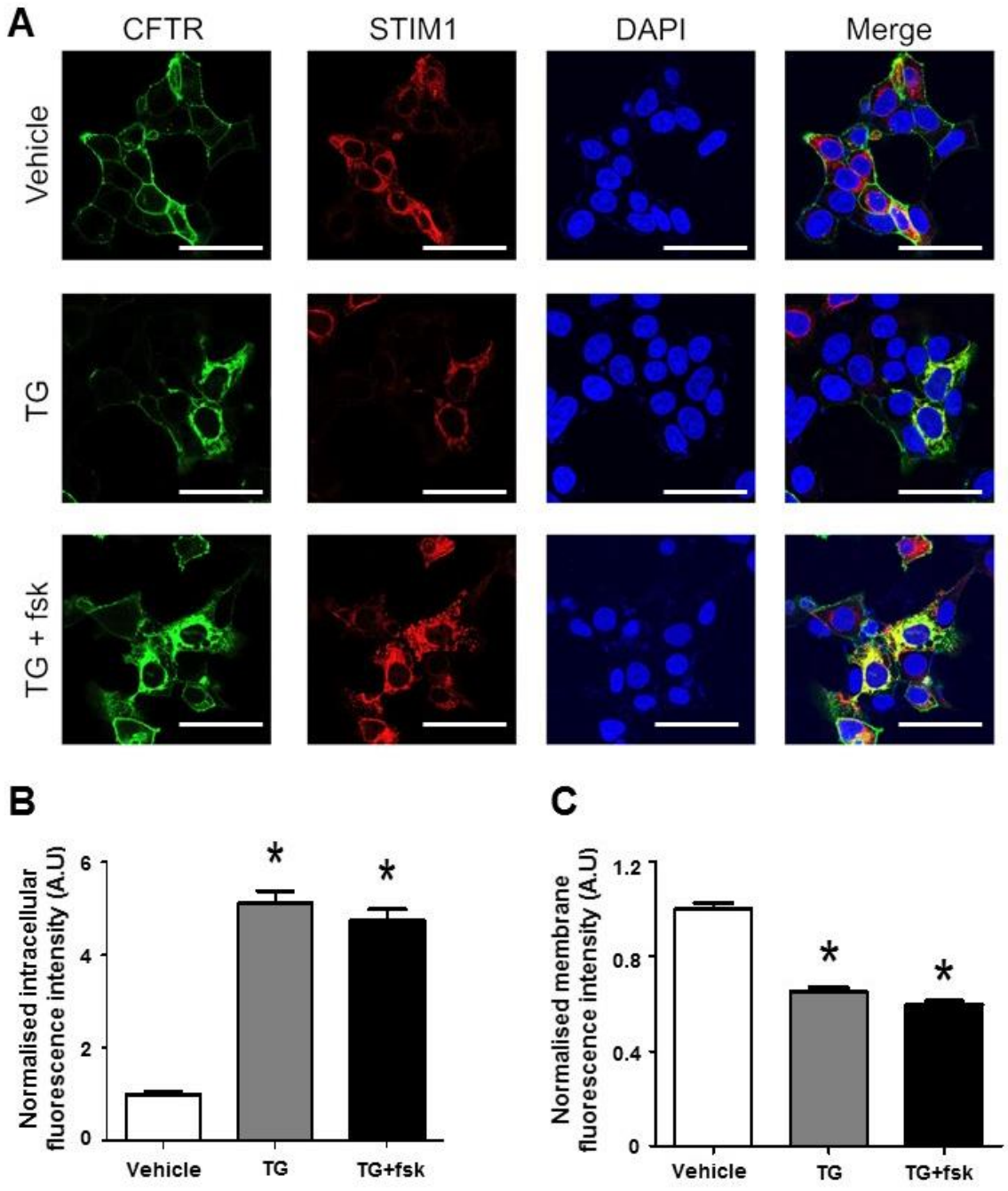

Figure 4.11. PKA phosphorylation of CFTR does not affect thapsigargin-induced internalisation of CFTR. (A) Representative images showing the effect of vehicle (n=323 cells), 200 nM thapsigargin (TG; n=279 cells) and TG + forskolin (fsk; n=289 cells). Cells were transfected with GFP CFTR (green) and STIM1 mCherry (red). Nuclei were counter stained with DAPI (blue). Scale bar represents 50 µM. Changes in relative **(B)** intracellular and **(C)** membrane fluorescence, Data are mean ± SEM (coverslips were imaged in duplicate from 3 independent experiments). Scale bar represents 50 µm *p<0.001 compared to vehicle treated cells.

4.7.2 Inhibitors of PKA and PKC have no effect on thapsigargin-induced internalisation of CFTR

In order to further investigate whether the cAMP/PKA pathway played a role in Ca^{2+} induced CFTR internalisation, cells were pre-treated with the PKA inhibitor, H89. H89 inhibits the effect of PKA through competitive inhibition of ATP binding to the catalytic subunit of PKA (Engh et al., 1996). Cells were also pre-treated with the PKC inhibitor, staurosporine to determine whether phosphorylation by this kinase plays a role in internalisation. Staurosporine inhibits the action of PKC by binding to the catalytic subunit of PKC (Tamaoki et al., 1986, Ward and O'Brian, 1992).

On average, exposure to thapsigargin caused an increase in intracellular fluorescence of CFTR to 2.0 ± 0.2 A.U (n=258 cells, $p<0.001$) compared to cells treated with vehicle (1.0 ± 0.04 A.U, n=254 cells). In comparison, cells exposed to thapsigargin after pre-treatment with staurosporine (100 nM) showed an increase in intracellular fluorescence to 2.2 ± 0.1 A.U (n=284 cells, $p<0.001$). Similarly, cells pre-treated with H89 (0.5 μM) showed an increase in fluorescence to 2.6 ± 0.1 A.U (n=238 cells, $p<0.05$, Fig. 4.12B).

Likewise, plasma membrane fluorescence of CFTR decreased to 0.6 ± 0.02 A.U ($p<0.001$) in thapsigargin treated cells, compared to a fluorescence of 1.0 ± 0.02 A.U in cells treated with vehicle. Similarly, cells exposed to thapsigargin after pre-treatment with staurosporine showed a decrease in fluorescence to 0.6 ± 0.01 A.U ($p<0.001$) and cells pre-treated with H89 showed a decrease to 0.59 ± 0.02 A.U ($p<0.001$, Fig. 4.12C).

A similar trend was seen in the changes in co-localisation between CFTR and STIM1. Cells exposed to vehicle had a co-localisation of 31.2 ± 1.8% which was increased to 46.2 ± 2.2% ($p<0.05$) when cells were exposed to thapsigargin. A similar increase in co-localisation was seen when cells were exposed to staurosporine (50.1 ± 1.7%, $p<0.05$) or H89 (48.4 ± 2.0%, $p<0.05$).

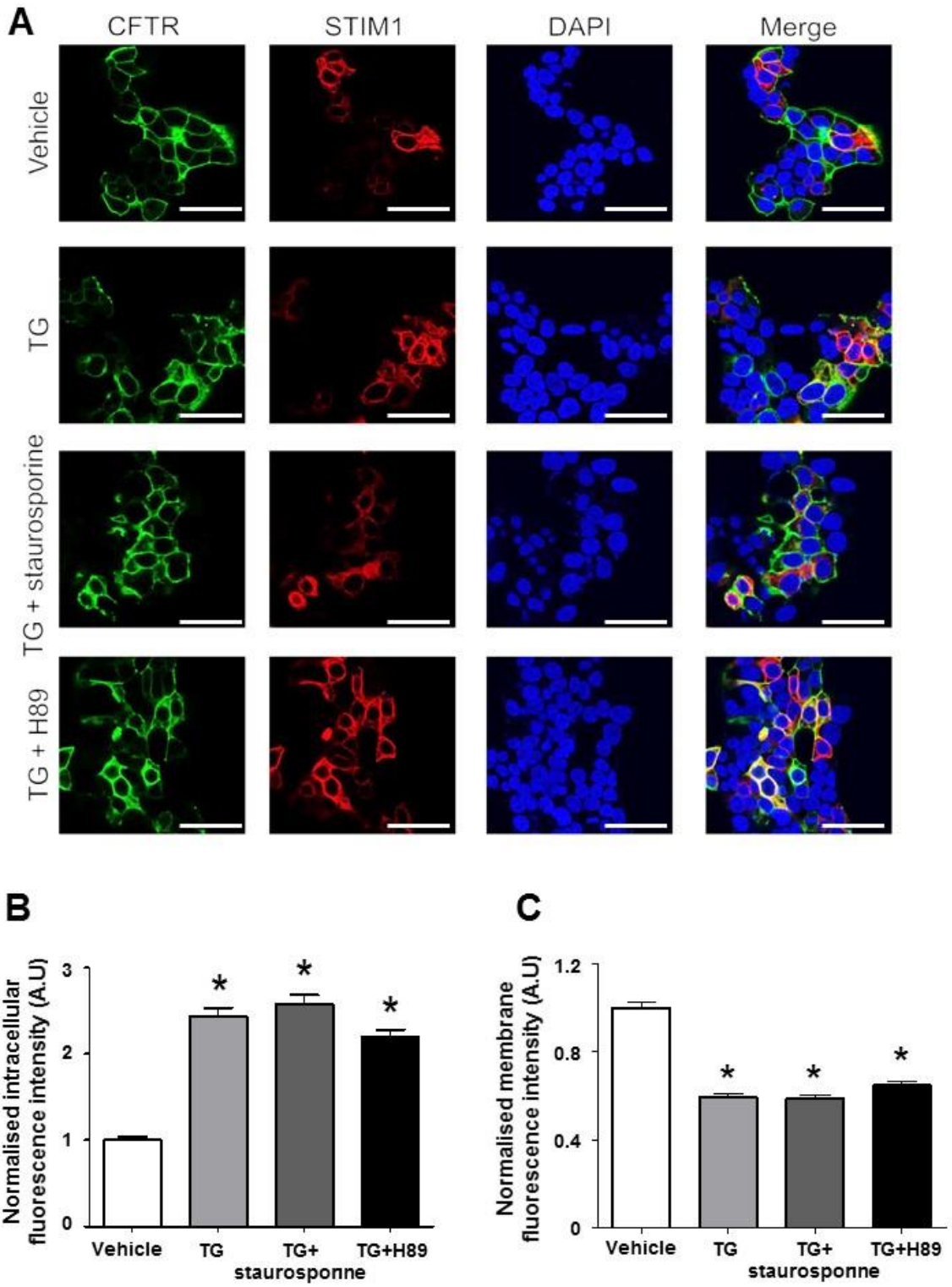

Figure 4.12. Inhibitors of PKA or PKC do not affect thapsigargin-induced internalisation of CFTR. (A) Representative images showing the effect of vehicle (n=254 cells), 200 nM thapsigargin (TG; n=258 cells), TG + 100 nM staurosporine (n=284 cells) and TG + 0.5 µM H89 (n=238 cells). Cells were transfected with GFP CFTR (green) and STIM1 mCherry (red). Nuclei were counter stained with DAPI (blue). Changes in relative **(B)** intracellular and **(C)** membrane fluorescence, Data are mean ± SEM (coverslips were imaged in duplicate from 3 independent experiments). Scale bar represents 50 µm *p<0.001 compared to vehicle treated cells.

4.7.3 Increasing cAMP via forskolin prevents cigarette smoke-induced CFTR internalisation

The data discussed above showed that increasing cAMP, and therefore phosphorylation of CFTR, had no effect on the thapsigargin-induced internalisation of CFTR. Likewise, inhibition of PKA with H89 had no effect on the thapsigargin-induced internalisation of CFTR. To determine whether cigarette smoke-induced CFTR internalisation was also insensitive to PKA phosphorylation, cells were pre-treated with either forskolin or the inhibitor, H89 and then exposed to cigarette smoke.

The data in fig 4.13 shows that in marked contrast to the data in figure 4.11, in cells pre-treated with forskolin, cigarette smoke failed to induce CFTR internalisation. This effect of forskolin was affected by H89 and so was clearly a PKA dependent effect. On average, in cells exposed to air and pre-treated with vehicle, CFTR had an intracellular fluorescence of 1.0 ± 0.1 A.U (n=237 cells), similar to cells pre-treated with 5 µM forskolin (1.3 ± 0.2 A.U; n= 242 cells) and cells treated with forskolin and 0.5 µM H89 (1.6 ± 1.0 A.U; 232 cells). Exposure to cigarette smoke caused an increase in intracellular fluorescence to 6.8 ± 1.2 A.U (n=235 cells, $p<0.001$), which was prevented by pre-treatment with forskolin (1.4 ± 0.3 A.U; n= 245 cells, $p<0.001$). On the other hand, pre-treatment of smoke exposed cells with forskolin and H89 showed an increase in intracellular fluorescence that was similar to cells treated with vehicle (6.6 ± 1.0 A.U; n= 235 cells, $p<0.001$, Fig. 4.13B).

Changes in plasma membrane fluorescence showed similar trends. Cells exposed to air and treated with vehicle had a plasma membrane fluorescence of 1.0 ± 0.1 A.U, similar to cells pre-treated with forskolin (0.9 ± 0.1 A.U) and forskolin and H89 (0.9 ± 0.1 A.U). Smoke exposure caused a reduction in plasma membrane fluorescence to 0.6 ± 0.05 A.U ($p<0.001$) whereas cells pre-treated with forskolin had a higher plasma membrane fluorescence of 0.8 ± 0.04 A.U. In contrast, cells treated with forskolin and H89 showed a similar loss of plasma membrane fluorescence to cells exposed to smoke and treated with vehicle (0.5 ± 0.03 A.U, $p<0.001$, Fig. 4.13C).

Changes in co-localisation between CFTR and STIM1 showed the same trends. On average, cells exposed to air and treated with vehicle had a co-localisation of 35.8 ± 2.3%, which was increased to 58.3 ± 2.4% ($p<0.05$) when cells were exposed to smoke. The smoke induced increase in co-localisation was blunted to 43.5 ± 2.6%

(p<0.05) when cells were pre-treated with forskolin whereas cells exposed to air had a co-localisation of 34.4 ± 1.8%. Cells exposed to smoke and treated with forskolin and H89 had a co-localisation of 51.9 ± 2.6% (p<0.05) whereas cells exposed to air had a co-localisation of 45.4 ± 2.3%. Thus, these data suggest that phosphorylation of CFTR via the action of forskolin has different consequences for cells exposed to cigarette smoke or to an increase in cytosolic Ca^{2+} induced by thapsigargin.

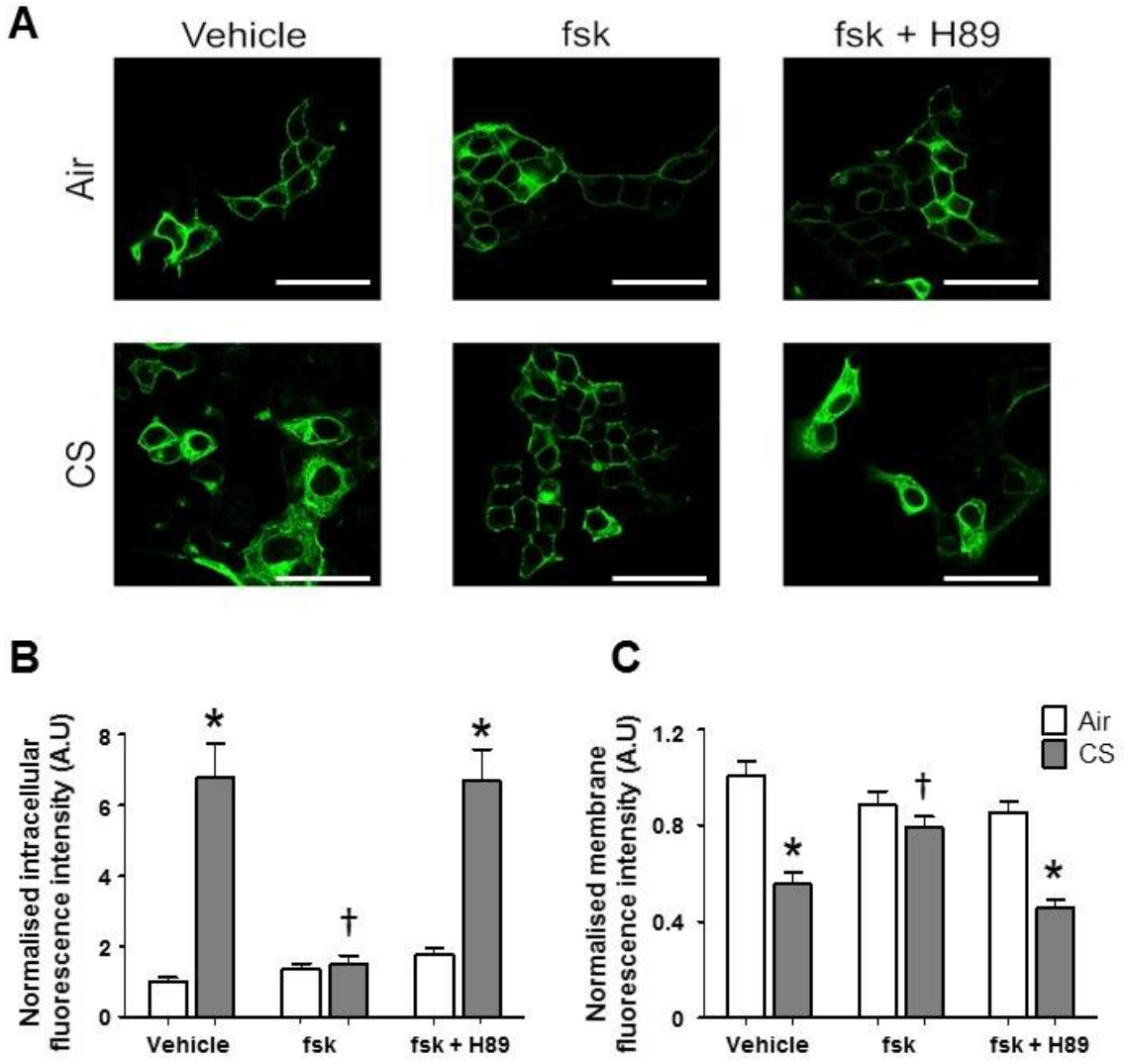

Figure 4.13. Phosphorylation of CFTR via PKA prevents smoke induced internalisation (A) Representative images showing the effect of air exposed cells treated with either vehicle (n=237 cells), 5 µM forskolin (fsk; n=242 cells) and fsk + 0.5 µM H89 (n=232 cells) or smoke (CS) exposed cells treated with vehicle (n=236 cells), fsk (n=245 cells) and fsk + H89 (n= 235 cells). Changes in relative **(B)** intracellular and **(C)** membrane fluorescence, Data are mean ± SEM (coverslips were imaged in duplicate from 3 independent experiments). Scale bar represents 50 µm. *p<0.001 compared to air + vehicle exposed cells † p<0.001 compared to CS + vehicle.

To determine whether the protective effect of forskolin was due to modulation of CS induced changes in Ca^{2+}, cells were pre-treated either 5 µM forskolin or vehicle and then Ca^{2+} measured. As with confocal imaging experiments, cells were pre-treated with 5 µM forskolin for 10 minutes before exposure to one research grade cigarette. On average, vehicle treated cells responded to cigarette smoke with an increase in ratio to 0.5 ± 0.1 ratio units from a baseline of 0.2 ± 0.02 ratio units. Likewise, cells pre-treated with forskolin showed an increase to 0.5 ± 0.1 ratio units from a baseline of 0.2 ± 0.02 ratio units. Cells treated with vehicle and exposed to air showed no changes in ratio (0.2 ± 0.03 ratio units compared to 0.2 ± 0.04 ratio units after exposure). Similarly, cells pre-treated with forskolin and exposed to air also showed no change in Fura-2 ratio (0.1 ± 0.01 ratio units compared to 0.2 ± 0.01 ratio units after exposure). Changes in area under the curve showed a similar trend where cells pre-treated with vehicle had an increase in AUC to 9.7 ± 3.7 ratio.min compared to 0.7 ± 0.3 ratio.min in air exposed cells. Similarly, cells pre-treated with forskolin showed an increase in AUC to 11.8 ± 5.2 ratio.min compared to 0.8 ± 0.3 ratio.min in air exposed cells (n=3, Fig. 4.14). These data suggest that the protective effect of forskolin on CFTR internalisation was not due to an inhibition of the smoke-induced rise in cytosolic Ca^{2+}.

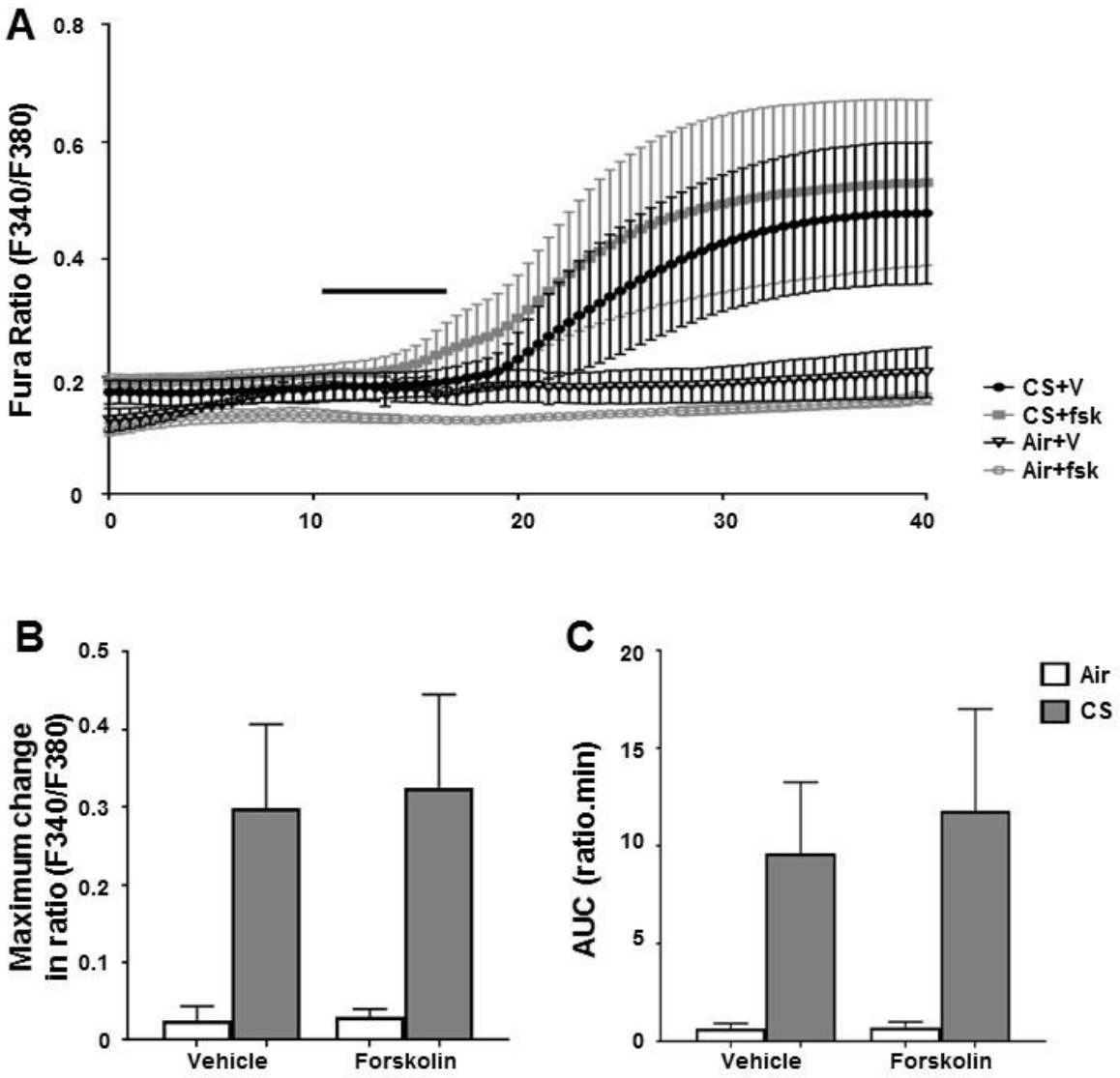

Figure 4.14. Forskolin pre-treatment has no effect on the smoke-induced increase in cytosolic Ca^{2+}. HEK 293T were loaded with Fura-2 AM for 30 mins. Cells were then exposed to one full research grade cigarette at a rate of one 35ml puff over 2s every 30s (13 puffs in total) or the equivalent of air. **(A)** Representative traces showing the changes in intracellular Ca^{2+} when cells were exposed to air or CS after pre-treatment with vehicle (V) or 5µM forskolin (fsk). Bar represents exposure period to either air or cigarette smoke (CS). Mean changes in **(B)** Fura-2 ratio and **(C)** area under the curve (AUC). Data are mean ± SEM (n=3).

4.8 The effect of calcineurin on CFTR internalisation

4.8.1 Inhibition of calcineurin prevents the thapsigargin-induced internalisation of CFTR

The data discussed above suggests that phosphorylation of CFTR via PKA is protective against CFTR internalisation induced by smoke. However, phosphorylation of CFTR had no effect on CFTR internalisation induced by an increase in cytosolic

Ca^{2+}. Thus, the data suggested that phosphorylation and dephosphorylation rates were important in determining CFTR internalisation. As an increase in cytosolic Ca^{2+} was common in both the response to cigarette smoke exposure and thapsigargin, the role of Ca^{2+} dependent phosphatase, calcineurin, was investigated. Cyclosporin A binds to the immunophilin cyclophilin, forming a complex which binds to and inhibits calcineurin (Schreiber and Crabtree, 1992, Galat, 1993). As a control, okadaic acid which inhibits protein phosphatase 1 and 2A was also tested. Cells were pre-treated with each drug for 30 minutes before the addition of thapsigargin.

On average, exposure to 200 nM thapsigargin caused an increase in intracellular fluorescence of CFTR to 6.0 ± 0.3 A.U (n=330 cells, $p<0.05$) from a baseline of 1.0 ± 0.05 A.U (n=356 cells). This increase was blunted when cells were pre-treated with 1 µM cyclosporin A (1.7 ± 0.1 A.U, n=363 cells, $p<0.05$), whereas pre-treatment with 10 nM okadaic acid had no effect (5.4 ± 0.3 A.U, n=321 cells, Fig. 4.15B). Likewise, plasma membrane fluorescence of CFTR decreased to 0.6 ± 0.02 A.U when cells were treated with TG, compared to vehicle treated cells (1.0 ± 0.02 A.U). This decrease was prevented by cyclosporin A pre-treatment (0.9 ± 0.02 A.U), however, okadaic acid had no effect on the TG-induced decrease in plasma membrane fluorescence (0.6 ± 0.02 A.U, Fig. 4.15C).

Co-localisation between CFTR and STIM1 was also analysed. On average, thapsigargin caused an increase in co-localisation to 39.0 ± 2.4% ($p<0.05$) compared to 18.5 ± 1.6% in vehicle treated cells. Pre-treatment of cells with cyclosporin A caused a reduction in co-localisation to 27.1 ± 1.9% ($p<0.05$) whereas pre-treatment with okadaic acid had no effect (32.8 ± 2.4%, $p<0.05$).

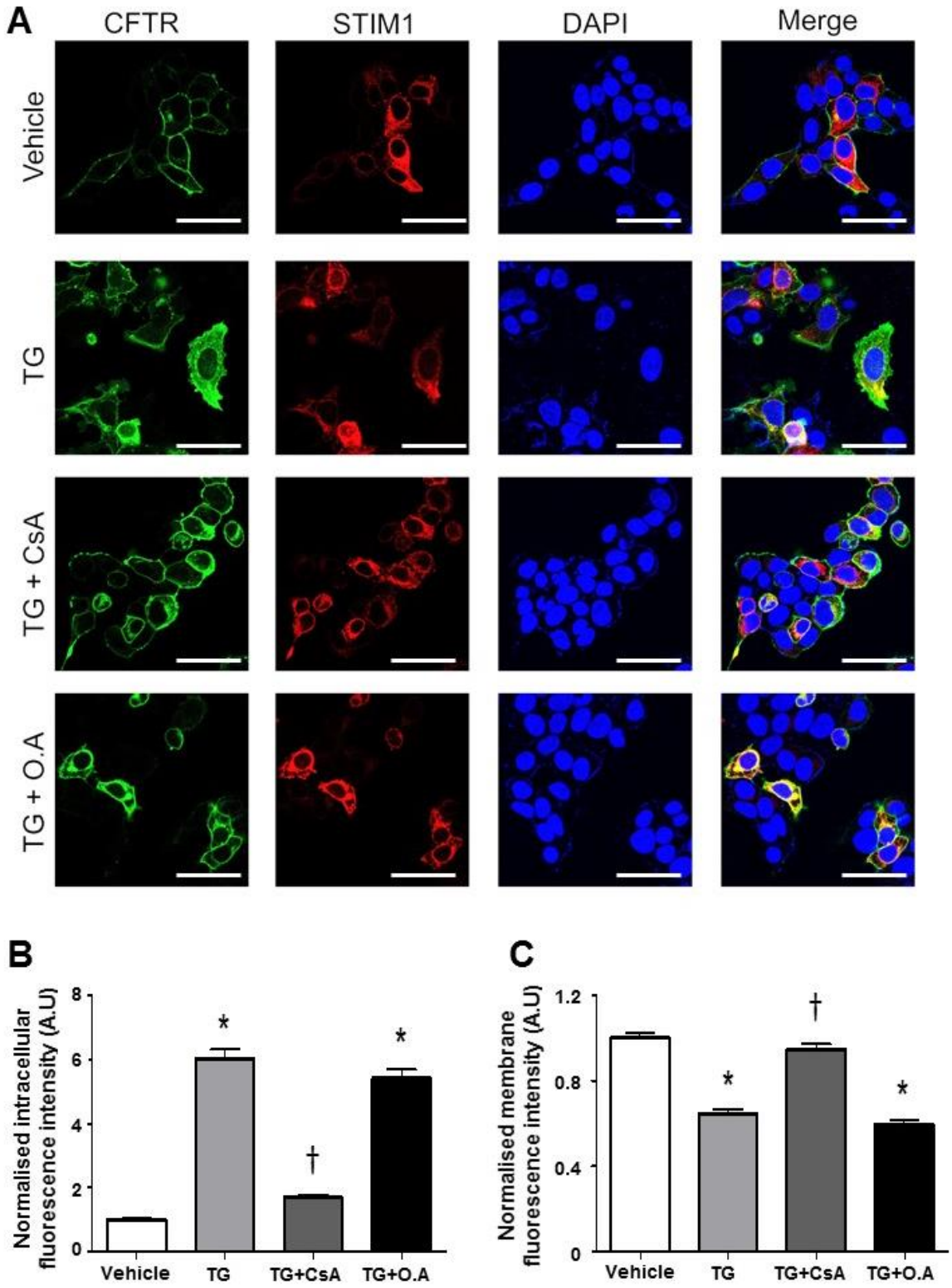

Figure 4.15. Effect of phosphatase inhibitors on thapsigargin-induced CFTR internalisation. Representative images showing the effect of (A) vehicle (n=356 cells), 200 nM thapsigargin (TG, n=330 cells), TG + 1 µM cyclosporin A (n=363 cells) and TG + 10 nM okadaic acid (n=321 cells). Cells were transfected with CFTR (green) and STIM1 (red). Nuclei were counter stained with DAPI (blue). Changes in (B) intracellular and (C) membrane fluorescence under conditions indicated. Data are mean ± SEM (coverslips were imaged in duplicate from 3 independent experiments). Scale bar represents 50 µm. *p<0.0001 compared to vehicle † p<0.0001 compared to TG.

4.8.2 An increase in cytosolic Ca^{2+} stimulates calcineurin phosphatase activity

A direct effect of thapsigargin on calcineurin phosphatase activity was also tested using a colorimetric assay. Various controls were employed to verify the sensitivity of the assay. When exposed to the PP1 and PP2A inhibitor, okadaic acid, calcineurin phosphatase activity was 1.4 ± 0.2 A.U compared to total activity in the assay (1.0 A.U). Treatment with the Ca^{2+} chelator, EGTA (1 mM), decreased calcineurin activity in the assay to 0.1 ± 0.3 A.U. When treated in combination with okadaic acid and EGTA, to inhibit PP1, PP2A and calcineurin, calcineurin activity was inhibited to 0.1 ± 0.1 A.U. Human recombinant calcineurin (40 U) was also assayed as a positive control, on average, the protein caused an increase in activity to 1.5 ± 0.4 A.U (n=3, Fig. 4.16A).

Alongside the controls, the effect of agonists used in imaging experiments was also tested. On average, 200 nM thapsigargin caused an increase in calcineurin phosphatase activity to 1.4 ± 0.1 A.U compared to vehicle treated cells (1.0 A.U; n=3, $p<0.05$). When treated with 1 µM cyclosporin A and thapsigargin, the phosphatase activity was reduced to 1.0 ± 0.04 A.U (n=3). Treatment with 10 nM okadaic acid had no effect on the thapsigargin induced increase (1.2 ± 0.1 A.U, n=3, Fig. 4.16B).

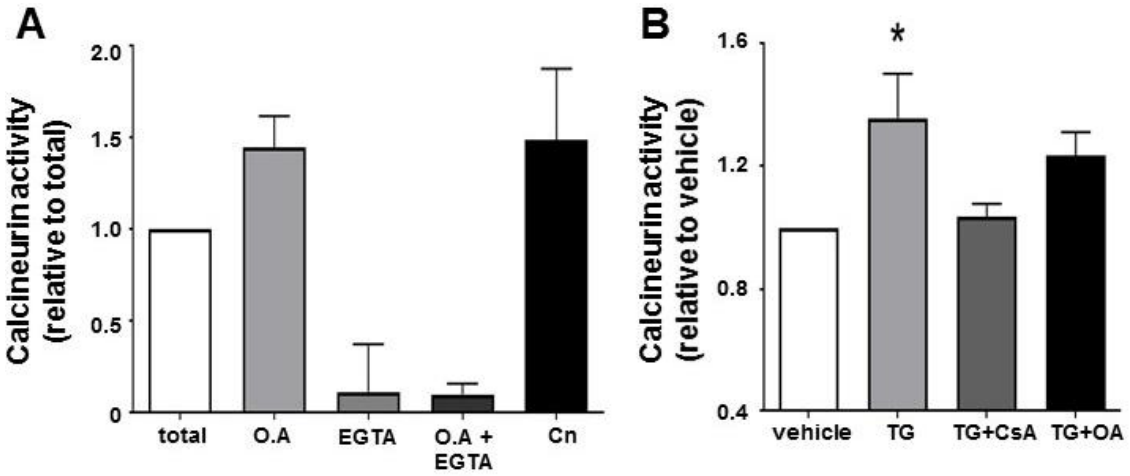

Figure 4.16. An increase in cytosolic calcium causes an increase in calcineurin phosphatase activity. Calcineurin phosphatase activity was measured using the Enzo Life Sciences calcineurin activity assay. Cells were treated with the conditions indicated and lysed. Excess phosphate was then removed from the sample and total calcineurin activity measured. **(A)** Changes in calcineurin phosphatase activity when treated with; okadaic acid (O.A), EGTA and human recombinant calcineurin (Cn). Data have been normalised to total phosphatase activity. **(B)** Changes in phosphatase activity when cells were exposed to thapsigargin (TG) and various inhibitors. Data have been normalised to vehicle. Data are mean ± SEM (n=3) *$p<0.05$ when compared to vehicle.

4.8.3 Inhibition of calcineurin in cigarette smoke exposed cells prevents internalisation of CFTR

The effect of calcineurin inhibition on smoke induced CFTR internalisation was also tested. As earlier, cells were pre-treated with either cyclosporin A or okadaic acid for 30 minutes before exposure to either 13 puffs of cigarette smoke or air. On average, exposure to smoke caused an increase in internal fluorescence of CFTR to 5.8 ± 0.3 A.U (n= 241 cells, $p<0.001$) compared to 1.0 ± 0.1 A.U (n=235 cells) when exposed to air. Pre-treatment with cyclosporin A blunted the increase in internal fluorescence induced by smoke to 1.4 ± 0.1 A.U (n=246 cells, $p<0.001$) whereas cells treated with air showed no change in fluorescence (0.9 ± 0.1 A.U; n= 240 cells). When treated with okadaic acid, cells exposed to smoke showed an increase in internal fluorescence to 5.4 ± 0.3 A.U (n=321 cells, $p<0.001$) compared to cells treated with air (0.7 ± 0.1 A.U, n=330 cells, Fig. 4.17B).

Likewise, exposure to cigarette smoke caused a decrease in plasma membrane fluorescence of CFTR to 0.6 ± 0.1 A.U compared to 1.0 ± 0.1 A.U ($p<0.001$) when exposed to air. Pre-treatment with cyclosporin A blunted the decrease in membrane fluorescence induced by CS to 0.9 ± 0.02 A.U similar to cells exposed to air (0.9 ± 0.1 A.U). When treated with okadaic acid, cells treated with CS showed a decrease in membrane fluorescence to 0.6 ± 0.02 A.U compared to cells treated with air (0.9 ± 0.1 A.U, $p<0.001$, Fig. 4.17C).

Cells were also co-transfected with STIM1. On average, the co-localisation between CFTR and STIM1 in cells exposed to air and treated with vehicle was 37.6 ± 2.1%. The co-localisation increased to 55.3 ± 2.7% ($p<0.05$) when cells were exposed to smoke. This increase in co-localisation induced by smoke was blunted to 41.8 ± 2.2% ($p<0.05$) when cells were pre-treated with cyclosporin A whereas cells exposed to air had a co-localisation of 31.4 ± 1.6%. Cells exposed to smoke and treated with okadaic acid had a co-localisation of 53.7 ± 2.4% ($p<0.05$) whereas cells exposed to air had a co-localisation of 42.4 ± 2.2%.

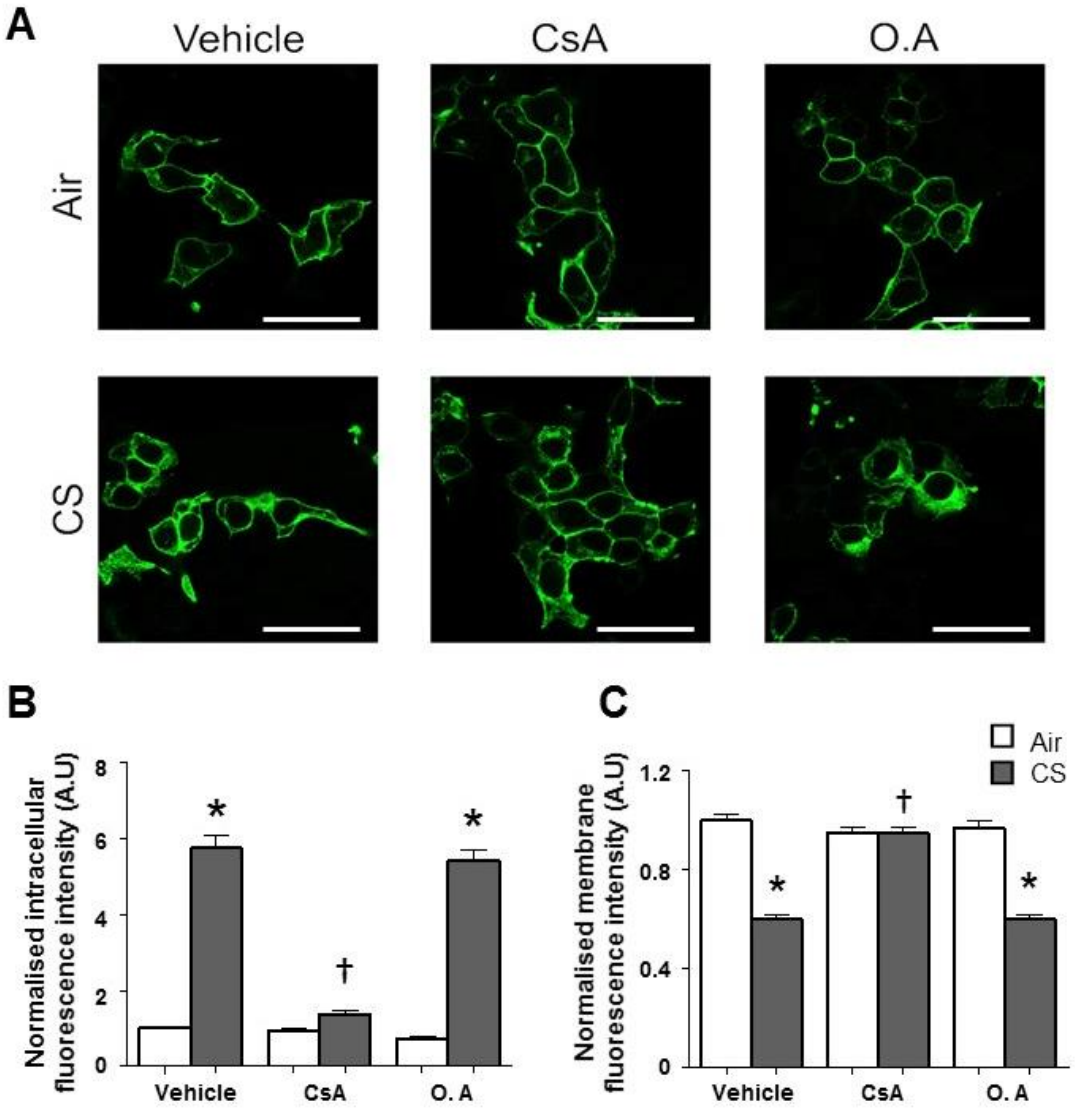

Figure 4.17. Effect of phosphatase inhibitors on smoke-induced CFTR internalisation. (A) Representative images showing the effect of air (n=235 cells), air + 1 µM cyclosporin A (CsA; n=240 cells), air + 10 nM okadaic acid (O.A; n=330 cells) or cigarette smoke (CS; n= 241 cells), CS + CsA (n=246 cells) and CS + O.A (n=321 cells) in cells transfected with GFP CFTR. Changes in **(B)** intracellular and **(C)** membrane fluorescence under conditions indicated. Data are mean ± SEM (coverslips were imaged in duplicate from 3 independent experiments). Scale bar represents 50 µm. *p<0.0001 compared to air + vehicle † p<0.0001 compared to CS + vehicle.

4.8.4 Exposure to cigarette smoke causes an increase in calcineurin phosphatase activity

The effect of cigarette smoke exposure on calcineurin phosphatase activity was also tested. As earlier, the assay was run with several controls, which displayed similar trends. Cells were exposed to 3 puffs of cigarette smoke and the phosphatase

activity assayed. Note that cells exposed to the standard 13 puffs showed highly variable results (data not shown).

As earlier, various controls were used to validate the assay. Exposure to okadaic acid caused an increase in calcineurin activity to 2.5 ± 0.7 A.U whereas treatment with EGTA inhibited activity to 0.3 ± 0.1 A.U, as did treatment with okadaic acid and in EGTA in combination (0.2 ± 0.1 A.U). As a positive control, human recombinant calcineurin was also assayed, and was found to cause an increase in activity to 9.0 ± 2.8 A.U (n=4-7, Fig. 4.18A). On average, exposure to cigarette smoke caused an increase in calcineurin activity to 2.4 ± 0.3 A.U when compared to air exposed cells (1.0, $p<0.05$). Cyclosporin A blunted the smoke induced increase in calcineurin activity to 1.1 ± 0.1 A.U which was similar to air exposed cells (0.9 ± 0.1 A.U). On the other hand, pre-treatment with okadaic acid still caused an increase in calcineurin activity to 1.9 ± 0.2 A.U, compared to air exposed cells (1.0 ± 0.1 A.U; n=7, Fig. 4.18B).

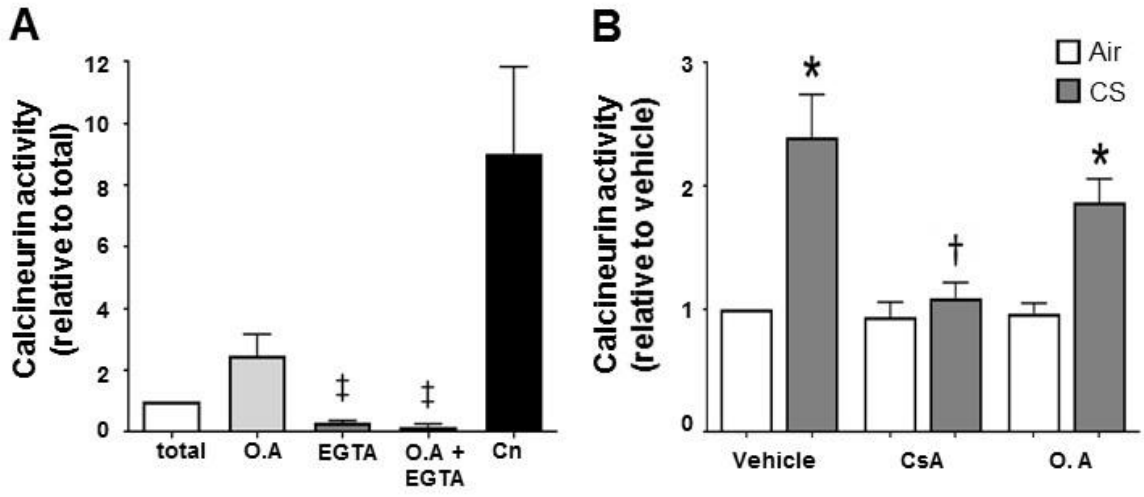

Figure 4.18. Cigarette smoke exposure causes an increase in calcineurin phosphatase activity. Calcineurin phosphatase activity was measured using the Enzo Life Sciences calcineurin activity assay. Cells were treated with the conditions indicated and lysed. Excess phosphate was then removed from the sample and total calcineurin activity measured. **(A)** Changes in calcineurin phosphatase activity under various control conditions employed in the assay; okadaic acid (O.A), EGTA and human recombinant calcineurin (Cn). Data have been normalised to total phosphatase activity (n= 4-7). **(B)** Changes in phosphatase activity when cells were exposed to air or cigarette smoke (CS); cyclosporin A (CsA; n=7). ‡ $p<0.05$ compared to Cn. *$p<0.05$ compared to air exposed cells. † $p<0.05$ compared to CS.

4.8.5 Inhibition of calcineurin prevents a smoke-induced reduction in airway surface liquid height

One of the major effects of cigarette smoke exposure is to decrease the height of the ASL and increase the production of mucus, due to a loss of CFTR from the plasma membrane (Rasmussen et al., 2014). To test whether calcineurin inhibition could be protective against the smoke-induced decrease in ASL height, primary human bronchial epithelial cells (HBEC) were used to study the effect of cyclosporin A on the ASL. Cells exposed to air had an ASL height of 8.3 ± 0.3 µm at 30 minutes post exposure compared to a starting height of 8.7 ± 0.2 µm (n=8 transwells). Cells subsequently maintained a height of approximately 7.7 µm for the duration of the experiment. In comparison, cells exposed to cigarette smoke showed a decrease in the height of the ASL to 5.0 ± 0.3 µm (n=7 transwells, $p<0.05$) at 30 mins post exposure compared to a starting height of 8.1 ± 0.3 µm. The ASL height subsequently started to recover, reaching a height of 7.3 ± 0.1 µm at 2 hours post exposure (n=7 transwells, Fig. 4.19B).

HBECs were also pre-treated with cyclosporin A for 30 mins before exposure to either air or smoke. Cells exposed to air had a starting ASL height of 8.7 ± 0.4 µm (n=8 transwells) and this height stayed fairly constant for the duration of the experiment. Cells pre-treated with cyclosporin A and exposed to smoke had a starting height of 8.2 ± 0.3 µm and showed a small but significantly less decline in ASL height compared to CS and vehicle exposed cells, with a decrease in height to 7.0 ± 0.4 µm at 30 minutes post exposure to cigarette smoke. Like vehicle treated cells, the ASL height subsequently recovered to a height to 7.6 ± 0.2 µm at 2 hours post cigarette smoke exposure (n=7 transwells, Fig. 4.19). These data indicated that pre-treatment with cyclosporin A could protect the ASL from a smoke-induced reduction in height, further implicating calcineurin as a key effector in smoke-induced internalisation of CFTR.

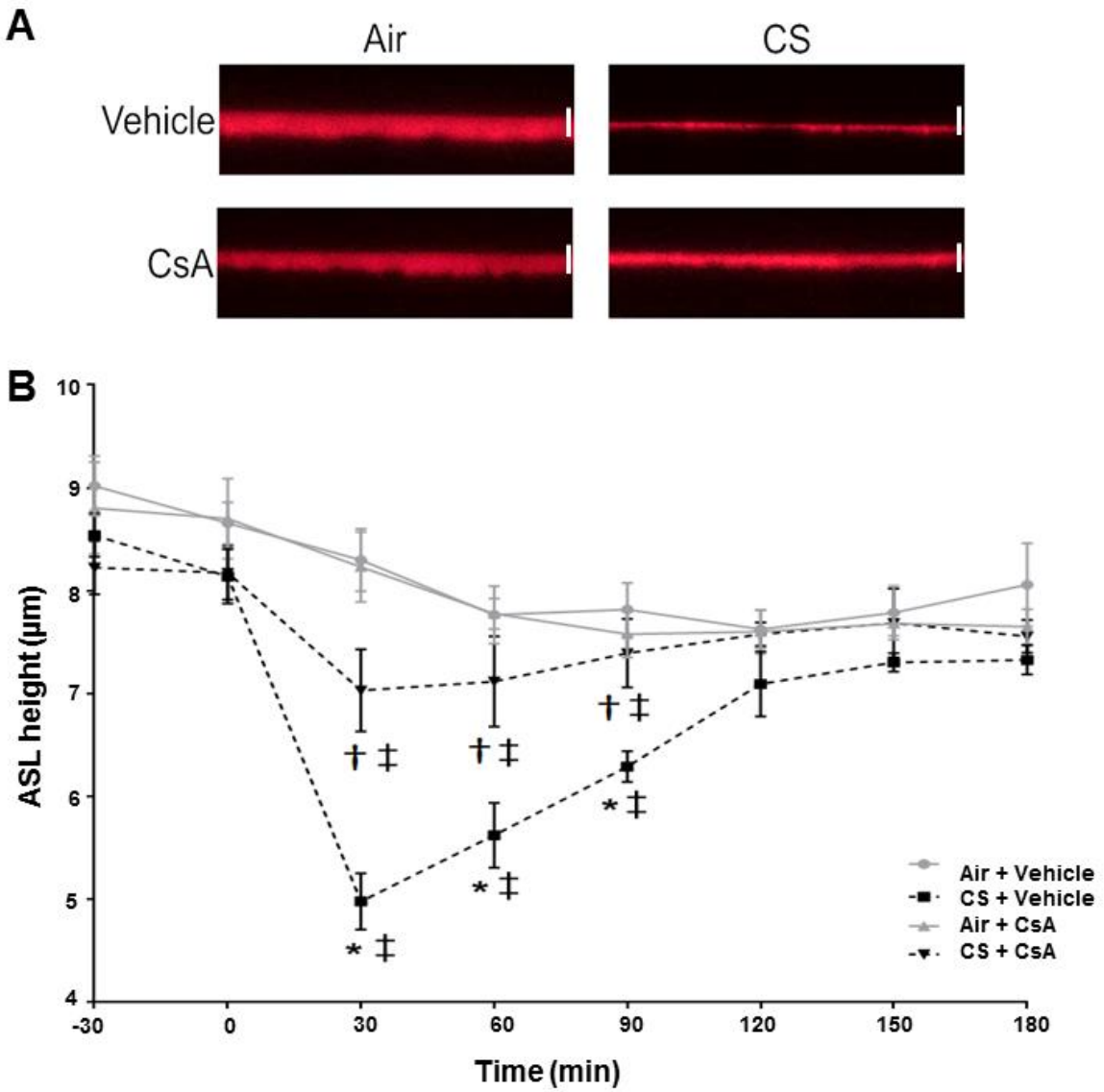

Figure 4.19. Cyclosporin A protects against a smoke-induced decrease in airway surface liquid height. Airway surface liquid (ASL) in human bronchial epithelial cells was labelled with tetramethylrhodamine conjugated dextran and perfluorocarbon was added mucosally to prevent evaporation of the ASL. **(A)** Representative images showing ASL height 30 minutes after cultures were exposed to either 13 puffs of air or cigarette smoke and treated as indicated. Scale bar represents 10 µm. **(B)** Time course showing changes in ASL height under conditions indicated. Data are mean ± SEM (n=7-8 transwells from 3 independent donors). Scale bar represents 10 µm. *p<0.05 compared to air exposed cultures. † p<0.05 compared to CS + vehicle. ‡ p<0.05 compared to t=0.

4.8.6 Calcineurin does not affect physiological increases in ASL height in response to G protein-coupled receptor agonists

The role of calcineurin under physiological conditions was also tested by exposing cells to adenosine (Ado; ~200 µM) after pre-treating cells with cyclosporin A or

vehicle overnight. Adenosine acts on the A_{2B} receptor causing an increase in cAMP and stimulation of CFTR (Tarran et al., 2005). Cells exposed to vehicle showed an increase in ASL height to 6.5 ± 0.2 µm (n=9 transwells) after being exposed to adenosine for 10 minutes, compared to a starting height of 5.8 ± 0.1 µm. The ASL height subsequently started to recover with the height falling to 5.7 ± 0.2 µm at 1 hour post exposure and remaining at that height for the rest of the experiment. In comparison, cells treated with vehicle showed no increases in ASL height overtime and the ASL height stayed at approximately 5.6 ± 0.2 µm for 6 hours (n=8 transwells, Fig. 4.20).

Cells exposed to cyclosporin A overnight appeared to respond normally to adenosine. Similar to vehicle treated cells, cells pre-treated with cyclosporin A showed an increase in ASL height to 6.8 ± 0.3 µm (n=9 transwells) after exposure to adenosine for 10 minutes, compared to a starting height of 5.6 ± 0.1 µm. Cells subsequently showed a recovery in ASL height, with the height at 6 hours being 6.0 ± 0.1 µm. In contrast, cells treated with vehicle only showed no changes in ASL height for the duration of the experiment, with the height remaining at ~5.6 ± 0.2 µm (n=8 transwells, Fig. 4.20). These data indicated that calcineurin had no effect on the response of CFTR to physiological agonists. Together with the previous ASL height data, these data indicate CFTR is regulated by calcineurin only under conditions of stress.

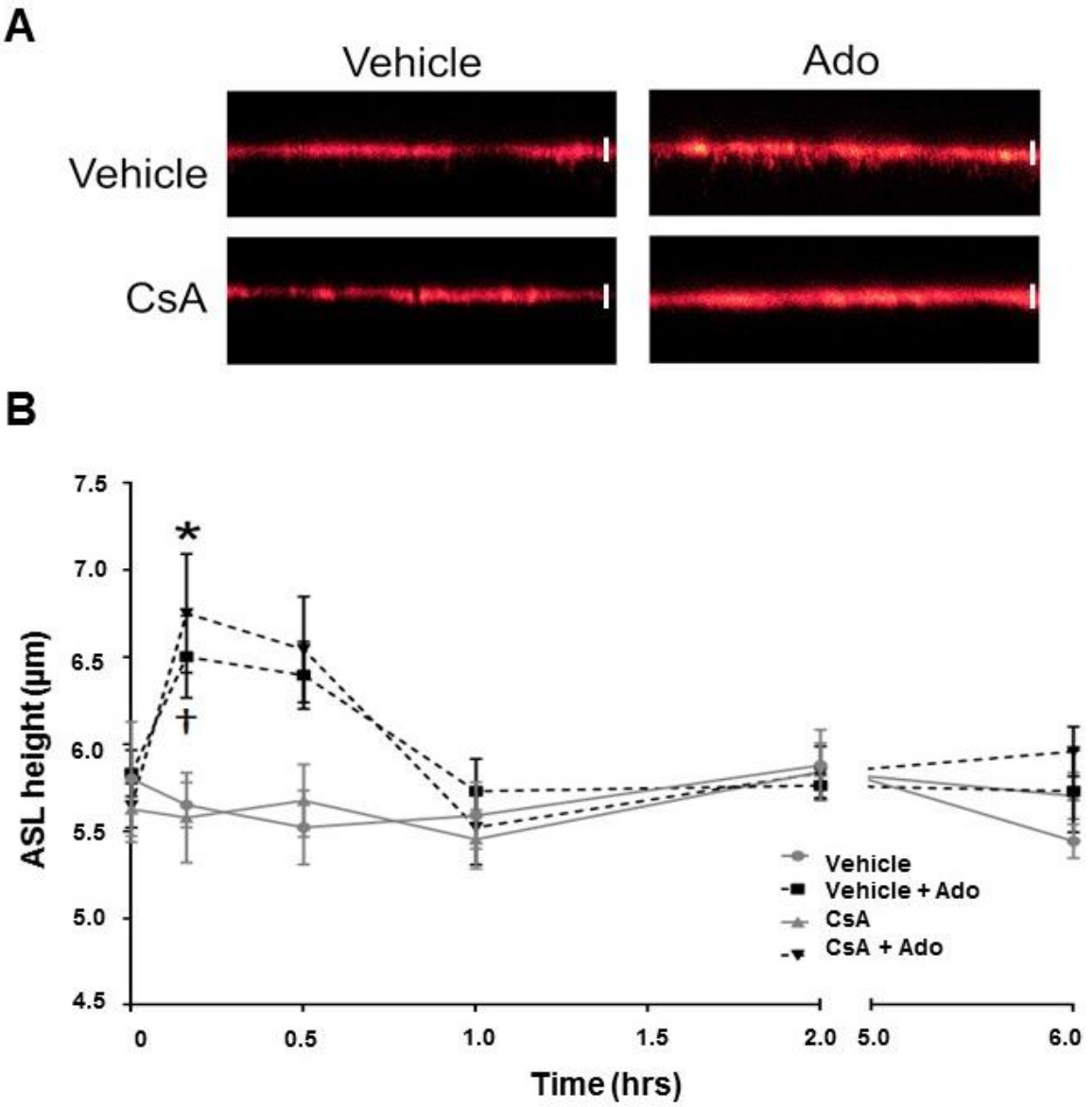

Figure 4.20. Cyclosporin A has no effect on the response of CFTR to adenosine induced increases in ASL height. (A) Airway surface liquid (ASL) in human bronchial epithelial cells was labelled with tetramethylrhodamine conjugated dextran and perfluorocarbon was added mucosally to prevent evaporation of the ASL. Representative images showing ASL height at 10 minutes post exposure to either powdered adenosine (Ado; ~200 µM) suspended in PFC or vehicle, as indicated. **(B)** Time course showing changes in ASL height under conditions indicated. Data are mean ± SEM (n=9 transwells, measured in triplicate, from 3 independent donors). Scale bar represents 10 µm. * represents a significant difference between cells treated with Ado compared to cells treated with vehicle. † represents a significant difference between cells treated with CsA + Ado compared to cells treated with CsA alone.

As a further physiological control, HBECs were also exposed to uridine 5'-triphosphate (UTP, ~200 µM). Within the airways, release of UTP stimulates the $P2Y_2$ receptor and causes activation of the Gq pathway to increase cytosolic Ca^{2+}

and subsequently stimulate Cl^- efflux through CaCC (Tarran et al., 2001b). As with earlier experiments, HBECS were exposed to UTP after pre-treatment with cyclosporin A or vehicle to test whether calcineurin could affect the function of the Ca^{2+} activated chloride channel. Cells were treated with either vehicle or cyclosporin A overnight as earlier.

Cells exposed to vehicle overnight showed an increase in ASL height to 7.4 ± 0.3 µm following 10 minutes exposure to UTP, from a starting height of 5.9 ± 0.3 µm. The ASL height subsequently fell to 6.8 ± 0.4 µm at 1 hour post exposure and recovered to 6.0 ± 0.1 µm at 6 hours post exposure. In contrast, cells treated with vehicle had an ASL that maintained a height of approximately 5.7 µm for the duration of the experiment.

Cells pre-treated with cyclosporin A overnight showed an increase in ASL height to 7.4 ± 0.3 µm following 10 minutes exposure to UTP, compared to a starting height of 6.0 ± 0.1 µm. Cells subsequently showed a decline in ASL height to 6.5 ± 0.2 µm at 1 hour post exposure and a recovery to 5.8 ± 0.1 µm at 6 hours. Cells treated with cyclosporin A showed no substantial changes in ASL height for the duration of the experiment. Thus, the data indicated the response to UTP was similar between cells pre-treated with vehicle and cyclosporin A. Therefore, calcineurin must have no role in regulating the response of the Ca^{2+} activated chloride channel to physiological agonists.

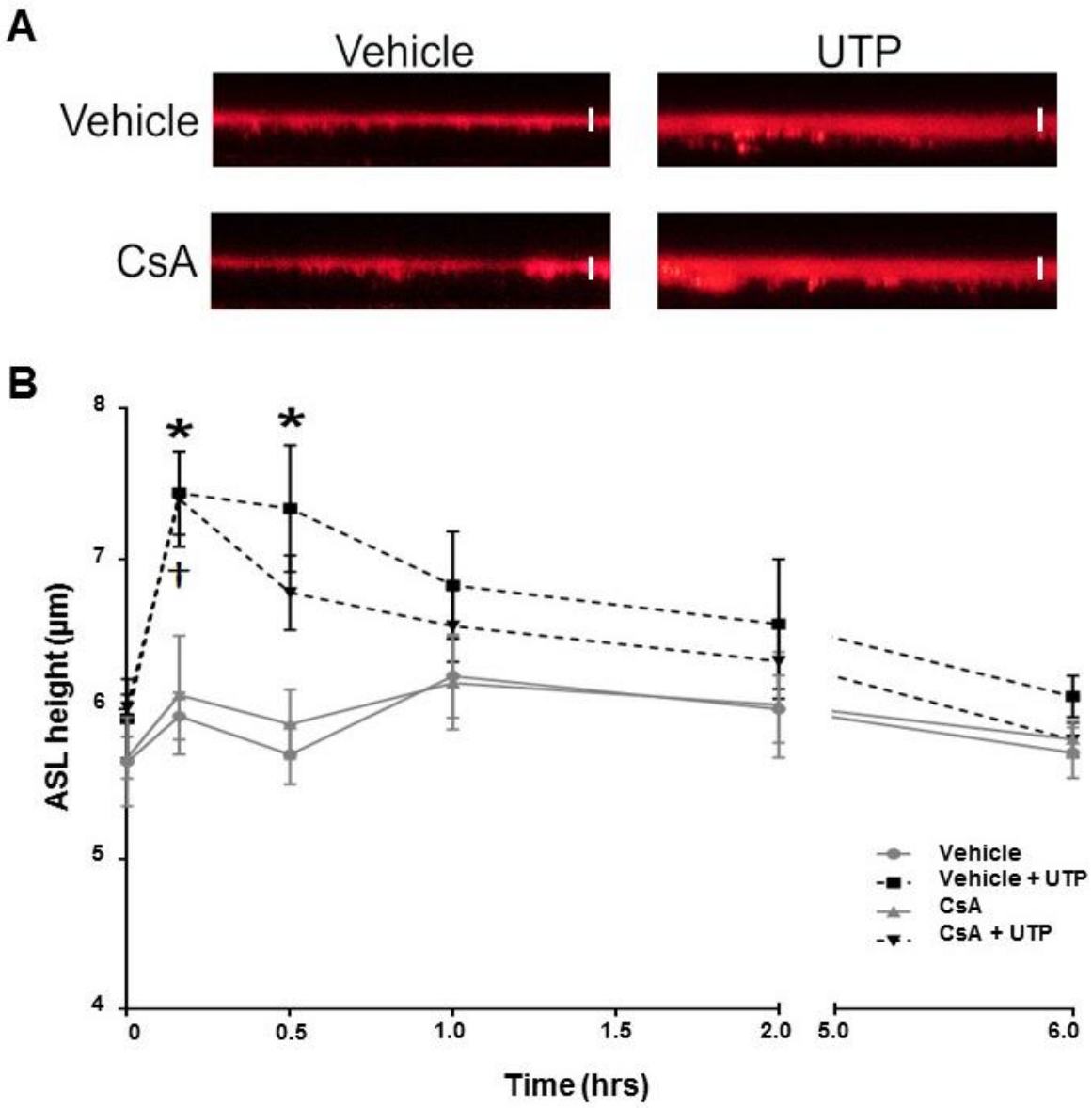

Figure 4.21. Cyclosporin A has no effect on uridine 5'-triphosphate mediated increases in airway surface liquid height responses. Airway surface liquid (ASL) in human bronchial epithelial cells was labelled with tetramethylrhodamine conjugated dextran and perfluorocarbon was added mucosally to prevent evaporation of the ASL. **(A)** Representative images showing ASL height at t=10 min after exposure to either powdered uridine 5'-triphosphate (UTP; ~200 µM) suspended in PFC or vehicle, as indicated. **(B)** Time course showing changes in ASL (n=8-9 transwells from 3 independent donors). Scale bar represents 10 µM. * represents a significant difference between cells treated with uridine 5'-triphosphate (UTP) compared to cells treated with vehicle. † represents a significant difference between cells treated with CsA + UTP compared to cells treated with CsA alone.

4.9 Discussion

In the following section, I will attempt to summarise the effects of increases in cytosolic Ca^{2+}, induced by either cigarette smoke or pharmacological agents, on CFTR (also detailed in Fig. 4.22). Data in the previous chapter showed that a range of Ca^{2+} agonists elicited different changes in cytosolic Ca^{2+} signals in terms of their magnitude and duration. These differences were correlated to differences in the degree of CFTR-mediated conductance loss. The data from confocal microscopy experiments detailed in this chapter also allowed the differences in Ca^{2+} responses to be correlated to differences in the degree of CFTR internalisation seen. Although not as evident in confocal microscopy experiments, ATP was seen to cause a smaller degree of intracellular accumulation of CFTR. These data provide further evidence for the finding that differences in the kinetics of cytosolic Ca^{2+} increases can modulate CFTR residency at the plasma membrane. Initial experiments showed that an increase in cytosolic Ca^{2+} lead to changes in CFTR localisation that were of a similar magnitude to cigarette smoke induced changes. This data supports the finding by Rasmussen and colleagues (2014) that the smoke-induced increase in cytosolic Ca^{2+} is primarily responsible for the effects seen on CFTR (Rasmussen et al., 2014).

Initial experiments found that, as reported by others, cigarette smoke exposure caused a reduction in CFTR present at the plasma membrane and an increase of the protein in the intracellular space. Rasmussen and colleagues (2014) first suggested that CFTR is internalised because of smoke exposure (Rasmussen et al., 2014). However, smoke exposure has been shown by other groups to affect CFTR function. For example, Cantin and colleagues (2006) showed that cigarette smoke exposure caused a reduction in nasal potential difference consistent with a reduction in CFTR activity (Cantin et al., 2006). Furthermore, Raju et al., (2013) showed that the defects in CFTR function are not limited to airway epithelia. Using sweat chloride analysis and intestinal current measurements, the researchers showed reduced CFTR activity in smokers compared to non-smokers (Raju et al., 2013).

The effect of an increase in cytosolic Ca^{2+} was found to be specific to CFTR and had no effect on Ano1 as the location of this channel did not change in response to an increase in cytosolic Ca^{2+}. Ano1 encodes CaCC which secretes Cl^- into the airways, secondary to CFTR (Anderson and Welsh, 1991, Namkung et al., 2011). Consequently, CaCC also plays a role in fluid secretion and changes in ASL height in

response to agonists released into the airways (Tarran et al., 2002). Therefore, Cl^- secretion via CaCC could be protective against the effects of an increase in Ca^{2+} or smoke on CFTR mediated Cl^- secretion. Indeed, it has been previously suggested that in cystic fibrosis, where Cl^- secretion through CFTR is compromised, activation of CaCC could be of therapeutic value (Boucher et al., 1989, Knowles et al., 1991). However, it has been suggested that the secretion induced by CaCC would be insufficient to compensate for the loss of CFTR, suggesting that CaCC activity would be unlikely to counteract the loss of Cl^- secretion from CFTR (Rab et al., 2013).

The specificity of the effect of smoke has also been previously reported by Rasmussen et al., (2014) and Clunes et al., (2012) who found that smoke had no effect on ENaC total protein or Ano1 expression (Clunes et al., 2012, Rasmussen et al., 2014). Interestingly, Virgin et al (2010) found that cigarette smoke condensate exposure caused a decrease in CaCC-mediated conductance in murine sinonasal epithelial cells (Virgin et al., 2010). In contrast to human epithelial cells, where CFTR is principally responsible for Cl^- secretion, CaCC plays a predominant role in Cl^- secretion from murine cells (Clarke et al., 1994). This provides evidence for cigarette smoke affecting the primary Cl^- conductance within the cell.

To assess the route taken by CFTR once internalised, different organelles were labelled with markers and CFTR co-localisation with the markers was assessed. Under the normal endocytic trafficking route taken by CFTR, the channel is internalised by clathrin mediated endocytosis (Bradbury et al., 1994, Prince et al., 1994). Following internalisation, CFTR can be routed to early endosomes from where CFTR can be transported to recycling endosomes to be returned to the plasma membrane. Alternatively, CFTR could be ubiquitinated, causing the protein to be routed from early endosomes to lysosomes for degradation (Ameen et al., 2007). Rasmussen and colleagues (2014) postulated that lysosomal function may be compromised after exposure to smoke, due to smoke stimulating the emptying of lysosomal Ca^{2+} stores, and therefore CFTR may not follow a normal trafficking process (Rasmussen et al., 2014). Indeed, co-localisation between LAMP1 and CFTR did not change when cells were exposed to an increase in cytosolic Ca^{2+}, suggesting that CFTR was not degraded following an increase in cytosolic Ca^{2+}.

Co-localisation of CFTR with the ER markers calreticulin and STIM1 indicated that CFTR is trafficked to the endoplasmic reticulum following an increase in cytosolic Ca^{2+}. This suggests that CFTR follows a retrograde transport pathway whereby CFTR internalised into endosomes is transported to the ER following exposure to an increase in Ca^{2+} (Bonifacino and Rojas, 2006). Friedman and colleagues (2013) showed that the endoplasmic reticulum and endosomes can form sustained contact sites and that these contact sites can be used for transfer of proteins (Friedman et al., 2010, Friedman et al., 2013). Retrograde transport can also involve transport to the *trans* Golgi network, and CFTR can be transported to the *trans* Golgi network from late endosomes (Ameen et al., 2007). However, the experiments detailed above showed no change in CFTR in the Golgi network following an increase in cytosolic Ca^{2+}. As transport to the Golgi network is usually seen in retrograde transport, it is possible that a more detailed time course would be needed to fully assess whether CFTR located in the Golgi changes after an increase in cytosolic Ca^{2+}.

The data showed that inhibition the MEK/ERK pathway negated the effect of a Ca^{2+}-induced internalisation of CFTR. The MEK/ERK pathway is a ubiquitous signalling pathway that is comprised of a mitogen activated protein kinase (MAPK) kinase kinase that phosphorylates a MAPK kinase which in turn phosphorylates MAPK. In the ERK pathway, Raf functions as the MAPKKK, MEK (MAPK/ERK) as MAPKK and ERK as MAPK. The pathway can regulate other kinases, as well as cellular processes such as proliferation, differentiation, and cell survival (Bonni et al., 1999, Kolch, 2000, Whitmarsh and Davis, 2000, Shaul and Seger, 2007). Our lab has previously shown that the MEK/ERK pathway is involved in the smoke induced diminution of CFTR. Further, the same inhibitors as those used in these experiments were able to inhibit smoke-induced internalisation of CFTR (Xu et al., 2015). Similarly, Hellerman and colleagues (2002) found that acute exposure of human bronchial epithelial cells to cigarette smoke condensate caused an increase in ERK1/2 activity. Further, the authors also linked the activation of MAPK activity and NFκB to an increase in proinflammatory cytokines (Hellermann et al., 2002).

Studies have correlated an increase in cytosolic Ca^{2+} with the activation of ERK 1/2 and MEK 1/2 in lens epithelial tissue and neurons (Rosen et al., 1994, Li et al., 2005). Indeed, studies from our lab have shown that inhibition of the MEK/ERK pathway had no effect on the Ca^{2+} increase induced by smoke (Marklew, 2016) .

Paradoxically, ERK has been associated with an increase in CFTR activity in renal epithelial cells. Jansson and colleagues found that fluid secretion from renal cells was coupled to increases in Cl^- secretion through CFTR, which were in turn mediated by the Src-MEK/ERK pathway (Jansson et al., 2012). The consequences of the activation of the MEK/ERK pathway has been shown to depend on the strength and magnitude of the activation (Agell et al., 2002). For example, previous studies have shown that sustained activation of the pathway can lead to cell cycle arrest inked to either apoptosis or proliferation, depending on the cell type (Qiu and Green, 1992, Cook et al., 1997). However, the profile of the activation of the MEK/ERK pathway by smoke has not been characterised. Together with the data detailed in this chapter, these findings suggest that activation of the MEK/ERK pathway is secondary to the Ca^{2+} increase induced by cigarette smoke. However, further characterisation of the activation profile of the MEK/ERK pathway in airway cells would be needed as these studies could help elucidate how activation of the pathway could have different effects on CFTR.

Various inhibitors employed to investigate the role of PKC and serine/threonine phosphatases suggested that these pathways play no role in Ca^{2+}-induced internalisation of CFTR. Rasmussen and colleagues (2014) similarly found that these same pathways also play no role in CFTR internalisation induced by cigarette smoke (Rasmussen et al., 2014). Interestingly, my experiments showed that when cells were pre-treated with forskolin, cigarette smoke no longer caused internalisation of CFTR, suggesting that PKA phosphorylation protects CFTR. Similarly, inhibition of PKA 'rescued' the internalisation of CFTR induced by smoke but had no effect in cells treated with a pharmacological Ca^{2+} agonist. Experiments also showed that forskolin pre-treatment did not affect the change in cytosolic Ca^{2+} induced by cigarette smoke, suggesting the effect of forskolin on CFTR internalisation was downstream to the increase in cytosolic Ca^{2+}. Likewise, others have found that forskolin was able to prevent endocytosis of wild type CFTR in cell lines including pancreatic cells and T84 cells (Bradbury et al., 1992, Prince et al., 1994, Howard et al., 1996). Lukacs et al., (1997) further suggested that phosphorylation of CFTR prevented CFTR removal from the plasma membrane by promoting the movement of CFTR held in internal stores to the plasma membrane (Lukacs et al., 1997).

Conversely, in my studies, forskolin pre-treatment had no effect on Ca^{2+}-induced internalisation of CFTR. Whilst no other studies have investigated the effect of an increase in cytosolic Ca^{2+} on CFTR internalisation, as discussed in chapter 4, others have shown that an increase in Ca^{2+} in the presence of forskolin can cause a reduction in CFTR activity (Bozoky et al., 2017). Therefore, it seems that when cells are exposed to an increase in cytosolic Ca^{2+}, phosphorylation via PKA is not able to protect CFTR. Arguably, smoke exposure would cause numerous effects within the cell. It is possible that besides the increase in cytosolic Ca^{2+}, another consequence of smoke exposure is responsible for this discrepancy between the effect of smoke and an increase in cytosolic Ca^{2+}.

Imaging experiments showed that inhibition of the Ca^{2+} dependent phosphatase, calcineurin, prevented both smoke-induced and thapsigargin-induced internalisation of CFTR. Thus, calcineurin plays a key role in regulating CFTR internalisation. Calcineurin, also known as protein phosphatase 2B, requires Ca^{2+} and calmodulin for activation, specifically, calcineurin is activated by sustained elevations in cytosolic Ca^{2+} (Crabtree, 1999, Rusnak and Mertz, 2000). Although calcineurin is found in multiple mammalian tissues, the role of this phosphatase has been extensively studied in neuronal cells, where calcineurin is responsible for hippocampal long term depression and nerve regeneration. Calcineurin itself is composed of an A and B subunit, both of which are necessary for activity of the phosphatase (Klee et al., 1979). The A subunit contains the catalytic domain and the regulatory domain which is composed to a calmodulin binding domain and an autoinhibitory domain whilst the B subunit of the phosphatase contains the Ca^{2+} binding region (Kincaid et al., 1988, Rusnak and Mertz, 2000).

Interestingly, Lai et al., (1999) found that in extracts from rat brain, calcineurin is linked to dynamin 1. Furthermore, the researchers found that the link between calcineurin and dynamin was Ca^{2+} dependent. They correlated an increase in cytosolic Ca^{2+} to the dephosphorylation of dynamin, which resulted in the translocation of the calcineurin-dynamin complex to a cluster of proteins involved in clathrin mediated endocytosis, allowing calcineurin to dephosphorylate other proteins (Lai et al., 1999). Further evidence for the interaction between calcineurin and dynamin comes from the observation that calcineurin has been found to be associated with the cytoskeleton, as is dynamin (Earnest et al., 1996). Given that

inhibition of dynamin via dynasore was found to inhibit CFTR internalisation, these data from Lai and colleagues provide a functional link between my data showing a role for calcineurin and dynamin in Ca^{2+}-induced internalisation of CFTR (Fig. 4.22). Consequently, testing whether there is an interaction between calcineurin and dynamin, either using co-immunoprecipitation or knockdown of either protein could provide a direct link between smoke-induced activation of calcineurin and changes in dynamin activity.

Calcineurin has also been shown to regulate the activity of CFTR itself. Fischer and colleagues (1998) found that calcineurin could inhibit the activation of CFTR by either PKA or PKC. Furthermore, they found forskolin stimulation evoked larger currents after calcineurin inhibition. However, it has been suggested that calcineurin does not regulate CFTR in all cell types, Fischer and colleagues found that in epithelial cell lines, inhibition of endogenous calcineurin did not affect CFTR, suggesting CFTR function is not governed by calcineurin, similar to findings from ASL height data. The researchers suggested that the effect of calcineurin on CFTR may depend on the subcellular location of calcineurin (Fischer et al., 1998). My data has thus far suggested that phosphorylation of CFTR may be an important determinant of whether the channel is internalised. However, the data from Fischer and colleagues along with data in the literature describing the effect of calcineurin on dynamin suggest the phosphorylation status of multiple proteins, including CFTR, may need to be further investigated to understand the internalisation of CFTR.

As discussed in section 1.7 cigarette smoke is thought to cause Ca^{2+} release from lysosomal stores. Furthermore, lysosomal Ca^{2+} release through the TRPML1 channel has been shown to activate calcineurin directly. Since calcineurin is activated by direct increases in cytosolic Ca^{2+}, these data provide a direct mechanistic link between CS induced release of lysosomal Ca^{2+} and CFTR internalisation (Fig. 4.22). The pathway has been characterised as regulating autophagy independently of the mTOR pathway (Medina et al., 2015). Rasmussen and colleagues found inhibition of the mTOR pathway has no effect on CFTR internalisation (Rasmussen et al., 2014). Thus, investigating whether cigarette smoke causes Ca^{2+} release through the TRPML1 channel could be of value in further understanding how cigarette smoke affects intracellular Ca^{2+} signalling.

Studies have suggested that there is a link between calcineurin and activation of the ERK pathway, which is of interest, given that activation of the ERK pathway has been shown to play a role in CFTR internalisation. Kinase suppressor of Ras 2 (KSR2) acts as a scaffold and positive regulator of the ERK signalling cascade (Kornfeld et al., 1995, Sundaram and Han, 1995, Therrien et al., 1995, Kolch, 2000). Using mass spectrometry analysis, Dougherty and colleagues (2009) found that KSR2 can interact with calcineurin. Furthermore, using metabolic [^{32}P] labelling, the researchers showed that calcineurin dephosphorylated KSR2 and so was able to regulate KSR2 movement to the plasma membrane and an increase ERK activity in response to increases in cytosolic Ca^{2+} (Dougherty et al., 2009). Conversely, MAPKs themselves have also been shown to affect calcineurin. It has been shown that activation of MAPK can either further activate or inhibit calcineurin-NFAT signalling, depending on the cell type (Molkentin, 2004). These data suggest that further study is needed into the interaction between calcineurin and the MEK/ERK pathway after smoke exposure in airway epithelia.

It has been suggested that A kinase anchoring proteins (AKAPs), which bind PKA and localise its actions to specific domains in the cell can form a macromolecular complex (Colledge and Scott, 1999). In particular, the mAKAP complex has been shown to contain PKA, Ca^{2+}, components of the MEK/ERK pathway, the guanine nucleotide exchange factor (Epac), the ryanodine receptor, phosphodiesterases and phosphatases including calcineurin in cardiac myocytes (Marx et al., 2000, Dodge-Kafka et al., 2005, Dodge-Kafka and Kapiloff, 2006). The complex has been suggested to integrate changes in intracellular cAMP and Ca^{2+} to nuclear processes (Dodge-Kafka et al., 2005). Furthermore, a similar complex has also been found in neuronal cells, where AKAP79, PKA and calcineurin have been shown to form a complex (Coghlan et al., 1995). Within airway epithelia, ezrin has been shown to be an AKAP associated with PKA and CFTR, however, it has not been found to be associated with calcineurin (Sun et al., 2000, Tasken and Aandahl, 2004). These findings suggest that there may be more components to the regulation of CFTR by changes in Ca^{2+}, the MEK/ERK pathway and calcineurin.

Conversely, it has been shown that calcineurin can also indirectly positively regulate CFTR function. Using co-immunoprecipitation, Borthwick and colleagues (2007) showed that annexin 2, the Ca^{2+} binding protein S100A10, and CFTR form a complex

dependent on cAMP and PKA. Further, they showed that the formation of this complex was dependent on calcineurin, as inhibition of calcineurin was able to prevent complex formation (Borthwick et al., 2007). Whilst these data suggest calcineurin plays a role in the activation of CFTR, Fischer et al., (1998) speculated that the location of calcineurin may be important in regulating its effect on CFTR (Fischer et al., 1998). Therefore, it could be possible that the increase in Ca^{2+} of the magnitude caused by thapsigargin or cigarette smoke interferes with the role of calcineurin in forming a macromolecular complex or causes relocation of the phosphatase. Thus, further experiments using co-immunoprecipitation to test whether Ca^{2+} agonists interfere with complex formation would be of value.

The findings detailed in HEK 293 cells were validated in airway cells. Inevitably, HEK 293 cells present a model system which has much simpler dynamics/signalling pathways than highly specialised airway epithelial cells. Indeed, when grown in a polarised manner, airway cells have highly compartmentalised signalling machinery for CFTR located at the apical pole of the cell (Guggino and Stanton, 2006). Thus, I attempted to validate my findings in HBECS to determine whether similar dynamics were at play in a more complex system. Cigarette smoke exposure caused a rapid reduction in ASL height, and similar changes in ASL have been previously reported (Clunes et al., 2012, Rasmussen et al., 2014). The height of the ASL is principally determined by transepithelial ion flux; therefore, a smoke-induced reduction in CFTR function causes a reduction in ASL height (Boucher, 1999, Clunes et al., 2012). Furthermore, an abnormal ASL height has been suggested to be linked to an impairment of mucociliary clearance and an increased prevalence of bacterial infections (Verkman et al., 2003, Fahy and Dickey, 2010). Indeed, patients with COPD have been found to have a higher incidence of chronic infection (Stämpfli and Anderson, 2009). Cyclosporin A prevented the smoke-induced decrease in ASL height, presumably by preventing the loss of CFTR from the membrane. This is of interest because restoring CFTR function in CF patients has been shown to reduce the prevalence of lung infection (Hisert et al., 2017).

Phosphatases have been previously shown to regulate ASL height. Thelin and colleagues (2005) showed that PP2A, which is active in the absence of divalents, can regulate CFTR in airway epithelial cells (Rusnak and Mertz, 2000, Thelin et al., 2005). Using affinity purification and co-immunoprecipitation, the researchers found

that PP2A binds to the C terminus of CFTR. Furthermore, an inhibition of the interaction between PP2A and CFTR resulted in an increase in Cl^- secretion through CFTR and the height of the ASL (Thelin et al., 2005). The resting ASL height of cultures pre-treated with cyclosporin A, either acutely or overnight, showed no difference to cultures pre-treated with vehicle only. These data suggested that calcineurin is not active under resting conditions, as an increase in activity would be expected to cause a higher ASL height.

Further evidence for calcineurin having no role in regulating resting ASL height came from the finding that calcineurin inhibition had no effect on changes in ASL height in response to physiological agonists. The effect of calcineurin of CFTR function was tested using adenosine, which stimulates the $A2_B$ receptor, and is an agonist for CFTR function. Similar to the data presented in this chapter, it has been previously been shown that adenosine causes a small and rapid increase in ASL height (Tarran et al., 2006b). A role for adenosine in the regulation of ASL height has also been shown by the findings that inhibition of the $A2_B$ receptor results in cultures being unable to regulate ASL height (Tarran et al., 2005). Furthermore, a sustained basal level of adenosine, which continuously stimulates the $A2_B$ receptor, has been shown to be critical for the regulation of ASL height (Lazarowski et al., 2004). The effect of calcineurin on Cl^- secretion through calcium activated chloride channel activity was also tested, using UTP to stimulate $P2Y_2$ receptors (Tarran et al., 2006a). A similar temporal change in ASL height induced by UTP has been previously reported, with the transient nature of the response likely due to breakdown of UTP by ecto-nucleotidases (Tarran et al., 2001b). The data showed that calcineurin inhibition had no effect on Cl^- secretion through either CFTR or CaCC when stimulated with physiological agonists. Therefore, it may be possible that calcineurin only plays a role in regulating CFTR under conditions of stress.

In summary, the main findings of this chapter are;

- An increase in cytosolic Ca^{2+} causes a loss of CFTR at the plasma membrane and movement of the protein to the intracellular space.

- CFTR is trafficked to the endoplasmic reticulum following an increase in cytosolic Ca^{2+}.

- The phosphorylation status of CFTR has different consequences for cells exposed to cigarette smoke or to an increase in cytosolic Ca^{2+}.
- The MEK/ERK pathway plays a role in Ca^{2+}-induced internalisation of CFTR.
- The Ca^{2+} dependent phosphatase, calcineurin, plays a central role in the internalisation of CFTR following exposure to either cigarette smoke or to an increase in cytosolic Ca^{2+} induced by thapsigargin.
- Inhibition of calcineurin can protect the ASL against a smoke-induced reduction in height but this phosphatase plays no role in the response of CFTR to physiological agonists.

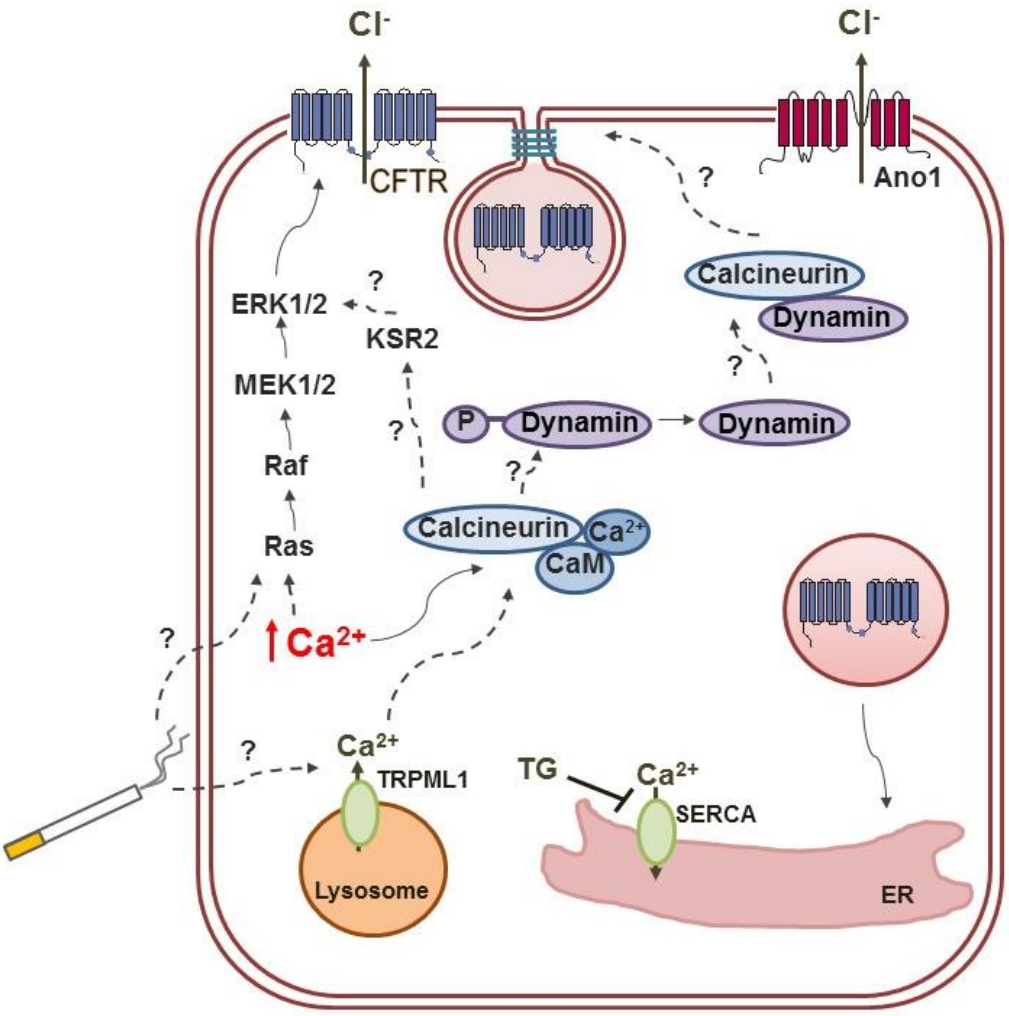

Figure 4.22. Summary of the cellular effects of cigarette smoke and an increase in cytosolic Ca^{2+} on CFTR surface expression. Data detailed in this chapter showed exposure to either thapsigargin (TG) or cigarette smoke caused an increase in cytosolic Ca^{2+}. The work in this thesis did not show an increase in Ca^{2+} activates the MEK/ERK pathway, however this effect has been detailed in the literature. Nevertheless, a role for the MEK/ERK pathway in thapsigargin-induced CFTR internalisation was indicated by my data. Furthermore, my data linked an increase in cytosolic Ca^{2+} to the activation of calcineurin. CFTR was subsequently found to be internalised via a dynamin-dependent mechanism and routed to the endoplasmic reticulum. The location of Ano1, on the other hand, was unaffected by cigarette smoke or an increase in Ca^{2+}. Potential mechanisms deduced from the literature are indicated by dashed arrows. Cigarette smoke has been linked to activation of the MEK/ERK pathway. Cigarette smoke, through the effects of reactive oxygen species, and increases in cytosolic Ca^{2+} has also been speculated to cause an increase in cytosolic Ca^{2+} arising from the lysosomal stores. Lysosomal Ca^{2+} release through TRPML1 channels, have been linked to the activation of calcineurin. Furthermore, the activation of calcineurin has been linked to dephosphorylation of the ERK pathway regulator, KSR2, with the consequent effect of increasing ERK activity. Thus, there may be some cross-talk between the activation of the MEK/ERK pathway and calcineurin. Calcineurin is also known to dephosphorylate dynamin and other proteins involved in endocytosis, suggesting that calcineurin may act to internalise CFTR via its effects on dynamin.

Chapter 5.0 Concluding Discussion

5.1 Summary of main findings

The aim of my project was to investigate the effect of an increase in cytosolic Ca^{2+} on CFTR function and to determine the mechanism underlying how an increase cytosolic Ca^{2+} affects CFTR activity. Much of my work was carried out using HEK 293T cells transiently transfected with CFTR as this cell system represents a model which can be easily manipulated and reproduce the effects of cigarette smoke on epithelial cells (Rasmussen et al., 2014). Using the whole cell configuration of the patch clamp technique, I found that increases in cytosolic Ca^{2+}, elicited by a range of pharmacological agonists, caused a decrease in CFTR-mediated conductance. By using fluorescent Ca^{2+} measurements to give an approximation of the changes in cytosolic Ca^{2+}, I found that the loss of CFTR-mediated conductance was temporally related to the increases in cytosolic Ca^{2+}. Furthermore, Ca^{2+} imaging experiments also helped deduce that a transient increase in cytosolic Ca^{2+} was sufficient to cause a reduction in CFTR-mediated conductance. Further to these findings, inhibition of dynamin prevented the loss of CFTR-mediated conductance after exposure to an agonist which caused an increase in cytosolic Ca^{2+}. These data suggested that increases in cytosolic Ca^{2+} stimulated the removal of CFTR from the plasma membrane via a dynamin-dependent mechanism.

Confocal microscopy was used to assess changes in CFTR localisation after an increase in cytosolic Ca^{2+}. These experiments revealed that the loss of CFTR from the plasma membrane followed changes in cytosolic Ca^{2+}, similar to that seen in patch clamp experiments. These data also linked the reduction in CFTR-mediated conductance to a loss of CFTR channels expressed at the plasma membrane. In addition, imaging experiments indicated that the Ca^{2+}-induced loss of CFTR from the plasma membrane was accompanied by a reciprocal increase in intracellular fluorescence, further suggesting that CFTR was internalised. A comparison of the changes in CFTR expression induced by pharmacological Ca^{2+} agonists and smoke exposure revealed both agonists caused a similar pattern of change in CFTR expression. Taken together, these data provide strong evidence that a smoke-induced increase in Ca^{2+} was the primary cause for loss of CFTR from the plasma membrane. Additionally, an increase in cytosolic Ca^{2+} stimulated the relocation of CFTR from the plasma membrane to the endoplasmic reticulum, without routing the

protein to lysosomes for degradation, as shown for the change in CFTR localisation induced by smoke exposure (Rasmussen et al., 2014, Marklew, 2016). The similarity between smoke exposure and pharmacological Ca^{2+} agonists was also seen in the MEK/ERK pathway, where inhibition of the pathway prevented Ca^{2+}-induced CFTR internalisation (Xu et al., 2015). Together, these data suggested that exposure to either a Ca^{2+} agonist or cigarette smoke caused similar cellular effects and induced a similar pattern of trafficking in CFTR.

Initial electrophysiology experiments studied the effect of an increase in cytosolic Ca^{2+} after forskolin had been used to stimulate phosphorylation of CFTR. To determine whether there was a difference in the effect of Ca^{2+} increases on phosphorylated and unphosphorylated CFTR, parallel confocal imaging experiments were carried out. These experiments revealed that the pre-treatment of HEK 293 cells with forskolin had no effect on Ca^{2+}-induced CFTR internalisation. Interestingly, the same manoeuvre in cigarette smoke exposed cells prevented CFTR internalisation. These data suggested that PKA dependent phosphorylation of CFTR had different consequences for CFTR depending on the agonist used to stimulate internalisation, thus uncovering a divergence in the effects of cigarette smoke *vs* increases in Ca^{2+} induced by pharmacological agents.

Further to the finding that the phosphorylation status of CFTR may be an important determinant of CFTR internalisation, the Ca^{2+} dependent phosphatase, calcineurin, was found to play a key role in CFTR internalisation. Using confocal microscopy, calcineurin inhibition was found to prevent loss of CFTR from the plasma membrane after exposure to either cigarette smoke or a Ca^{2+} agonist. Furthermore, cigarette smoke and pharmacological Ca^{2+} agonists were both found to directly increase calcineurin phosphatase activity; these data further indicated that this phosphatase could determine CFTR internalisation. Importantly, these findings were replicated in primary human bronchial epithelial cells, where calcineurin inhibition prevented a cigarette smoke-induced reduction in ASL height. Conversely, calcineurin inhibition had no effect on physiological changes in ASL height induced by G protein-coupled receptor agonists. Together, these data suggest that calcineurin may not regulate CFTR activity under resting conditions but may only be active under conditions of stress.

5.2 Clinical significance of findings for smoke related disease

The major disease associated with smokers is chronic obstructive pulmonary disease. As detailed in section 1.5.2, the presentation of the disease is clinically seen as either emphysema, chronic bronchitis, or most commonly, a combination of both (Siafakas et al., 1995). Furthermore, the progression of both emphysema and chronic bronchitis has been proposed to be, in part, mediated by a smoke-induced reduction in CFTR function and expression at the plasma membrane (Bodas et al., 2011, Clunes et al., 2012). My data identified the activation of the Ca^{2+} dependent phosphatase, calcineurin as causative in smoke-induced CFTR internalisation. Likewise, my data showed that calcineurin inhibition with cyclosporin A prevented loss of CFTR at the plasma membrane after smoke exposure.

Cyclosporin A is currently in use clinically as an immunosuppressant. The drug has been widely used as part of treatment regimens for the prevention of graft rejection and in the cure of autoimmune diseases (Stellato et al., 1992, MacDonald, 2001). These findings suggest that cyclosporin A could be easily administered to patients with smoke related diseases. However, it has been suggested that smokers have a lower absorption of formulations of cyclosporin A used clinically. These differences have been attributed to a reduction in the availability of the drug in the intestine due to increased intestinal peristalsis caused by nicotine (Fagiolino et al., 2014). Nevertheless, a study looking at the effect of environmental tobacco smoke exposure and cardiovascular disease found that the association was lower in patients who were already being prescribed cyclosporin A, suggesting the drug may have some efficacy *in vivo* in combating the effects of cigarette smoke (Pope 3rd et al., 2001).

In addition to oral formulations of cyclosporin A, aerosolised cyclosporin A also been prescribed for the treatment of lung diseases as this method of application has been associated with increased bioavailability of the drug (Fukaya et al., 2003). Furthermore, administration of aerosolised cyclosporin A has been associated with a stabilisation of pulmonary function in progressive diseases such as bronchiolitis obliterans (Iacono et al., 1997). This is of interest because these studies indicate cyclosporin A could be readily used to treat smoke induced lung disease. Therefore, inhibition of calcineurin with cyclosporin A could represent a viable method of negating the effects of cigarette smoke on the airway.

Although my studies used cyclosporin A to inhibit calcineurin, clinically, tacrolimus is also available as an immunosuppressant that acts through the inhibition of calcineurin (Jørgensen et al., 2003). Furthermore, studies have suggested that tacrolimus has a higher efficacy than cyclosporin A in preventing graft rejection (Group, 1994a, Group, 1994b). Thus, tacrolimus could also represent a potential treatment strategy to prevent smoke-induced airway disease.

5.3 Future experiments

The data presented in this study help to further understand how changes in cytosolic Ca^{2+} modulate the expression and activity of CFTR at the plasma membrane. However, there are still many experiments that could be performed to provide a more detailed mechanistic understanding of the effects of increases in cytosolic Ca^{2+} and cigarette smoke on CFTR. Many of the experiments carried out in this thesis used HEK 293 cells as an expression system as exogenous protein can be easily introduced and studied in this cell line. The experiments conducted in this thesis would be much more difficult in highly specialised epithelial cells as these cells are not as easily manipulated (Zhu et al., 1998). Thus, validating my findings in other cell lines would be of value. Accordingly, Balch and colleagues observed that the trafficking pattern of CFTR is different in BHK and CHO cells versus HEK and HeLa cells. Furthermore, trafficking has been suggested to be different between epithelial and non-epithelial cell lines (Bertrand and Frizzell, 2003). Previous studies have also found cAMP dependent membrane trafficking is not seen in non-epithelial cell lines, suggesting the trafficking machinery is specialised in epithelial cells in comparison to non-epithelial cell lines (Dho et al., 1993, Hug et al., 1997, Bertrand and Frizzell, 2003). Additionally, trafficking has been shown to be different in cells grown as polarised monolayers or unpolarised (Cholon et al., 2010). Therefore, experiments investigating the relocation of CFTR following an increase in cytosolic Ca^{2+} may need to be repeated in polarised epithelial cells such as primary human bronchial epithelial cells.

CFTR was found to be routed to the ER, after either an increase in cytosolic Ca^{2+} or smoke exposure. However, the experiments only looked at CFTR localisation 30 minutes after exposure to an increase in cytosolic Ca^{2+}. Therefore, a more detailed time course using various intracellular organelle markers would be needed to fully determine the trafficking of CFTR after exposure to an increase in cytosolic Ca^{2+}.

Thus far, the fate of CFTR after being transported to the ER has not been investigated. The retrograde transport of CFTR through the ER has been associated with ER associated degradation (ERAD) of the protein. Indeed, Xiong and colleagues (1999) showed that proteins in the ER membrane could be targeted for ERAD (Xiong et al., 1999). Whether a similar process takes place after an increase in cytosolic Ca^{2+} or smoke exposure could help further understand the fate of CFTR after it reaches the ER.

The data detailed in chapter 4 showed increases in cAMP, and so the phosphorylation of CFTR by PKA had different effects on CFTR internalisation. When exposed to cigarette smoke, phosphorylation of CFTR relieved internalisation whereas the phosphorylation status of CFTR had no effect on internalisation stimulated using pharmacological Ca^{2+} agonists. Further investigating this difference could help understand how the phosphorylation status of CFTR affects endocytic trafficking of the channel. Various antibodies are available which only bind to CFTR when phosphorylated by PKA (Hegedűs et al., 2009). Furthermore, antibodies to distinguish between various sites on the R domain are available. For example, antibodies which bind at phosphorylation sites, 737, 700, 768 and 813, all of which are predicted to be phosphorylated by PKA. Western blots to determine changes in the phosphorylation of these sites could help further understand the different effects PKA phosphorylation had on CFTR internalisation when exposed to either a Ca^{2+} agonist or cigarette smoke.

As detailed in section 4.9, calcineurin has been physically associated with dynamin in neuronal cells (Lai et al., 1999). My experiments linked inhibition of dynamin and calcineurin independently to the prevention of CFTR internalisation. Knockdown of either calcineurin or dynamin using siRNA could help determine whether both these proteins are needed for CFTR internalisation. Whether an increase in Ca^{2+} causes calcineurin to be physically associated with dynamin would help not only further characterise the mechanism of smoke exposure on CFTR internalisation, but also the role of calcineurin in airway epithelial cells. As the experiments detailed in this thesis used pharmacological inhibitors for calcineurin, knock down of the phosphatase using siRNA could also help provide further evidence for the role of calcineurin in CFTR internalisation.

As discussed in section 4.9, calcineurin is associated with AKAPs, PKA, various phosphatases, phosphodiesterase's and components of the MEK/ERK pathway in cardiac myocytes and neuronal cells (Dodge-Kafka and Kapiloff, 2006). To my knowledge, no one has investigated whether components of the MEK/ERK pathway and calcineurin are part of a macromolecular complex with CFTR. The association of calcineurin with these proteins could be tested using co-immunoprecipitation. If calcineurin was found to be associated with these proteins, it could help understand how calcineurin regulates CTFR, as a complex such as this would create a specialised region bringing together multiple proteins involved in the regulation of CFTR activity. Alternatively, calcineurin has been shown to critical to development of a macromolecular complex involving CFTR, annexin 2 and S100A10 (Borthwick et al., 2007). This complex has been suggested to be necessary for the function of CFTR. Co-immunoprecipitation of CFTR with these proteins could help understand if calcineurin affects CFTR activity by disrupting the formation of this complex.

I used confocal microscopy to measure changes in plasma membrane resident CFTR; however, studies measuring changes in expression of protein at the plasma membrane have typically used surface biotinylation as a sensitive assay (Prince et al., 1994, Lukacs et al., 1997, Silvis et al., 2009). This technique involves labelling proteins expressed at the plasma membrane with biotin and measuring changes in biotinylated proteins after treatment. Thus, directly measuring whether calcineurin inhibition could cause the retention of CFTR at the plasma membrane after an increase in cytosolic Ca^{2+} would be of value.

The MEK/ERK pathway represents a common signalling cascade that is thought to be activated by either an increase in cytosolic Ca^{2+} or cigarette smoke exposure (Rosen et al., 1994, Li et al., 2005, McCubrey et al., 2005). The studies detailed in this thesis used pharmacological inhibitors to test the involvement of this pathway in CFTR internalisation. To more definitively test the role of this pathway, antibodies against phospho-Erk1/2 could be used to show activation of MEK/ERK signals (Xu et al., 2015). The activation of the MEK/ERK signalling cascade and calcineurin has been shown to be co-dependent. Identifying whether there is some cross talk between these two events after smoke exposure would help decipher the downstream events that takes place. Therefore, western blots testing for activation of

the pathway after treatment with cyclosporin A could help identify whether activation of calcineurin is upstream or downstream of the MEK/ERK pathway.

The experiments in this thesis used pharmacological agents to replicate the effect of cigarette smoke. Sassano et al., (2017) identified multiple cigarette smoke constituents linked to an increase in cytosolic Ca^{2+}. Thus, the identification of constituents of cigarette smoke may prove useful in replicating the effects in smoke on Ca^{2+} more closely. Amongst the constituents, nicotine-derived nitrosamine ketone (NNK) was found to cause a substantial increase in cytosolic Ca^{2+} (Sassano et al., 2017). Based on the data detailed in this thesis, I would predict that NNK would also cause a reduction in CFTR-mediated conductance and dynamin-dependent internalisation of the channel. However, Li et al., (2010) showed that exposure of Calu-3 cells to NNK caused an increase in CFTR activity, measured using either iodide efflux or short-circuit current changes (Li et al., 2010). Together, these findings are intriguing as they suggest that there may be another underlying mechanism for Ca^{2+} to affect CFTR at the plasma membrane. However, a clear difference is that Sassano et al., (2017) exposed cells to NNK overnight whilst the experiments in this thesis only studied the effect of acute increases in cytosolic Ca^{2+}. Whilst the acute effect of NNK on cytosolic Ca^{2+} would need to be studied, measuring the effect of NNK on CFTR could be of value in further understanding how changes in cytosolic Ca^{2+} affect CFTR function and expression.

Many of the experiments detailed in this thesis used thapsigargin to mimic the effect of cigarette smoke exposure. Whilst the temporal profile of smoke induced increases in cytosolic Ca^{2+} have been characterised, any possible long-term effects have not been studied. Interestingly, it has been suggested that a process of Ca^{2+} induced Ca^{2+} signal remodelling can occur in the heart, causing changes to cellular architecture (Berridge et al., 2003, Berridge, 2006a, Berridge, 2006b). In cystic fibrosis, the capacity of the endoplasmic reticulum stores has been shown to be increased in comparison to wild type cells. Furthermore, the cigarette smoke component, cadmium has been linked to an inhibition of SERCA (Biagioli et al., 2008, Mekahli et al., 2011). Further to changes in the endoplasmic reticulum structure, mitochondrial stores have also been found to be altered in cystic fibrosis. Similar to the endoplasmic reticulum store, the capacity of the mitochondrial stores are enlarged in CF patients (Feigal and Shapiro, 1979). Rasmussen and colleagues

showed that the mitochondria and endoplasmic reticulum buffered some of the increased cytosolic Ca^{2+} after smoke exposure. Therefore, changes in the expression of the SERCA and mitochondrial buffering capacity would have important consequences for the effect of long term smoke exposure on Ca^{2+} homeostasis (Rasmussen et al., 2014). It is possible that chronic elevations in cytosolic Ca^{2+} cause stores to increase their buffering capacity. Consequently, it would be interesting to measure the capacity of these stores in cells derived from smokers or exposed to cigarette smoke chronically in comparison to cells from non-smokers. Thus, characterising whether chronic smoke exposure could cause similar changes in the Ca^{2+} signalling architecture, such as the expression of SERCA, would be of interest in further understanding the effect of smoke on cellular processes.

Finally, further understanding the proteins involved in the Ca^{2+} response to cigarette smoke would be of value as identification of these proteins could lead to novel targets in preventing a smoke-induced increase in cytosolic Ca^{2+}. One approach to identify these proteins would be to screen cells derived from species on various points on the phylogenetic tree. Thus, identifying a cell line incapable of reproducing the effect of smoke on cytosolic Ca^{2+} could allow for further study of the differences in the Ca^{2+} signalling machinery and identification of the proteins involved in the response to cigarette smoke. Preliminary data using this approach are detailed in the appendix.

5.4 Final conclusions

In conclusion, my work has shown that changes in cytosolic Ca^{2+} are able to modulate the expression and activity of CFTR at the plasma membrane. These findings help provide a better understanding of how changes in cytosolic Ca^{2+} affect CFTR as well as how changes in Ca^{2+} induced by smoke affect CFTR. Furthermore, I have identified calcineurin as being a key target which coupled an increase in cytosolic Ca^{2+} to a decrease in CFTR, regardless of whether cigarette smoke or pharmacological agents induced this. Thus, I hypothesise that an increase in cytosolic Ca^{2+} regardless of the agonist, causes an increase in calcineurin phosphatase activity which may cause dephosphorylation of CFTR and its subsequent translocation from the plasma membrane to the endoplasmic reticulum. Finally, my data suggests inhibition of calcineurin may have important implications for

the correction the ASL hydration in smokers and the treatment of smoke related disease.

Appendix The Effect of Cigarette Smoke on Cytosolic Ca^{2+} in Eukaryotes

A.1 Introduction

As discussed in section 1.6, cigarette smoke exposure has been shown to cause an increase in cytosolic Ca^{2+} with a corresponding decrease in the expression of CFTR and height of the airway surface liquid in HBECs. An increase in cytosolic Ca^{2+} elicited by smoke has been shown in numerous cell lines, including differentiated airway cells and undifferentiated non-airway cell lines including HEK 293 cells (Rasmussen et al., 2014). As the increase in cytosolic Ca^{2+} seems to be the principle step in the changes elicited by cigarette smoke, a better understanding of what underlies the change in Ca^{2+} would be of value. To this end, I sought to characterise the response to cigarette smoke in cell lines chosen from various branches on the phylogenetic tree, to determine if all species respond in a similar manner.

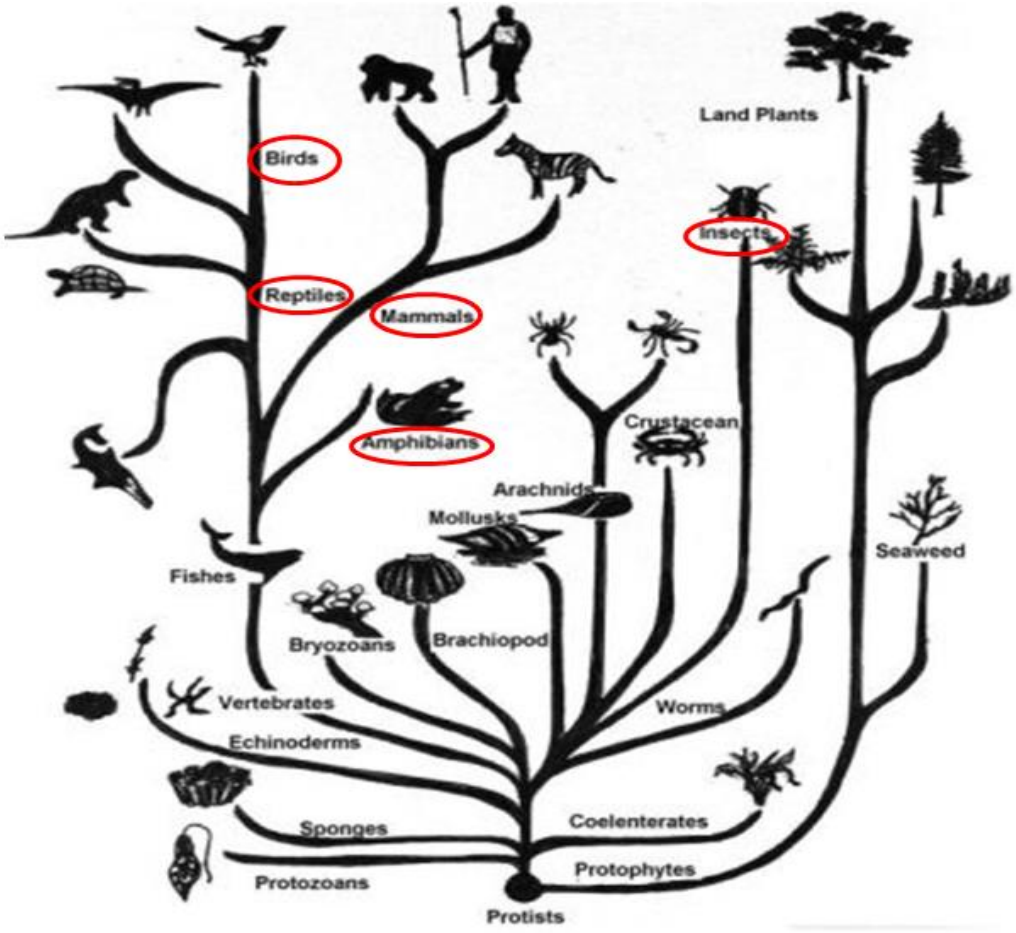

Figure A.1. Phylogenetic tree of life. Phylogenetic tree representing different evolutionary relationships between species. Species studied in this chapter are indicated. Image taken from 'The Evidence of Evolution' by Nicholas Hotton.

A.2 Cigarette smoke exposure causes an increase in cytosolic Ca^{2+} in cell lines chosen from various branches on the phylogenetic tree

A.2.1 Mammalian cells

To investigate the effect of cigarette smoke on cytosolic Ca^{2+}, HEK 293T cells were chosen as a model cell line for mammalian cells as the response to smoke in these cells has been previously documented (Rasmussen et al., 2014). Fura-2 loaded cells were exposed to 13 x 35 ml puffs over 2s every 30s which was the equivalent of one reference cigarette. Cells were otherwise exposed to room air as a control. Exposure to one cigarette caused an increase in ratio to 2.1 ± 0.5 ratio units from a baseline of 0.7 ± 0.02 ratio units. In comparison, air exposed cells showed little change in ratio (0.7 ± 0.2 ratio units from a baseline of 0.8 ± 0.1 ratio units; n=3, Fig. A.2B). Similarly, the area under the curve in smoke exposed cells was increased to 530.3 ± 66.0 ratio.min compared to 67.7 ± 22.2 ratio.min in air exposed cells (n=3, Fig. A.2C).

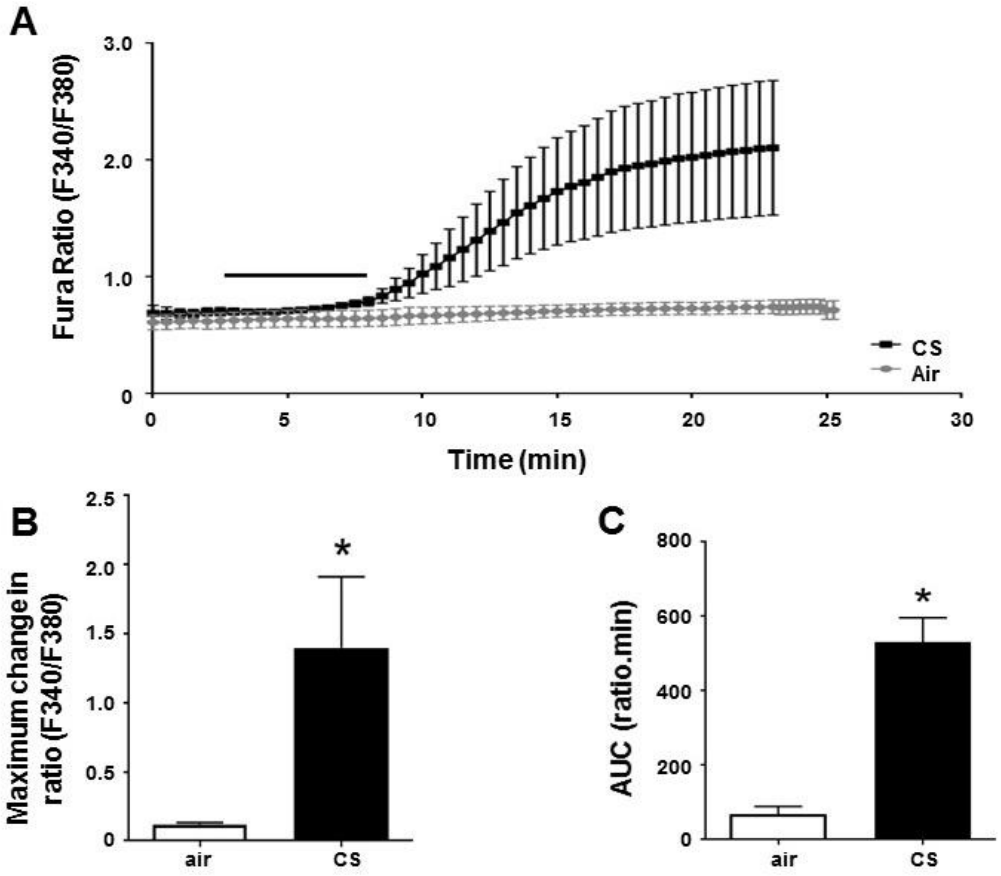

Figure A.2. Cigarette smoke exposure causes an increase in intracellular Ca^{2+} in HEK 293T cells. HEK 293T were loaded with Fura-2 AM for 30 mins. Cells were then exposed to one full research grade cigarette at a rate of one 35ml puff over 2s every 30s (13 puffs in total) or the equivalent of air. **(A)** Representative traces showing the changes in intracellular Ca^{2+}. Bar represents exposure period to either air or cigarette smoke (CS). Mean changes in **(B)** Fura-2 ratio and **(C)** area under the curve (AUC). Data are mean ± SEM (n=3). *p<0.05 compared to air.

A.2.2 Avian cells

To further understand what determines the change in cytosolic Ca^{2+} in response to smoke exposure, cells from species at various positions on the phylogenetic tree were screened. Chicken fibroblast (SL-29) cells exposed to cigarette smoke showed an increase in ratio to 0.7 ± 0.02 ratio units from a baseline of 0.4 ± 0.1 ratio units. In contrast, air exposed cells showed little change in ratio (0.5 ± 0.1 ratio units compared to 0.4 ± 0.1 ratio units before exposure). AUC followed the same trend, where smoke exposed cells showed an increase to 215.7 ± 33.0 ratio.min compared to 35.7 ± 19.0 ratio.min in air exposed cells (n=3, $p<0.05$, Fig. A.3).

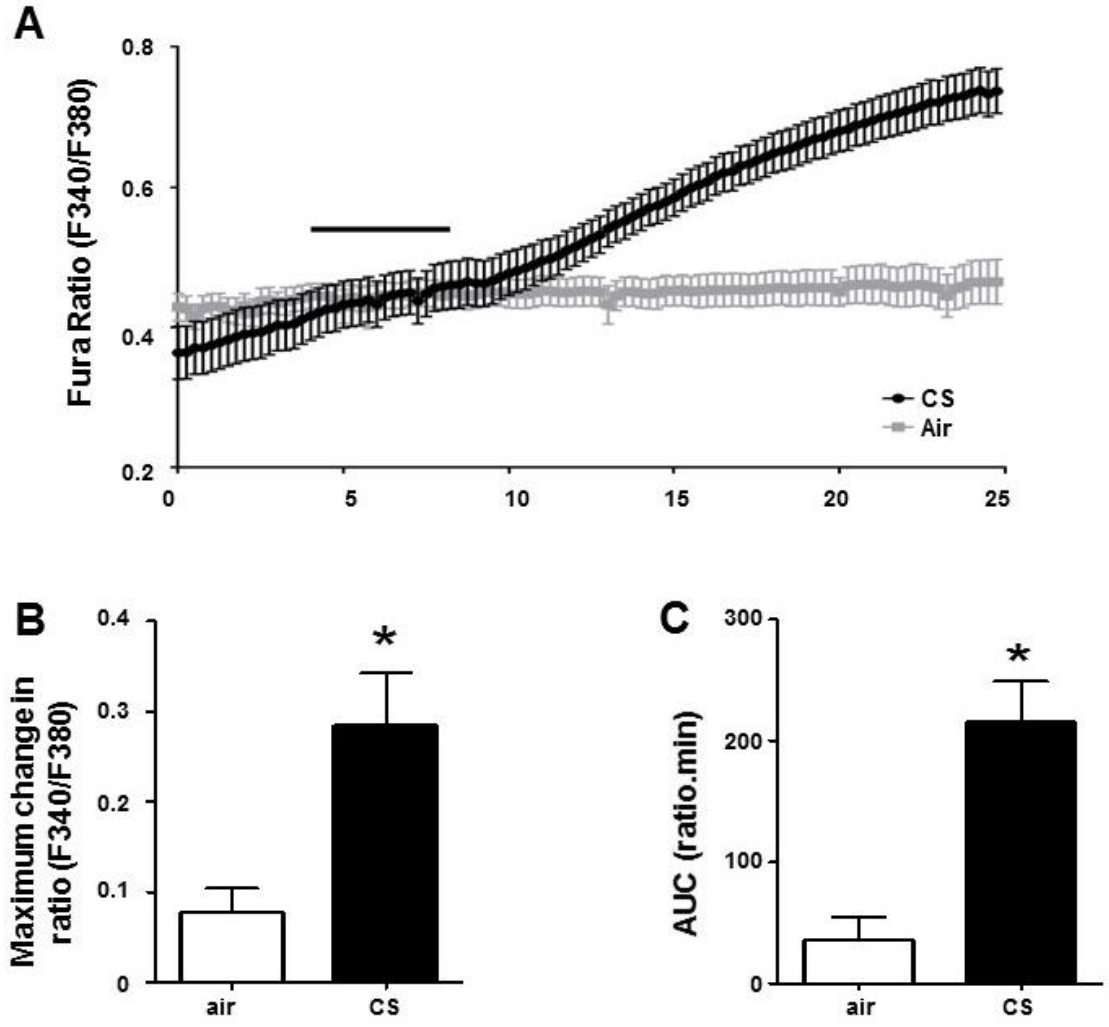

Figure A.3. Cigarette smoke exposure causes an increase in intracellular Ca^{2+} in SL-29 cells. Embryonic chicken cells, SL-29, were loaded with Fura-2 AM for 30 mins. Cells were then exposed to one full research grade cigarette at a rate of one 35ml puff over 2s every 30s (13 puffs in total) or the equivalent of air. **(A)** Representative traces showing the changes in intracellular Ca^{2+}. Bar represents exposure period to either air or cigarette smoke (CS). Mean changes in **(B)** Fura-2 ratio and **(C)** area under the curve (AUC). Data are mean ± SEM (n=3). *$p<0.05$ compared to air.

A.2.3 Reptilian cells

Reptilian cells were also chosen to study the effect of smoke on changes in cytosolic Ca^{2+}. Splenic viper (VSW) cells exposed to cigarette smoke responded with an increase in ratio of 1.0 ± 0.1 ratio units compared to 0.6 ± 0.1 ratio units before exposure. In contrast, air caused no change in the Fura-2 ratio (0.4 ± 0.02 ratio units compared to 0.4 ± 0.03 ratio units before exposure). Likewise, the AUC increased to 338.1 ± 25.8 ratio.min in smoke exposed cells, compared to 48.4 ± 25.7 ratio.min in air exposed cells (n=3, $p<0.05$, Fig. A.4).

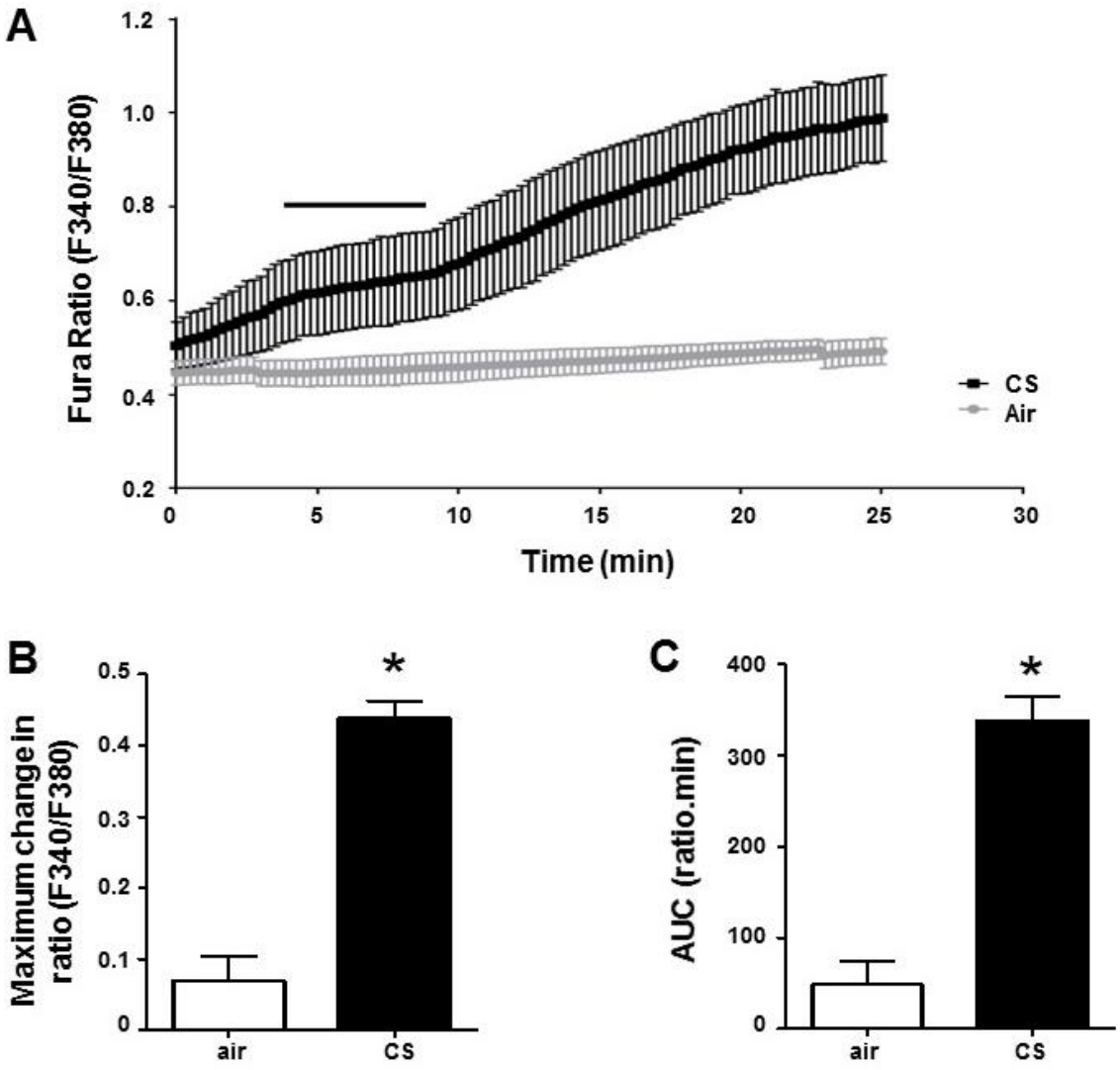

Figure A.4. Cigarette smoke exposure causes an increase in intracellular Ca^{2+} in VSW cells. Splenic viper cells, VSW, were loaded with Fura-2 AM for 30 mins. Cells were then exposed to one full research grade cigarette at a rate of one 35ml puff over 2s every 30s (13 puffs in total) or the equivalent of air. **(A)** Representative traces showing the changes in intracellular Ca^{2+}. Bar represents exposure period to either air or cigarette smoke (CS). Mean changes in **(B)** Fura-2 ratio and **(C)** area under the curve (AUC). Data are mean ± SEM (n=3). *$p<0.05$ compared to air.

A.2.4 Amphibian cells

As the previous cell lines tested showed an increase in Ca^{2+} comparable to mammalian cells, amphibian cells were tested as they represent an earlier offshoot of the phylogenetic tree (Fig. A.1). Cells derived from xenopus laevis kidney (A6) were exposed to cigarette smoke or air. On average, exposure to smoke caused an increase in ratio to 0.9 ± 0.1 ratio units compared to 0.4 ± 0.03 ratio units before exposure. In comparison, air exposed cells showed an increase to 0.5 ± 0.04 ratio units compared to 0.3 ± 0.04 ratio units (n=3, Fig. A.5B). Likewise, AUC increased to 559.5 ± 212.2 ratio.min in smoke exposed cells compared to 185.9 ± 61.7 ratio.min in air exposed cells (n=3, Fig. A.5C) indicating amphibian cells also respond to cigarette smoke.

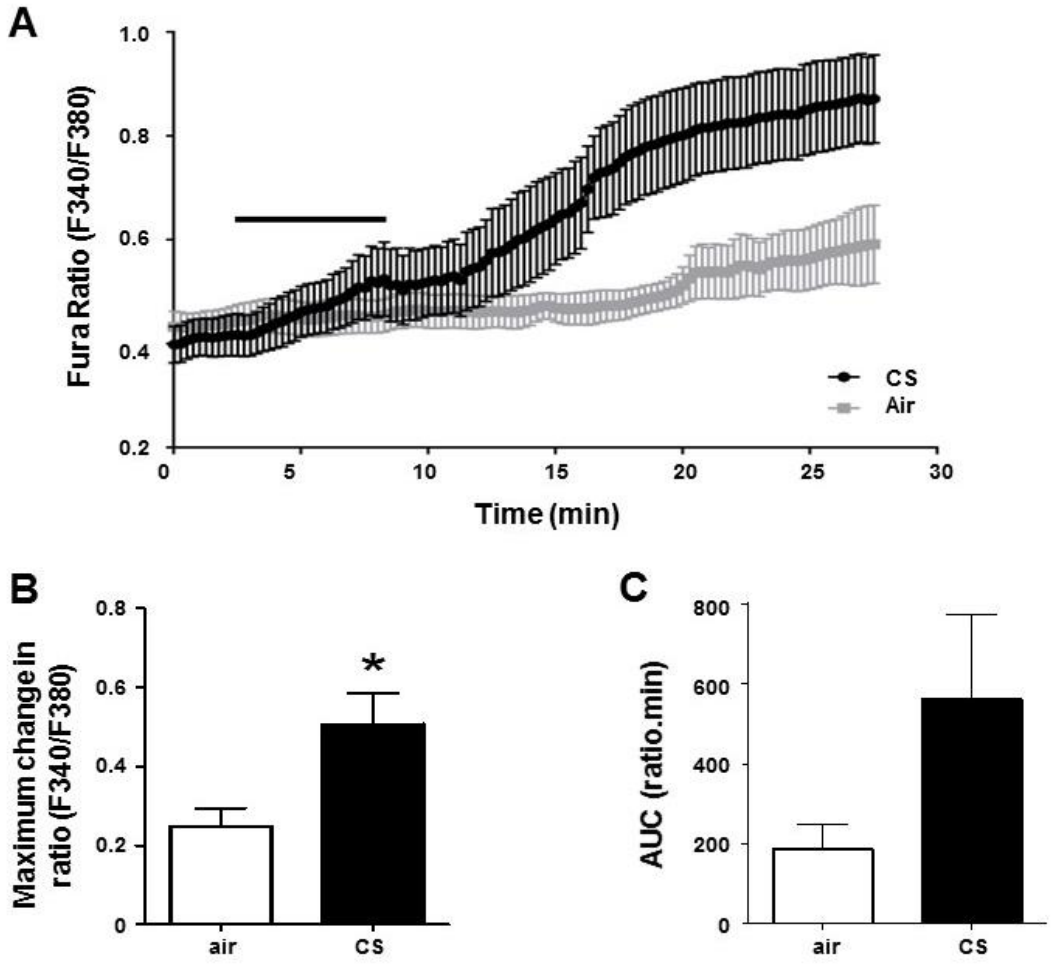

Figure A.5. Cigarette smoke exposure causes an increase in intracellular Ca^{2+} in A6 cells. Frog kidney cells, A6, were loaded with Fura-2 AM for 30 mins. Cells were then exposed to one full research grade cigarette at a rate of one 35ml puff over 2s every 30s (13 puffs in total) or the equivalent of air. **(A)** Representative traces showing the changes in intracellular Ca^{2+}. Bar represents exposure period to either air or cigarette smoke (CS). Mean changes in **(B)** Fura-2 ratio and **(C)** area under the curve (AUC). Data are mean ± SEM (n=3) *p<0.05 compared to air.

A.2.5 Insect cells

The divergence from vertebrates and insects represents a major split in the phylogenetic tree, with the deviation from human evolution occurring earlier than previous species that have been tested (Ayala et al., 1998). Therefore, cells from ovarian fall armyworms (Sf9) were tested (Fig. A.1). On average, exposure to cigarette smoke caused an increase in ratio to 0.5 ± 0.1 ratio units compared to 0.2 ± 0.01 ratio units before exposure. In comparison, cells exposed to air showed little change in ratio (0.3 ± 0.1 ratio units compared to 0.2 ± 0.04 ratio units; n=3, Fig. A.6). Likewise, the AUC in smoke exposed cells increased to 5.4 ± 1.7 ratio.min compared to 2.3 ± 0.6 ratio.min in air exposed cells (n=3, Fig. A.6C). Although the data did not reach significance, there was a trend towards an increase in Ca^{2+} upon exposure to cigarette smoke. Thus, it is likely that an increase in the number of experiments would cause the trend to reach significance.

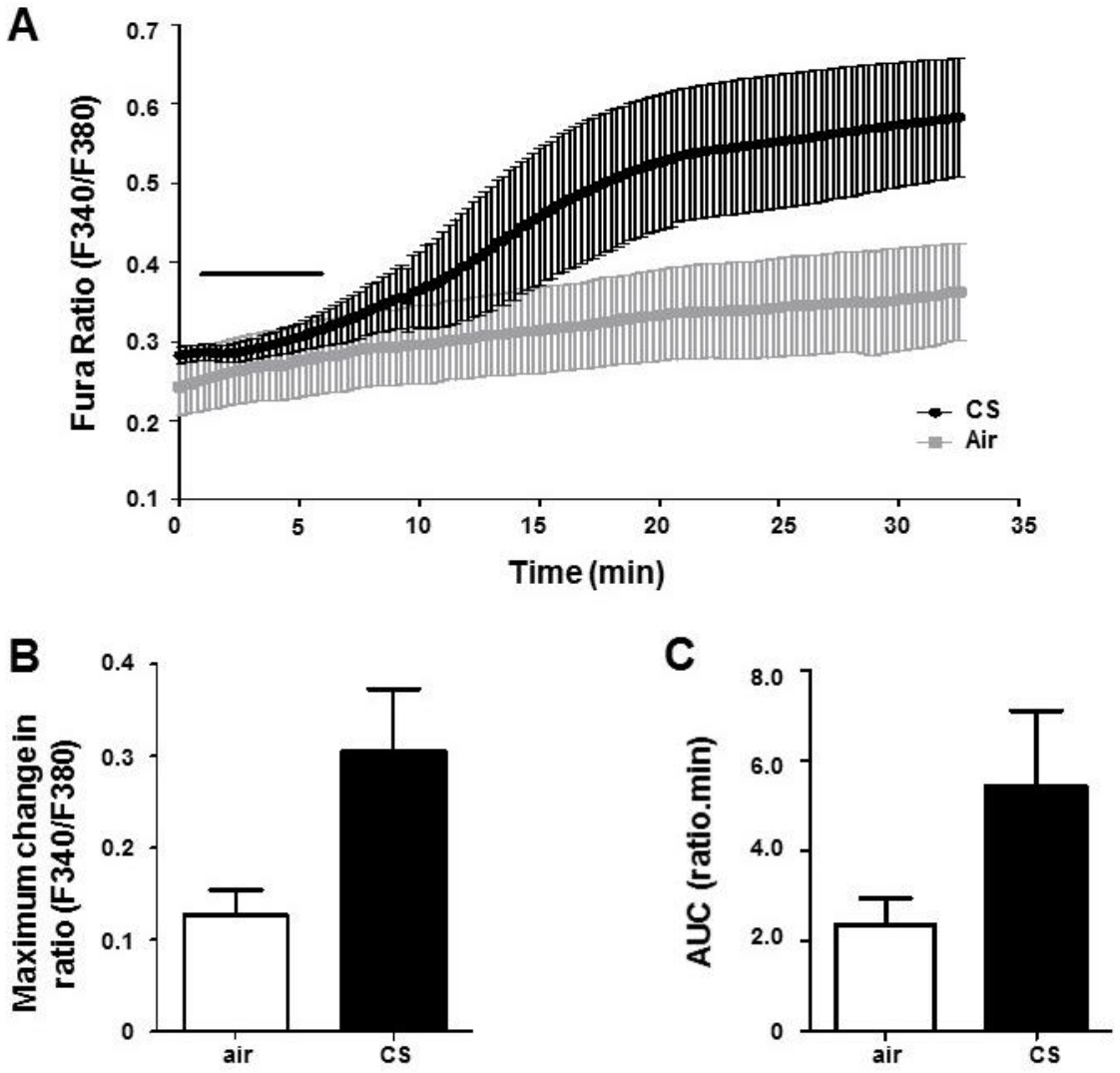

Figure A.6. Cigarette smoke exposure causes an increase in intracellular Ca^{2+} in Sf9 cells. Ovarian fall armyworm cells, Sf9, were loaded with Fura-2 AM for 30 mins. Cells were then exposed to one full research grade cigarette at a rate of one 35ml puff over 2s every 30s (13 puffs in total) or the equivalent of air. **(A)** Representative traces showing the changes in intracellular Ca^{2+}. Bar represents exposure period to either air or cigarette smoke (CS). Mean changes in **(B)** Fura-2 ratio and **(C)** area under the curve (AUC). Data are mean ± SEM (n=3).

A.3 Discussion

Tobacco smoke exposure has been shown to cause internalisation of CFTR in both airway and non-airway cell lines', suggesting this phenomenon is not reliant on the highly-specialised nature of airway epithelium (Rasmussen et al., 2014). Rasmussen and colleagues previously tested multiple mammalian cell lines. Therefore, it could be possible that the increase in Ca^{2+} in response to cigarette smoke evolved as a protective mechanism. To further understand what governs the response to cigarette smoke, I tested whether cell lines from various offshoots on the phylogenetic tree would elicit a similar response. Cells from birds, reptiles, amphibians, and insects all showed an increase in cytosolic Ca^{2+} in response to smoke exposure. Thus, these data provide further support for the hypothesis from Rasmussen and colleagues that the response of cells to cigarette smoke is a fundamental response (Rasmussen et al., 2014).

Recently, several cigarette smoke constituents have been identified as being causative in the increase in cytosolic Ca^{2+} induced by cigarette smoke (Sassano et al., 2017). However, the mechanism by which these components act to increase cytosolic Ca^{2+} has not been elucidated. On the other hand, exposure to whole cigarette smoke has been shown to cause an increase in cytosolic Ca^{2+} via Ca^{2+} release from the lysosomal store, without any release from ER or mitochondrial stores (Rasmussen et al., 2014). The basic Ca^{2+} signalling machinery has been documented in many species. Indeed, it has been suggested that the machinery is highly regulated and has been evolutionary conserved (Plattner and Verkhratsky, 2015). The presence of Ca^{2+} influx and efflux channels as well as organellar Ca^{2+} stores has been documented in species varying from humans to bacteria (Berridge et al., 2000, Raeymaekers et al., 2002). Furthermore, it has been shown that Ca^{2+} signalling was present when plant and animal ancestors split, with plants possessing Ca^{2+} influx channels and Ca^{2+} binding proteins (Edel and Kudla, 2015, Plattner, 2015). Later in the phylogenetic tree, when animal and fungi ancestors split, animals developed a large increase in specialised Ca^{2+} genes. Examples of these proteins include calcineurin and calmodulin. However, fungi do express calcineurin like proteins and these proteins have been found to respond to the same kinases and phosphatases as those in mammalian cells (Goldman et al., 2014). Thus, these findings further indicate a range of species possess the basic Ca^{2+} signalling machinery (Plattner and Verkhratsky, 2015).

Since all the species tested showed a similar profile in the Ca^{2+} response to smoke, it is possible that cells derived from animals which split from mammals earlier on the phylogenetic tree would need to be tested. Further down the phylogenetic tree would be choanoflagellates, which are unicellular organisms closest to humans. However, choanoflagellates have also been shown to have several of the Ca^{2+} channels seen in mammalian cells, including transient receptor potential channels (TRP) and Orai channels needed for store-operated Ca^{2+} entry as well as the calcium sensor STIM1 (Cai, 2008, Cai and Clapham, 2012). Going back earlier in the evolutionary tree would be yeasts. However, *S. cerevisiae* possess TRP channels on vacuoles which are organelles similar to lysosomes (Palmer et al., 2001). Indeed, vacuoles have been studied as a model for mammalian lysosomal function, suggesting that yeasts also have the machinery capable of responding to smoke (Li and Kane, 2009).

All of the species studied were eukaryotic; therefore, prokaryotic organisms could also be studied. However, these organisms are known to have a low cytosolic Ca^{2+} and plasma membrane Ca^{2+} extrusion pumps and exchangers (Gangola and Rosen, 1987, Shemarova and Nesterov, 2005). Furthermore, bacterial Ca^{2+} channels have been shown to have similar functional and pharmacological properties to eukaryotic cells (Matsushita et al., 1989). Although the Ca^{2+} signalling machinery is more complex in eukaryotic systems, prokaryotic organisms have a basic Ca^{2+} signalling system, similar to mammalian cells suggesting that these organisms may possess the machinery needed to respond to smoke (Marchadier et al., 2016).

One other avenue that could be pursued would be to test water breathing animals. All the cell lines tested were from air breathing animals and therefore, it is possible that in water breathing animals, the response to smoke may differ enough to determine what governs the Ca^{2+} increase. Fish have been shown to have Ca^{2+} homeostatic mechanisms that are comparable to vertebrates, however, it has been suggested that fish can tolerate bigger fluctuations in Ca^{2+} than land-dwelling vertebrates (Hanssen et al., 1989, Flik and Verbost, 1993).

Overall, the data showed that species which diverged from humans in the order of hundreds of millions of years ago all responded to cigarette smoke, suggesting this response is fundamental across many phyla. As changes in cytosolic Ca^{2+} can signal

changes in several processes, smoke exposure would likely have detrimental consequences for any cell type exposed. If a species could be found that showed an atypical response to cigarette smoke, further analysis of the genome of this species could help identify which proteins are involved in the Ca^{2+} response to smoke.

References

ABDULLAH, L., CONWAY, J., COHN, J. & DAVIS, C. 1997. Protein kinase C and Ca2+ activation of mucin secretion in airway goblet cells. *American Journal of Physiology-Lung Cellular and Molecular Physiology,* 273**,** L201-L210.

ABU-ARISH, A., PANDZIC, E., GOEPP, J., MATTHES, E., HANRAHAN, J. W. & WISEMAN, P. W. 2015. Cholesterol Modulates CFTR Confinement in the Plasma Membrane of Primary Epithelial Cells. *Biophysical Journal,* 109**,** 85-94.

AGELL, N., BACHS, O., ROCAMORA, N. & VILLALONGA, P. 2002. Modulation of the Ras/Raf/MEK/ERK pathway by Ca 2+, and calmodulin. *Cellular signalling,* 14**,** 649-654.

ALEKSANDROV, A. A., ALEKSANDROV, L. & R RIORDAN, J. 2002. Nucleoside triphosphate pentose ring impact on CFTR gating and hydrolysis. *FEBS letters,* 518**,** 183-188.

ALEKSANDROV, A. A., ALEKSANDROV, L. A. & RIORDAN, J. R. 2007. CFTR (ABCC7) is a hydrolyzable-ligand-gated channel. *Pflügers Archiv-European Journal of Physiology,* 453**,** 693-702.

ALEKSANDROV, A. A. & RIORDAN, J. R. 1998. Regulation of CFTR ion channel gating by MgATP. *FEBS letters,* 431**,** 97-101.

ALESSI, D. R., CUENDA, A., COHEN, P., DUDLEY, D. T. & SALTIEL, A. R. 1995. PD 098059 is a specific inhibitor of the activation of mitogen-activated protein kinase kinase in vitro and in vivo. *Journal of Biological Chemistry,* 270**,** 27489-27494.

AMARAI, J. F., MARSHALLI, J. & SMITHL, A. E. 1992. Processing of mutant cystic fibrosis transmembrane conductance regulator is temperature-sensitive. *nature,* 358**,** 27.

AMEEN, N., SILVIS, M. & BRADBURY, N. A. 2007. Endocytic trafficking of CFTR in health and disease. *J Cyst Fibros,* 6**,** 1-14.

ANDERSON, M. P. & GREGORY, R. J. 1991. Demonstration that CFTR is a chloride channel by alteration of its anion selectivity. *Science,* 253**,** 202.

ANDERSON, M. P., RICH, D. P., GREGORY, R. J., SMITH, A. E. & WELSH, M. J. 1991. Generation of cAMP-Activated Chloride Currents by Expression of CFTR. *Science,* 251**,** 679-682.

ANDERSON, M. P. & WELSH, M. J. 1991. Calcium and cAMP activate different chloride channels in the apical membrane of normal and cystic fibrosis epithelia. *Proceedings of the National Academy of Sciences,* 88**,** 6003-6007.

ANTIGNY, F., NOREZ, C., BECQ, F. & VANDEBROUCK, C. 2011. CFTR and Ca2+ signaling in cystic fibrosis. *Frontiers in pharmacology,* 2**,** 67.

AXELROD, D. 2001. Total internal reflection fluorescence microscopy in cell biology. *Traffic,* 2**,** 764-774.

AYALA, F. J., RZHETSKY, A. & AYALA, F. J. 1998. Origin of the metazoan phyla: molecular clocks confirm paleontological estimates. *Proceedings of the National Academy of Sciences,* 95**,** 606-611.

BABA, Y., HAYASHI, K., FUJII, Y., MIZUSHIMA, A., WATARAI, H., WAKAMORI, M., NUMAGA, T., MORI, Y., IINO, M. & HIKIDA, M. 2006. Coupling of STIM1 to store-operated Ca2+ entry through its constitutive and inducible movement in the endoplasmic reticulum. *Proceedings of the National Academy of Sciences,* 103**,** 16704-16709.

BAKER, J. M., HUDSON, R. P., KANELIS, V., CHOY, W.-Y., THIBODEAU, P. H., THOMAS, P. J. & FORMAN-KAY, J. D. 2007. CFTR regulatory region interacts with NBD1 predominantly via multiple transient helices. *Nature structural & molecular biology,* 14**,** 738-745.

BAKOWSKI, D., NELSON, C. & PAREKH, A. B. 2012. Endoplasmic reticulum–mitochondria coupling: local Ca2+ signalling with functional consequences. *Pflügers Archiv-European Journal of Physiology,* 464**,** 27-32.

BALGHI, H., ROBERT, R., RAPPAZ, B., ZHANG, X., WOHLHUTER-HADDAD, A., EVAGELIDIS, A., LUO, Y., GOEPP, J., FERRARO, P. & ROMÉO, P. 2011. Enhanced Ca2+ entry due to Orai1 plasma membrane insertion increases IL-8 secretion by cystic fibrosis airways. *The FASEB Journal,* 25**,** 4274-4291.

BANNYKH, S. I., BANNYKH, G. I., FISH, K. N., MOYER, B. D., RIORDAN, J. R. & BALCH, W. E. 2000. Traffic pattern of cystic fibrosis transmembrane regulator through the early exocytic pathway. *Traffic,* 1**,** 852-870.

BARGON, J., TRAPNELL, B. C., CHU, C.-S., ROSENTHAL, E. R., YOSHIMURA, K., GUGGINO, W. B., DALEMANS, W., PAVIRANI, A., LECOCQ, J. P. & CRYSTAL, R. G. 1992. Down-regulation of cystic fibrosis transmembrane conductance regulator gene expression by agents that modulate intracellular divalent cations. *Molecular and cellular biology,* 12**,** 1872-1878.

BECQ, F., JENSEN, T. J., CHANG, X.-B., SAVOIA, A., ROMMENS, J. M., TSUI, L. C., BUCHWALD, M., RIORDAN, J. R. & HANRAHAN, J. W. 1994. Phosphatase inhibitors activate normal and defective CFTR chloride channels. *Proceedings of the National Academy of Sciences,* 91**,** 9160-9164.

BENNETT, W. D., DAVISKAS, E., HASANI, A., MORTENSEN, J., FLEMING, J. & SCHEUCH, G. 2010. Mucociliary and cough clearance as a biomarker for therapeutic development. *J Aerosol Med Pulm Drug Deliv,* 23**,** 261-72.

BERGER, H., TRAVIS, S. & WELSH, M. 1993. Regulation of the cystic fibrosis transmembrane conductance regulator Cl-channel by specific protein kinases and protein phosphatases. *Journal of Biological Chemistry,* 268**,** 2037-2047.

BERGER, H. A., ANDERSON, M., GREGORY, R. J., THOMPSON, S., HOWARD, P. W., MAURER, R. A., MULLIGAN, R., SMITH, A. E. & WELSH, M. J. 1991. Identification and regulation of the cystic fibrosis transmembrane conductance regulator-generated chloride channel. *Journal of Clinical Investigation,* 88**,** 1422.

BERNARD, K., BOGLIOLO, S., SORIANI, O. & EHRENFELD, J. 2003. Modulation of calcium-dependent chloride secretion by basolateral SK4-like channels in a human bronchial cell line. *The Journal of membrane biology,* 196**,** 15-31.

BERRIDGE, M. J. 2006a. Calcium microdomains: organization and function. *Cell calcium,* 40**,** 405-412.

BERRIDGE, M. J. 2006b. Remodelling Ca2+ signalling systems and cardiac hypertrophy. *Biochem Soc Trans,* 34**,** 228-31.

BERRIDGE, M. J., BOOTMAN, M. D. & RODERICK, H. L. 2003. Calcium signalling: dynamics, homeostasis and remodelling. *Nat Rev Mol Cell Biol,* 4**,** 517-29.

BERRIDGE, M. J., LIPP, P. & BOOTMAN, M. D. 2000. The versatility and universality of calcium signalling. *Nat Rev Mol Cell Biol,* 1**,** 11-21.

BERTRAND, C. A. & FRIZZELL, R. A. 2003. The role of regulated CFTR trafficking in epithelial secretion. *American Journal of Physiology-Cell Physiology,* 285**,** C1-C18.

BIAGIOLI, M., PIFFERI, S., RAGGHIANTI, M., BUCCI, S., RIZZUTO, R. & PINTON, P. 2008. Endoplasmic reticulum stress and alteration in calcium homeostasis are involved in cadmium-induced apoptosis. *Cell calcium,* 43**,** 184-195.

BILLET, A. & HANRAHAN, J. W. 2013. The secret life of CFTR as a calcium-activated chloride channel. *The Journal of physiology,* 591**,** 5273-5278.

BILLET, A., LUO, Y., BALGHI, H. & HANRAHAN, J. W. 2013. Role of tyrosine phosphorylation in the muscarinic activation of the cystic fibrosis transmembrane conductance regulator (CFTR). *J Biol Chem,* 288**,** 21815-23.

BODAS, M., MIN, T., MAZUR, S. & VIJ, N. 2011. Critical modifier role of membrane-cystic fibrosis transmembrane conductance regulator-dependent ceramide signaling in lung injury and emphysema. *J Immunol,* 186**,** 602-13.

BOESE, S. H., GLANVILLE, M., AZIZ, O., GRAY, M. A. & SIMMONS, N. L. 2000. Ca2+ and cAMP-activated Cl- conductances mediate Cl- secretion in a mouse renal inner medullary collecting duct cell line. *J Physiol,* 523 Pt 2**,** 325-38.

BONIFACINO, J. S. & ROJAS, R. 2006. Retrograde transport from endosomes to the trans-Golgi network. *Nature reviews Molecular cell biology,* 7**,** 568-579.

BONNI, A., BRUNET, A., WEST, A. E., DATTA, S. R., TAKASU, M. A. & GREENBERG, M. E. 1999. Cell survival promoted by the Ras-MAPK signaling pathway by transcription-dependent and-independent mechanisms. *Science,* 286**,** 1358-1362.

BOOTMAN, M. D., COLLINS, T. J., PEPPIATT, C. M., PROTHERO, L. S., MACKENZIE, L., DE SMET, P., TRAVERS, M., TOVEY, S. C., SEO, J. T., BERRIDGE, M. J., CICCOLINI, F. & LIPP, P. 2001. Calcium signalling--an overview. *Semin Cell Dev Biol,* 12**,** 3-10.

BORTHWICK, L. A., MCGAW, J., CONNER, G., TAYLOR, C. J., GERKE, V., MEHTA, A., ROBSON, L. & MUIMO, R. 2007. The formation of the cAMP/protein kinase A-dependent annexin 2–S100A10 complex with cystic fibrosis conductance regulator protein (CFTR) regulates CFTR channel function. *Molecular biology of the cell,* 18**,** 3388-3397.

BOUCHER, R. C. 1999. Molecular insights into the physiology of the ‘thin film’of airway surface liquid. *The Journal of Physiology,* 516**,** 631-638.

BOUCHER, R. C. 2004. Relationship of airway epithelial ion transport to chronic bronchitis. *Proc Am Thorac Soc,* 1**,** 66-70.

BOUCHER, R. C., CHENG, E., PARADISO, A. M., STUTTS, M. J., KNOWLES, M. R. & EARP, H. S. 1989. Chloride secretory response of cystic fibrosis human airway epithelia. Preservation of calcium but not protein kinase C-and A-dependent mechanisms. *Journal of Clinical Investigation,* 84**,** 1424.

BOZOKY, Z., AHMADI, S., MILMAN, T., KIM, T. H., DU, K., DI PAOLA, M., PASYK, S., PEKHLETSKI, R., KELLER, J. P. & BEAR, C. E. 2017. Synergy of cAMP

and calcium signaling pathways in CFTR regulation. *Proceedings of the National Academy of Sciences***,** 201613546.

BOZOKY, Z., KRZEMINSKI, M., CHONG, P. A. & FORMAN-KAY, J. D. 2013. Structural changes of CFTR R region upon phosphorylation: a plastic platform for intramolecular and intermolecular interactions. *FEBS Journal,* 18**,** 4407-4416.

BRADBURY, N., JILLING, T., BERTA, G., SORSCHER, E., BRIDGES, R. & KIRK, K. 1992. Regulation of plasma membrane recycling by CFTR. *Science (New York, NY),* 256**,** 530.

BRADBURY, N. A., COHN, J. A., VENGLARIK, C. J. & BRIDGES, R. J. 1994. Biochemical and biophysical identification of cystic fibrosis transmembrane conductance regulator chloride channels as components of endocytic clathrin-coated vesicles. *Journal of Biological Chemistry,* 269**,** 8296-8302.

BRINI, M. & CARAFOLI, E. 2009. Calcium pumps in health and disease. *Physiological reviews,* 89**,** 1341-1378.

BUTTON, B., CAI, L.-H., EHRE, C., KESIMER, M., HILL, D. B., SHEEHAN, J. K., BOUCHER, R. C. & RUBINSTEIN, M. 2012. A periciliary brush promotes the lung health by separating the mucus layer from airway epithelia. *Science,* 337**,** 937-941.

CAI, X. 2008. Unicellular Ca2+ signaling 'toolkit'at the origin of metazoa. *Molecular biology and evolution,* 25**,** 1357-1361.

CAI, X. & CLAPHAM, D. E. 2012. Ancestral Ca2+ signaling machinery in early animal and fungal evolution. *Molecular biology and evolution,* 29**,** 91-100.

CALCRAFT, P. J., RUAS, M., PAN, Z., CHENG, X., ARREDOUANI, A., HAO, X., TANG, J., RIETDORF, K., TEBOUL, L., CHUANG, K. T., LIN, P., XIAO, R., WANG, C., ZHU, Y., LIN, Y., WYATT, C. N., PARRINGTON, J., MA, J., EVANS, A. M., GALIONE, A. & ZHU, M. X. 2009. NAADP mobilizes calcium from acidic organelles through two-pore channels. *Nature,* 459**,** 596-600.

CANESSA, C. M., SCHILD, L., BUELL, G., THORENS, B., GAUTSCHI, I., HORISBERGER, J.-D. & ROSSIER, B. C. 1994. Amiloride-sensitive epithelial Na+ channel is made of three homologous subunits. *Nature,* 367**,** 463.

CANT, N., POLLOCK, N. & FORD, R. C. 2014. CFTR structure and cystic fibrosis. *Int J Biochem Cell Biol,* 52**,** 15-25.

CANTIN, A. M., HANRAHAN, J. W., BILODEAU, G., ELLIS, L., DUPUIS, A., LIAO, J., ZIELENSKI, J. & DURIE, P. 2006. Cystic fibrosis transmembrane conductance

regulator function is suppressed in cigarette smokers. *Am J Respir Crit Care Med,* 173**,** 1139-44.

CAPUTO, A., CACI, E., FERRERA, L., PEDEMONTE, N., BARSANTI, C., SONDO, E., PFEFFER, U., RAVAZZOLO, R., ZEGARRA-MORAN, O. & GALIETTA, L. J. 2008. TMEM16A, a membrane protein associated with calcium-dependent chloride channel activity. *Science,* 322**,** 590-4.

CHAMBERS, L. A., ROLLINS, B. M. & TARRAN, R. 2007. Liquid movement across the surface epithelium of large airways. *Respir Physiol Neurobiol,* 159**,** 256-70.

CHAPPE, V., HINKSON, D., ZHU, T., CHANG, X. B., RIORDAN, J. & HANRAHAN, J. 2003. Phosphorylation of protein kinase C sites in NBD1 and the R domain control CFTR channel activation by PKA. *The Journal of physiology,* 548**,** 39-52.

CHAPPE, V., HINKSON, D. A., HOWELL, L. D., EVAGELIDIS, A., LIAO, J., CHANG, X.-B., RIORDAN, J. R. & HANRAHAN, J. W. 2004. Stimulatory and inhibitory protein kinase C consensus sequences regulate the cystic fibrosis transmembrane conductance regulator. *Proceedings of the National Academy of Sciences,* 101**,** 390-395.

CHAPPE, V., IRVINE, T., LIAO, J., EVAGELIDIS, A. & HANRAHAN, J. W. 2005. Phosphorylation of CFTR by PKA promotes binding of the regulatory domain. *The EMBO journal,* 24**,** 2730-2740.

CHENG, J., MOYER, B. D., MILEWSKI, M., LOFFING, J., IKEDA, M., MICKLE, J. E., CUTTING, G. R., LI, M., STANTON, B. A. & GUGGINO, W. B. 2002. A Golgi-associated PDZ domain protein modulates cystic fibrosis transmembrane regulator plasma membrane expression. *Journal of Biological Chemistry,* 277**,** 3520-3529.

CHEPIGA, T., MORTON, M., MURPHY, P., AVALOS, J., BOMBICK, B., DOOLITTLE, D., BORGERDING, M. & SWAUGER, J. 2000. A comparison of the mainstream smoke chemistry and mutagenicity of a representative sample of the US cigarette market with two Kentucky reference cigarettes (K1R4F and K1R5F). *Food and Chemical Toxicology,* 38**,** 949-962.

CHO, H., JOO, N. & WINE, J. 2011. Defective Fluid Secretion from Submucosal Glands of Nasal Turbinates from CFTR-/-and CFTRDF508/DF508 Pigs. PLoS.

CHOLON, D. M., O'NEAL, W. K., RANDELL, S. H., RIORDAN, J. R. & GENTZSCH, M. 2010. Modulation of endocytic trafficking and apical stability of CFTR in

primary human airway epithelial cultures. *American Journal of Physiology-Lung Cellular and Molecular Physiology,* 298**,** L304-L314.

CLANCY, J., ROWE, S. M., ACCURSO, F. J., AITKEN, M. L., AMIN, R. S., ASHLOCK, M. A., BALLMANN, M., BOYLE, M. P., BRONSVELD, I. & CAMPBELL, P. W. 2012. Results of a phase IIa study of VX-809, an investigational CFTR corrector compound, in subjects with cystic fibrosis homozygous for the F508del-CFTR mutation. *Thorax,* 67**,** 12-18.

CLAPHAM, D. E. 2007. Calcium signaling. *Cell,* 131**,** 1047-1058.

CLARE, J. J. 2010. Targeting ion channels for drug discovery. *Discov Med,* 9**,** 253-60.

CLARKE, L. L., GRUBB, B. R., YANKASKAS, J. R., COTTON, C. U., MCKENZIE, A. & BOUCHER, R. C. 1994. Relationship of a non-cystic fibrosis transmembrane conductance regulator-mediated chloride conductance to organ-level disease in Cftr (-/-) mice. *Proceedings of the National Academy of Sciences,* 91**,** 479-483.

CLUNES, L. A., BRIDGES, A., ALEXIS, N. & TARRAN, R. 2008. In vivo versus in vitro airway surface liquid nicotine levels following cigarette smoke exposure. *J Anal Toxicol,* 32**,** 201-7.

CLUNES, L. A., DAVIES, C. M., COAKLEY, R. D., ALEKSANDROV, A. A., HENDERSON, A. G., ZEMAN, K. L., WORTHINGTON, E. N., GENTZSCH, M., KREDA, S. M., CHOLON, D., BENNETT, W. D., RIORDAN, J. R., BOUCHER, R. C. & TARRAN, R. 2012. Cigarette smoke exposure induces CFTR internalization and insolubility, leading to airway surface liquid dehydration. *Faseb j,* 26**,** 533-45.

COGHLAN, V. M., PERRINO, B. A., HOWARD, M. & LANGEBERG, L. K. 1995. Association of protein kinase A and protein phosphatase 2B with a common anchoring protein. *Science,* 267**,** 108.

COLLEDGE, M. & SCOTT, J. D. 1999. AKAPs: from structure to function. *Trends in cell biology,* 9**,** 216-221.

CONTRERAS, J. E., SÁEZ, J. C., BUKAUSKAS, F. F. & BENNETT, M. V. 2003. Gating and regulation of connexin 43 (Cx43) hemichannels. *Proceedings of the National Academy of Sciences,* 100**,** 11388-11393.

CONWAY, J. D., BARTOLOTTA, T., ABDULLAH, L. H. & DAVIS, C. W. 2003. Regulation of mucin secretion from human bronchial epithelial cells grown in

murine hosted xenografts. *American Journal of Physiology-Lung Cellular and Molecular Physiology,* 284**,** L945-L954.

COOK, S. J., BELTMAN, J., CADWALLADER, K. A., MCMAHON, M. & MCCORMICK, F. 1997. Regulation of mitogen-activated protein kinase phosphatase-1 expression by extracellular signal-related kinase-dependent and Ca2+-dependent signal pathways in Rat-1 cells. *Journal of Biological Chemistry,* 272**,** 13309-13319.

COOPER, J., HILL, S. J. & ALEXANDER, S. P. 1997. An endogenous A2B adenosine receptor coupled to cyclic AMP generation in human embryonic kidney (HEK 293) cells. *British journal of pharmacology,* 122**,** 546-550.

CRABTREE, G. R. 1999. Generic signals and specific outcomes: signaling through Ca2+, calcineurin, and NF-AT. *Cell,* 96**,** 611-614.

DAHAN, D., EVAGELIDIS, A., HANRAHAN, J. W., HINKSON, D. A., JIA, Y., LUO, J. & ZHU, T. 2001. Regulation of the CFTR channel by phosphorylation. *Pflugers Arch,* 443 Suppl 1**,** S92-6.

DALEMANS, W. & BARBRY, P. 1991. Altered Chloride Ion Channel Kinetics Associated with the (Delta) F508 Cystic Fibrosis Mutation. *Nature,* 354**,** 526.

DALHAMN, T. 1959. The effect of cigarette smoke on ciliary activity in the upper respiratory tract. *AMA archives of otolaryngology,* 70**,** 166-168.

DAVIS, C. W. & DICKEY, B. F. 2008. Regulated airway goblet cell mucin secretion. *Annu. Rev. Physiol.,* 70**,** 487-512.

DAVIS, K. A. & COWLEY, E. A. 2006. Two-pore-domain potassium channels support anion secretion from human airway Calu-3 epithelial cells. *Pflügers Archiv,* 451**,** 631-641.

DAVIS, P. B. 2006. Cystic fibrosis since 1938. *Am J Respir Crit Care Med,* 173**,** 475-82.

DE MÉNORVAL, M.-A., MIR, L. M., FERNÁNDEZ, M. L. & REIGADA, R. 2012. Effects of dimethyl sulfoxide in cholesterol-containing lipid membranes: a comparative study of experiments in silico and with cells. *PloS one,* 7**,** e41733.

DHO, S., GRINSTEIN, S. & FOSKETT, J. K. 1993. Plasma membrane recycling in CFTR-expressing CHO cells. *Biochimica et Biophysica Acta (BBA)-Molecular Basis of Disease,* 1225**,** 78-82.

DI BENEDETTO, G., MAGNUS, C., GRAY, P. & MEHTA, A. 1991. Calcium regulation of ciliary beat frequency in human respiratory epithelium in vitro. *The Journal of Physiology,* 439**,** 103.

DODGE-KAFKA, K. L. & KAPILOFF, M. S. 2006. The mAKAP signaling complex: integration of cAMP, calcium, and MAP kinase signaling pathways. *European journal of cell biology,* 85**,** 593-602.

DODGE-KAFKA, K. L., SOUGHAYER, J., PARE, G. C., MICHEL, J. J. C., LANGEBERG, L. K., KAPILOFF, M. S. & SCOTT, J. D. 2005. The protein kinase A anchoring protein mAKAP coordinates two integrated cAMP effector pathways. *Nature,* 437**,** 574-578.

DONALDSON, S. H., HIRSH, A., LI, D. C., HOLLOWAY, G., CHAO, J., BOUCHER, R. C. & GABRIEL, S. E. 2002. Regulation of the epithelial sodium channel by serine proteases in human airways. *Journal of Biological Chemistry,* 277**,** 8338-8345.

DOUGHERTY, M. K., RITT, D. A., ZHOU, M., SPECHT, S. I., MONSON, D. M., VEENSTRA, T. D. & MORRISON, D. K. 2009. KSR2 is a calcineurin substrate that promotes ERK cascade activation in response to calcium signals. *Molecular cell,* 34**,** 652-662.

DRANSFIELD, M. T., WILHELM, A. M., FLANAGAN, B., COURVILLE, C., TIDWELL, S. L., RAJU, S. V., GAGGAR, A., STEELE, C., TANG, L. P. & LIU, B. 2013. Acquired cystic fibrosis transmembrane conductance regulator dysfunction in the lower airways in COPD. *CHEST Journal,* 144**,** 498-506.

DUDLEY, D. T., PANG, L., DECKER, S. J., BRIDGES, A. J. & SALTIEL, A. R. 1995. A synthetic inhibitor of the mitogen-activated protein kinase cascade. *Proceedings of the National Academy of Sciences,* 92**,** 7686-7689.

DUNCIA, J. V., SANTELLA, J. B., HIGLEY, C. A., PITTS, W. J., WITYAK, J., FRIETZE, W. E., RANKIN, F. W., SUN, J.-H., EARL, R. A. & TABAKA, A. C. 1998. MEK inhibitors: the chemistry and biological activity of U0126, its analogs, and cyclization products. *Bioorganic & medicinal chemistry letters,* 8**,** 2839-2844.

EARNEST, S., KHOKHLATCHEV, A., ALBANESI, J. P. & BARYLKO, B. 1996. Phosphorylation of dynamin by ERK2 inhibits the dynamin-microtubule interaction. *FEBS letters,* 396**,** 62-66.

EDEL, K. H. & KUDLA, J. 2015. Increasing complexity and versatility: how the calcium signaling toolkit was shaped during plant land colonization. *Cell Calcium,* 57**,** 231-246.

EICHSTAEDT, S., GABLER, K., BELOW, S., MULLER, C. & HILDEBRANDT, J. P. 2008. Phospholipase C-activating plasma membrane receptors and calcium

signaling in immortalized human airway epithelial cells. *J Recept Signal Transduct Res,* 28**,** 591-612.

ELLGAARD, L. & HELENIUS, A. 2003. Quality control in the endoplasmic reticulum. *Nature reviews Molecular cell biology,* 4**,** 181-191.

ENGH, R. A., GIROD, A., KINZEL, V., HUBER, R. & BOSSEMEYER, D. 1996. Crystal structures of catalytic subunit of cAMP-dependent protein kinase in complex with isoquinolinesulfonyl protein kinase inhibitors H7, H8, and H89 structural implications for selectivity. *Journal of Biological Chemistry,* 271**,** 26157-26164.

EVANS, J. & SANDERSON, M. 1999. Intracellular calcium oscillations regulate ciliary beat frequency of airway epithelial cells. *Cell calcium,* 26**,** 103-110.

FAGIOLINO, P., VÁZQUEZ, M., IBARRA, M., MAGALLANES, L., GUEVARA, N. & FOTAKI, N. 2014. Sex-and smoke-related differences in gastrointestinal transit of cyclosporin A microemulsion capsules. *European journal of pharmaceutical sciences: official journal of the European Federation for Pharmaceutical Sciences,* 63**,** 140-146.

FAHY, J. V. & DICKEY, B. F. 2010. Airway mucus function and dysfunction. *N Engl J Med,* 363**,** 2233-47.

FARINHA, C. M., MATOS, P. & AMARAL, M. D. 2013. Control of cystic fibrosis transmembrane conductance regulator membrane trafficking: not just from the endoplasmic reticulum to the Golgi. *Febs j,* 280**,** 4396-406.

FARINHA, C. M., NOGUEIRA, P., MENDES, F., PENQUE, D. & AMARAL, M. D. 2002. The human DnaJ homologue (Hdj)-1/heat-shock protein (Hsp) 40 co-chaperone is required for the in vivo stabilization of the cystic fibrosis transmembrane conductance regulator by Hsp70. *Biochemical Journal,* 366**,** 797-806.

FAVATA, M. F., HORIUCHI, K. Y., MANOS, E. J., DAULERIO, A. J., STRADLEY, D. A., FEESER, W. S., VAN DYK, D. E., PITTS, W. J., EARL, R. A. & HOBBS, F. 1998. Identification of a novel inhibitor of mitogen-activated protein kinase kinase. *Journal of Biological Chemistry,* 273**,** 18623-18632.

FEIGAL, R. J. & SHAPIRO, B. L. 1979. Mitochondrial calcium uptake and oxygen consumption in cystic fibrosis. *Nature,* 278**,** 276-277.

FISCHER, H., ILLEK, B. & MACHEN, T. E. 1998. Regulation of CFTR by protein phosphatase 2B and protein kinase C. *Pflügers Archiv European Journal of Physiology,* 436**,** 175-181.

FISCHER, H. & MACHEN, T. E. 1996. The tyrosine kinase p60c-src regulates the fast gate of the cystic fibrosis transmembrane conductance regulator chloride channel. *Biophysical Journal,* 71**,** 3073-3082.

FLIK, G. & VERBOST, P. 1993. Calcium transport in fish gills and intestine. *Journal of Experimental Biology,* 184**,** 17-29.

FRIEDMAN, J. R., DIBENEDETTO, J. R., WEST, M., ROWLAND, A. A. & VOELTZ, G. K. 2013. Endoplasmic reticulum–endosome contact increases as endosomes traffic and mature. *Molecular biology of the cell,* 24**,** 1030-1040.

FRIEDMAN, J. R., WEBSTER, B. M., MASTRONARDE, D. N., VERHEY, K. J. & VOELTZ, G. K. 2010. ER sliding dynamics and ER–mitochondrial contacts occur on acetylated microtubules. *The Journal of cell biology,* 190**,** 363-375.

FUKAYA, H., IIMURA, A., HOSHIKO, K., FUYUMURO, T., NOJI, S. & NABESHIMA, T. 2003. A cyclosporin A/maltosyl-α-cyclodextrin complex for inhalation therapy of asthma. *European Respiratory Journal,* 22**,** 213-219.

FULCHER, M. L., GABRIEL, S., BURNS, K. A., YANKASKAS, J. R. & RANDELL, S. H. 2005. Well-differentiated human airway epithelial cell cultures. *Human Cell Culture Protocols***,** 183-206.

FULCHER, M. L. & RANDELL, S. H. 2013. *Human nasal and tracheo-bronchial respiratory epithelial cell culture*, Springer.

GADSBY, D. C. & NAIRN, A. C. 1999. Control of CFTR channel gating by phosphorylation and nucleotide hydrolysis. *Physiological Reviews,* 79**,** S77-S107.

GAILLARD, E. A., KOTA, P., GENTZSCH, M., DOKHOLYAN, N. V., STUTTS, M. J. & TARRAN, R. 2010. Regulation of the epithelial Na+ channel and airway surface liquid volume by serine proteases. *Pflügers Archiv-European Journal of Physiology,* 460**,** 1-17.

GALAT, A. 1993. Peptidylproline cis-trans-isomerases: immunophilins. *The FEBS Journal,* 216**,** 689-707.

GALIONE, A. & CHURCHILL, G. C. 2002. Interactions between calcium release pathways: multiple messengers and multiple stores. *Cell Calcium,* 32**,** 343-54.

GANESAN, S., COMSTOCK, A. T. & SAJJAN, U. S. 2013. Barrier function of airway tract epithelium. *Tissue barriers,* 1**,** e24997.

GANGOLA, P. & ROSEN, B. 1987. Maintenance of intracellular calcium in Escherichia coli. *Journal of Biological Chemistry,* 262**,** 12570-12574.

GAO, Z., CHEN, T., WEBER, M. J. & LINDEN, J. 1999. A2B adenosine and P2Y2 receptors stimulate mitogen-activated protein kinase in human embryonic kidney-293 cells cross-talk between cyclic AMP and protein kinase C pathways. *Journal of Biological Chemistry,* 274**,** 5972-5980.

GARCIA-CABALLERO, A., RASMUSSEN, J. E., GAILLARD, E., WATSON, M. J., OLSEN, J. C., DONALDSON, S. H., STUTTS, M. J. & TARRAN, R. 2009. SPLUNC1 regulates airway surface liquid volume by protecting ENaC from proteolytic cleavage. *Proceedings of the National Academy of Sciences,* 106**,** 11412-11417.

GENTZSCH, M., CHANG, X.-B., CUI, L., WU, Y., OZOLS, V. V., CHOUDHURY, A., PAGANO, R. E. & RIORDAN, J. R. 2004. Endocytic trafficking routes of wild type and ΔF508 cystic fibrosis transmembrane conductance regulator. *Molecular biology of the cell,* 15**,** 2684-2696.

GERALD, L. B. & BAILEY, W. C. 2002. Global initiative for chronic obstructive lung disease. *J Cardiopulm Rehabil,* 22**,** 234-44.

GOLDMAN, A., ROY, J., BODENMILLER, B., WANKA, S., LANDRY, C. R., AEBERSOLD, R. & CYERT, M. S. 2014. The calcineurin signaling network evolves via conserved kinase-phosphatase modules that transcend substrate identity. *Molecular cell,* 55**,** 422-435.

GOLDSTEIN, J. L., ANDERSON, R. G. & BROWN, M. S. 1979. Coated pits, coated vesicles, and receptor-mediated endocytosis. *Nature,* 279**,** 679-685.

GONG, X., BURBRIDGE, S. M., COWLEY, E. A. & LINSDELL, P. 2002. Molecular determinants of Au (CN) 2− binding and permeability within the cystic fibrosis transmembrane conductance regulator Cl− channel pore. *The Journal of physiology,* 540**,** 39-47.

GRAY, M., HARRIS, A., COLEMAN, L., GREENWELL, J. & ARGENT, B. 1989. Two types of chloride channel on duct cells cultured from human fetal pancreas. *American Journal of Physiology-Cell Physiology,* 257**,** C240-C251.

GRAY, M., WINPENNY, J., PORTEOUS, D., DORIN, J. & ARGENT, B. 1994. CFTR and calcium-activated chloride currents in pancreatic duct cells of a transgenic CF mouse. *American Journal of Physiology-Cell Physiology,* 266**,** C213-C221.

GROUP, E. F. M. L. S. 1994a. Randomised trial comparing tacrolimus (FK506) and cyclosporin in prevention of liver allograft rejection. *The Lancet,* 344**,** 423-428.

GROUP, U. M. F. L. S. 1994b. A comparison of tacrolimus (FK 506) and cyclosporine for immunosuppression in liver transplantation. *N Engl J Med,* 1994**,** 1110-1115.

GRYNKIEWICZ, G., POENIE, M. & TSIEN, R. Y. 1985. A new generation of Ca2+ indicators with greatly improved fluorescence properties. *J Biol Chem,* 260**,** 3440-50.

GUGGINO, W. B. & STANTON, B. A. 2006. New insights into cystic fibrosis: molecular switches that regulate CFTR. *Nat Rev Mol Cell Biol,* 7**,** 426-36.

HALLER, T., DIETL, P., DEETJEN, P. & VÖLKL, H. 1996. The lysosomal compartment as intracellular calcium store in MDCK cells: a possible involvement in InsP3-mediated Ca2+ release. *Cell calcium,* 19**,** 157-165.

HALLOWS, K. R., RAGHURAM, V., KEMP, B. E., WITTERS, L. A. & FOSKETT, J. K. 2000. Inhibition of cystic fibrosis transmembrane conductance regulator by novel interaction with the metabolic sensor AMP-activated protein kinase. *The Journal of clinical investigation,* 105**,** 1711-1721.

HAMILL, O. P., MARTY, A., NEHER, E., SAKMANN, B. & SIGWORTH, F. J. 1981. Improved patch-clamp techniques for high-resolution current recording from cells and cell-free membrane patches. *Pflugers Arch,* 391**,** 85-100.

HANSSEN, R., LAFEBER, F., FLIK, G. & BONGA, S. W. 1989. Ionic and total calcium levels in the blood of the European eel (Anguilla anguilla): effects of stanniectomy and hypocalcin replacement therapy. *Journal of Experimental Biology,* 141**,** 177-186.

HEDA, G. D., TANWANI, M. & MARINO, C. R. 2001. The ΔF508 mutation shortens the biochemical half-life of plasma membrane CFTR in polarized epithelial cells. *American Journal of Physiology-Cell Physiology,* 280**,** C166-C174.

HEGEDŰS, T., ALEKSANDROV, A., MENGOS, A., CUI, L., JENSEN, T. J. & RIORDAN, J. R. 2009. Role of individual R domain phosphorylation sites in CFTR regulation by protein kinase A. *Biochimica et Biophysica Acta (BBA)-Biomembranes,* 1788**,** 1341-1349.

HELLERMANN, G. R., NAGY, S. B., KONG, X., LOCKEY, R. F. & MOHAPATRA, S. S. 2002. Mechanism of cigarette smoke condensate-induced acute inflammatory response in human bronchial epithelial cells. *Respiratory research,* 3**,** 22.

HERMANS, C. & BERNARD, A. 1999. Lung epithelium–specific proteins: characteristics and potential applications as markers. *American journal of respiratory and critical care medicine,* 159**,** 646-678.

HILL, D. B. & BUTTON, B. 2012. Establishment of respiratory air–liquid interface cultures and their use in studying mucin production, secretion, and function. *Mucins: Methods and Protocols***,** 245-258.

HINSHAW, J. 2000. Dynamin and its role in membrane fission 1. *Annual review of cell and developmental biology,* 16**,** 483-519.

HISERT, K. B., HELTSHE, S. L., POPE, C., JORTH, P., WU, X., EDWARDS, R. M., RADEY, M., ACCURSO, F. J., WOLTER, D. J. & COOKE, G. 2017. Restoring CFTR Function Reduces Airway Bacteria and Inflammation in People With Cystic Fibrosis and Chronic Lung Infections. *American Journal of Respiratory And Critical Care Medicine*.

HOVENBERG, H., DAVIES, J. & CARLSTEDT, I. 1996. Different mucins are produced by the surface epithelium and the submucosa in human trachea: identification of MUC5AC as a major mucin from the goblet cells. *Biochemical Journal,* 318**,** 319.

HOWARD, M., JILLING, T. & FRIZZELL, R. A. 1996. cAMP-regulated trafficking of epitope-tagged CFTR. *Kidney International,* 49**,** 1642-1648.

HTTPS://WWW.CFTR2.ORG/. *Clinical and Functional Translation of CFTR* [Online]. [Accessed 23 May 2017].

HUG, M., THIELE, I. & GREGER, R. 1997. The role of exocytosis in the activation of the chloride conductance in Chinese hamster ovary cells (CHO) stably expressing CFTR. *Pflügers Archiv,* 434**,** 779-784.

IACONO, A. T., SMALDONE, G. C., KEENAN, R. J., DIOT, P., DAUBER, J. H., ZEEVI, A., BURCKART, G. J. & GRIFFITH, B. P. 1997. Dose-related reversal of acute lung rejection by aerosolized cyclosporine. *American journal of respiratory and critical care medicine,* 155**,** 1690-1698.

INESI, G. & SAGARA, Y. 1992. Thapsigargin, a high affinity and global inhibitor of intracellular Ca2+ transport ATPases. *Archives of biochemistry and biophysics,* 298**,** 313-317.

JANSSON, K., NGUYEN, A.-N. T., MAGENHEIMER, B. S., REIF, G. A., ARAMADHAKA, L. R., BELLO-REUSS, E., WALLACE, D. P., CALVET, J. P. & BLANCO, G. 2012. Endogenous concentrations of ouabain act as a cofactor to stimulate fluid secretion and cyst growth of in vitro ADPKD models via

cAMP and EGFR-Src-MEK pathways. *American Journal of Physiology-Renal Physiology,* 303**,** F982-F990.

JIA, L., LIU, Z., SUN, L., MILLER, S. S., AMES, B. N., COTMAN, C. W. & LIU, J. 2007. Acrolein, a toxicant in cigarette smoke, causes oxidative damage and mitochondrial dysfunction in RPE cells: protection by (R)-alpha-lipoic acid. *Invest Ophthalmol Vis Sci,* 48**,** 339-48.

JIA, Y., MATHEWS, C. J. & HANRAHAN, J. W. 1997. Phosphorylation by protein kinase C is required for acute activation of cystic fibrosis transmembrane conductance regulator by protein kinase A. *Journal of Biological Chemistry,* 272**,** 4978-4984.

JØRGENSEN, K. A., KOEFOED-NIELSEN, P. & KARAMPERIS, N. 2003. Calcineurin phosphatase activity and immunosuppression. A review on the role of calcineurin phosphatase activity and the immunosuppressive effect of cyclosporin A and tacrolimus. *Scandinavian journal of immunology,* 57**,** 93-98.

KAHL, B., HERRMANN, M., EVERDING, A. S., KOCH, H. G., BECKER, K., HARMS, E., PROCTOR, R. A. & PETERS, G. 1998. Persistent infection with small colony variant strains of Staphylococcus aureus in patients with cystic fibrosis. *Journal of Infectious Diseases,* 177**,** 1023-1029.

KILBURN, K. H. 1968. A Hypothesis for Pulmonary Clearance and Its Implications 1, 2, 3. *American Review of Respiratory Disease,* 98**,** 449-463.

KILPATRICK, B. S., EDEN, E. R., SCHAPIRA, A. H., FUTTER, C. E. & PATEL, S. 2013. Direct mobilisation of lysosomal Ca2+ triggers complex Ca2+ signals. *J Cell Sci,* 126**,** 60-6.

KIM, S. J. & SKACH, W. R. 2012. Mechanisms of CFTR Folding at the Endoplasmic Reticulum. *Front Pharmacol,* 3**,** 201.

KIM, V. & CRINER, G. J. 2013. Chronic bronchitis and chronic obstructive pulmonary disease. *American journal of respiratory and critical care medicine,* 187**,** 228-237.

KINCAID, R. L., NIGHTINGALE, M. S. & MARTIN, B. M. 1988. Characterization of a cDNA clone encoding the calmodulin-binding domain of mouse brain calcineurin. *Proceedings of the National Academy of Sciences,* 85**,** 8983-8987.

KLEE, C., CROUCH, T. & KRINKS, M. 1979. Calcineurin: a calcium-and calmodulin-binding protein of the nervous system. *Proceedings of the National Academy of Sciences,* 76**,** 6270-6273.

KLEIN, H., ABU-ARISH, A., TRINH, N. T. N., LUO, Y., WISEMAN, P. W., HANRAHAN, J. W., BROCHIERO, E. & SAUVÉ, R. 2016. Investigating CFTR and KCa3. 1 protein/protein interactions. *PloS one,* 11**,** e0153665.

KLENCHIN, V. A. & MARTIN, T. F. 2000. Priming in exocytosis: attaining fusion-competence after vesicle docking. *Biochimie,* 82**,** 399-407.

KNOWLES, M. R. & BOUCHER, R. C. 2002. Mucus clearance as a primary innate defense mechanism for mammalian airways. *The Journal of clinical investigation,* 109**,** 571-577.

KNOWLES, M. R., CLARKE, L. L. & BOUCHER, R. C. 1991. Activation by extracellular nucleotides of chloride secretion in the airway epithelia of patients with cystic fibrosis. *New England Journal of Medicine,* 325**,** 533-538.

KOLCH, W. 2000. Meaningful relationships: the regulation of the Ras/Raf/MEK/ERK pathway by protein interactions. *Biochemical Journal,* 351**,** 289-305.

KONGSUPHOL, P., CASSIDY, D., HIEKE, B., TREHARNE, K. J., SCHREIBER, R., MEHTA, A. & KUNZELMANN, K. 2009. Mechanistic insight into control of CFTR by AMPK. *J Biol Chem,* 284**,** 5645-53.

KONSTAS, A.-A., KOCH, J.-P. & KORBMACHER, C. 2003. cAMP-dependent activation of CFTR inhibits the epithelial sodium channel (ENaC) without affecting its surface expression. *Pflügers Archiv European Journal of Physiology,* 445**,** 513-521.

KORNFELD, K., HOM, D. B. & HORVITZ, H. R. 1995. The ksr-1 gene encodes a novel protein kinase involved in Ras-mediated signaling in C. elegans. *Cell,* 83**,** 903-913.

KREINDLER, J. L., JACKSON, A. D., KEMP, P. A., BRIDGES, R. J. & DANAHAY, H. 2005. Inhibition of chloride secretion in human bronchial epithelial cells by cigarette smoke extract. *Am J Physiol Lung Cell Mol Physiol,* 288**,** L894-902.

LAI, M. M., HONG, J. J., RUGGIERO, A. M., BURNETT, P. E., SLEPNEV, V. I., DE CAMILLI, P. & SNYDER, S. H. 1999. The calcineurin-dynamin 1 complex as a calcium sensor for synaptic vesicle endocytosis. *Journal of Biological Chemistry,* 274**,** 25963-25966.

LAZAROWSKI, E. R. & BOUCHER, R. C. 2001. UTP as an extracellular signaling molecule. *Physiology,* 16**,** 1-5.

LAZAROWSKI, E. R., TARRAN, R., GRUBB, B. R., VAN HEUSDEN, C. A., OKADA, S. & BOUCHER, R. C. 2004. Nucleotide release provides a mechanism for

airway surface liquid homeostasis. *Journal of Biological Chemistry,* 279**,** 36855-36864.

LI, C., RAMJEESINGH, M., WANG, W., GARAMI, E., HEWRYK, M., LEE, D., ROMMENS, J. M., GALLEY, K. & BEAR, C. E. 1996. ATPase activity of the cystic fibrosis transmembrane conductance regulator. *Journal of Biological Chemistry,* 271**,** 28463-28468.

LI, C., SCHUETZ, J. D. & NAREN, A. P. 2010. Tobacco carcinogen NNK transporter MRP2 regulates CFTR function in lung epithelia: implications for lung cancer. *Cancer letters,* 292**,** 246-253.

LI, D. W.-C., LIU, J.-P., MAO, Y.-W., XIANG, H., WANG, J., MA, W.-Y., DONG, Z., PIKE, H. M., BROWN, R. E. & REED, J. C. 2005. Calcium-activated RAF/MEK/ERK signaling pathway mediates p53-dependent apoptosis and is abrogated by αB-crystallin through inhibition of RAS activation. *Molecular biology of the cell,* 16**,** 4437-4453.

LI, S. C. & KANE, P. M. 2009. The yeast lysosome-like vacuole: endpoint and crossroads. *Biochimica et Biophysica Acta (BBA)-Molecular Cell Research,* 1793**,** 650-663.

LIN, B. H., TSAI, M. H., LII, C. K. & WANG, T. S. 2015. IP3 and calcium signaling involved in the reorganization of the actin cytoskeleton and cell rounding induced by cigarette smoke extract in human endothelial cells. *Environmental toxicology*.

LINSDELL, P. 2016. Anion conductance selectivity mechanism of the CFTR chloride channel. *Biochimica et Biophysica Acta (BBA)-Biomembranes,* 1858**,** 740-747.

LINSDELL, P. 2017. Architecture and functional properties of the CFTR channel pore. *Cellular and Molecular Life Sciences,* 74**,** 67-83.

LINSDELL, P. & HANRAHAN, J. W. 1998. Adenosine triphosphate–dependent asymmetry of anion permeation in the cystic fibrosis transmembrane conductance regulator chloride channel. *The Journal of general physiology,* 111**,** 601-614.

LINSDELL, P., TABCHARANI, J. A., ROMMENS, J. M., HOU, Y.-X., CHANG, X.-B., TSUI, L.-C., RIORDAN, J. R. & HANRAHAN, J. W. 1997. Permeability of wild-type and mutant cystic fibrosis transmembrane conductance regulator chloride channels to polyatomic anions. *The Journal of general physiology,* 110**,** 355-364.

LIU, C. & HERMANN, T. E. 1978. Characterization of ionomycin as a calcium ionophore. *Journal of Biological Chemistry,* 253**,** 5892-5894.

LIU, F., ZHANG, Z., CSANÁDY, L., GADSBY, D. C. & CHEN, J. 2017. Molecular Structure of the human CFTR ion channel. *Cell,* 169**,** 85-95. e8.

LOO, M. A., JENSEN, T. J., CUI, L., HOU, Y. X., CHANG, X. B. & RIORDAN, J. R. 1998. Perturbation of Hsp90 interaction with nascent CFTR prevents its maturation and accelerates its degradation by the proteasome. *The EMBO journal,* 17**,** 6879-6887.

LUBAMBA, B., DHOOGHE, B., NOEL, S. & LEAL, T. 2012. Cystic fibrosis: insight into CFTR pathophysiology and pharmacotherapy. *Clin Biochem,* 45**,** 1132-44.

LUKACS, G. L., CHANG, X.-B., BEAR, C., KARTNER, N., MOHAMED, A., RIORDAN, J. R. & GRINSTEIN, S. 1993. The delta F508 mutation decreases the stability of cystic fibrosis transmembrane conductance regulator in the plasma membrane. Determination of functional half-lives on transfected cells. *Journal of Biological Chemistry,* 268**,** 21592-21598.

LUKACS, G. L., SEGAL, G., KARTNER, N., GRINSTEIN, S. & ZHANG, F. 1997. Constitutive internalization of cystic fibrosis transmembrane conductance regulator occurs via clathrin-dependent endocytosis and is regulated by protein phosphorylation. *Biochem. J,* 328**,** 353-361.

LUO, J., PATO, M. D., RIORDAN, J. R. & HANRAHAN, J. W. 1998. Differential regulation of single CFTR channels by PP2C, PP2A, and other phosphatases. *American Journal of Physiology-Cell Physiology,* 274**,** C1397-C1410.

LUZ, S., KONGSUPHOL, P., MENDES, A., ROMEIRAS, F., SOUSA, M., SCHREIBER, R., MATOS, P., JORDAN, P., MEHTA, A. & AMARAL, M. 2011. Contribution of casein kinase 2 and spleen tyrosine kinase to CFTR trafficking and protein kinase A-induced activity. *Molecular and cellular biology,* 31**,** 4392-4404.

LYTTON, J., WESTLIN, M. & HANLEY, M. R. 1991. Thapsigargin inhibits the sarcoplasmic or endoplasmic reticulum Ca-ATPase family of calcium pumps. *J Biol Chem,* 266**,** 17067-71.

MA, H.-P., SAXENA, S. & WARNOCK, D. G. 2002. Anionic phospholipids regulate native and expressed epithelial sodium channel (ENaC). *Journal of Biological Chemistry,* 277**,** 7641-7644.

MACDONALD, A. S. 2001. A worldwide, phase III, randomized, controlled, safety and efficacy study of a sirolimus/cyclosporine regimen for prevention of acute

rejection in recipients of primary mismatched renal allografts. *Transplantation,* 71**,** 271-280.

MACIA, E., EHRLICH, M., MASSOL, R., BOUCROT, E., BRUNNER, C. & KIRCHHAUSEN, T. 2006. Dynasore, a cell-permeable inhibitor of dynamin. *Dev Cell,* 10**,** 839-50.

MALL, M., GONSKA, T., THOMAS, J., SCHREIBER, R., SEYDEWITZ, H., KUEHR, J., BRANDIS, M. & KUNZELMANN, K. 2003. Modulation of Ca2+-activated Cl- secretion by basolateral K+ channels in human normal and cystic fibrosis airway epithelia. *Pediatric research,* 53**,** 608-618.

MALL, M., WISSNER, A., SCHREIBER, R., KUEHR, J., SEYDEWITZ, H., BRANDIS, M., GREGER, R. & KUNZELMANN, K. 2000. Role of K (V) LQT1 in cyclic adenosine monophosphate-mediated Cl (-) secretion in human airway epithelia. *American journal of respiratory cell and molecular biology,* 23**,** 283-289.

MARCHADIER, E., OATES, M. E., FANG, H., DONOGHUE, P. C., HETHERINGTON, A. M. & GOUGH, J. 2016. Evolution of the Calcium-Based Intracellular Signaling System. *Genome Biology and Evolution,* 8**,** 2118-2132.

MARKLEW, A. J. 2016. *Exploring the mechanisms behind cigarette smoke-induced internalization of CFTR.* PhD Thesis, Newcastle University.

MARKS, B. & MCMAHON, H. T. 1998. Calcium triggers calcineurin-dependent synaptic vesicle recycling in mammalian nerve terminals. *Current biology,* 8**,** 740-749.

MARX, S. O., REIKEN, S., HISAMATSU, Y., JAYARAMAN, T., BURKHOFF, D., ROSEMBLIT, N. & MARKS, A. R. 2000. PKA phosphorylation dissociates FKBP12. 6 from the calcium release channel (ryanodine receptor): defective regulation in failing hearts. *Cell,* 101**,** 365-376.

MATSUI, H., GRUBB, B. R., TARRAN, R., RANDELL, S. H., GATZY, J. T., DAVIS, C. W. & BOUCHER, R. C. 1998a. Evidence for periciliary liquid layer depletion, not abnormal ion composition, in the pathogenesis of cystic fibrosis airways disease. *Cell,* 95**,** 1005-1015.

MATSUI, H., RANDELL, S. H., PERETTI, S. W., DAVIS, C. W. & BOUCHER, R. C. 1998b. Coordinated clearance of periciliary liquid and mucus from airway surfaces. *Journal of Clinical Investigation,* 102**,** 1125-1131.

MATSUSHITA, T., HIRATA, H. & KUSAKA, I. 1989. Calcium channels in bacteria. *Annals of the New York Academy of Sciences,* 560**,** 426-429.

MCCANN, J. & WELSH, M. 1990. Regulation of Cl− and K+ channels in airway epithelium. *Annual review of physiology,* 52**,** 115-135.

MCCUBREY, J., LAHAIR, M. & FRANKLIN, R. 2005. Reactive oxygen species-induced activation of the MAP kinase signaling pathways. *Antioxidants & redox signaling,* 8**,** 1775-1789.

MEACHAM, G. C., LU, Z., KING, S., SORSCHER, E., TOUSSON, A. & CYR, D. M. 1999. The Hdj-2/Hsc70 chaperone pair facilitates early steps in CFTR biogenesis. *The EMBO Journal,* 18**,** 1492-1505.

MEACHAM, G. C., PATTERSON, C., ZHANG, W., YOUNGER, J. M. & CYR, D. M. 2001. The Hsc70 co-chaperone CHIP targets immature CFTR for proteasomal degradation. *Nature cell biology,* 3**,** 100-105.

MEDINA, D. L., DI PAOLA, S., PELUSO, I., ARMANI, A., DE STEFANI, D., VENDITTI, R., MONTEFUSCO, S., SCOTTO-ROSATO, A., PREZIOSO, C. & FORRESTER, A. 2015. Lysosomal calcium signalling regulates autophagy through calcineurin and TFEB. *Nature cell biology,* 17**,** 288-299.

MEIKLE, P. J., BROOKS, D. A., RAVENSCROFT, E. M., YAN, M., WILLIAMS, R. E., JAUNZEMS, A. E., CHATAWAY, T. K., KARAGEORGOS, L. E., DAVEY, R. C. & BOULTER, C. D. 1997. Diagnosis of lysosomal storage disorders: evaluation of lysosome-associated membrane protein LAMP-1 as a diagnostic marker. *Clinical chemistry,* 43**,** 1325-1335.

MEKAHLI, D., BULTYNCK, G., PARYS, J. B., DE SMEDT, H. & MISSIAEN, L. 2011. Endoplasmic-reticulum calcium depletion and disease. *Cold Spring Harbor perspectives in biology,* 3**,** a004317.

MERCER, B. A. & D ARMIENTO, J. M. 2006. Emerging role of MAP kinase pathways as therapeutic targets in COPD. *International journal of chronic obstructive pulmonary disease,* 1**,** 137.

MILNER, R., BAKSH, S., SHEMANKO, C., CARPENTER, M., SMILLIE, L., VANCE, J., OPAS, M. & MICHALAK, M. 1991. Calreticulin, and not calsequestrin, is the major calcium binding protein of smooth muscle sarcoplasmic reticulum and liver endoplasmic reticulum. *Journal of Biological Chemistry,* 266**,** 7155-7165.

MISONOU, Y., ASAHI, M., YOKOE, S., MIYOSHI, E. & TANIGUCHI, N. 2006. Acrolein produces nitric oxide through the elevation of intracellular calcium levels to induce apoptosis in human umbilical vein endothelial cells: implications for smoke angiopathy. *Nitric Oxide,* 14**,** 180-187.

MOLKENTIN, J. D. 2004. Calcineurin–NFAT signaling regulates the cardiac hypertrophic response in coordination with the MAPKs. *Cardiovascular research,* 63**,** 467-475.

MORAN, A. R., NORIMATSU, Y., DAWSON, D. C. & MACDONALD, K. D. 2014. Aqueous cigarette smoke extract induces a voltage-dependent inhibition of CFTR expressed in Xenopus oocytes. *American Journal of Physiology-Lung Cellular and Molecular Physiology,* 306**,** L284-L291.

MORAN, O. & ZEGARRA-MORAN, O. 2008. On the measurement of the functional properties of the CFTR. *J Cyst Fibros,* 7**,** 483-94.

MORGAN, A. J. & JACOB, R. 1994. Ionomycin enhances Ca2+ influx by stimulating store-regulated cation entry and not by a direct action at the plasma membrane. *Biochem J,* 300 (Pt 3)**,** 665-72.

MORGAN, A. J., PLATT, F. M., LLOYD-EVANS, E. & GALIONE, A. 2011. Molecular mechanisms of endolysosomal Ca2+ signalling in health and disease. *Biochem J,* 439**,** 349-74.

MOSER, S. L., HARRON, S. A., CRACK, J., FAWCETT, J. P. & COWLEY, E. A. 2008. Multiple KCNQ potassium channel subtypes mediate basal anion secretion from the human airway epithelial cell line Calu-3. *Journal of Membrane Biology,* 221**,** 153-163.

MOYER, B. D., DENTON, J., KARLSON, K. H., REYNOLDS, D., WANG, S., MICKLE, J. E., MILEWSKI, M., CUTTING, G. R., GUGGINO, W. B. & LI, M. 1999. A PDZ-interacting domain in CFTR is an apical membrane polarization signal. *The Journal of clinical investigation,* 104**,** 1353-1361.

MURPHY, T. F., BRAUER, A. L., ESCHBERGER, K., LOBBINS, P., GROVE, L., CAI, X. & SETHI, S. 2008. Pseudomonas aeruginosa in chronic obstructive pulmonary disease. *American journal of respiratory and critical care medicine,* 177**,** 853-860.

NAKAMURA, N., RABOUILLE, C., WATSON, R., NILSSON, T., HUI, N., SLUSAREWICZ, P., KREIS, T. E. & WARREN, G. 1995. Characterization of a cis-Golgi matrix protein, GM130. *The Journal of cell biology,* 131**,** 1715-1726.

NAMKUNG, W., PHUAN, P. W. & VERKMAN, A. S. 2011. TMEM16A inhibitors reveal TMEM16A as a minor component of calcium-activated chloride channel conductance in airway and intestinal epithelial cells. *J Biol Chem,* 286**,** 2365-74.

NEHER, E. 1992. [6] Correction for liquid junction potentials in patch clamp experiments. *Methods in enzymology,* 207**,** 123-131.

NEVILLE, D. C., ROZANAS, C. R., TULK, B. M., TOWNSEND, R. R. & VERKMAN, A. 1998. Expression and Characterization of the NBD1-R Domain Region of CFTR: Evidence for Subunit− Subunit Interactions. *Biochemistry,* 37**,** 2401-2409.

NEVILLE, D. C., TOWNSEND, R. R., ROZANAS, C. R., VERKMAN, A., PRICE, E. M. & GRUIS, D. B. 1997. Evidence for phosphorylation of serine 753 in CFTR using a novel metal-ion affinity resin and matrix-assisted laser desorption mass spectrometry. *Protein Science,* 6**,** 2436-2445.

OKIYONEDA, T., HARADA, K., TAKEYA, M., YAMAHIRA, K., WADA, I., SHUTO, T., SUICO, M. A., HASHIMOTO, Y. & KAI, H. 2004. ΔF508 CFTR pool in the endoplasmic reticulum is increased by calnexin overexpression. *Molecular biology of the cell,* 15**,** 563-574.

PALMER, C. P., ZHOU, X.-L., LIN, J., LOUKIN, S. H., KUNG, C. & SAIMI, Y. 2001. A TRP homolog in Saccharomyces cerevisiae forms an intracellular Ca2+-permeable channel in the yeast vacuolar membrane. *Proceedings of the National Academy of Sciences,* 98**,** 7801-7805.

PARADISO, A. M., RIBEIRO, C. M. & BOUCHER, R. C. 2001. Polarized signaling via purinoceptors in normal and cystic fibrosis airway epithelia. *J Gen Physiol,* 117**,** 53-67.

PARK, C. Y., HOOVER, P. J., MULLINS, F. M., BACHHAWAT, P., COVINGTON, E. D., RAUNSER, S., WALZ, T., GARCIA, K. C., DOLMETSCH, R. E. & LEWIS, R. S. 2009. STIM1 clusters and activates CRAC channels via direct binding of a cytosolic domain to Orai1. *Cell,* 136**,** 876-890.

PATEL, S. & DOCAMPO, R. 2010. Acidic calcium stores open for business: expanding the potential for intracellular Ca2+ signaling. *Trends Cell Biol,* 20**,** 277-86.

PICCIANO, J. A., AMEEN, N., GRANT, B. D. & BRADBURY, N. A. 2003. Rme-1 regulates the recycling of the cystic fibrosis transmembrane conductance regulator. *American Journal of Physiology-Cell Physiology,* 285**,** C1009-C1018.

PICCIOTTO, M., COHN, J., BERTUZZI, G., GREENGARD, P. & NAIRN, A. 1992. Phosphorylation of the cystic fibrosis transmembrane conductance regulator. *Journal of Biological Chemistry,* 267**,** 12742-12752.

PICHER, M., BURCH, L. H. & BOUCHER, R. C. 2004. Metabolism of P2 Receptor Agonists in Human Airways IMPLICATIONS FOR MUCOCILIARY CLEARANCE AND CYSTIC FIBROSIS. *Journal of Biological Chemistry,* 279**,** 20234-20241.

PIND, S., RIORDAN, J. R. & WILLIAMS, D. B. 1994. Participation of the endoplasmic reticulum chaperone calnexin (p88, IP90) in the biogenesis of the cystic fibrosis transmembrane conductance regulator. *Journal of Biological Chemistry,* 269**,** 12784-12788.

PLATTNER, H. 2015. Molecular aspects of calcium signalling at the crossroads of unikont and bikont eukaryote evolution–the ciliated protozoan Paramecium in focus. *Cell calcium,* 57**,** 174-185.

PLATTNER, H. & VERKHRATSKY, A. 2015. The ancient roots of calcium signalling evolutionary tree. *Cell Calcium,* 57**,** 123-132.

POHUNEK, P. 2004. Development, structure and function of the upper airways. *Paediatric respiratory reviews,* 5**,** 2-8.

POPE 3RD, C., EATOUGH, D., GOLD, D., PANG, Y., NIELSEN, K., NATH, P., VERRIER, R. & KANNER, R. 2001. Acute exposure to environmental tobacco smoke and heart rate variability. *Environmental health perspectives,* 109**,** 711.

PRINCE, L., WORKMAN JR, R. & MARCHASE, R. 1994. Rapid endocytosis of the cystic fibrosis transmembrane conductance regulator chloride channel. *Proceedings of the National Academy of Sciences of the United States of America,* 91**,** 5192-5196.

QIU, M.-S. & GREEN, S. H. 1992. PC12 cell neuronal differentiation is associated with prolonged p21 ras activity and consequent prolonged ERK activity. *Neuron,* 9**,** 705-717.

RAB, A., ROWE, S. M., RAJU, S. V., BEBOK, Z., MATALON, S. & COLLAWN, J. F. 2013. Cigarette smoke and CFTR: implications in the pathogenesis of COPD. *Am J Physiol Lung Cell Mol Physiol,* 305**,** L530-41.

RAEYMAEKERS, L., WUYTACK, E., WILLEMS, I., MICHIELS, C. & WUYTACK, F. 2002. Expression of a P-type Ca 2+-transport ATPase in Bacillus subtilis during sporulation. *Cell calcium,* 32**,** 93-103.

RAGHURAM, V., MAK, D.-O. D. & FOSKETT, J. K. 2001. Regulation of cystic fibrosis transmembrane conductance regulator single-channel gating by bivalent PDZ-domain-mediated interaction. *Proceedings of the National Academy of Sciences,* 98**,** 1300-1305.

RAJU, S. V., JACKSON, P. L., COURVILLE, C. A., MCNICHOLAS, C. M., SLOANE, P. A., SABBATINI, G., TIDWELL, S., TANG, L. P., LIU, B., FORTENBERRY, J. A., JONES, C. W., BOYDSTON, J. A., CLANCY, J. P., BOWEN, L. E., ACCURSO, F. J., BLALOCK, J. E., DRANSFIELD, M. T. & ROWE, S. M. 2013. Cigarette smoke induces systemic defects in cystic fibrosis transmembrane conductance regulator function. *Am J Respir Crit Care Med,* 188**,** 1321-30.

RAJU, S. V., LIN, V. Y., LIU, L., MCNICHOLAS, C. M., KARKI, S., SLOANE, P. A., TANG, L., JACKSON, P. L., WANG, W. & WILSON, L. 2017. The Cystic Fibrosis Transmembrane Conductance Regulator Potentiator Ivacaftor Augments Mucociliary Clearance Abrogating Cystic Fibrosis Transmembrane Conductance Regulator Inhibition by Cigarette Smoke. *American Journal of Respiratory Cell and Molecular Biology,* 56**,** 99-108.

RAMACHANDRAN, S., XIE, L. H., JOHN, S. A., SUBRAMANIAM, S. & LAL, R. 2007. A novel role for connexin hemichannel in oxidative stress and smoking-induced cell injury. *PLoS One,* 2**,** e712.

RASMUSSEN, J. E., SHERIDAN, J. T., POLK, W., DAVIES, C. M. & TARRAN, R. 2014. Cigarette smoke-induced Ca2+ release leads to cystic fibrosis transmembrane conductance regulator (CFTR) dysfunction. *J Biol Chem,* 289**,** 7671-81.

RENNOLDS, J., BUTLER, S., MALONEY, K., BOYAKA, P. N., DAVIS, I. C., KNOELL, D. L., PARINANDI, N. L. & CORMET-BOYAKA, E. 2010. Cadmium regulates the expression of the CFTR chloride channel in human airway epithelial cells. *Toxicological sciences,* 116**,** 349-358.

RIBEIRO, C. M. P., PARADISO, A. M., LIVRAGHI, A. & BOUCHER, R. C. 2003. The mitochondrial barriers segregate agonist-induced calcium-dependent functions in human airway epithelia. *The Journal of general physiology,* 122**,** 377-387.

RIORDAN, J. R. 2005. Assembly of functional CFTR chloride channels. *Annu Rev Physiol,* 67**,** 701-18.

RIORDAN, J. R., ROMMENS, J. M., KEREM, B.-S., ALON, N. & ROZMAHEL, R. 1989. Identification of the cystic fibrosis gene: cloning and characterization of complementary DNA. *Science,* 245**,** 1066.

RIZZUTO, R., DE STEFANI, D., RAFFAELLO, A. & MAMMUCARI, C. 2012. Mitochondria as sensors and regulators of calcium signalling. *Nature reviews Molecular cell biology,* 13**,** 566-578.

ROSEN, L. B., GINTY, D. D., WEBER, M. J. & GREENBERG, M. E. 1994. Membrane depolarization and calcium influx stimulate MEK and MAP kinase via activation of Ras. *Neuron,* 12**,** 1207-1221.

ROSSI, A. H., SALMON, W. C., CHUA, M. & DAVIS, C. W. 2007. Calcium signaling in human airway goblet cells following purinergic activation. *American Journal of Physiology-Lung Cellular and Molecular Physiology,* 292**,** L92-L98.

ROSSI, A. H., SEARS, P. R. & DAVIS, C. W. 2004. Ca2+ dependency of 'Ca2+-independent'exocytosis in SPOC1 airway goblet cells. *The Journal of physiology,* 559**,** 555-565.

ROWE, S. M. & VERKMAN, A. S. 2013. Cystic fibrosis transmembrane regulator correctors and potentiators. *Cold Spring Harbor perspectives in medicine,* 3**,** a009761.

RUSNAK, F. & MERTZ, P. 2000. Calcineurin: form and function. *Physiological reviews,* 80**,** 1483-1521.

SAGARA, Y., FERNANDEZ-BELDA, F., DE MEIS, L. & INESI, G. 1992. Characterization of the inhibition of intracellular Ca2+ transport ATPases by thapsigargin. *Journal of Biological Chemistry,* 267**,** 12606-12613.

SAINT-CRIQ, V. & GRAY, M. A. 2017. Role of CFTR in epithelial physiology. *Cellular and Molecular Life Sciences,* 74**,** 93-115.

SAKMANN, B. & NEHER, E. 1984. Patch clamp techniques for studying ionic channels in excitable membranes. *Annual review of physiology,* 46**,** 455-472.

SASSANO, M. F., GHOSH, A. & TARRAN, R. 2017. Tobacco Smoke Constituents Trigger Cytoplasmic Calcium Release. *Applied In Vitro Toxicology*.

SCHREIBER, R., NITSCHKE, R., GREGER, R. & KUNZELMANN, K. 1999. The cystic fibrosis transmembrane conductance regulator activates aquaporin 3 in airway epithelial cells. *Journal of Biological Chemistry,* 274**,** 11811-11816.

SCHREIBER, S. L. & CRABTREE, G. R. 1992. The mechanism of action of cyclosporin A and FK506. *Immunology today,* 13**,** 136-142.

SCHROEDER, B. C., CHENG, T., JAN, Y. N. & JAN, L. Y. 2008. Expression cloning of TMEM16A as a calcium-activated chloride channel subunit. *Cell,* 134**,** 1019-29.

SEAVILLEKLEIN, G., AMER, N., EVAGELIDIS, A., CHAPPE, F., IRVINE, T., HANRAHAN, J. W. & CHAPPE, V. 2008. PKC phosphorylation modulates PKA-dependent binding of the R domain to other domains of CFTR. *American Journal of Physiology-Cell Physiology,* 295**,** C1366-C1375.

SEIBERT, F. S., TABCHARANI, J. A., CHANG, X.-B., DULHANTY, A. M., MATHEWS, C., HANRAHAN, J. W. & RIORDAN, J. R. 1995. cAMP-dependent protein kinase-mediated phosphorylation of cystic fibrosis transmembrane conductance regulator residue Ser-753 and its role in channel activation. *Journal of Biological Chemistry,* 270**,** 2158-2162.

SHAUL, Y. D. & SEGER, R. 2007. The MEK/ERK cascade: from signaling specificity to diverse functions. *Biochimica et Biophysica Acta (BBA)-Molecular Cell Research,* 1773**,** 1213-1226.

SHEMAROVA, I. & NESTEROV, V. 2005. Evolution of mechanisms of Ca 2+-signaling: role of calcium ions in signal transduction in prokaryotes. *Journal of Evolutionary Biochemistry and Physiology,* 41**,** 12-19.

SHEN, B., FINKBEINER, W., WINE, J., MRSNY, R. & WIDDICOMBE, J. 1994. Calu-3: a human airway epithelial cell line that shows cAMP-dependent Cl- secretion. *American Journal of Physiology-Lung Cellular and Molecular Physiology,* 266**,** L493-L501.

SHEPPARD, D. N., GRAY, M. A., GONG, X., SOHMA, Y., KOGAN, I., BENOS, D. J., SCOTT-WARD, T. S., CHEN, J. H., LI, H., CAI, Z., GUPTA, J., LI, C., RAMJEESINGH, M., BERDIEV, B. K., ISMAILOV, II, BEAR, C. E., HWANG, T. C., LINSDELL, P. & HUG, M. J. 2004. The patch-clamp and planar lipid bilayer techniques: powerful and versatile tools to investigate the CFTR Cl- channel. *J Cyst Fibros,* 3 Suppl 2**,** 101-8.

SHEPPARD, D. N. & WELSH, M. J. 1999. Structure and function of the CFTR chloride channel. *Physiological reviews,* 79**,** S23-S45.

SHORT, D. B., TROTTER, K. W., RECZEK, D., KREDA, S. M., BRETSCHER, A., BOUCHER, R. C., STUTTS, M. J. & MILGRAM, S. L. 1998. An apical PDZ protein anchors the cystic fibrosis transmembrane conductance regulator to the cytoskeleton. *Journal of Biological Chemistry,* 273**,** 19797-19801.

SIAFAKAS, N., VERMEIRE, P., PRIDE, N. A., PAOLETTI, P., GIBSON, J., HOWARD, P., YERNAULT, J., DECRAMER, M., HIGENBOTTAM, T. & POSTMA, D. 1995. Optimal assessment and management of chronic obstructive pulmonary disease (COPD). *European Respiratory Journal,* 8**,** 1398-1420.

SILVA, P., STOFF, J., FIELD, M., FINE, L., FORREST, J. N. & EPSTEIN, F. H. 1977. Mechanism of active chloride secretion by shark rectal gland: role of Na-K-

ATPase in chloride transport. *American Journal of Physiology-Renal Physiology,* 233**,** F298-F306.

SILVIS, M. R., BERTRAND, C. A., AMEEN, N., GOLIN-BISELLO, F., BUTTERWORTH, M. B., FRIZZELL, R. A. & BRADBURY, N. A. 2009. Rab11b regulates the apical recycling of the cystic fibrosis transmembrane conductance regulator in polarized intestinal epithelial cells. *Molecular biology of the cell,* 20**,** 2337-2350.

SIMET, S. M., SISSON, J. H., PAVLIK, J. A., DEVASURE, J. M., BOYER, C., LIU, X., KAWASAKI, S., SHARP, J. G., RENNARD, S. I. & WYATT, T. A. 2010. Long-term cigarette smoke exposure in a mouse model of ciliated epithelial cell function. *Am J Respir Cell Mol Biol,* 43**,** 635-40.

SKACH, W. R. 2000. Defects in processing and trafficking of the cystic fibrosis transmembrane conductance regulator. *Kidney international,* 57**,** 825-831.

SMITH, S. S., STEINLE, E. D., MEYERHOFF, M. E. & DAWSON, D. C. 1999. Cystic fibrosis transmembrane conductance regulator. *The Journal of general physiology,* 114**,** 799-818.

SOLER, N., TORRES, A., EWIG, S., GONZALEZ, J., CELIS, R., EL-EBIARY, M., HERNANDEZ, C. & RODRIGUEZ-ROISIN, R. 1998. Bronchial microbial patterns in severe exacerbations of chronic obstructive pulmonary disease (COPD) requiring mechanical ventilation. *American journal of respiratory and critical care medicine,* 157**,** 1498-1505.

STÄMPFLI, M. R. & ANDERSON, G. P. 2009. How cigarette smoke skews immune responses to promote infection, lung disease and cancer. *Nature Reviews Immunology,* 9**,** 377-384.

STANLEY, P., WILSON, R., GREENSTONE, M., MACWILLIAM, L. & COLE, P. 1986. Effect of cigarette smoking on nasal mucociliary clearance and ciliary beat frequency. *Thorax,* 41**,** 519-523.

STELLATO, C., DE PAULIS, A., CICCARELLI, A., CIRILLO, R., PATELLA, V., CASOLARO, V. & MARONE, G. 1992. Anti-inflammatory effect of cyclosporin A on human skin mast cells. *Journal of investigative dermatology,* 98**,** 800-804.

STEWART, G., GLANVILLE, M., AZIZ, O., SIMMONS, N. & GRAY, M. 2001. Regulation of an outwardly rectifying chloride conductance in renal epithelial cells by external and internal calcium. *Journal of Membrane Biology,* 180**,** 49-64.

STUTTS, M. J., CANESSA, C. M., OLSEN, J. C. & HAMRICK, M. 1995. CFTR as a cAMP-dependent regulator of sodium channels. *Science,* 269**,** 847.

SUN, F., HUG, M. J., BRADBURY, N. A. & FRIZZELL, R. A. 2000. Protein kinase A associates with cystic fibrosis transmembrane conductance regulator via an interaction with ezrin. *Journal of Biological Chemistry,* 275**,** 14360-14366.

SUNDARAM, M. & HAN, M. 1995. The C. elegans ksr-1 gene encodes a novel Raf-related kinase involved in Ras-mediated signal transduction. *Cell,* 83**,** 889-901.

SWIATECKA-URBAN, A., BROWN, A., MOREAU-MARQUIS, S., RENUKA, J., COUTERMARSH, B., BARNABY, R., KARLSON, K. H., FLOTTE, T. R., FUKUDA, M. & LANGFORD, G. M. 2005. The short apical membrane half-life of rescued ΔF508-cystic fibrosis transmembrane conductance regulator (CFTR) results from accelerated endocytosis of ΔF508-CFTR in polarized human airway epithelial cells. *Journal of Biological Chemistry,* 280**,** 36762-36772.

SWIATECKA-URBAN, A., DUHAIME, M., COUTERMARSH, B., KARLSON, K. H., COLLAWN, J., MILEWSKI, M., CUTTING, G. R., GUGGINO, W. B., LANGFORD, G. & STANTON, B. A. 2002. PDZ domain interaction controls the endocytic recycling of the cystic fibrosis transmembrane conductance regulator. *Journal of Biological Chemistry,* 277**,** 40099-40105.

TAMAGNINI, F., SCULLION, S., BROWN, J. T. & RANDALL, A. D. 2014. Low concentrations of the solvent dimethyl sulphoxide alter intrinsic excitability properties of cortical and hippocampal pyramidal cells. *PloS one,* 9**,** e92557.

TAMAOKI, T., NOMOTO, H., TAKAHASHI, I., KATO, Y., MORIMOTO, M. & TOMITA, F. 1986. Staurosporine, a potent inhibitor of phospholipidCa++ dependent protein kinase. *Biochemical and biophysical research communications,* 135**,** 397-402.

TAMASHIRO, E., XIONG, G., ANSELMO-LIMA, W. T., KREINDLER, J. L., PALMER, J. N. & COHEN, N. A. 2009. Cigarette smoke exposure impairs respiratory epithelial ciliogenesis. *American journal of rhinology & allergy,* 23**,** 117-122.

TARRAN, R. 2004. Regulation of airway surface liquid volume and mucus transport by active ion transport. *Proc Am Thorac Soc,* 1**,** 42-6.

TARRAN, R. & BOUCHER, R. C. 2002. Thin-film measurements of airway surface liquid volume/composition and mucus transport rates in vitro. *Cystic fibrosis methods and protocols***,** 479-492.

TARRAN, R., BUTTON, B. & BOUCHER, R. C. 2006a. Regulation of normal and cystic fibrosis airway surface liquid volume by phasic shear stress. *Annu Rev Physiol,* 68**,** 543-61.

TARRAN, R., BUTTON, B., PICHER, M., PARADISO, A. M., RIBEIRO, C. M., LAZAROWSKI, E. R., ZHANG, L., COLLINS, P. L., PICKLES, R. J., FREDBERG, J. J. & BOUCHER, R. C. 2005. Normal and cystic fibrosis airway surface liquid homeostasis. The effects of phasic shear stress and viral infections. *J Biol Chem,* 280**,** 35751-9.

TARRAN, R., GRUBB, B. R., GATZY, J. T., DAVIS, C. W. & BOUCHER, R. C. 2001a. The relative roles of passive surface forces and active ion transport in the modulation of airway surface liquid volume and composition. *The Journal of general physiology,* 118**,** 223-236.

TARRAN, R., GRUBB, B. R., PARSONS, D., PICHER, M., HIRSH, A. J., DAVIS, C. W. & BOUCHER, R. C. 2001b. The CF salt controversy: in vivo observations and therapeutic approaches. *Mol Cell,* 8**,** 149-58.

TARRAN, R., LOEWEN, M. E., PARADISO, A. M., OLSEN, J. C., GRAY, M. A., ARGENT, B. E., BOUCHER, R. C. & GABRIEL, S. E. 2002. Regulation of murine airway surface liquid volume by CFTR and Ca2+-activated Cl− conductances. *The Journal of general physiology,* 120**,** 407-418.

TARRAN, R., TROUT, L., DONALDSON, S. H. & BOUCHER, R. C. 2006b. Soluble mediators, not cilia, determine airway surface liquid volume in normal and cystic fibrosis superficial airway epithelia. *The Journal of general physiology,* 127**,** 591-604.

TASKEN, K. & AANDAHL, E. M. 2004. Localized effects of cAMP mediated by distinct routes of protein kinase A. *Physiological reviews,* 84**,** 137-167.

THELIN, W. R., KESIMER, M., TARRAN, R., KREDA, S. M., GRUBB, B. R., SHEEHAN, J. K., STUTTS, M. J. & MILGRAM, S. L. 2005. The cystic fibrosis transmembrane conductance regulator is regulated by a direct interaction with the protein phosphatase 2A. *Journal of Biological Chemistry,* 280**,** 41512-41520.

THERRIEN, M., CHANG, H. C., SOLOMON, N. M., KARIM, F. D., WASSARMAN, D. A. & RUBIN, G. M. 1995. KSR, a novel protein kinase required for RAS signal transduction. *Cell,* 83**,** 879-888.

THORNTON, D. J., ROUSSEAU, K. & MCGUCKIN, M. A. 2008. Structure and function of the polymeric mucins in airways mucus. *Annu. Rev. Physiol.,* 70**,** 459-486.

TOWNSEND, R. R., LIPNIUNAS, P. H., TULK, B. M. & VERKMAN, A. 1996. Identification of protein kinase A phosphorylation sites on NBD1 and R domains of CFTR using electrospray mass spectrometry with selective phosphate ion monitoring. *Protein Science,* 5**,** 1865-1873.

TREHARNE, K. J., XU, Z., CHEN, J.-H., BEST, O. G., CASSIDY, D. M., GRUENERT, D. C., HEGYI, P., GRAY, M. A., SHEPPARD, D. N. & KUNZELMANN, K. 2009. Inhibition of protein Kinase CK2 closes the CFTR Cl- channel, but has no effect on the cystic fibrosis mutant ΔF508-CFTR. *Cellular Physiology and Biochemistry,* 24**,** 347-360.

TUDER, R. M. & PETRACHE, I. 2012. Pathogenesis of chronic obstructive pulmonary disease. *The Journal of clinical investigation,* 122**,** 2749-2755.

VALLET, V., CHRAIBI, A., GAEGGELER, H.-P., HORISBERGER, J.-D. & ROSSIER, B. C. 1997. An epithelial serine protease activates the amiloride-sensitive sodium channel. *Nature,* 389**,** 607-610.

VERGANI, P., LOCKLESS, S. W., NAIRN, A. C. & GADSBY, D. C. 2005. CFTR channel opening by ATP-driven tight dimerization of its nucleotide-binding domains. *Nature,* 433**,** 876-880.

VERKMAN, A. S., SONG, Y. & THIAGARAJAH, J. R. 2003. Role of airway surface liquid and submucosal glands in cystic fibrosis lung disease. *Am J Physiol Cell Physiol,* 284**,** C2-15.

VIRGIN, F. W., AZBELL, C., SCHUSTER, D., SUNDE, J., ZHANG, S., SORSCHER, E. J. & WOODWORTH, B. A. 2010. Exposure to cigarette smoke condensate reduces calcium activated chloride channel transport in primary sinonasal epithelial cultures. *Laryngoscope,* 120**,** 1465-9.

VON ESSEN, M., MENNÉ, C., NIELSEN, B. L., LAURITSEN, J. P. H., DIETRICH, J., ANDERSEN, P. S., KARJALAINEN, K., ØDUM, N. & GEISLER, C. 2002. The CD3γ leucine-based receptor-sorting motif is required for efficient ligand-mediated TCR down-regulation. *The Journal of Immunology,* 168**,** 4519-4523.

WANG, S., YUE, H., DERIN, R. B., GUGGINO, W. B. & LI, M. 2000. Accessory protein facilitated CFTR-CFTR interaction, a molecular mechanism to potentiate the chloride channel activity. *Cell,* 103**,** 169-179.

WANG, W., EL HIANI, Y., RUBAIY, H. N. & LINSDELL, P. 2014. Relative contribution of different transmembrane segments to the CFTR chloride channel pore. *Pflügers Archiv-European Journal of Physiology,* 466**,** 477-490.

WANG, W. & LINSDELL, P. 2012. Conformational change opening the CFTR chloride channel pore coupled to ATP-dependent gating. *Biochimica et biophysica acta,* 1818**,** 851.

WARD, N. E. & O'BRIAN, C. A. 1992. Kinetic analysis of protein kinase C inhibition by staurosporine: evidence that inhibition entails inhibitor binding at a conserved region of the catalytic domain but not competition with substrates. *Molecular pharmacology,* 41**,** 387-392.

WEIXEL, K. & BRADBURY, N. 2001. Endocytic adaptor complexes bind the C-terminal domain of CFTR. *Pflügers Archiv European Journal of Physiology,* 443**,** S70-S74.

WHITMARSH, A. J. & DAVIS, R. J. 2000. Signal transduction: a central control for cell growth. *Nature,* 403**,** 255-256.

WICKSTRÖM, C., DAVIES, J., ERIKSEN, G., VEERMAN, E. & CARLSTEDT, I. 1998. MUC5B is a major gel-forming, oligomeric mucin from human salivary gland, respiratory tract and endocervix: identification of glycoforms and C-terminal cleavage. *Biochemical Journal,* 334**,** 685.

WIDDICOMBE, J. H. & WINE, J. J. 2015. Airway gland structure and function. *Physiological reviews,* 95**,** 1241-1319.

WORLD HEALTH ORGANISATION. 2014. *The top 10 causes of death* [Online]. Available: http://www.who.int/mediacentre/factsheets/fs310/en/ [Accessed 6 Aug 2014].

WORTHINGTON, E. N. & TARRAN, R. 2011. Methods for ASL measurements and mucus transport rates in cell cultures. *Cystic Fibrosis: Diagnosis and Protocols, Volume II: Methods and Resources to Understand Cystic Fibrosis***,** 77-92.

WRIGHT, A. M., GONG, X., VERDON, B., LINSDELL, P., MEHTA, A., RIORDAN, J. R., ARGENT, B. E. & GRAY, M. A. 2004. Novel regulation of cystic fibrosis transmembrane conductance regulator (CFTR) channel gating by external chloride. *Journal of Biological Chemistry,* 279**,** 41658-41663.

WU, X.-S., MCNEIL, B. D., XU, J., FAN, J., XUE, L., MELICOFF, E., ADACHI, R., BAI, L. & WU, L.-G. 2009. Ca2+ and calmodulin initiate all forms of

endocytosis during depolarization at a nerve terminal. *Nature neuroscience,* 12**,** 1003-1010.

WWW.GENET.SICKKIDS.ON.CA/CFTR. *Cystic Fibrosis Mutation Database* [Online]. Available: http://www.genet.sickkids.on.ca/app [Accessed 5 May 2017].

XIONG, X., CHONG, E. & SKACH, W. R. 1999. Evidence that endoplasmic reticulum (ER)-associated degradation of cystic fibrosis transmembrane conductance regulator is linked to retrograde translocation from the ER membrane. *Journal of Biological Chemistry,* 274**,** 2616-2624.

XU, X., BALSIGER, R., TYRRELL, J., BOYAKA, P. N., TARRAN, R. & CORMET-BOYAKA, E. 2015. Cigarette smoke exposure reveals a novel role for the MEK/ERK1/2 MAPK pathway in regulation of CFTR. *Biochim Biophys Acta,* 1850**,** 1224-32.

YANG, Y., JANICH, S., COHN, J. A. & WILSON, J. M. 1993. The common variant of cystic fibrosis transmembrane conductance regulator is recognized by hsp70 and degraded in a pre-Golgi nonlysosomal compartment. *Proceedings of the National Academy of Sciences,* 90**,** 9480-9484.

YANG, Y. D., CHO, H., KOO, J. Y., TAK, M. H., CHO, Y., SHIM, W. S., PARK, S. P., LEE, J., LEE, B., KIM, B. M., RAOUF, R., SHIN, Y. K. & OH, U. 2008. TMEM16A confers receptor-activated calcium-dependent chloride conductance. *Nature,* 455**,** 1210-5.

YOSHIDA, T. & TUDER, R. M. 2007. Pathobiology of cigarette smoke-induced chronic obstructive pulmonary disease. *Physiol Rev,* 87**,** 1047-82.

YOUNG, A., GENTZSCH, M., ABBAN, C. Y., JIA, Y., MENESES, P. I., BRIDGES, R. J. & BRADBURY, N. A. 2009. Dynasore inhibits removal of wild-type and ΔF508 cystic fibrosis transmembrane conductance regulator (CFTR) from the plasma membrane. *Biochemical Journal,* 421**,** 377-385.

YU, Y., PLATOSHYN, O., SAFRINA, O., TSIGELNY, I., YUAN, J. X. J. & KELLER, S. H. 2007. Cystic fibrosis transmembrane conductance regulator (CFTR) functionality is dependent on coatomer protein I (COPI). *Biology of the Cell,* 99**,** 433-444.

ZHOU, J.-J., FATEHI, M. & LINSDELL, P. 2008. Identification of positive charges situated at the outer mouth of the CFTR chloride channel pore. *Pflügers Archiv-European Journal of Physiology,* 457**,** 351.

ZHOU, Z., HU, S. & HWANG, T. C. 2001. Voltage-dependent flickery block of an open cystic fibrosis transmembrane conductance regulator (CFTR) channel pore. *The Journal of Physiology,* 532**,** 435-448.

ZHU, M. X., MA, J., PARRINGTON, J., CALCRAFT, P. J., GALIONE, A. & EVANS, A. M. 2010. Calcium signaling via two-pore channels: local or global, that is the question. *Am J Physiol Cell Physiol,* 298**,** C430-41.

ZHU, G., ZHANG, Y., XU, H., JIANG, C. 1998 Identification of endogenous outward currents in the human embryonic kidney (HEK 293) cell line. *Journal of Neuroscience Methods,* 81, 73-83.